2006 Biophysical Society Discussions
October 19-22, 2006
Molecular Motors: Point Counterpoint

The Biophysical Society Discussions are special meetings that focus on outstanding problems in a field with a view to solving them. The format of the Biophysical Discussions is unique in that broad audience participation and discussion are emphasized to encourage the emergence of new insights and ideas. The Discussions differ from other scientific meetings in that the role of the session chairs and invited speakers is primarily to provide a framework for discussion of work relevant to specific unresolved problems in the field, rather than to present and discuss data from the speakers' laboratories. We have asked the speakers at this Discussions meeting to give short talks (5-10 min) that present an overview of the problem assigned to them by their chair, to allow maximal time for discussion by meeting participants.

The Discussions this Fall will be the first to focus on molecular motors since the reinstatement of the meetings in 1994, when Roger Cooke organized the meeting entitled “Molecular Motors: Structure, Mechanics, and Energy Transduction”. We believe that it is appropriate to revisit this topic at this time for several reasons. First, many new motors have been identified since 1994 and common themes regarding their mechanisms of function are becoming increasingly apparent. Second, the development of new techniques for imaging motors has made studies in live cells feasible, opening an exciting new era of studies with the potential to provide information directly relevant to motor function in cellular processes, such as mitosis and morphogenesis. Third, there is a growing appreciation that molecular motors play an important role in human disease – motors are now a focus of increasing interest as potential drug targets. Finally, as noted above, the format of the Discussions has changed appreciably since 1994 and is still evolving, and we believe that significant new insights and research directions will emerge through the interchange of ideas that the new format will encourage.

The 2006 Discussions, entitled "Molecular Motors: Point Counterpoint", will highlight unresolved problems in the field and compare known mechanisms with those emerging for different motors, bringing in work from proteins that undergo similar changes, but are not conventionally considered motors. The immediate, unresolved questions in the field will be posed in a special opening talk by Yale Goldman, a leader in the motors field. The meeting sessions will address unanswered questions regarding motor stepping, force generation and transduction, directionality, regulation, and force production in the cell. The posters and reviews will broaden participation by attendees and highlight work that may not otherwise be a focus of discussion. An overview of the ideas developed during the meeting and new directions that have been forged will be given by Joe Howard at the end of the meeting.

We anticipate that the 2006 Discussions meeting will define the outstanding problems in the field and develop new ideas and approaches to address them. These new approaches are likely to include new initiatives in drug design and screening, given that molecular motors are now known to play essential roles in cellular processes that, when disrupted, result in cancer, heart failure, blindness/deafness, and other disabling human diseases.

Sharyn A. Endow and Steven S. Rosenfeld, Co-organizers
Organizing Committee: Steven M. Block, Hideo Higuchi, F. Jon Kull, Ron Milligan, H. Lee Sweeney, Rich Vallee, Claudia Veigel

Abstract for Biophysical Discussions Meeting

Yale E. Goldman, Pennsylvania Muscle Institute, University of Pennsylvania

Challenges in Molecular Motor Research

Biophysical Discussions have had a strong influence on molecular motor research. In 1994, Roger Cooke organized the Biophysical Discussions meeting on 'Molecular Motors: Structure, Mechanics and Energy Transduction' in Airlie, Virginia. He brought together for the first time then disparate groups working on myosin, kinesin and dynein. Now, research on these three classical motor protein families is so well integrated, with so much cross-talk of results and approaches, that their separate existence is a distant memory. Some other meetings having high impact are the Biophysical Society 'Motility Subgroup', Gordon Research Conferences on 'Motility and Contractile Systems', 'Muscle & Molecular Motors' and 'Single Molecule Approaches to Biology', the last one initiated by Lori S. Goldner in 2006. Steven M. Block organized meetings on 'Single Molecule Biophysics' (note the initials) at the Aspen Center for Physics in 2003 and 2005. These meetings incorporated molecular motors, nucleic acid processing enzymes, macromolecular folding and unfolding, nucleosomes, ribosomes, and technology for their manipulation and interrogation. The cross-over of technology among these areas, the operating principles of the molecular machines, and many aspects of their structures make considering them together and comparing them a productive exercise. Sharyn Endow and Steve Rosenfeld have taken an interesting approach for the present meeting to ensure that the mechanisms among the various motor families are compared and contrasted, along with nontraditional motors. Our goals over the next few days are to define the outstanding problems in the field, devise ways to solve them, and forge new research directions that impact on the relevant cellular processes. Each session considers functional characteristics among several of the motor families to promote cross-fertilization of ideas and approaches.

I was asked to present an introductory lecture on opportunities and challenges in our field. Here I list some of the important uncertainties in the mechanism of molecular motors, organized according to the sessions we'll attend at the meeting. Many of these points have been answered for one class of molecular motor, but not the others. I plan to expand on these in the talk.

<u>Walking, Limping and Processivity</u>

1. In the hand-over-hand mechanism, how do the motor domains communicate with their partners to modulate maintain the ATPase cycle out of phase?
2. Are there processive motility mechanisms other than hand-over-hand?
3. How do single-headed processive motors stay associated with their filament?
4. Are the two heads of a motor equivalent?
5. What functional advantage is conferred by asymmetries in two-headed species?
6. How do the motors achieve flexibility of path and obstacle avoidance?
7. How do molecular machines such as helicases, polymerases and ribosomes, included more recently in the motor club, move along their tracks?

Overview

Mechano-Chemistry

1. What are the structural changes that take place during the ATPase cycle that produce force and motion?
2. When force or torque is generated, how is it amplified by the structure (e.g. lever arms) into larger motion?
3. How do the states in the ATPase cycle modulate affinity of the motor for the nucleotide and the cytoskeletal filament, in some cases at quite a distance?
4. How do the cytoskeletal filaments modulate the nucleotide affinities, and the rates and equilibria of the elementary steps of the ATPase cycle?
5. How can we obtain high-resolution structures of motors complexed to cytoskeletal filaments?
6. Beyond being tracks and activators, what roles do actin and microtubules serve?
7. How do the motors succeed in efficient energy transduction in the chaotic, fluctuating 'perfect storm' of their viscous cellular environment?
8. Do molecular motors capture thermal energy as Brownian ratchets? Are there other roles of thermal fluctuations?
9. Where is energy stored in the protein?
10. What kinetic tuning optimizes a motor for its cellular role?
11. How do mechanical factors such as the force and compliance of the load modulate the ATPase cycle?
12. What operating mechanisms co-exist with other mechano-chemical proteins, such as ion channels, pumps and receptors?

Directionality

1. Does the orientation of a lever arm or linker determine the stroke direction?
2. Is directionality determined by a well-defined domain?
3. How is directionality of the non-traditional motors, such as nucleic acid processors, determined?
4. Why do N-terminal and C-terminal motors usually travel in opposite directions?
5. How do motors reverse direction?
6. Is reversal regulated and how?
7. How varied are the mechanisms among the molecular motor families?
8. Are the mechanisms of the most unconventional motors fundamentally different from the standard bearers?
9. Do motors serve as anchors as well as transporters?
10. How do filament polymerization and depolymerization interact with molecular motors?
11. What can we learn from bacteria that swim by changes in helicity.

Regulation

1. How does cellular signal transduction switch motors on and off and regulate their rate?
2. How is the cargo specified?
3. How is cargo bound to the motor and released at the proper moments?
4. How is the destination specified?
5. Do cargos modulate dimerization and thereby signaling between heads?

6. When interacting with a cargo, how do motors cooperate or provoke each other among individuals of one isoform and between isoforms and families?
7. Do scaffolds and adaptor proteins operate in several contexts?

Higher Levels of Integration

1. How do motors deal with the crowded cellular environment and the complex network of filaments?
2. What happens at cross-overs between like and disparate filaments?
3. How do the motors get to their site of action and then get back to any storage reservoirs?
4. How do supramolecular complexes assemble at their site of action?
5. What regulates their assembly and the degradation of mis-assembled complexes and ones that have fulfilled their missions?
6. How do motors interact with membranes, applying forces and receiving signals?
7. What are the components and their interactions within supermolecular compartments, such as the cleavage furrow, the lamellopodium and the spindle?
8. How do cytoskeletal filaments confer appropriate mechanics on the cell? How is this process regulated?
9. How do molecular motors assist the actin and microtubules in determining cell shape?

Beyond this Biophysical Discussions Meeting

1. Can we design specific activators and inhibitors that will be useful scientifically and clinically?
2. How does our molecular understanding help to elaborate developmental morphogenesis, tissue size and shape, and repair.
3. Can we use molecular motors and/or their operating principles in man-made nanoscale devices?
4. Can we quantitatively model a whole cell, then multicellular networks?

Conclusions

1. Progress on each of the three classical molecular motor families, and on many other mechano-enzymes, filaments, and NTPases, informs research on all of the rest.
2. These challenges and further ones missing from this list should keep us fascinated, busy and funded.

The problem of processivity

R.A. Cross

Introduction

Can progress on the kinesin mechanism tell us anything about how ribosomes work? Can understanding the myosins help us with the walking mechanism of dynein? In this first session we will hear reviews of recent progress in these 4 systems from experts in each field, and explore the possibility that their operating principles overlap.

As an aid to discussion, I list here a set of biophysical questions that might reasonably be asked of each of these systems. Everyone working in the field will have their own favourite formulations, and my list is not intended to be definitive or comprehensive – my purpose here is just to provide an uncontroversial low-resolution map of the problem of processivity, as a navigational aid to readers of these discussion papers.

1. What do single steps look like at high spatial and temporal resolution? Is the step a unitary event? Do single mechanical steps map to single chemical kinetic steps?

Mechanoenzymes run through a cycle of conformational changes, which is driven by, a coupled cycle of transitions between chemical kinetic states. At least one of the chemical kinetic state changes, and perhaps more than one, produces a change in the shape or the binding proclivities of the motor, resulting in the generation of force, or motion, or both. One way to pose the problem of mechanism is to ask, which state-transitions result in displacements? By recording the stepping behaviour of mechanoenzymes at very high spatial and temporal resolution, we can try to gauge how much force or displacement is generated by each chemical kinetic step.

2. How (and how fast) do the moving parts of the motor move?

Molecular motors are like macroscopic motors in as much as they have moving parts – it is just that the moving parts of a molecule, a “soft machine”, are much more elastic and much more dynamic than the parts of a macroscopic machine. To understand the operating principles of a molecular machine, we can try to divide up its structure into modular moving parts, perhaps corresponding to molecular domains and subdomains, and ask about the dynamics of the parts. In the case of processive mechanoenzymes, we are interested in particular in the connections that link the two (or more) collaborating motor domains (heads).

3. What do(es) the waiting state(s) look like?

This question is particularly relevant to processive motors. It seems that in several processive motors, the mechanical cycle of chemically-driven conformational changes pauses at some point, and requires that some condition test TRUE before the cycle can continue. Perhaps this property of arresting in a so-called waiting state, with further progress conditional on a specific chemical kinetic event, represents a kind of signature for processivity. The redevelopment of a waiting state at the end of each chemical cycle may allow walking motors like kinesin and myosin V (and perhaps dynein?) to resynchronise the mechanochemical cycles of their two heads. By finding out what the

waiting state looks like (Both heads bound? One head bound?) we can begin to analyse how this synchronisation works.

4. Which mechanochemical steps are strain-dependent? How does stiffness vary during the mechanochemical cycle?

The defining property of a mechanoenzyme is that its state-transitions result in the development of force. This force produces strain, corresponding to distortion in the structure of the motor. Chemical kinetic state-transitions that generate strain will have rate constants that are sensitive to externally-applied strain. This property of strain dependence in the chemical kinetics evinces the reciprocal coupling of the chemical and mechanical cycles of the motor. By understanding which chemical kinetic equilibria are strain dependent, we can identify the force-generating steps in the cycle. For processive mechanoenzymes, strain appears to be used as a means of communication between linked domains of the same molecule. By applying strain to its partner, a force-generating domain can signal its activity and prompt the partner to modify its actions appropriately – most obviously for kinesin-1 and myosin V, where backwards strain on the lead head serves to stabilise its attachment to the track, whilst forwards strain on the trail head accelerates its release. A special case of this kind of coordination arises if the stiffness of the motor varies during the kinetic cycle.

5. Tracking mechanisms - how and why do processive motors stay on track? Is track-switching possible? Why do / do not motors rotate around the axis of the track?

For several processive motors, there is more than one potential route along the track. Microtubules are the most extreme example, wherein the motor binding sites are arranged along several different helices. How does the motor pick out its route? One contributory factor may be the electrostatic charge distribution on the microtubule surface, which may tend to set up an electrostatic barrier between protofilaments, guiding the motor to step down between two ridges of charge. Another contributory factor can be the power stroke itself, which in some motors at least can have on-axis and off-axis components. There may be other mechanisms by which one track-binding head can guide the other to a particular destination. Much more work is needed in this area.

6. Non-equivalent steps – what are the structural and kinetic origins of limping?

Sometimes, motors limp, indicating that rather than every step being exactly equivalent, alternate steps are equivalent. Kinesin-1 can be given a permanent limp by mutating one of its heads to slow down its kinetic cycle. Interestingly however, limping can also sometimes occur for wild type (homodimeric) motors. In alternate-sides hand-over-hand (walking) schemes, the trail head passes alternately to the left or right of the lead head, producing an asymmetry – why this asymmetry sometimes produces a limp and sometimes does not is unclear: but even the fact that it happens sometimes tells us that there is an asymmetry.

7. Mechanisms for amplifying stroke size & **biasing attachment direction – lever arms and neck linkers**

One mechanistic advantage of processivity is that one head can (indeed must) guide the actions of the other(s). Much interest continues in the problem of how this occurs. In myosin in particular, it seems that lever arms can come in a variety of lengths, and that the lever must be the correct length if the leading head is to be guided to the correct, straight-ahead, target site along the actin filament – a little shorter or longer, and the motor rotates corkscrew-fashion around the axis of the actin filament. Meanwhile, the active motion of the lever arm is amplifying an underlying, driving motion in the motor head. The lever arm also acts as a strain sensor, its stiffness allowing strain to be transmitted between heads and used to coordinate the actions of the two heads. Longer levers are expected to be less stiff. Processivity requires that the properties of the underlying head are matched to the length and the stiffness of the lever arm. Understanding how this works, in myosin and in other systems, is a considerable challenge.

8. Mechanochemical coupling – Tight coupling? Loose coupling? Variable coupling? Variable step sizes?

My last question is a note-to-self about gearing in molecular motors. For kinesin, it is now reasonably clear that in most cases at least, steps are tightly coupled in a 1:1 relationship to ATP turnover. This is even clearer in the case of the F1 ATPase. For kinesin-1, expending 1 ATP molecule per 8 nm step means that processive stepping is energetically inefficient except at high loads. There have been reports that in more elaborate processive systems like myosin thick filaments, there exist mechanisms for changing gear. So far, there is no convincing evidence for this.

Conclusions

Processivity is useful both to cells and to experimentalists: mechanisms of processivity take the basal force-generating activity of a motor and overlays it or leverages it, so as to produce longer steps, prolonged contact, and a specified trajectory along the track. The central point is that one motor domain or head collaborates with and guides one or more others, specifying when and where the partner(s) bind and generate force. We can think of each collaborator within a processive system as having inputs and outputs - several channels of mechanical and chemical inputs, a stage of integration, and an output, or perhaps several outputs. The general problem is to understand the mechanisms by which the inputs are sensed and then processed into outputs. By focussing our attention on one motor domain within a processive system and asking how external influences modify its mechanochemical function, we can find out not only about mechanisms of processivity, but also about mechanisms of force generation.

How myosin motors work

James Spudich, Zev Bryant, Alex Dunn, Stirling Churchman, David Altman, Ben Spink, Jung-Chi Liao, David Parker, Scott Delp, Tom Purcell, Mike Stern, Shirley Sutton, and Hans Warrick. Department of Biochemistry and Department of Bioengineering, Stanford University, Stanford, CA 94305

The molecular basis of how myosin motors work has been significantly advanced over the last few years by a wide variety of studies from several different laboratories using myosin V. There is little doubt that this motor moves processively by stepping arm-over-arm, walking along the 36-nm pseudo-repeat of an actin filament, hydrolyzing one ATP per step, and using its six light chain long lever arm to provide a large stroke in its direction of movement. It is also clear that intramolecular tension sensing establishes a bias in the behavior of the two heads with regard to nucleotide kinetics that allow the rear head to most often release from the actin by binding ATP. This intramolecular tension sensing is important for unidirectional processive stepping of the myosin V motor and of processive motors in general [Spudich, J.A. (2006). Molecular motors take tension in stride. *Cell* 126:242-244] (Fig. 1).

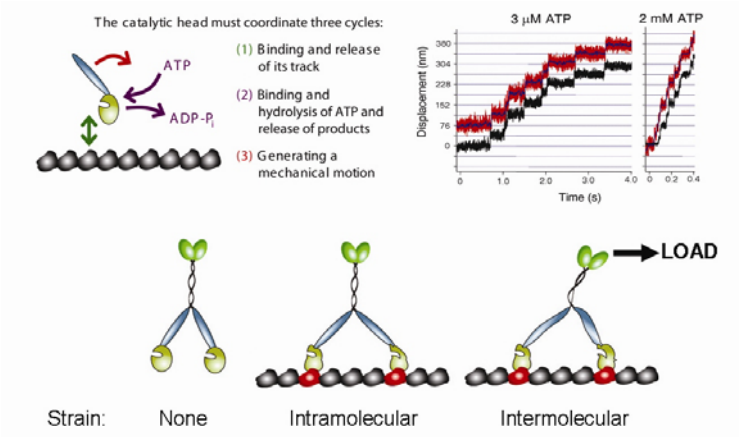

Figure 1. Coordinating molecular motor movement. (Top, left) Schematic diagram indicating the three cycles that molecular motors must coordinate. (Top, right) Single myosin V molecules stepping along an actin filament observed with an optical trap. The red steps are the displacement of a bead pulled by the myosin, and the black steps are the movements of the laser trap to allow a fixed and constant load. At 3 μM ATP under low load, ATP concentration is rate limiting, P_i and ADP have already exited the active site, and the motor's long dwell times reflect the on-rate of binding of ATP. The mean dwell time is ~0.36 s, and the second order on-rate constant for ATP binding is k_{on} = (1 step / 0.36 s) / 3 μM = ~0.9 $\mu M^{-1}s^{-1}$. In contrast, at saturating ATP (2 mM) the ADP release becomes rate limiting, and the observed mean dwell time is ~0.08 s indicating a first order off-rate constant for ADP of ~12 s^{-1}. [Data from Rief, M., Rock, R.S., Mehta, A.D., Mooseker, M.S., Cheney, R.E. and Spudich, J.A. (2000). Myosin-V stepping kinetics: A molecular model for processivity. *Proc Natl Acad Sci USA* 97:9482-9486]. (Bottom left) Schematic drawing of a homodimeric motor with its two heads in identical configuration and experiencing no tension. (Bottom middle) A motor walking along a polarized track with no external load and experiencing intramolecular tension causing the active site to be conformationally distorted in different ways for each head. Note that there are preferred binding sites of processive motors along their track, which results from the structures of both the motors and the track itself. This is very evident in the case of the actin filament, which has two right-handed long-pitch strands with a helical pseudo-repeat of ~36 nm. Myosins V and VI both prefer to step along this pseudo-repeat rather than undergo the necessary distortions to bind to other actin monomers. Such preferred binding sites are indicated schematically in red. (Bottom right) A motor walking to the left under a backward external load that distorts the motor domains in a different manner, leading to different changes in enzyme kinetics compared to those resulting from the intramolecular tension.

One limitation in further elucidation of the mechanism of myosin V movement is the need for higher time resolution for visualizing events associated with the very rapid transition that a rear head experiences as it releases from the actin and moves 72 nm forward before rebinding the filament. Alex Dunn is leading an effort to improve time resolution by tracking single gold nanoparticle-myosin V conjugates using darkfield imaging. A small (30-60 nm) gold particle is attached to one of the two lever arms of dimeric myosin V (Fig. 2).

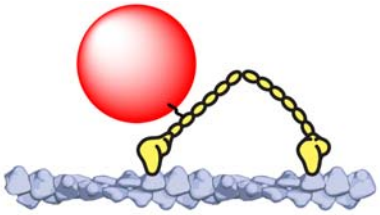

Figure 2

Gold nanoparticles scatter visible light extremely efficiently, making it possible to track their motion under darkfield imaging with sub-millisecond time resolution. In addition, the asymmetric attachment of the gold particle allows us to directly observe elements of the catalytic cycle that must be inferred from optical trapping experiments, which follow the myosin V center of mass. Data tracking gold nanoparticle-myosin V conjugates with high temporal resolution will be presented, as well as the mechanistic implications of our results.

A second limitation in further elucidation of the mechanism of myosin V movement is the need for better methods for visualizing single nucleotide molecules as they bind and release from the myosin five during its processive movement. The elegant experiments in 1998 from the laboratory of Toshio Yanagida [Ishijima, A., Kojima, H., Funatsu, T., Tokunaga, M., Higuchi, H., Tanaka, H., and Yanagida, T. (1998) Simultaneous observation of individual ATPase and mechanical events by a single myosin molecule during interaction with actin. *Cell* 92:161-171] remain the only such measurements to have been made. In order to visualize single nucleotide molecules, Ishijima et al. used total internal reflection fluorescence microscopy (TIRF) to limit the excitation volume of dye labeled nucleotides, and nucleotide concentration was reduced to sub-micromolar levels. An unacceptable background of fluorescence occurs at above a concentration of ~10-30 nM when using TIRF.

Stirling Churchman is leading an effort to develop a new approach for visualizing fluorescent nucleotide attaching and detaching from myosin V during its processive movement. We previously developed a technique allowing for the simultaneous co-localization of two chromatically differing fluorophores called single-molecule high resolution co-localization (SHREC). We employed SHREC to measure the end-to-end distances of dsDNA and to directly observe myosin V molecules walking hand-over-hand [Churchman, L.S., Ökten, Z., Rock, R.S., Dawson, J.F. and Spudich, J.A. (2005). Single molecule high-resolution colocalization of Cy3 and Cy5 attached to macromolecules measures intramolecular distances through time. *Proc Natl Acad Sci USA* 102:1419-1423]. We are adapting the SHREC technique to observe myosin V's nucleotide dynamics using dye-labeled ATP molecules. Circular zero-mode waveguides have been

used to increase nucleotide concentration to 7.5 μM to directly observe nucleotide incorporation by DNA polymerase [Levene, M.J., Korlach, J., Turner, S.W., Foquet, M. Craighead, H.G. and Webb, W.W. (2003). Zero-mode waveguides for single-molecule analysis at high concentrations. *Science* 299:682-686]. We are using linear zero-mode waveguides to study myosin V's mechanochemical cycle due to the long actin filaments necessary for the assay (Fig. 3). We have fabricated linear zero-mode waveguides with a range of widths and are characterizing them computationally and experimentally. Using ~ 50-nm wide linear zero-mode waveguides we have increased the working concentration of labeled ATP to greater than 1 μM. We have developed an experimental geometry that places actin filaments along the bottom of the linear zero-mode waveguides and allows myosin V molecules to be observed while walking processively along them.

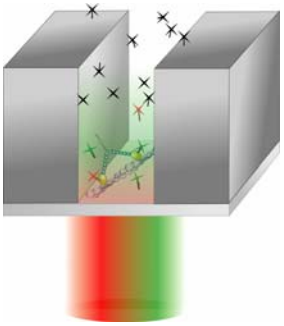

Figure 3.

In addition to the above studies, Jung-Chi Liao, David Parker, and Scott Delp are developing computational approaches to examine various aspects of myosin V as well as other myosin motors. Normal mode analysis of the myosin neck region, for example, is being examined. A novel computational algorithm has been developed that can predict dwell-time distributions of any complex kinetics and conduct global fitting for dwell-time distributions under various conditions. Using this new algorithm, we simulated the possible mechanochemical mechanism of one head of myosin V. By fitting the data of dwell-time distributions under different applied forces and nucleotide concentrations, we conclude that the power stroke does not occur simultaneously with the P_i release step nor the ADP release step. Our analysis suggests that the power stroke happens after the P_i release step and before the ADP release step.

While myosin V is proving to follow the basic tenets of a conventional tightly-coupled swinging cross bridge model, the fascinating myosin VI molecule has been full of surprises and challenges with regard to conventional thinking. The light chain binding domain of this motor is unusual in that it has only one IQ domain, and a second light chain is bound to a unique insert just beyond the converter domain. It's not clear how the unique insert might contribute to lever arm movement, but at best myosin VI appears to have a lever arm that is only two light chains long. Nevertheless, the molecule still steps processively 36 nm along an actin filament. Some of this discrepancy between lever arm length and step size is proving to be explained by an ~80-residue proximal tail domain that is highly flexible [Rock, R.S., Ramamurthy, B., Dunn, A.R., Beccafico, S., Rami, B.R., Morris, C., Spink, B.J., Franzini-Armstrong, C., Spudich, J.A., and Sweeney, H.L.

(2005). A flexible domain is essential for the large step size and processivity of myosin VI. *Molecular Cell* 17:603-609]. Ben Spink is leading an effort to understand the proximal tail domain in more detail. But the proximal tail domain can not explain everything. There must be a substantial stroke to bias the directionality of this highly diffusive motor. Indeed, we have shown that myosin VI has an unexpectedly large step size (at least 12 nm) given its structure [Rock, *et al*. (2005). *Mol Cell* 17:603-609].

Myosin VI moves in the opposite direction to that of myosin II and myosin V [Wells, A.L., Lin, A.W., Chen, L.Q., Safer, D., Cain, S.M., Hasson, T., Carragher, B.O., Milligan, R.A., and Sweeney, H.L. (1999). Myosin VI is an actin-based motor that moves backwards. *Nature* 401:505-508]. The unique insert stretch of amino acids inserted between the converter domain and the lever arm was proposed by Wells, *et al*. to provide the structural basis of directionality reversal. In support of this model, the unique insert mediates a ~120° redirection of the lever arm in the presumed post-stroke conformation of myosin VI crystallized by Anne Houdusse and coworkers [Menetrey, J., Bahloul, A., Wells, A.L., Yengo, C.M., Morris, C.A., Sweeney, H.L., and Houdusse, A. (2005). The structure of the myosin VI motor reveals the mechanism of directionality reversal. *Nature* 435:779-785]. However, this redirection alone is insufficient to account for the large (-) end directed stroke of a myosin VI S1 construct [Rock, *et al*. (2005). *Mol Cell* 17:603-609].

In a study led by Zev Bryant, we have elucidated a number of structural requirements that myosin VI must undergo as it transitions from its pre-stroke state to its post-stroke state. We are using the previous approaches that we applied to myosin II [Uyeda, T.Q.P., Abramson, P.D., and Spudich, J.A. (1996). The neck region of the myosin motor domain acts as a lever arm to generate movement. *Proc. Natl. Acad. Sci. USA 93*:4459-4464] and myosin V [Purcell, T.J., Morris, C., Spudich, J.A., and Sweeney, H.L. (2002). Role of the lever arm in the processive stepping of myosin V. *Proc Natl Acad Sci USA* 99:14159-14164] to map out motions in the molecule required to explain our in vitro motility and single molecule analyses. Thus, in order to map out the motion of the converter domain and lever arm, we have generated a series of truncated myosin VI constructs and characterized the size and direction of the power stroke for each construct using dual-labeled gliding filament assays and optical trapping. Motors truncated near the end of the converter domain generate (+) end directed motion, whereas longer constructs move toward the (-) end. Our results suggest that the lever arm rotates ~180° between pre- and post-stroke conformations, which accounts for the very large stroke size observed with this motor and provides for the needed large mechanical stroke to bias the directionality of the myosin VI movement that would be expected from conventional lever arm concepts.

Kinesin Motor Mechanics: Binding, Stepping, Tracking, Gating, Limping...and Some Newly Discovered Rotational States

Steven M. Block
Department of Biological Sciences and Department of Applied Physics
Stanford University, Stanford, CA 94305

In keeping with the spirit of a discussions meeting, I present here a personal perspective on the current state of kinesin motor mechanics. Nearly a generation has passed since the discovery of the motor named kinesin (Vale et al., 1985), and the subsequent development of the very first single-molecule gliding-filament and bead assays for motility (Howard et al., 1989; Block et al., 1990), which helped to establish the modern field of *single-molecule biophysics*. Discrete steps of single molecules were first measured for kinesin (Svoboda et al., 1993), followed shortly thereafter by reports of similar steps for myosin (Finer et al., 1994; Ishijima et al., 1994). Since then, literally thousands of single-molecule experiments have been performed on a whole variety of molecular motors, all with the aim of discovering how these remarkable protein machines function. Considerable progress has been achieved, but key questions still abound, and this remains a very lively field of endeavor. I discuss below my current thinking on several questions about kinesin mechanics, listed in no particular order of precedence. I hold no illusions that everyone will share my views on the answers to these questions, but I hope to provoke a more thoughtful examination, and set the record straight on at least a few points. By choice, and in keeping with the topic of this session, the questions that I've posed relate directly to the nanoscale mechanics of kinesin motion. However, these same questions are intimately and inevitably linked to other aspects of kinesin structure, biochemistry, and cellular function.

Does kinesin take sub-steps? If so, over what time and distance scales?

In our original paper describing single kinesin stepping, the steps were found to subtend a distance of 8 nm, and they took place instantaneously on the time scale of the experiment. Here, the data acquisition rate was 1 kHz (after anti-alias filtering at the Nyquist frequency, 0.5 kHz), and records were software-filtered to 200 Hz, for a characteristic time of 5 ms (Svoboda et al., 1993). Quite a number of models to explain kinesin motion have since been entertained which predict that the 8-nm step should be composed of substeps of one form or another. Substeps are by no means unreasonable to contemplate, for a variety of plausible reasons (see below).

Two papers have claimed to identify substeps within the kinesin cycle. I don't believe that either paper presented a sufficiently compelling case that substeps exist. In both instances, there appear to have been similar flaws in methodology. The first paper, a collaborative effort by Vale and Spudich (Coppin et al., 1996) reported the existence of a comparatively long-lived intermediate state during the forward step, lasting on the order of 10-20 ms, which separated the 8-nm step into two distinct components of 5- and 3-nm (with the 5-nm component being the most clearly resolved). However, the starting and ending points of the steps in data records were (*a*) scored entirely 'by eye' from (*b*) traces filtered with a 15-ms median filter. Under these circumstances, no statistically meaningful plateaus can exist whose characteristic times are comparable to that of the smoothing filter (15 ms). Although the data were sampled at 2 kHz, this did not mean that they were trust-

worthy at a data interval of 0.5 ms, because the bandwidth of the analog position signal was limited to 110 Hz, corresponding to a characteristic time of 9 ms. In retrospect, it seems likely that the ms-long plateaus seen in the noisy records were the consequence of a data selection artifact. Since 1996, the time resolution for the routine recording of kinesin stepping has steadily improved, particularly for smaller beads subjected to higher loads, where it now routinely achieves ~1 ms or better [see, for example, (Guydosh and Block, 2006)]. No group has ever duplicated these findings.

The second paper, the result of a collaborative effort by the Yanagida and Higuchi labs (Nishiyama et al., 2001), achieved substantially higher temporal resolution, and reported substeps lasting on the order of 50 μs, some 200-fold faster than those reported by (Coppin et al., 1996). Here again, though, the same two issues resurface, associated with (*a*) data sampling by selection and (*b*) a failure to assess the effects of instrument bandwidth. Because of the presence of noise, individual records of steps showed no clear evidence of substeps. However, a subset of records displayed small fluctuations (seen as plateaus) during their rising phase for a step: these records were separated from those that rose more smoothly (again, 'by eye') and placed in two further batches, with plateaus lasting either 50-100 μs or >100 μs, then separately averaged together. Such a selection procedure, followed by averaging, seems guaranteed to reinforce any random fluctuations (noise) that may have contributed to the plateaus, along with genuine signals (if any). The traces with apparent 50-100 μs plateaus seemed to divide the 8-nm step into two equal components of 4 nm. However, although data were acquired at 100 kHz using dark-field laser illumination onto a quadrant photodetector (QPD), signals had been passed through a 20 kHz analog low-pass filter before digitizing, so the characteristic response time of the measurements was 50 μs. This time is remarkable similar to their measurement of the average time constant for the abrupt rising phase of a step [Fig. 3 of (Nishiyama et al., 2001)], which came to 48 μs. It is not meaningful to extract timing information in the "10 μs range" when instrument response times are restricted to comparable intervals.

More recently, Cross's group has reinvestigated the question of kinesin substeps, and reported finding no evidence for these down to their experimental cut-off time, estimated to at approximately 30 μs (Carter and Cross, 2005). In their case, the measurement system, based on bright-field imaging onto a QPD, had a combined bandwidth of 46 kHz (~21 μs), but in most cases data were sampled at 80 kHz and averaged down to 20 kHz (~50 μs) for analysis. The effective bandwidth is therefore quite comparable to that of the instrument employed by the Yanagida and Higuchi group. However, steps were scored here by an automated algorithm, and not binned by eye into categories for subsequent averaging. My own group has also sought evidence of kinesin substeps. In unpublished work, we found no evidence for these with an instrument that uses back focal plane detection of scattered laser light onto a position-sensitive detector (PSD). Our photodetection subsystem has an analog bandwidth of ~200 kHz, but the computer data acquisition was limited to ~35 kHz, corresponding to a characteristic system response time of ~30 μs. We concur with (Carter and Cross, 2005) that no substeps can be found down to this response time, and steps are still instantaneous on the timescale of our measurements.

None of this is to say, however, that kinesin substeps don't exist! The Yanagida group has argued that the size of the 'characteristic distance', δ, for kinesin movement (Schnitzer et al., 2000), a parameter that can be derived from force velocity curves, *implies the existence of substeps*, given that its value is ~3 nm, which is only a fraction the full 8-nm step (Nishiyama et al., 2002). However, I do

not accept that argument as being decisive. As we have previously noted in (Wang et al., 1998), the physical interpretation of the characteristic distance, δ, is highly model-dependent, and several very different classes of biochemical pathways can lead to force-velocity relationships with a similar Boltzmann-type shape. In some of these pathways, the characteristic distance corresponds directly to a measurement of the step size (Abbondanzieri et al., 2005), but in others, it corresponds instead to the distance to a transition state, which is always less than the step size. It therefore seems possible that a value of $\delta \sim 3$ nm could be reconciled with either full-stepping or substepping pathways; additional evidence is required to decide the issue.

Could substeps be accommodated? Yes, provided these are exceedingly short-lived. An unloaded kinesin head can diffuse over 8 nm in a time of ~10 μs (based on approximating the head as a 10-nm diameter sphere diffusing in water through 8 nm, according to $\langle x^2 \rangle \approx 2Dt$). However, this first-passage time rises exponentially fast when the head is forced to move against a load of any size (Howard, 2001). If the actual kinesin step consists, for example, of (*a*) an initial conformational change followed by (*b*) a diffusional component that carries the head the remainder of the way to its next microtubule binding site, then it seems possible that evidence for substeps may be very difficult to discover, in practice. That difficulty would be exacerbated if the distance subtended by the conformational component constituted a comparatively small fraction of the overall step (say, ~2 nm, measured at the common stalk joining the heads) and the diffusional distance is larger.

What's the kinesin walking pattern ('waddle model'), and what do we learn about its mechanics from this?

At least four single-molecule experiments bear directly on this question (Hua et al., 2002; Asbury et al., 2003; Kaseda et al., 2003; Yildiz et al., 2004). The Gelles lab (Hua et al., 2002) found that the short kinesin stalk of a recombinant Drosophila construct (K448 with a C-terminal biotinylation site) was torsionally rigid, a finding that contrasted sharply with earlier measurements of the stalk from full-length bovine kinesin, which was found to be surprisingly flexible overall, permitting $k_B T$ of energy to twist the stalk by more than one full rotation (Hunt and Howard, 1993). The rigidity of the short recombinant stalk allowed them to track the rotational Brownian motion of microtubules moved by single kinesin molecules. That movement was found to be tightly bounded, and did not produce large angular motions of 180° or more during stepping motion. In their paper, Gelles and coworkers introduced important terminology for three different types of kinesin walk: *symmetric hand-over-hand* (where the two heads exchange leading and trailing positions on the microtubule, but the 3D structure of the kinesin molecule is preserved at all equivalent points in the step cycle), *asymmetric hand-over-hand* (where the kinesin heads exchange positions on the microtubule, but the initial and final states of the molecule are not symmetry-related, implying that alternate steps must differ in essential ways), and *inchworm* (where one head always leads and the other always trails during the cycle of advancement; all inchworm models are necessarily symmetric). The failure to observe large angular changes in the stalk ruled out the symmetric hand-over-hand (HoH) model, which would have produced 180° stalk rotations. The body of evidence was therefore interpreted as favoring the inchworm model. However, as Hua et al. were careful to point out, the asymmetric HoH model could not be ruled out altogether by their data, although it would place severe constraints on the ways in which the molecule might move between stepping states. They wrote: "*Thus, although our experimental results do not rigorously exclude an asymmetric hand-over-hand mecha-*

nism, we regard as improbable the existence of two structures that simultaneously satisfy all of the requirements outlined above."

The subsequent discovery of 'limping' in kinesin, where the average kinetics of *every other step* switch between a faster and a slower stepping phase, proved that kinesin dimers advance through an **asymmetric HoH** motion, and that this motion is inconsistent with either the inchworm or symmetric HoH patterns. This is because kinesin dimers were found to alternate between two distinct (identifiable) states with each step, precisely as required by the asymmetric HoH model, which alone breaks symmetry: no such alternation can exist in either the (symmetric) inchworm or symmetric HoH models. Limping kinesins were generated in two rather distinct ways, using recombinant constructs of *Drosophila* kinesin. Work by (Kaseda et al., 2003) produced *heterodimers* with one 'wild-type' head and the other head slowed by a mutation to the nucleotide binding pocket (R14A), which reduces the microtubule-stimulated ATPase rate by nearly 20-fold. Independent work by (Asbury et al., 2003) found that appropriate *homodimer* constructs of kinesin would also limp, provided that their stalk regions were sufficiently short. In fact, the degree of limping was found to be anti-correlated with the length of the stalk.

Reports of kinesin limping were very soon followed by some compelling experiments from Paul Selvin's group that followed the motion of an individual dimeric kinesin head labeled by a single fluorophore, using video centroid tracking accurate to nearly one nanometer (Yildiz et al., 2004). Kinesin heads (with labels on the heavy chain placed sufficiently close to the head domain) appeared to advance in a series of ~16 nm steps, a result consistent with HoH motion but inconsistent with inchworm motion, which would have produced ~8 nm steps instead. Importantly, however, and in contrast to the two earlier limping experiments, the centroid-tracking experiments *do not distinguish* between symmetric and asymmetric HoH motion; a fact that seems to have eluded more than one review writer. Modeling of biochemical kinetic results by (Schief et al., 2004) also supported HoH motions, as opposed to inchworming. Because the results of the Selvin lab support either symmetric or asymmetric HoH stepping models, whereas the results of the Gelles lab support either inchworm or asymmetric HoH models, the only stepping pattern consistent with both sets of results is asymmetric HoH motion. This, of course, is fully consistent with the two limping reports, which unambiguously indicated asymmetric HoH motion. All in all, the body of evidence in favor of the asymmetric HoH model is very compelling.

We still don't know what causes limping in homodimer constructs, but our experimental results suggest that it is unlikely to be simply an artifact of the linking geometry to the bead itself. Kinesin homodimers with short stalks limp whether bound to beads by streptavidin- or by antibody-based linkages. The degree of limping correlates with the length of the stalk and the value of the external load, and is most pronounced when the load is highest. This result is not consistent with some form of nonspecific interaction between one of the heads and the bead, an interaction that would be destabilized (and therefore diminished) at higher loads; this explanation therefore gives the wrong sign for the load-dependence. Moreover, if one head were to interact transiently with the bead for a significant portion of the cycle (as required for this explanation to hold), then the position of the bead would tend to report the position of a single head, rather than the centroid of the molecule (the stalk position), leading to alternating step sizes as well as step timing, contrary to observation. Dimers that are cross-linked by disulfide linkages between cysteines introduced into

the proximal dimerization domain at the base of the stalk continue to limp, suggesting that helix misregistration of the coiled-coil region cannot be responsible for the phenomenon (Block lab; *unpublished data*). However, there are several other candidate explanations that are currently under test, and some of these involve torsional effects of the heads with respect to the stalk.

Given the body of evidence in support of an asymmetric HoH stepping pattern, an obvious question arises as to how symmetry is actually broken for kinesin, which surely involves the microtubule itself. A corollary of the asymmetric HoH walk is that there must be *two intrinsically different kinds of steps* taken by kinesin molecules (call these a 'left' step and a 'right' step), and that these steps differ in both their trajectories (i.e., in the underlying molecular geometry) and also in their biochemical kinetics. Notwithstanding, the left and right kinesin steps are generated by head domains that are nominally identical in amino acid sequence (a least for homodimers), and the same head can generate either a left or a right step depending on its microenvironment. The consequences of this are far-reaching and profound, I believe.

How do the two kinesin heads manage to stay out of phase with one another during the stepping cycle (i.e., How are they 'gated')?

The temporal sequencing involved in stepping requires some form of communication between the heads to synchronize their biochemical cycles in precisely such a way as to maintain them out of phase, or else processivity would rapidly be lost. Furthermore, the evidence that kinesin's 8-nm step is tightly coupled to the hydrolysis of a single ATP molecule (Hua et al., 1997; Schnitzer and Block, 1997; Coy et al., 1999) also implies some form of coordination between the cycles of the two heads. In fact, kinetic data on single-headed motors support the notion that processivity derives from head coordination (Berliner et al., 1995; Hancock and Howard, 1998). The only realistic basis for such a gating mechanism would seem to be the mechanical strain that develops between heads during stepping itself. In principle, there are two plausible candidates for communicating this strain: through the regions joining the two kinesin heads, i.e., the neck linker regions and the common stalk, or from the heads through the microtubule protofilament. Of course, these are not mutually exclusive. Furthermore, whenever discussing the effects of strain on movement, one must remain mindful of the inherent reciprocity between the mechanics and the biochemistry: the load can affect the binding and hydrolysis, but binding and hydrolysis equally well affect the forces generated. These are intimately linked.

Broadly speaking, two general classes of gating mechanism have been entertained. In one (the so-called 'gated rear head' mechanism), the mechanical release of the trailing head from the microtubule leading head is accelerated by internal strain (Hancock and Howard, 1999). Experimental support for this picture comes from the work of (Crevel et al., 2004; Schief et al., 2004), who reported that strain accelerates the detachment rate of the rear head. In the other model (the so-called 'gated front head' mechanism), ATP binding to the leading head is suppressed through internal strain (Rosenfeld et al., 2003; Klumpp et al., 2004). Note that these are not mutually exclusive, either, so mixed models are feasible. Work on head unbinding forces by Ishiwata group has also helped to establish the notion that kinesin's affinity for nucleotide is dependent on the directionality of an external load, and the apparent K_D of a kinesin head for ADP is weakened up to sevenfold for rearwards versus forward load (Uemura and Ishiwata, 2003).

Additional evidence supporting a gated front head mechanism comes from recent work by (Guydosh and Block, 2006) on the effects of nucleotide analogs (AMP-PNP and ADP·BeF_x) on single-molecule motion driven by ATP. The addition of low concentrations of these non-hydrolyzable analogs causes stepping kinesin molecules to enter into long pauses, until the analogs can be released and ultimately exchanged for ATP. After a pause induced by an analog, it was discovered that processive stepping could only resume once the kinesin molecule took an obligatory, terminal *backstep*, exchanging the positions of its leading and trailing heads, which allows release of the bound analog from the (new) front head. Preferential release of the analog from the front head, as opposed to the rear head, implies that the kinetics of the two heads are *differentially affected* when both are bound to the microtubule. Kinesin, then, would seem to be the proverbial 'back seat driver,' where the passenger head in the rear directs the driver head in the front!

Where in the kinesin biochemical pathway is forward motion produced?

According to (Hancock and Howard, 1999), release of stored strain upon unbinding of the trailing head permits the leading head to power an 8-nm advance of the entire molecule. According to (Rice et al., 1999), ATP binding induces the docking of the neck linker on the leading head to produce motion of the partner head. My own group has found that the effective binding rate for ATP is load-dependent, which indicates that ATP binding, or a transition closely coupled to it, generates the forward step (Block et al., 2003). When taken together with other biochemical results, modeling of our data suggests that ATP binding is highly reversible and followed by some kind of conformational (and less reversible) change, leading to a mechanical step broadly consistent with the model of (Rice et al., 1999). The recent finding by (Guydosh and Block, 2006) that the duration of the terminal backstep before the resumption of forward movement (from a pause induced by a nucleotide analog) depends on ATP concentration strengthens the case for a mechanical step triggered by ATP binding, and further argues against the alternative picture that the release of strain permits a step.

Is the backstepping cycle a reversal of the forward cycle, and does kinesin generate ATP under super-stall loads that force it to move backwards?

Occasional backsteps have been reported since the very first studies of kinesin stepping under load (Svoboda and Block, 1994), and their relative frequency—but not necessarily their duration—clearly depends on the applied load, because (*trivially!*) the forward and backward single-molecule stepping frequencies must exactly balance at stall, when velocity drops to zero. Most often, backsteps are solitary, flanked by forward steps on either side in records of processive motion. The dependence of backstepping phenomena on ATP levels, and their interpretation, must be considered controversial for the present. The frequency of backstepping did not appear to be very dependent on [ATP] in the work of (Nishiyama et al., 2002), although the durations of backsteps were, and these findings were interpreted in terms of a biased Brownian ratchet model. The authors went so far as to suggest that the effective temperature of the motor protein would reach 834K (536°C), which seems preposterously high, especially in view of the fact that proteins cannot remain out of thermal equilibrium with their surrounding milieu for so much as a microsecond at a time, which is less than the time required to complete an 8-nm step by diffusion. Backstep rates were also reportedly independent of load, a result later confirmed by (Carter and Cross, 2005), who extended this result to the regime of larger, super-stall forces, which were discovered to induce processive

backstepping. Their recent experiments also found that the dwell times for both forward and backward steps decreased with increasing [ATP], suggesting that ATP binding is a requirement for both forward and backward stepping (but not necessarily its hydrolysis).

Is processive backstepping simply movement in reverse, and could ATP possibly be synthesized during load-induced, processive backstepping? Carter & Cross tend to think not, and they suggested that there "*is at present no evidence that backward stepping is coupled to ATP turnover.*" Hackney has pointed out that the product of the kinesin stall force (~7 pN) and step size (8 nm) is less than the energy that he estimated to be released during ATP hydrolysis at physiological ATP, P_i, and ADP levels (87 pN nm) (Hackney, 2005), so a stall is not an equilibrium state. He suggests that backsteps are therefore unlikely to represent a simple reversal of the kinesin pathway. However, it may be useful to examine more carefully the rearward motion of kinesin molecules at forces only slightly in excess of stall to see if the experimentally-observed behavior is truly incompatible with the energetics of ATP synthesis. One cautionary note: Fisher has pointed out that, unlike the relative *frequencies* of forward and rearward stepping, which may in principle be modulated by ATP concentration, the average *dwell times* for forward and rearward steps are generally coupled, and these must always rise or fall *together* with changing ATP levels (Fisher and Kim, 2005). The data in Fig. 5 of (Nishiyama et al., 2002) seem broadly consistent with this requirement (at first glance).

Conversely, when kinesin is sped up by an assisting force, is it going through its normal biochemical cycle or by some other pathway?

The original report that kinesin could be sped up by as much as three-fold beyond its normal unloaded velocity in response to external forward loads (Coppin et al., 1997) is no longer considered credible, and in retrospect seems likely to have been an artifact of experimental geometry (which may have allowed kinesin to release and 'skip' forward), and the manner in which loads were applied, which did not include force-clamped conditions. However, kinesin does speed up moderately under forward loads, and this is particularly true at for low ATP levels, below the apparent K_M for movement (Block et al., 2003; Carter and Cross, 2005). The speed-up under forward load is predicted by simple pathway models that invoke a single load-dependent transition with Boltzmann-type behavior (Block et al., 2003) and also by discrete-state stochastic models with 3D energy landscapes (Fisher and Kim, 2005).

If the application of forward load simply pulled the trailing head in front of the leading head and caused the neck linker to dock or undergo some other conformational change [one possible version of the Rice et al. 1999 scenario; see also (Carter and Cross, 2005)], then we might not expect to see any speed-up in velocity at limiting [ATP], which would disfavor this docking. This is food for thought.

When stepping processively, does kinesin spend most of its time in a two-heads bound state or a one-head bound state?

This is a very interesting and controversial question, and one that bears directly on mechanism. The many electron micrographic reconstructions that have been performed on kinesin and its relatives are not informative here, because they are not carried out under physiological conditions, especially with respect to the kinesin concentration. Biochemical experiments by Hackney argued that because the rear head of kinesin is competent to synthesize ATP, it must remain bound to the

microtubule for most of the kinetic cycle. The experiments of (Yildiz et al., 2004) which found 16-nm steps for a single labeled head of the stepping dimer also lend strong support to a two-heads-bound model, because otherwise they would likely have observed alternating steps of two different values that add up to 16 nm, instead. This is because if one head stays unbound during a significant fraction of the cycle time, it will not be located directly above its microtubule binding site, but instead at a position much closer to its partner head: this motion will produce a positional offset that will affect *every other* step. As discussed in (Yildiz et al., 2003; Yildiz et al., 2004), attaching the fluorophore dye to a position close to the common stalk can also introduce an offset leading to alternation in the apparent step size: this is a similar geometric phenomenon. Head detachment experiments performed by the Ishiwata group, however, suggest that only a single head may be bound while kinesin is in the ADP nucleotide state (Uemura et al., 2002). The addition of AMP-PNP (assumed to act as an ATP analog) forces kinesin into a state characterized by twice the unbinding force and twice the elastic modulus (Kawaguchi and Ishiwata, 2001). However, it seems possible that one head may be weakly bound while the other is strongly bound; nevertheless, both heads remain attached to their microtubule binding sites through most of the cycle under normal stepping conditions. The recent model advanced by (Carter and Cross, 2005), however, has kinesin bound instead by a single 'holdfast' head, while its partner head remains predominantly unloaded and is free to explore the energy landscape via diffusion. This picture was supported by their observation that there was little change found in the positional variance throughout the stepping cycle (although there are several alternative explanations for this that are consistent with two heads bound). On its face, though, the current (Carter and Cross, 2005) model is not easily reconciled with the data of (Yildiz et al., 2004). So what's bound: one head, or both? Could it be that only one head is tightly bound while its partner remains loosely bound throughout most of the cycle?

Is the head-neck linker docking model correct (and does it suffice to explain actual stepping)? Does kinesin undertake a conformational 'power stroke', or something like it (and if so, how large is it)?

The neck linker docking model of (Rice et al., 1999) was developed on the basis of structural and EPR data obtained with kinesin monomers, and it successfully explains a great deal about kinesin's structural states on microtubules in the ADP- and ATP-bound states (as implied by nucleotide analogs intended to mimic these states). A largely qualitative model for the stepping cycle of the kinesin dimer was developed directly from these data. Critical analysis of the neck-linker docking model can be found in a review by (Schief and Howard, 2001). Two of the more salient criticisms, which I and others have also discussed (Block, 1998), are these. First, the kinesin neck linker region is only ~11-13 amino acids long, and is therefore is unlikely to generate a physical displacement of even so much as 2 nm (depending on the shape of the polypeptide chain), which compares rather unfavorably with the size of the kinesin step at 8 nm. This shortfall is all the more dramatic when one considers that the asymmetric HoH model requires that each head domain move through 16 nm to produce the 8-nm molecular step, during which only one of the two neck linkers becomes docked. A second criticism arises from subsequent work by (Rice et al., 2003) that estimated the free energy associated with neck-linker docking, and found it to be just ~3 kJ/mol (note that k_BT is 2.6 kJ/mol), which is very weakly favorable from a thermodynamic perspective, and represents only a minute fraction (~5%) of the free energy released through ATP hydrolysis (50-60 kJ/mol, or ~20 k_BT). Kinesin is known to be at least 50% efficient (Block, 1995), so this is an unsatisfactory re-

sult. Further free energy may be recovered during the complete kinesin cycle via other energy-release mechanisms, in principle, notably through microtubule binding, but it seems implausible that kinesin could move in any sustained way against ~6 pN loads (as it does) when that would require (2 nm × 6 pN) = 12 pN nm (~3 k_BT) of free energy per step from the docking component. Hackney has argued, on the basis of a series of oxygen isotope exchange experiments (Hackney, 2005), that the free energy released during the ATP binding step for a kinesin head on a microtubule is substantially larger than k_BT, at ~34 kJ/mol (13 k_BT); he attributed the low energy values obtained by Rice et al. to their use of AMP-PNP, a nonhydrolyzable analog, instead of ATP. However, these purely energetic considerations do not establish whether any of the free energy released may actually be communicated to the neck linker region through docking, or power other changes. The issue remains open.

Because (Carter and Cross, 2005) found that ATP was required for load-induced backsteps, they proposed that rearward steps may involve some sort of head *undocking*, in which case ATP may actually serve to undock the neck linker, that is, exactly contrary to the original proposal of (Rice et al., 1999). An alternative explanation, based on the findings of (Guydosh and Block, 2006), would be that the neck linker is unable to dock when the leading head is strained, either through the application of external load or through the internal strain created by an attached trailing head.

The Yanagida group has advocated an entirely Brownian-ratchet based mechanism, where entropy rectifies the kinesin steps (Taniguchi et al., 2005). Based on measurements of the temperature-dependence of forward and rearward stepping rates, they found that the binding of the 'free' head in the leading position (for a forward step) was entropically favored over binding to the trailing position (for a backward step) by approximately 4 k_BT. Added to the approximately 1-2 k_BT thought to represent neck-linker docking (but recall the *caveats* above), this could provide roughly 6 k_BT of energetic bias to power asymmetric, unidirectional motion.

Higuchi's group has reported one controversial experiment that purported to measure the displacement associated with power-generating portion of the kinesin cycle (Kamei et al., 2005), by scoring the binding displacement towards the microtubule plus-end for beads coated with monomeric kinesin. In this fashion, they obtained an apparent 'stroke size' of 3.5 nm, which they associated with the kinesin head. Unfortunately, however, their results cannot be considered definitive, because they may equally well be interpreted as arising from a binding artifact, coming from the changing experimental geometry during the binding event, which can induce a small movement of a kinesin-attached bead that depends on the radius of the bead, the length of the kinesin stalk, etc.. To address this alternative explanation, it would be necessary to show that the 3.5 nm displacement was robust, and independent of bead size and kinesin length. Furthermore, their results (if not a binding artifact) are more consistent with the 'step' being coupled to ADP release than to ATP binding, which seems troubling.

So, does kinesin move by a power stroke or by a Brownian ratchet mechanism?!

The answer is, "Yes!" ☺ It's important to realize that these two mechanisms are not mutually exclusive, so this question poses a *false dichotomy*. Furthermore, reaction pathways, particularly those that pass through one or more energetically unfavorable transition states on their way to an energetically favored minimum—and that constitutes the vast majority of all enzymatic reactions—

require additional energy which they transiently 'borrow' from the thermal bath in order to proceed at a finite rate, according to the usual Kramer/Eyring/Arrhenius rate picture. So, in a narrow sense, an awful lot of biochemical reactions might reasonably be construed as "Brownian ratchets." One therefore has to be exceedingly careful about definitions when discussing these candidate mechanisms. Given kinesin's small head size and large step size, I and others pointed out early on (Block, 1995) that diffusion was likely to play a significant role in transporting a head from one microtubule binding site to the next. A better question to ask, then, might be this: "What fraction of the overall kinesin step distance is associated with energetically-favored conformational motions (i.e., power strokes or similar) and what fraction is associated mainly with diffusion (i.e., Brownian movement, facilitated or otherwise)." Even here, the purists will cheerfully point out that any distinctions between these things are not as clear-cut as one might hope. If the kinesin head is displaced by some combination of thermal energy and elastic energy release (where the source of the latter can be entropic or electrostatic), which lead to a change in its shape as well as to a change in its position and/or orientation, does this qualify as a "thermal motion" or a "conformational change?" Technically, it's both, and we're once again faced with a false dichotomy.

How does kinesin manage to track parallel to a single protofilament of the microtubule?

No one really knows. There is excellent, longstanding evidence that kinesin tracks closely along a path parallel to that of a single protofilament (Kuo et al., 1991; Ray et al., 1993), and even kinesin dimers subjected to sideways loads continue to track faithfully along protofilament paths (Block et al., 2003). Furthermore, we now know that kinesin moves hand-over-hand as it does so. However, these experiments do *not* establish whether kinesin moves along a single protofilament or whether it moves astride two adjacent protofilaments (Block and Svoboda, 1995; Cross, 1995; Block, 1998). Recently, (Yajima and Cross, 2005), using marked microtubules where axial rotation could be scored, reported that a torsional component of motion was imparted by kinesin monomers functioning in a multi-motor, gliding-filament assay. They presented a model where free kinesin head tends to diffuse and bind to the most proximal microtubule binding site; however, to explain their data, they needed to invoke some additional tilting or conformational shift to explained sustained counterclockwise rotation. However, because the relationship between monomer and dimer stepping remains unknown, it is still unclear what all this means with respect to protofilament tracking by the dimer, which could still move along a single protofilament or sit astride a pair of these.

Are there any unusual observations to consider that bear on kinesin walking?

Yes! My lab has been tracking the thermally-driven angular positions of the kinesin stalk when individual dimers are bound to microtubules under a variety of conditions. These positions are reported by fluorescently-marked beads attached to the end of the stalk. To our surprise, we find that the stalk can adopt a series of *discrete rotational states* that slowly evolve and interconvert over time, with very interesting dynamics. I hope that the time allotted to my presentation will permit me to share some of these new data with you, as well as to touch on the other important questions considered here.

Is there any hope for eventual agreement?

All the current difficulties aside, a consensus model may possibly be emerging, if only in fits and starts. Put another way, there are several variations on a theme that are now being played, albeit with a certain dissonance and counterpoint, and that theme goes, more or less, as follows:

1) The binding of ATP to the front kinesin head in a microtubule-bound dimer releases significant energy.
2) That energetic release drives some form of conformational change, with neck linker docking representing the leading candidate for such a change. This change results in a mainly plus-end directed motion of the rear partner head through a comparatively small displacement, perhaps just 1-2 nm or thereabouts.
3) From this state, the unbound partner head, which has ADP on it, undertakes a biased diffusional search for its next forward binding site on the microtubule (with a finite probability of reaching a rearward binding site instead).
4) The heads have now swapped their relative positions, and in so doing, the centroid of the molecule has advanced by 8.2 nm along the microtubule, the tubulin dimer repeat distance. The previous two steps are both completed very rapidly, in a time less than ~100 μs.
5) After the partner head has reached its forward binding site, ADP is released (leaving an empty site) and this new front head binds tightly to the microtubule, thereby leading to internal strain (perhaps communicated through the neck regions, or perhaps through the microtubule). This strain tends to suppress the premature binding of ATP to the front head until the rear head had a chance to hydrolyze its own ATP and release phosphate. (Binding to the forward site may also induce additional conformations, including the possibility of motions that are not strictly parallel to the microtubule long axis.)
6) Following phosphate release from the rear head (above), strain is relieved. This allows the empty front head to rebind ATP for the next step.
7) As a consequence of all of the above, the mechanochemistry of the front and rear heads of kinesin is intrinsically different, with heads swapping roles at each step, maintaining their biochemical cycles out of phase. All in all, kinesin motion is tightly coupled to ATP hydrolysis, with 1 ATP consumed per 8-nm step, which arises from the strict alternation of the two heads moving in an asymmetric, hand-over-hand fashion.

Epilogue: In light of all the uncertainty associated with the foregoing discussion, and the limited extent of our present knowledge, it continues to astonish me how often my colleagues have seemed ready to declare victory based on their latest insight, experimental discovery, or model, only to be humbled—or at least transiently silenced!—by the next set of experiments to be published. A great deal more remains to be discovered about motor proteins. Nature is vastly more subtle, and generally smarter, than we tend to give her credit for being.

ACKNOWLEDGEMENTS

I'm very grateful to Adrian Fehr, Braulio Gutierrez, and Nicholas Guydosh of the Block Lab for their discussions and comments on this manuscript. My work was supported, until recently, by a grant from the NIGMS.

REFERENCES

Abbondanzieri, E. A., Greenleaf, W. J., Shaevitz, J. W., Landick, R., and Block, S. M. (2005). Direct observation of base-pair stepping by RNA polymerase. ***Nature*** **438**: 460-465.

Asbury, C. L., Fehr, A. N., and Block, S. M. (2003). Kinesin moves by an asymmetric hand-over-hand mechanism. ***Science*** **302**: 2130-2134.

Berliner, E., Young, E. C., Anderson, K., Mahtani, H. K., and Gelles, J. (1995). Failure of a single-headed kinesin to track parallel to microtubule protofilaments. ***Nature*** **373**: 718-721.

Block, S. M. (1995). Nanometres and piconewtons: the macromolecular mechanics of kinesin. ***Trends Cell Biol*** **5**: 169-175.

Block, S. M. (1998). Kinesin: what gives? ***Cell*** **93**: 5-8.

Block, S. M., Asbury, C. L., Shaevitz, J. W., and Lang, M. J. (2003). Probing the kinesin reaction cycle with a 2D optical force clamp. ***Proc Natl Acad Sci U S A*** **100**: 2351-2356.

Block, S. M., Goldstein, L. S., and Schnapp, B. J. (1990). Bead movement by single kinesin molecules studied with optical tweezers. ***Nature*** **348**: 348-352.

Block, S. M., and Svoboda, K. (1995). Analysis of high resolution recordings of motor movement. ***Biophys J*** **68**: 2305S-2395S; discussion 2395S-2415S.

Carter, N. J., and Cross, R. A. (2005). Mechanics of the kinesin step. ***Nature*** **435**: 308-312.

Coppin, C. M., Finer, J. T., Spudich, J. A., and Vale, R. D. (1996). Detection of sub-8-nm movements of kinesin by high-resolution optical-trap microscopy. ***Proc Natl Acad Sci U S A*** **93**: 1913-1917.

Coppin, C. M., Pierce, D. W., Hsu, L., and Vale, R. D. (1997). The load dependence of kinesin's mechanical cycle. ***Proc Natl Acad Sci U S A*** **94**: 8539-8544.

Coy, D. L., Wagenbach, M., and Howard, J. (1999). Kinesin takes one 8-nm step for each ATP that it hydrolyzes. ***J Biol Chem*** **274**: 3667-3671.

Crevel, I. M., Nyitrai, M., Alonso, M. C., Weiss, S., Geeves, M. A., and Cross, R. A. (2004). What kinesin does at roadblocks: the coordination mechanism for molecular walking. ***Embo J*** **23**: 23-32.

Cross, R. A. (1995). On the hand-over-hand footsteps of kinesin heads. ***J Muscle Res Cell Motil*** **16**: 91-94.

Finer, J. T., Simmons, R. M., and Spudich, J. A. (1994). Single myosin molecule mechanics: piconewton forces and nanometre steps. ***Nature*** **368**: 113-119.

Fisher, M. E., and Kim, Y. C. (2005). Kinesin crouches to sprint but resists pushing. ***Proc Natl Acad Sci U S A*** **102**: 16209-16214.

Guydosh, N. R., and Block, S. M. (2006). Backsteps induced by nucleotide analogs suggest the front head of kinesin is gated by strain. ***Proc Natl Acad Sci U S A*** **103**: 8054-8059.

Hackney, D. D. (2005). The tethered motor domain of a kinesin-microtubule complex catalyzes reversible synthesis of bound ATP. ***Proc Natl Acad Sci U S A*** **102**: 18338-18343.

Hancock, W. O., and Howard, J. (1998). Processivity of the motor protein kinesin requires two heads. ***J Cell Biol*** **140**: 1395-1405.

Hancock, W. O., and Howard, J. (1999). Kinesin's processivity results from mechanical and chemical coordination between the ATP hydrolysis cycles of the two motor domains. ***Proc Natl Acad Sci U S A*** **96**: 13147-13152.

Howard, J. (2001). Mechanics of Motor Proteins and the Cytoskeleton (Sunderland, MA: Sinauer Associates).

Howard, J., Hudspeth, A. J., and Vale, R. D. (1989). Movement of microtubules by single kinesin molecules. ***Nature*** **342**: 154-158.

Hua, W., Chung, J., and Gelles, J. (2002). Distinguishing inchworm and hand-over-hand processive kinesin movement by neck rotation measurements. ***Science*** **295**: 844-848.

Hua, W., Young, E. C., Fleming, M. L., and Gelles, J. (1997). Coupling of kinesin steps to ATP hydrolysis. ***Nature*** **388**: 390-393.

Hunt, A. J., and Howard, J. (1993). Kinesin swivels to permit microtubule movement in any direction. ***Proc Natl Acad Sci U S A*** **90**: 11653-11657.

Ishijima, A., Harada, Y., Kojima, H., Funatsu, T., Higuchi, H., and Yanagida, T. (1994). Single-molecule analysis of the actomyosin motor using nano-manipulation. ***Biochem Biophys Res Commun*** **199**: 1057-1063.

Kamei, T., Kakuta, S., and Higuchi, H. (2005). Biased binding of single molecules and continuous movement of multiple molecules of truncated single-headed kinesin. ***Biophys J*** **88**: 2068-2077.

Kaseda, K., Higuchi, H., and Hirose, K. (2003). Alternate fast and slow stepping of a heterodimeric kinesin molecule. ***Nat Cell Biol*** **5**: 1079-1082.

Kawaguchi, K., and Ishiwata, S. (2001). Nucleotide-dependent single- to double-headed binding of kinesin. ***Science*** **291**: 667-669.

Klumpp, L. M., Hoenger, A., and Gilbert, S. P. (2004). Kinesin's second step. ***Proc Natl Acad Sci U S A*** **101**: 3444-3449.

Kuo, S. C., Gelles, J., Steuer, E., and Sheetz, M. P. (1991). A model for kinesin movement from nanometer-level movements of kinesin and cytoplasmic dynein and force measurements. ***J Cell Sci Suppl*** **14**: 135-138.

Nishiyama, M., Higuchi, H., and Yanagida, T. (2002). Chemomechanical coupling of the forward and backward steps of single kinesin molecules. ***Nat Cell Biol*** **4**: 790-797.

Nishiyama, M., Muto, E., Inoue, Y., Yanagida, T., and Higuchi, H. (2001). Substeps within the 8-nm step of the ATPase cycle of single kinesin molecules. ***Nat Cell Biol*** **3**: 425-428.

Ray, S., Meyhofer, E., Milligan, R. A., and Howard, J. (1993). Kinesin follows the microtubule's protofilament axis. ***J Cell Biol*** **121**: 1083-1093.

Rice, S., Cui, Y., Sindelar, C., Naber, N., Matuska, M., Vale, R., and Cooke, R. (2003). Thermodynamic properties of the kinesin neck-region docking to the catalytic core. ***Biophys J*** **84**: 1844-1854.

Rice, S., Lin, A. W., Safer, D., Hart, C. L., Naber, N., Carragher, B. O., Cain, S. M., Pechatnikova, E., Wilson-Kubalek, E. M., Whittaker, M., *et al.* (1999). A structural change in the kinesin motor protein that drives motility. ***Nature*** **402**: 778-784.

Rosenfeld, S. S., Fordyce, P. M., Jefferson, G. M., King, P. H., and Block, S. M. (2003). Stepping and stretching. How kinesin uses internal strain to walk processively. ***J Biol Chem*** **278**: 18550-18556.

Schief, W. R., Clark, R. H., Crevenna, A. H., and Howard, J. (2004). Inhibition of kinesin motility by ADP and phosphate supports a hand-over-hand mechanism. ***Proc Natl Acad Sci U S A*** **101**: 1183-1188.

Schief, W. R., and Howard, J. (2001). Conformational changes during kinesin motility. ***Curr Opin Cell Biol*** **13**: 19-28.

Schnitzer, M. J., and Block, S. M. (1997). Kinesin hydrolyses one ATP per 8-nm step. ***Nature*** **388**: 386-390.

Schnitzer, M. J., Visscher, K., and Block, S. M. (2000). Force production by single kinesin motors. ***Nat Cell Biol*** **2**: 718-723.

Svoboda, K., and Block, S. M. (1994). Force and velocity measured for single kinesin molecules. ***Cell*** **77**: 773-784.

Svoboda, K., Schmidt, C. F., Schnapp, B. J., and Block, S. M. (1993). Direct observation of kinesin stepping by optical trapping interferometry. ***Nature*** **365**: 721-727.

Taniguchi, Y., Nishiyama, M., Ishii, Y., and Yanagida, T. (2005). Entropy rectifies the Brownian steps of kinesin. ***Nat Chem Biol*** **1**: 342-347.

Uemura, S., and Ishiwata, S. (2003). Loading direction regulates the affinity of ADP for kinesin. ***Nat Struct Biol*** **10**: 308-311.

Uemura, S., Kawaguchi, K., Yajima, J., Edamatsu, M., Toyoshima, Y. Y., and Ishiwata, S. (2002). Kinesin-microtubule binding depends on both nucleotide state and loading direction. ***Proc Natl Acad Sci U S A* 99**: 5977-5981.

Vale, R. D., Reese, T. S., and Sheetz, M. P. (1985). Identification of a novel force-generating protein, kinesin, involved in microtubule-based motility. ***Cell* 42**: 39-50.

Wang, M. D., Schnitzer, M. J., Yin, H., Landick, R., Gelles, J., and Block, S. M. (1998). Force and velocity measured for single molecules of RNA polymerase. ***Science* 282**: 902-907.

Yajima, J., and Cross, R. A. (2005). A torque component in the kinesin-1 power stroke. ***Nat Chem Biol* 1**: 338-341.

Yildiz, A., Forkey, J. N., McKinney, S. A., Ha, T., Goldman, Y. E., and Selvin, P. R. (2003). Myosin V walks hand-over-hand: single fluorophore imaging with 1.5-nm localization. ***Science* 300**: 2061-2065.

Yildiz, A., Tomishige, M., Vale, R. D., and Selvin, P. R. (2004). Kinesin walks hand-over-hand. ***Science* 303**: 676-678.

Step size and force generated by axonemal and cytoplasmic dynein

Hideo Higuchi*, Shiori Toba$, Tomonobu Watanabe* and Yoko Yano-Toyoshima#

* Biomedical and Engineering Research Organization, Tohoku university, Sendai, Japan
$ Kansai Advanced Research Center, National Institute of Information and Communications Technology, Kobe, Japan
# Department of Life Sciences, Graduate School of Arts and Sciences, University of Tokyo, Tokyo, Japan.

Summary

Structural differences between dynein and kinesin suggest a unique molecular mechanism of dynein motility. Measuring the mechanical properties of single molecule of dynein is crucial to reveal the mechanisms underlying its movement. In this study the step size and force produced by single molecules of axomemal 22S and cytoplasmic dyneins were measured using an optical trap and fluorescence imaging with a high temporal resolution. A single molecule of 22S dynein moved processively only at low concentrations of ATP (<20 μM), while cytoplasmic dynein exhibited processive movement at low and high ATP concentrations. The maximum force of both dyneins was 5-8 pN. Dynein exhibited forward and the occasional backward step of ~8 nm, that were independent of load. Visualization of dynein by negative stain electron microscopy shows that the ring domains partially overlap. This indicates that the large dynein heads take 16-nm steps using an overlapping hand-over-hand mechanism, while the dynein molecule takes steps of 8 nm.

Introduction

Axonemal dynein was the first microtubule motor protein to be discovered and functions as a molecular engine for the movement of cilia and flagella (1). Axonemal dynein constitutes the outer and inner arms of axonemes in cilia and flagella., Multiple forms (monomer, dimer, and trimer) of dyneins have been isolated from axonemes, even in a single species. More than 20 years after the first discovery of axonemal dynein (1), cytoplasmic dynein, a homodimer was identified (2) and found to be involved in the transport of organelles, in spindle assembly and chromosome segregation (3-7). Dynein transports cellular organelles toward the minus end of microtubules, whereas most kinesin molecules transport organelles toward the plus end. Both axonemal and cytoplasmic dynein consist of multiple subunits referred to as heavy chains (>500 kDa), intermediate chains (60–150 kDa), and light chains (<50 kDa). Each dynein heavy chain contains four conserved ATP (or ADP) binding sites, P1–P4. The P1 site is thought to be the major ATP catalytic site, but the functions of the P2-P4 sites are still unknown (8).

Systems with very high resolution have been developed to enable various aspects of theforce generation process by individual motor proteins to be observed. In this study we have summarized the force and step size measurements of dynein from our previous work (9, 10), report on recent advances and discuss several problems related to dynein.

Materials and Methods

Preparation of the dynein bead

Three headed 22S dynein was purified from *Tetrahymena thermophila* cilia (9). Fluorescent latex beads (1.0 μm in diameter) in buffer A (10 mM Tris-acetate, pH 7.5, 50 mM K-acetate, 4 mM $MgSO_4$, 1 mM EGTA,1 mM DTT) were incubated with various concentrations of 22S dynein on ice for 2 min and then a BSA solution (0.5 mg/ml after the mixing) was added (9).

Cytoplasmic dynein was purified from porcine brain and stored in liquid nitrogen (10). Just before the experiment, dynein was further purified by the binding to and releasing from the microtubules.

Polystyrene beads of 0.2 μm in diameter were coated with 1.4 mg/ml protein A for 30 min in solution B containing 10 mM Pipes, 25 mM K-acetate, 4 mM $MgSO_4$, and 1 mM EGTA (pH 7.0). The bead were then mixed in solution B containing 3 mg/ml BSA and 0.2 M KCl for 10 min. KCl prevents the beads from aggregating (10).

Bead Motility Assay.
Dynein-coated beads were trapped, and their positions were measured using an optical trapping system (9, 10). Experiments were performed in buffer A for axonemal 22S dynein and in solution B for cytoplasmic dynein containing an oxygen scavenging system at 25–27°C.

Quantum Dot Fluorescence Imaging with 1-nm Accuracy.
Quantum dots, the CdSe particles were cross-linked with protein-A by EDC and then mixed with cytoplasmic dynein (10). Dynein–CdSe complexes were observed under a fluorescence microscope (IX-71; Olympus) using evanescent illumination from a green laser. Fluorescence images were captured using a cooled electron multiplier–charge-coupled device (Ixon DV860; Andor Technology) at 2-ms intervals. The centroid of the bead in the images was determined by fitting the images to 2D Gaussian curves. Less than 10% of these complexes interacted with the microtubules, indicating that each complex binds with a single dynein molecule. The experiments were performed at 16°C.

Results

Demonstration of Bead Movement by Single Dynein Molecules.
To determine whether single molecules of dynein can move a bead processively, we prepared dynein-coated beads at various molar ratios of dynein to beads were prepared at the time of mixing and the beads were examined moving in the presence of ATP. The curve fits are given by $1 - \exp(-r/A)$ for the heads that were bound to the beads, where r is the molar ratio of dynein to a bead at the time of mixing and A is constant. The fractions of beads that bound to microtubules in the absence of ATP for axonemal 22S dynein and in the presence of 1 mM AMP-PNP for cytoplasmic dynein was almost the same as the fractions that moved processively in the presence of ATP. Dynein bound tightly to the microtubule in these conditions. This finding also provides support for the conclusion that single molecules move processively (11).

Force and step size of ciliary 22S dynein.
Fig. 1*a* shows a typical example of a time course of bead displacement driven by a single 22S dynein molecule at 3 μM ATP. As the ATP concentration increased, the pattern of bead displacement changed. At 10 μM ATP, the beads detached from the microtubules and were pulled back to the center of the trap before reaching a steady state force and the profile of the movement was then truncated (stopped??). At 20 μM ATP, the beads bound to the microtubules without any clear displacements where the travel distance was <40 nm. The velocity at low forces in the presence of 3 μM ATP was ~300 nm/s. The maximum force of 22S dynein measured from the maximal level of the displacement where the bead stayed for more than 0.2 s at ATP concentrations of 3 μM was 4.7 +- 0.6 pN (mean +- SD).

During force development, dynein molecules showed a stepwise displacement of 8 nm from 0.4 pN to the maximum force and frequently exhibited backward steps of ~8 nm (Fig. 1b). The ratio of backward steps to forward steps was ~20% and ~40% at forces of 1 and 4 pN. The results showed that the backward steps occurred more frequently at higher loads.

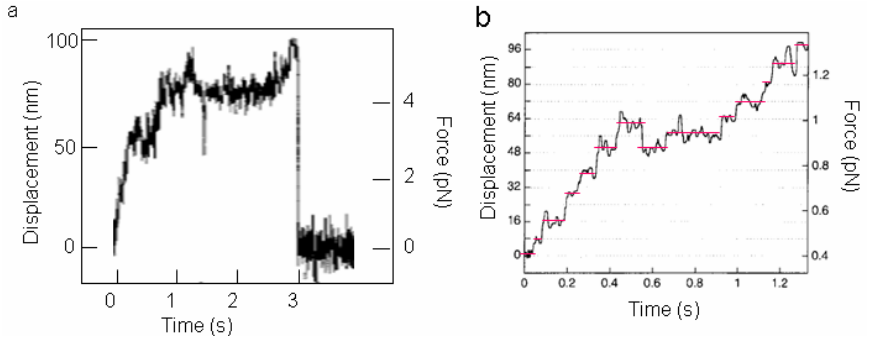

Fig 1. Time course of the displacement of a 22S dynein-coated bead in the presence of 3 μMATP. (a) Processive movement. (*b*) 8 nm steps. The figure is modified from the figure in reference 9.

Force and step size of cytoplasmic dynein

Single molecules of dynein moved processively and produced forces up to 7–8 pN in the presence of 1 mM ATP (Fig. 2*a*). However, when the beads were not coated with the protein low forces and velocities were often observed which were similar to those reported in a previous study (Fig. 2b). This result suggests that the presence of protein A is important for keeping dynein active.

The velocity at low forces and high ATP concentrations of ~800 nm/s is consistent with that observed in cells and *in vitro* assays (0.5–1.5 μm/s). At low ATP concentrations (10 μM), the velocity decreased and the stall force of ~7 pN was independent of the ATP concentration.

Single molecules of cytoplasmic dynein moved stepwise. Steps of 8 nm could be clearly detected in the expanded traces (Fig. 2*a*). Steps of 8 nm were observed even at zero forces. Backward 8-nm steps were also occasionally detected. The step size of 8 nm was independent of force over the range 0 to 7 pN and at ATP concentrations over the range 10 μM to 1 mM.

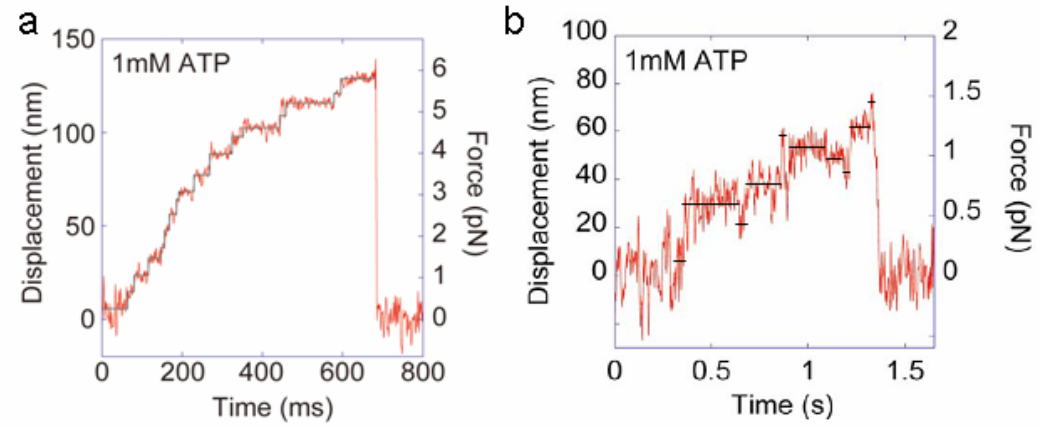

Fig 2. Stepwise movement of a single molecule of cytoplasmic dynein at a high concentration of ATP (1mM). (a) Force generation by dynein with the protein-A coating on the beads. The mixing ratio of dynein to bead is 40 :1 (b) Dynein was bound directly to beads without a coating of protein-A and then casein was added to block the bead surface. The mixing ratio of dynein to bead is very high, 300 :1. These figures are modified from the figures in reference 10.

Cytoplasmic dynein-quantum dots moved by 8-nm steps along the microtubules (Fig 3a). The positions parallel and perpendicular to the microtubule axis versus time were plotted (Fig 3b). The quantum dots traveled over ~100 nm along the microtubule axis over a period of one second (Fig. 3a).

In the perpendicular movement, the positions distributed in one envelope. The perpendicular diffusion of quantum dot was within ~20 nm (Fig 3b). The diagram illustrates a quantum dot linked to a microtubule via cytoplasmic dynein. If the dynein moves from one protofilament to another, the center of the distribution shifted ~50 nm (Fig 3c). This suggests that the diffusion along the perpendicular axis was restricted to a single microtubule protofilament.

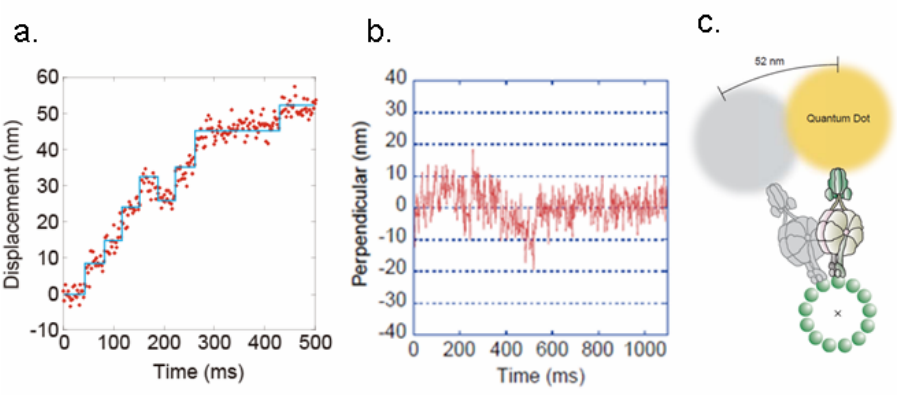

Fig 3. Parallel and perpendicular displacement of cytoplasmic dynein labeled with quantum dots. (a) Parallel displacement versus time plots of a dynein-quantum dot. (b) Perpendicular displacement versus time plots of a dynein-quantum dot. (c) Schematic diagram of the quantum dot-dynein bound to microtubule

The diameter of the ring-shaped dynein head is 15 nm, which is ~ 2-fold larger than the step size of 8 nm. Dynein was visualized using negative stain electron microscopy. Negative staining was performed in the presence of 1mM AMPPNP where cytoplasmic dynein bound tightly to the microtubule. The heads of dynein bound to the microtubule in the presence of AMPPNP are shown in Figures 4a-d. The majority of the two heads (72%, n=47) were bound to the microtubules in an overlapped fashion. In some cases the two heads did not appear to be completely overlapped completely but rather overlapped by half of a head or less (Fig. 4b, c). A small number of the two headed structures showed the heads were located separately (28 %, n=18) (Fig. 4 d).

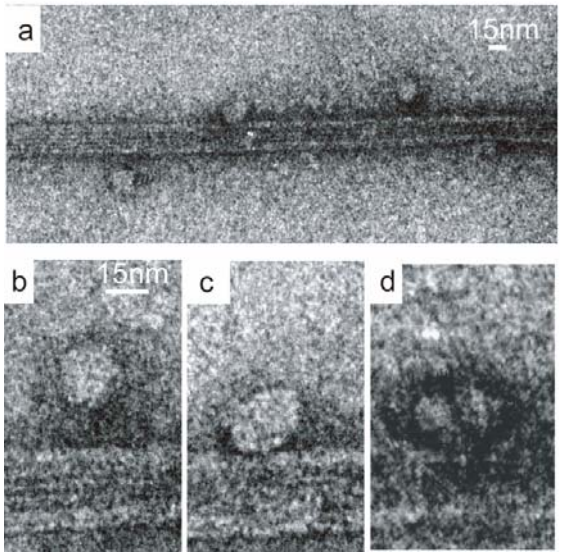

Fig. 4. Electron micrographs of negatively stained single dynein molecules bound to a microtubule and the model of the step process. (**a**) Micrographs taken at low magnifications of dynein molecules attached to a microtubule in the presence of 1mM AMPPNP. (**b-d**) Micrographs at a high magnification of a single dynein molecule on the microtubules. Almost all of the dynein rings or heads were almost completely overlapped (**b**) or show the two heads being only partially overlapped (**c**). (**d**) The two heads attached partially separately.

Discussion

The processive movement of 22S dynein can only be observed at low ATP concentrations (10 μM or lower). At higher concentrations of ATP (20 μM or higher), the 22S dynein-coated beads did not move more than 40 nm from the center of the optical trap. Axonemal outer dynein is known to

accelerate sliding velocity between adjacent doublet microtubules in flagellar movement (12, 13). To achieve the very fast sliding movement (~15 μm/s), the outer arm dynein most likely has a low duty ratio in the presence of high concentrations of ATP. At low ATP concentrations, the duty ratio of each head increased because the rate limiting state was a no nucleotide state where 22S dynein was strongly bound to the microtubule. The coordination of attachment of three heads may make the processive movement. Thus, 22S dynein can switch between the processive and nonprocessive modes using subtle changes in the ATP concentration. The stall force, ~5 pN, of 22S dynein was slightly lower than that, ~7 pN, for cytoplasmic dynein. The stall force for 22S dynein was reduced due to higher backward ratio or dissociation.

The maximum velocity (800 nm/s), stall force (7-8 pN) and the step size (8 nm) of the cytoplasmic dynein are strikingly similar to those reported for kinesin-1 (14). Hand-over-hand model for kinesin has been proposed previously (15-17). The result that dynein has one rate limiting state at the 8-nm step reported previously (10) supports the hand-over-hand model because the simple inchworm model requires two step reactions to produce one 8-nm step (15). Visualization of dynein by negative stain electron microscopy shows a phi (Φ)-shaped structure, indicating that the stems of the two heads are close to each other and the ring domains partially overlapped (18, 19). When the heads of dynein bind to the microtubule in the presence of AMPPNP they also overlap (Fig. 4a-c). Axonemal dynein within axonemes also showed an overlapping of heads as observed from electron micrographs (20, 21). Cytoplasmic dynein followed the path of a single microtubule protofilament because the perpendicular diffusion of quantum dot remained within a single protofilament. A possible model to explain the stepping movement is that the dynein heads are positioned axially along the microtubule similar to kinesin. Thus, the ring regions representing the dynein heads should overlap (Fig. 4 and 5). The large dynein heads take 16-nm steps using an overlapping hand-over-hand mechanism, while the dynein molecule takes 8 nm steps.

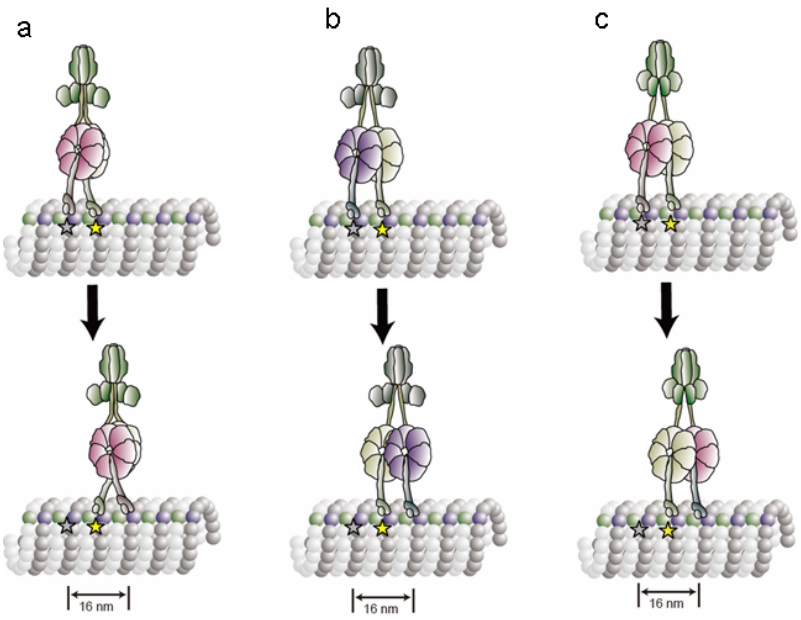

Fig. 5 The overlapping hand-over-hand model of stepping by a single dynein molecule. The dynein heads bind to a microtubule at sites separated by 8 nm. (a) The two heads are stacked. The trailing stalk head swings by 16 nm. (b) The trailing head passes the leading head by 16-nm to a make 8 nm step. (c) The trailing head passes across the leading head.

References

1. Gibbons, I. R. Studies on the Protein Components of Cilia from *Tetrahymena pyriformis*. (1963) *Proc. Natl. Acad. Sci. USA* **50,** 1002–1010.
2. Paschal, B. M. & Vallee, R. B. Retrograde transport by the microtubule-associated protein MAP 1C. (1987) *Nature (London)* **330,** 181–183.
3. Schnapp, B. J. & Reese, T. S. Dynein is the motor for retrograde axonal transport of organelles. (1989) *Proc. Natl. Acad. Sci. USA* **86,** 1548–1552.
4. Verde, F., Berrez, J. M., Antony, C. & Karsenti, E. Taxol-induced microtubule asters in mitotic extracts of Xenopus eggs: requirement for phosphorylated factors and cytoplasmic dynein. (1991) *J. Cell Biol.* **112,** 1177–1187.
5. Walczak, C. E., Vernos, I., Mitchison, T. J., Karsenti, E. & Heald, R. A model for the proposed roles of different microtubule-based motor proteins in establishing spindle bipolarity. (1998) *Curr. Biol.* **8,** 903–913.
6. Dujardin, D., Wacker, U. I., Moreau, A., Schroer, T. A., Rickard, J. E. & De Mey, J. R. Evidence for a role of CLIP-170 in the establishment of metaphase chromosome alignment. (1998) *J. Cell Biol.* **141,** 849–862.
7. Starr, D. A., Williams, B. C., Hays, T. S. & Goldberg, M. L. ZW10 helps recruit dynactin and dynein to the kinetochore. (1998) *J. Cell Biol.* **142,** 763–774.
8. Kon, T., Nishiura, M., Ohkura, R., Toyoshima, Y. Y. & Sutoh, K. Distinct functions of nucleotide-binding/hydrolysis sites in the four AAA modules of cytoplasmic dynein. (2004) *Biochemistry* **43,** 11266–11274.
9. Hirakawa, E., Higuchi, H. & Toyoshima, Y. Y. Processive movement of single 22S dynein molecules occurs only at low ATP concentrations. (2000) *Proc. Natl. Acad. Sci. USA* **97,** 2533–2537.
10. Toba, S., Watanabe, T. M., Yamaguchi-Okimoto, L., Toyoshima, Y. Y. & Higuchi, H. Overlapping hand-over-hand mechanism of single molecular motility of cytoplasmic dynein. (2006) *Proc. Natl. Acad. Sci. USA* **103,** 5741–5745.
11. Block, S. M., Goldstein, L. S. B. & Schnapp, B. J. Bead movement by single kinesin molecules studied with optical tweezers. (1990) *Nature (London)* **348**, 348–352.
12. Gibbons, B. H. & Gibbons, I. R. Functional recombination of dynein 1 with demembranated sea urchin sperm partially extracted with KCl. (1976) *Biochem. Biophys. Res. Commun.* **73**, 1–6.
13. Yano, Y. & Miki-Noumura, T. Recovery of sliding ability in arm-depleted flagellar axonemes after recombination with extracted dynein I. (1981) *J. Cell Sci.* **48,** 223–239.
14. Nishiyama, M., Higuchi, H. & Yanagida, T. Chemomechanical coupling of the forward and backward steps of single kinesin molecules. (2002) *Nat. Cell Biol.* **4,** 790–797.
15. Kaseda, K., Higuchi, H. & Hirose, K. Alternate fast and slow stepping of a heterodimeric kinesin molecule. (2003) *Nat. Cell Biol.* **5,** 1079–1082.
16. Asbury, C. L., Fehr, A. N. & Block, S. M. Kinesin moves by an asymmetric hand-over-hand mechanism. (2003) *Science* **302,** 2130–2134.
17. Yildiz, A., Tomishige, M., Vale, R. D.& Selvin, P. R. Kinesin walks hand-over-hand. (2004) *Science* **303,** 676–678.
18. Amos, L. A. Brain dynein crossbridges microtubules into bundles. (1989) *J. Cell Sci.* **93,** 19–28.
19. Toba, S. & Toyoshima, Y. Y. Dissociation of double-headed cytoplasmic dynein into single-headed species and its motile properties. (2004) *Cell Motil. Cytoskeleton* **58,** 281–289.
20. Goodenough, U. W. & Heuser, J. E. Substructure of the outer dynein arm. (1982) *J. Cell Biol.* **95,** 798–815.
21. Lupetti, P., Lanzavecchia, S., Mercati, D., Cantele, F., Dallai, R. & Mencarelli, C. Three-dimensional reconstruction of axonemal outer dynein arms in situ by electron tomography. (2005) *Cell Motil. Cytoskeleton* **62,** 69–83.

Speaker Paper 5

The ribosome as a molecular motor

Gary M. Skinner & Koen Visscher

University of Arizona, Dept of Physics, 1118 E. 4th Street, Tucson, AZ 85721

Abstract

Recent structural, biochemical and single-molecule biophysical studies have provided unprecedented insights into the molecular mechanism of the motion and forces generated by motor proteins such as kinesins and myosins. For large macromolecular complexes—with the ribosome being the poster child of these "huge" molecular machines—most single-molecule experiments are still under development, and are only starting to produce results fit for quantitative modeling. Ribosomes are thought to move in ratchet like manner along mRNA, with EF-G possibly acting as the rectifier. We have observed the 5'→3' motion of individual ribosomes along poly(U), as well as backward slippage when tension in the mRNA is increased using optical tweezers.

Ribosomes are amongst the most complex molecular motors known, when considering their size, the complex arrangements of RNA and proteins that make up their structure, and the biochemical cycle that underlies their motion. For example, the prokaryotic ribosome is a large ~2.5 MDa structure composed of 3 ribosomal RNA molecules which make up about half of the total mass, and more than fifty proteins. The structural complexity is in keeping with its functional complexity, which during elongation involves the selection of tRNA in accordance with the mRNA codon, catalysis of the

peptide bond formation, and subsequent motion along the mRNA template. Because we are mainly interested in ribosome motion we will not address initiation, termination and ribosome recycling, processes that are interesting in their own right. A full cycle of the translation elongation cycle, ignoring any intermediate states that may exist, is depicted in Fig. 1, and immediately suggests that the mechanochemical coupling of the ribosome is likely to be rather more complex than that of smaller and presumably simpler motors such as kinesin. The ribosome has 3 binding sites for tRNA partitioned between its small 30S and large 50S subunit: the Aminoacyl or A site; the Peptidyl or P site; and the Exit or E site. At the start of the cycle, peptidyl tRNA resides in the P site. Binding of aminoacyl tRNA occurs as a complex of tRNA•EF-Tu•GTP in the vacant A-site, catalyzed by the elongation factor Tu (EF-Tu) and GTP hydrolysis. Once aminoacyl tRNA has been bound in the A-site, the peptide bond is formed at the peptide transferase center (PTC) catalyzed by ribosomal RNA. To facilitate the next round of elongation, the

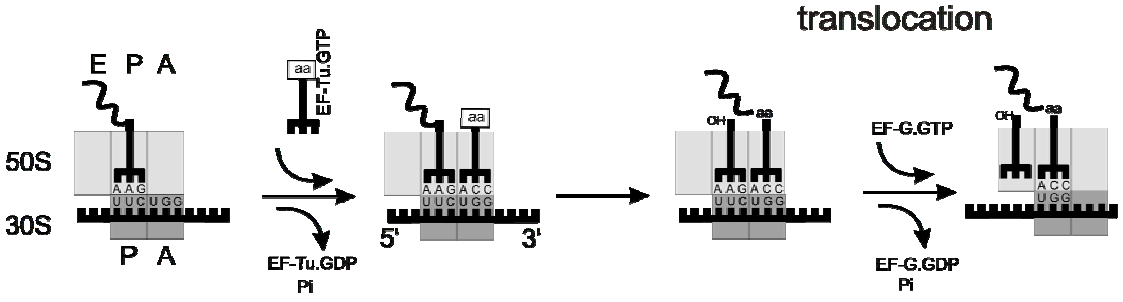

Fig. 1. The translation elongational cycle.

A-site is vacated during the so-called translocation step in which, the peptidyl tRNA (still in the A-site) and the deacylated tRNA (in the P-site) are moved to the P and E-site respectively; the associated mRNA is thought to be carried along, effectively moving the ribosome towards the 3'-end along the mRNA. The translocation event is strongly promoted by the binding and hydrolysis of EF-G•GTP[1,2]. This raises the question about

what precisely constitutes the motor: EF-G or the ribosome? The fact that elongation can occur in the absence of EF-G, albeit extremely slowly[3], argues that the ribosome is the actual motor facilitating motion, and naturally suggests a thermal ratchet type of mechanism to underlie motion. In principle, there are a multitude of molecular interactions within the ribosome that can provide the required energy, while directionality can result from the higher affinity of peptidyl tRNA for the P-site than the A-site. As translocation requires the disruption of a number of contacts between the tRNAs and the ribosome, the energy barrier for forward motion may be considerable, which could explain the extremely slow elongation rate in the absence of EF-G. The role of EF-G in this picture may simply be to reshape the energy landscape, i.e. lower some energy barriers while elevating others, so as to bias motion towards the 3'-end of the mRNA. Indeed, kinetic and biochemical analysis indicate that rapid hydrolysis upon binding of EF-G•GTP triggers conformational changes in both EF-G and the ribosome that "unlock" the ribosome after which tRNA-mRNA motion is thought to occur[4]. In particular, EF-G domain IV, which contacts the 30 S shoulder, is thought to play an essential role in opening up the decoding region. Deletion of this domain uncouples GTP hydrolysis and motion as shown by a ~1000-fold drop in the rate of elongation[5] while not affecting single round GTPase activity[1]. Interestingly, domain IV also mimics the anti-codon domain of the tRNA·EF-Tu complex and binds the A-site in the post translocation state[6], so that it may also serve to block any backward movement that might otherwise occur in the unlocked state. Although EF-G seems to couple GTP hydrolysis to motion, it remains to be seen if such coupling is tight or loose. For example, does each EF-G•GTP hydrolysis cycle result in a one-codon sized translocation step? How does the coupling

depend upon force? Single-molecule experiments can shed light on such questions, as has been demonstrated for the kinesin motor protein[7], particularly when XTP-dependent mutants of EF-Tu are used to isolate the GTP-dependent translocation step[8].

Step size and processivity. Translation is generally considered an orderly process in which mRNA is translated codon by codon, suggesting a step size of translocation of 1 codon, *i.e.* 3 nucleotides, or ~1.8 nm (contour length) but deviations from this regular pattern do occur. Best known are perhaps the +1 or -1 frameshifts that can occur and result in step sizes of 4 or 2 nucleotides[9]. However, these frameshifts very rarely occur spontaneously but rather are programmed and sequence-dependent. For example, -1 frameshifting requires two frameshift elements, the "slippery sequence" at the coding region and a pseudoknot or stem loop downstream, near the ribosome's entrance tunnel. Presumably the tension developed when a moving ribosome encounters such an obstacle triggers the -1 frameshift. Programmed frameshifts occur ~1-30% of the time, qualifying it as a rare event that causes only a single nucleotide-sized change in step size, and thus may be very hard to detect using single-molecule assays for ribosome motion. However, more dramatic events such as "hopping" and "sliding" in which the ribosome bypasses or slips over much longer regions of mRNA can also occur. For example, ribosomes from *E. coli* have been shown to hop with 100% efficiency over a large, 50 nucleotides long untranslated gap between codon 46 and 47 of the mature message of T4 topoisomerase subunit *gene 60, in vivo*[10]. Such hopping has very specific requirements: a take-off site and landing site codon that are similar in sequence; a terminator codon at the take-off point; a stem loop just downstream; and a specific amino acid sequence of the nascent

peptide from the 46 codons preceding the gap[10]. The latter is very interesting as it suggests some type of feedback in which the nascent peptide itself may control translation. Alternatively, when elongation is paused with the A-site kept unoccupied, *e.g.* by starving for aminoacyl-tRNA, peptidyl-tRNA-ribosome complexes, have been shown to "slide" for tens of nucleotides, or bypass the "hungry" codon before resuming translation downstream[11,12]. Unlike hopping, sliding is independent of any secondary structure in the untranslated region. As in the case of hopping, sliding depends upon the similarity of the P-site codon at the take-off and landing sites. While hopping, because of its specific requirements, is not expected to occur during single-molecule experiments, one can not rule out the possibility of sliding particularly at low concentrations of aminoacyl-tRNA when using homopolymeric messages.

Protein synthesis is a rather costly process and for reasons of efficiency alone one would expect a rather high processivity. The processivity of ribosomes has not yet been measured in ways analogous to other molecular motors using single molecule assays. However, the processivity error, defined as the fraction of premature terminated polypeptides during *in vivo* translation, has been estimated to be 20-30% for the *lacZ* gene in *E. coli*, yielding a loss of processivity frequency of ~$2\text{-}3\cdot10^{-4}$ per codon[13]. Several events can affect processivity: 1) False termination at a sense codon, which has been estimated, however, to only occur with a probability less than 10^{-5} per codon[14]. 2) Frameshifting into a stop-codon. Unprogrammed, spontaneous frameshifts, however, are also rare (order of 10^{-5} per codon for the *lacZ* gene[15]). 3) Drop-off or loss of the nascent polypeptide when the ester bond linking the peptide to tRNA is hydrolyzed by peptidyl-tRNA hydrolase[16]. 4) Termination by the action of tmRNA that appends an oligopeptide

tag to the polypeptide to aberrant protein for degradation[17]. Both drop-off and tmRNA tagging are associated with temporal stalls of the ribosome. At conditions of saturating concentrations one would expect ribosomes to be highly processive when moving along relatively featureless homopolymeric mRNA. Once ribosomes encounter obstacles such as downstream tertiary or secondary structure, stalling and loss of processivity can be expected. However, work by Noller's lab suggests that the ribosome serves as its own helicase capable of unwinding downstream RNA structure[18]. Ribosomes from *E. coli*, with the ribosomal proteins S3, S4, and S5 forming a ring structure presumably acting as a clamp, were shown to be highly processive on a stable 27 base pair RNA duplex[18]. However, this duplex is not identical to RNA hair pin structures ribosomes encounter *in vivo*. Such hair pins can have specific structures that facilitate additional contacts with the ribosome periphery, which for example have been discussed in the context of -1 frameshifting[19]. It seems reasonable to expect that such structures can also affect pausing and processivity. It is clear that, although some information is available, a detailed analysis of ribosome processivity is complex and lacking.

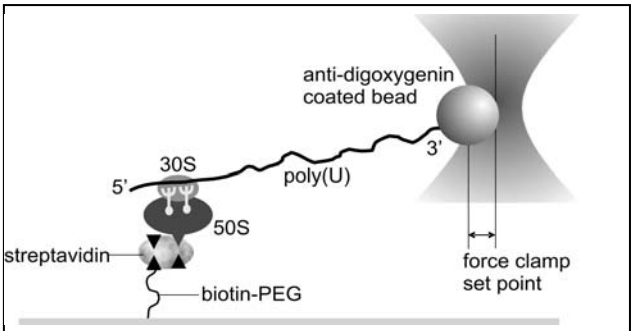

Fig. 2 A single-molecule assay for observing *E. coli* ribosome motion along mRNA using optical tweezers.

Single molecule experiments. We are developing *in vitro* assays to investigate (some of) these question in more details using single molecule experiments. As tension is thought to be of importance for -1 frameshifting and also may be able induce pausing or stalling and affect processivity, an assay was

chosen in which optical tweezers are used to apply controlled forces. One possible experimental geometry is depicted in Fig. 2. in which ribosomes from *E. coli.* have been surface-immobilized using a streptavidin binding aptamer inserted into the 23S rRNA[20]. The message used here is poly(U), which has been 3'-end labeled with dixoxygenin to attach a microscopic bead that will be held with optical tweezers. Upon addition of elongation buffer containing the protein factors, synthetases, amino acids, tRNA etc, motion of the ribosome along mRNA has been observed. At constant force and using the persistence length of poly(U)[21], ribosome velocities can then be computed in units of codons/s, and were found to be ~3 codons/s at room temperature, although velocities as high as ~14 codons/s have been found.

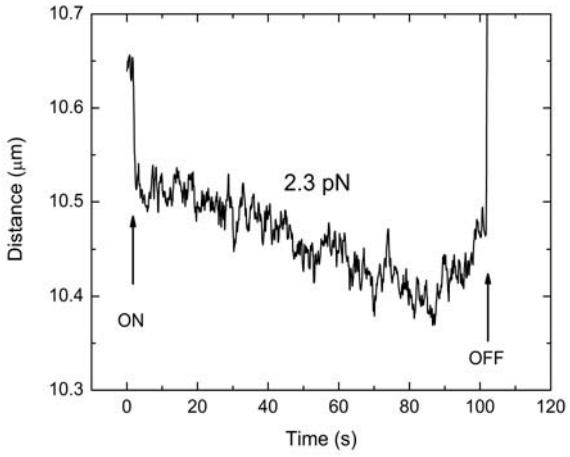

Fig. 3 One example of ribosome displacement along poly(U), at a rate of ~2.5 codons per second when applying a 2.3 pN load and taking the persistence length of poly(U) to be 1 nm. ON and OFF indicate the time period when the force clamp was operated at 2.3 pN. The experiment was performed at room temperature. The data has been corrected for stage drift using a marker attached to the microscope cover glass.

Interestingly, when comparing displacement records to controls in which ribosomes are stalled, the noise levels tend to have increased after elongation mix has been added. The source of these increased fluctuations was not due to any accumulation of aggregates in the optical trap and for now remains mysterious. Is it a reflection of the thermal ratchet behavior of this motor? Or, is this an artifact of the homopolymeric

nature of the message, and is the ribosome somehow scooting back and forth along the message somehow? The latter seems unlikely because one may argue that even a homopolymeric message has polarity that may be sensed by the ribosome. Furthermore, work by Rachel Green`s lab indicates that the length of the polypeptide synthesized is very tightly coupled to the length of the message indicating that forward 3'-end directed motion is preferred[22]. It was shown that poly(U) templates shorter than 5 codons produced no detectable levels of poly(Phe) in a TCA precipitation experiment that requires a at least 5 Phe residues for precipitation to occur. Thus, it was concluded, ribosomes move predominantly unidirectionally along poly(U) because any back and forth motion would have produced detectable Phe chains of 6 residues or longer[21]. However, one cannot rule out backward motion on longer messages, as the probability per codon of any backward motion may just be too low to detect in a precipitation assay. In fact, we have seen extended backward motion of ribosomes along poly(U) when forces of, but only when forces of 7-9 pN opposing 3'-end motion have been applied. However, thus far, single-molecule experiments have only produced the very first initial displacements records of ribosomes along mRNA[23]. There still is a way to go to be able to extract information that will shed new light on the issues such as mechanochemical coupling, processivity, step size and the mechanics and physics underlying ribosome motion motor.

1. Rodnina, M. V., Savelsbergh, A., Katunin, V. I. & Wintermeyer, W. Hydrolysis of GTP by elongation factor G drives tRNA movement on the ribosome. *Nature* **385,** 37-41 (1997).
2. Katunin, V. I., Savelsbergh, A., Rodnina, M. V. & Wintermeyer, W. Coupling of GTP hydrolysis by elongation factor g to translocation and factor recycling on the ribosome. *Biochem.* **41**, 12806-12812 (2002).
3. Belitsina, N.V., Tnalina, G.Z. & Spirin, A.S. Template-free ribosomal synthesis of polypeptides from aminoacyl-tRNAs. *Biosystems* **15**, 233-241 (1982).
4. Savelsbergh, A., Katunin, V.I., Mohr, D., Peske, F., Rodnina, M.V. & Wintermeyer, W. An elongation factor G-induced ribosome rearrangement precedes tRNA-mRNA translocation. *Mol. Cell* **11**, 1517-1523 (2003).
5. Green, R. & Noller, H. F. Ribosomes and translation. *Annu. Rev. Biochem.* **66,** 679-716 (1997).
6. Frank, J., and Agrawal, R.K. *Nature* **406**, 318-322 (2000).
7. Visscher, K., Schnitzer, M. J. & Block, S. M. Single kinesin molecules studied with a molecular force clamp. *Nature* **400**, 184-189 (1999).
8. Weijland, A., Parlato, G. & Parmeggiani, A. Elongation factor Tu D138N, a mutant with modified substrate specificity, as a tool to study energy consumption in protein biosynthesis. *Biochem.* **33**, 10711-10717 (1994).
9. Farabaugh, P.J., Programmed translational frameshifting. *Annu. Rev. Gen.* **30**, 507-528 (1996).
10. Weiss, R.B., Huang, W.M., and Dunn, D.M. A nascent peptide is required for ribosomal bypass of the coding gap in bacteriophage T4 gene *60*. *Cell* **62**, 117-126 (1990).

11. Gallant, J.A, and Lindsley D. Ribosomes can slide over and beyond "hungry" codons, resuming protein chain elongation many nucleotides downstream. *Proc. Natl. Acad. Sci. USA* **95**, 13771-13776 (1998).
12. Lindsley, D., Gallant, J., Doneanu, C., Bonthuis, P., Caldwell, S., and Fontelera, A. Spontaneous ribosome bypassing in growing cells. *J. Mol. Biol.* **349**, 261-272 (2005).
13. Dong, H., and Kurland, C.G. Ribosome mutants with altered accuracy translate with reduced processivity. *J. Mol. Biol.* **248**, 551-561 (1995).
14. Jorgensen, F., and Kurland, C.G. Processivity errors of gene expression in *Escherichia coli*. *J. Mol. Biol.* **215**, 511-521 (1990).
15. Atkins, J.F., Elseviers, D., and Gorini, L. Low activity of β-galactosidase of frameshift mutants in *Escherichia coli*. *Proc. Natl. Acad. Sci. USA* **69**, 1192-1195 (1972).
16. Menninger, J.R. peptidyl transfer RNA dissociation during protein synthesis from ribosomes of *Escherichia coli*. *J. Biol. Chem.* **251**,3392-3398 (1976).
17. Withey, J. H., and Friedman, D.I. A salvage pathway for protein synthesis: tmRNA and *Trans*-Translation *Annu. Rev. Microbiol.* **57**, 101-123 (2003).
18. Takyar, S., Hickerson, R.P., and Noller H.F. mRNA helicase activity of the ribosome. *Cell* **120**, 49-58 (2005).
19. Dulude, D., Baril, M. & Brakier-Gingras, L. Characterization of the frameshift stimulatory signal controlling programmed -1 ribosomal frameshift in the human immunodeficiency virus type 1. *Nucl. Acids Res.* **30**, 5094-5102 (2002).

20. Leonov, AA., Sergiev, P.V., Bogdanov, A.A, Brimacombe, R. & Dontsova O.A. Affinity purification of ribosomes with a lethal G2655C mutation in 23S rRNA that affects translocation. *J. Biol. Chem.* **278**, 25664-25670 (2003).
21. Seol, Y., Skinner, G.M. & Visscher K., "Elastic properties of a single-stranded charged homopolymeric ribonucleotide". *Phys. Rev. Lett.* **93**, 118102 (2004).
22. Southworth, D.R., Brunelle, J.L. & Green R. EFG-independent translocation of the mRNA:tRNA complex is promoted by modification of the ribosome with thiol-specific reagents. *J. Mol. Biol.* **324**, 611-623 (2002).
23. Vanzi, F., Vladimirov, S., Knudsen, C.R., Goldman Y.E. & Cooperman B.S. Protein synthesis by single ribosomes. *RNA* **9**, 1174-1179 (2003).

The strain of myosins working one-two-five.

Veigel C., Jankevics H. & J.E. Molloy
MRC National Institute for Medical Research, Mill Hill, London NW7 1AA, UK
Contact: jmolloy@nimr.mrc.ac.uk

THE AIM of this paper is to open discussion on the effect of distortion and strain on the kinetics of formation and subsequent lifetime of the acto-myosin cross-bridge. The words "strain" and "distortion" are often used interchangeably and are taken to mean either a mechanical deformation of the preformed acto-myosin complex or misalignment between the dissociated myosin and actin prior to binding. Here, we arbitrarily define "strain" as mechanical deformation of the bound actomyosin crossbridge and "distortion" as the distance between an ideally positioned (i.e. zero starting strain) myosin and its target actin binding site (Fig. 1). We can consider two examples in muscle where this distinction becomes physiologically relevant: Contraction of insect fibrillar flight muscle is controlled by thick and thin filament geometry. Mismatch between positions of myosin heads on the thick filament and target actin binding sites on the thin filaments means that few crossbridges can form even when the muscle is fully activated by calcium. However, both muscle stiffness and force rise dramatically when the muscle length is changed by a few percent (about 10nm per half sarcomere). This effect, known as *stretch activation*, arises because the externally applied length change causes filament sliding and reduces *distortion* by bringing thick and thin filament lattices into better register (3). One early study showed that stretch activation is periodic and repeats every 38nm (5). Several muscle types, including vertebrate smooth muscle and particularly molluscan catch muscle are capable of generating high force and stiffness with very low ATP turnover. Here, we believe that tension is maintained with good economy because *strain* in the bound cross-bridges causes deformation of their structure trapping ADP at the catalytic sites (6).

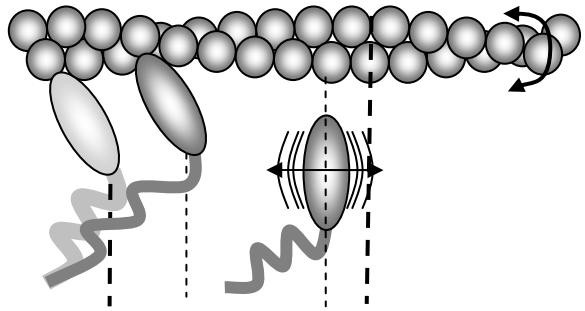

Figure 1. *The myosin cross-bridge can become strained after binding to actin (left) and because load is borne across the length of the molecule its structure might be deformed or bent. Myosin can exhibit thermal motion (right) before binding to actin and this would enable it to overcome a distortion distance from its actin binding site. Here the deforming load would be distributed across the molecule.*

The chance of a myosin head reaching a particular actin binding site can be calculated in terms of its "first passage time", the average time before the proteins make their first diffusional encounter (7). This depends upon *DISTORTION*, stiffness and viscous drag of the myosin head. The probability of an attached crossbridge undergoing its power stroke, or detaching from actin depends upon its *STRAIN* and stiffness (8). It is straightforward to define cross-bridge distortion and strain in vertebrate striated muscle, because the geometry of the two filament systems is known. We usually assume that thick and thin filaments are relatively rigid (in terms of distortion) and that their ultrastructure ensures there is little change in average crossbridge distortion with sarcomere length (9). However, we now want to know how strain and distortion affect the behaviour of non-muscle myosins, most of which do not exist in highly ordered arrays but instead act alone or in disordered "clumps". In order to start making sense of strain and distortion we need to first propose schemes that link the biochemical and mechanical cycles. These usually derive from the original Lymn-Taylor scheme (10). Fig. 2 (lower) enables us to start building a formalism for how strain and distortion might affect kinetics. Modelling

may then proceed by drawing free-energy diagrams that combine chemical and mechanical free energy terms and then producing dynamic solutions either by Monte Carlo or other numerical methods. The advent of single molecule techniques has greatly advanced our ability to test and refine such models. In particular, the use of optical tweezers enables measurement of force, stiffness and working stroke and opens the possibility to manipulate distortion and strain.

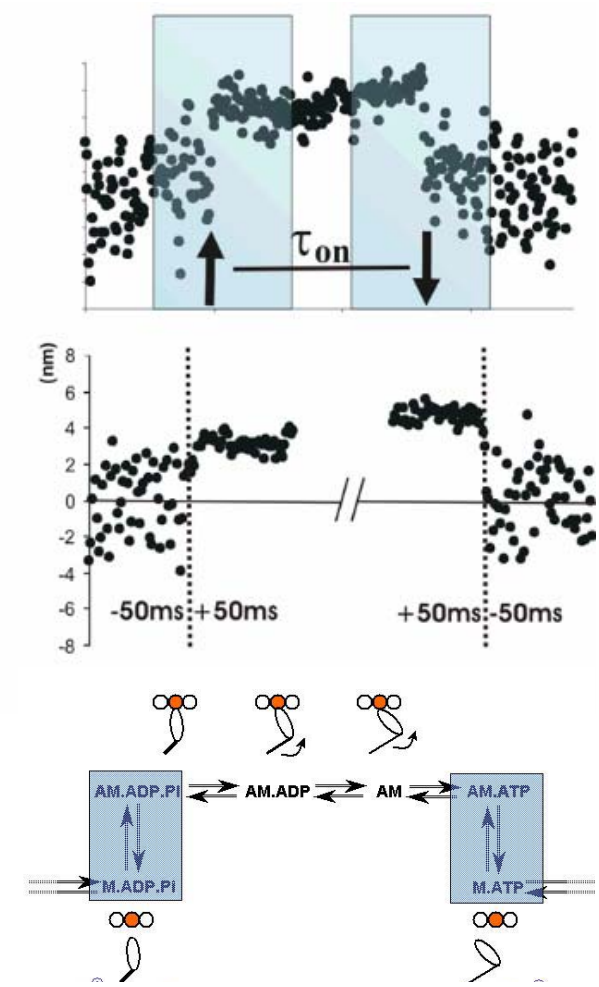

Figure 2. *Myosin 1c, like many other myosins, exhibits a two phase power stroke. Single events (upper) can be averaged by synchronising the data to the start and end point of each interaction (arrows on upper trace). The ensemble averaged data has better signal to noise because thermal fluctuations are averaged away (centre panel). The data can be interpreted in terms of the cross-bridge biochemical cycle (Lymn-Taylor scheme) with the additional feature that there are at least two, structurally distinct, force generating states (lower scheme). Taken from ref (2).*

OPTICAL TWEEZERS based single molecule experiments have enabled measurement of the time-course and amplitude of the working stroke (11-13). However, interpretation of data obtained from fast, intermittently interacting, myosins is still in debate (14). It was immediately evident that the archetypal myosin II from skeletal muscle produces most its movement, and presumably force, very rapidly after binding to actin. However, later work showed that myosin I (15), V (1, 16), VI (17) and smooth muscle myosin II (18) in fact generate movement in two discrete phases (Fig. 2). This followed the discovery that some myosins adopt structurally distinct conformations in rigor (apo) and ADP bound states (19, 20). It is, of course, tempting to link the second movement observed in optical trapping studies with the EM structural observations. The initial movement occurs within the time resolution of the measurements (which at best is ~ 1ms (21)) and is always the largest component. This is followed by a further movement after a delay of several tens of milliseconds. A recent study, made at very high time resolution (21), indicates that skeletal muscle myosin II exhibits the same phenomenon although the second movement is completed within just a few milliseconds of binding to actin.

It's been shown that myosin II binds tightly to actin from a nucleotide (or nucleotide analogue) loaded state or from the rigor (apo) state. Biochemical studies, show that there is a large drop in free energy when the proteins bind. So it is conceivable that if myosin "rocks" onto its actin binding site it might then produce movement as it binds even in the apo state. This was addressed in a recent study that showed a hydrolysis products starting state is a necessary prerequisite for movement and force production (22, 23). Binding from the apo state does not generate movement. So we strongly suspect that the large initial component of the working stroke correlates with phosphate release and the second movement occurs as the cross-bridge enters the rigor state (Fig. 2 scheme). So, what happens to the free

energy associated with the binding step?

Using optical tweezers it has been possible to apply rapid changes in strain during a single crossbridge cycle (18, 24, 25) and controlled loads to individual processive myosin Vs as they walk along actin (26). Furthermore, crossbridge distortion has been investigated by accurately positioning actin relative to the unbound myosin head and measuring the binding probability at different distortions (4, 21). The question then arises how strain and distortion dependence of acto-myosin interactions might manifest themselves in the motor mechanism and physiology of non-muscle myosins. For instance we would like to know if myosin can be "pulled off" actin in any of its biochemical states. We would also like to know which biochemical steps are reversible under normal loads or perhaps can be made to reverse under extreme (and possibly non-physiological) loading. Finally, what is the effect of load on the myosin atomic structure and what are the spring constants for different bending or torsional modes. We know that myosin II can readily swivel about its long axis (27, 28) and that its bending elasticity in the plane of the powerstroke is around 1-2pN.nm (25, 29) and his scales linearly with lever length (e.g. consistent with a spring at the base and not cantilever bending (30))

Strain and distortion in processive myosins:

Over the past 6 years, there have been many studies of the processive motor, myosin V and several clear conclusions about its mechanism arise from that body of work: Solution kinetic studies, show the rate of ADP release is known to be slow ($12s^{-1}$) and rate limits the cycle (31). Single headed myosin V should therefore spend >70% of its time bound to actin (in marked contrast to skeletal muscle myosin II). Intact, double-headed myosin V takes many 36nm steps along actin and processivity is found to be significantly higher than expected from kinetic studies using the monomer. This implies there is some mechanism that coordinates the ATPase cycles of the two heads. Single fluorophore imaging has allowed the resolution of the movement of individual heads and excludes inch-worm models and favours hand-over-hand mechanisms (32-34). Each head moves 72 nm for each ATP hydrolysed and the dimeric molecule advances 36nm for each step. Negative stain EM shows that the two heads bind actin monomers 36 nm apart and the lever arm shape at low ATP has a characteristic, strained, "*telemark*" appearance. Myosin V slightly understeps the pseudo repeat distance and video microscopy studies show a slow left-handed rotation as myosin V advances along actin. The working stroke of full length myosin V is 25nm consisting of 20nm initial step and then a further 5nm step following a brief delay (1, 35). Recombinant myosin V in which the lever arm was successively shortened had proportionately shorter power strokes (as originally discovered using myosin II (36)), and lower processivity (37). Meanwhile, another group found that 2-light chains were sufficient to produce 36nm stepping furthermore that stepping behaviour persists with just a single myosin V head (38, 39).

The load dependent stepping behaviour of intact, two-headed myosin V (26) and strain dependent lifetimes of single-headed interactions (24, 40) have been measured. But, there is a current controversy about how strain affects the bound myosin heads: One team finds that overall cross-bridge lifetime is extended by strains that resist its forward motion (pulling back on the motor) whereas forward directed, assisting, strains have rather little effect on kinetics (40). The other team found that both forward and reverse strain affected the lifetime of the first phase of the power stroke in an exponential manner as expected from the additional work term due to the applied load (Force* characteristic distance, ΔFd, or $\frac{1}{2}kd^2$, see Eqn 1.) but force had little effect on the second phase (limited by ATP binding) (24):

$$k = k_0 \bullet e^{-(\Delta Fd / k_b T)}$$ EQUATION 1.

When considering the mechanical mechanism of processive motors it is sensible to consider the effects of distortion on the binding probability of lead and trail heads as this will have an effect on run length.

At the instant of a given step, one head remains bound to actin whilst the other is free and this confers a geometrical relationship between the free head and actin filament. Knowing the distortion dependence of binding (4) one can start to model how this binding might be affected by distortion. The model presented in Fig 3. (legend) may be of some use when considering the behaviour of full length myosin V, recombinant myosin V constructs (e.g. (39, 41)) and other classes of processive motor like dimeric forms of myosin VI. When external load is applied to intact, processively moving, myosin V the two heads will share the load. But it is unclear how the external load will be borne, as this depends upon the shape and configuration of the heads. Furthermore, if one head detaches, the remaining head will bear all of the force and the dwell time of the "one-head bound" state will be of critical importance. The effect of strain on stepping kinetics of the intact molecule is non-linear and a comprehensive recent study made at super high loads, shows that myosin V, will process in the reverse direction along actin neither consuming or synthesising ATP (42).

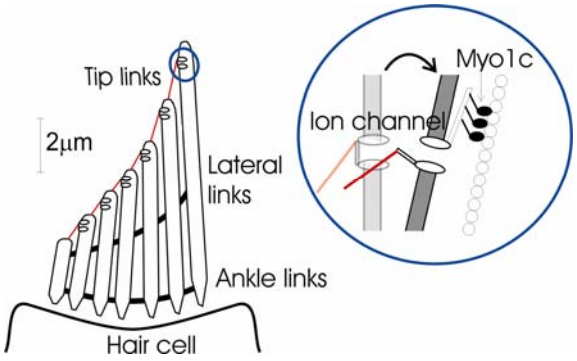

Figure 4*. Anatomy of the sterocilia of the hair cell and proposed insertion of myosin 1c at the sensory channel. Strain on the channel is transmitted to the leveram of the myosin 1c.*

Strain and distortion in a non-processive myosin:

Single headed myosin Is appear to be intermittent motors and many have uniformly slow kinetics compared to skeletal muscle myosin II. Most myosin Is generate force between the actin cytoskeleton and cellular membranes. We have been interested in the class myosin Ic that is found in liver and also within the stereocilia of hair cells within in the cochlea and vestibular system (Fig. 4). There is good evidence that this myosin is involved in the sensory adaptation process (43) and we have proposed that the strain-dependent force recovery by myosin I (44) might explain non-linearities observed in electrophysiological experiments. It would seem most likely that in their native context the myosin Ic's are unlikely to be arranged in an ordered array (but, that is not known). If so, distortion of individual molecules would be random and any distortion dependence would be likely to average out (like myosin II in the skeletal muscle sarcomere). In optical trapping experiments we find that this myosin, like the other myosin I's we have studied, exhibits a two-phase working stroke (see Fig. 1). It is believed that the tail region of the molecule binds to the receptor ion channel and the head binds to the actin filament bundle that runs through the central core of the stereocilium. The myosins essentially maintain a resting force that is sufficient to maintain the ion channel so that it is 'just closed' ($P_{open} \sim 0.1$) when the stereocilium is displaced this applies strain to the myosin heads which in response undergo rearrangement that tends to return the ion channel to its 'just closed' set-point. The total load in the system can be estimated from the ion channel conductance and these conductance signals bear similarities to the tension response of a single muscle fibre subjected to a sudden length perturbation. We are currently working to apply different loads to bound acto-myosin I complexes to better understand the non-linearities present in these relaxation processes.

We conclude that both strain and distortion are important in processive myosin motor mechanism whilst strain alone is important for most intermittent, non-muscle myosins.

FIGURE 3.

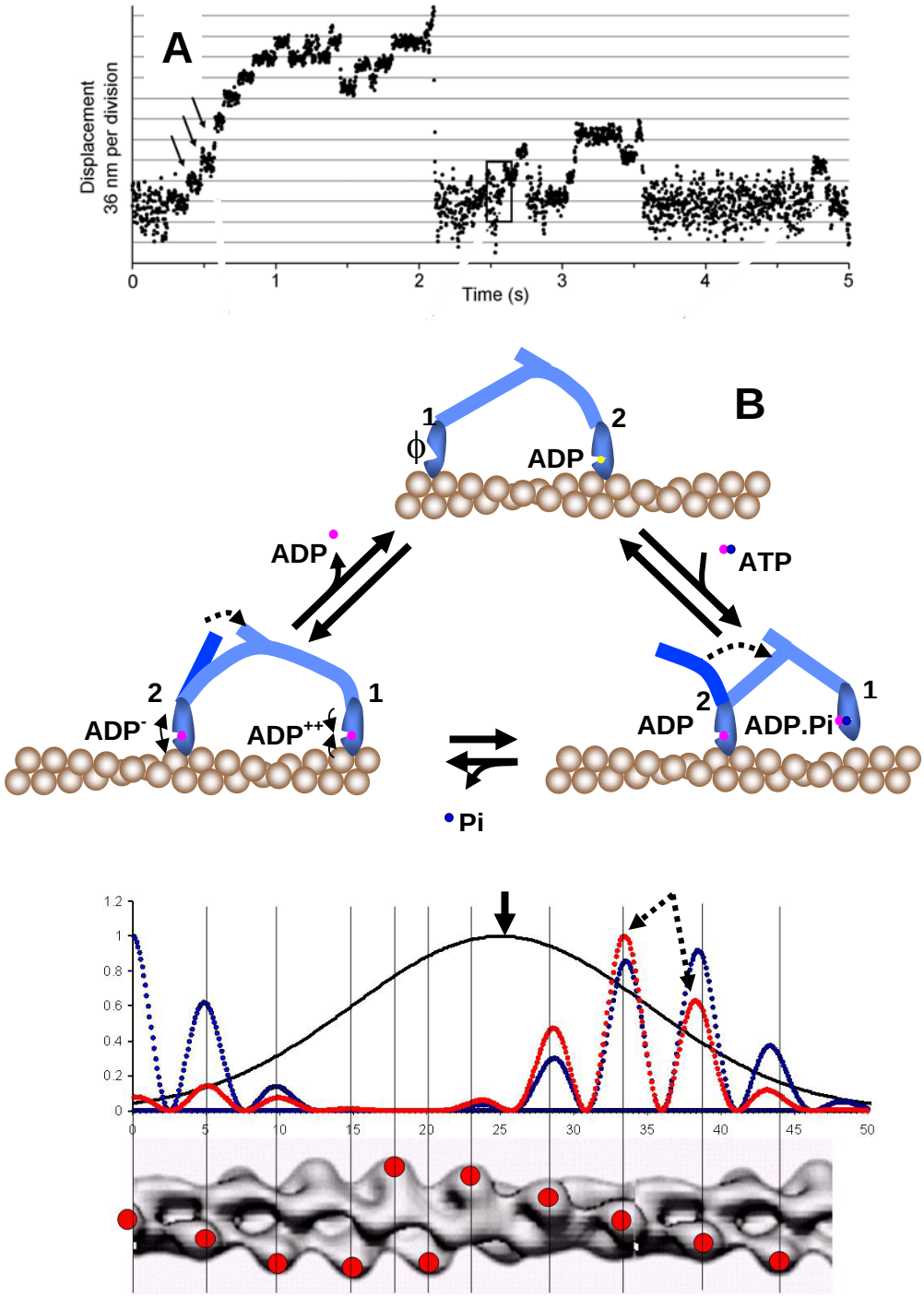

Figure 3. *A. Optical trapping record obtained using myosin V (1) showing 36 nm steps and individual interactions that indicate the powerstroke is 20+5 nm. These data led to a simple three-state model for myosin V procession. B. The mean position of the new lead head (head 1) falls short of its target binding site (arrow on lower graph). However, thermal excursions of the head (probability function, black curve) combine with actin site binding probability (blue curve based on ref (4)) to give a resultant binding probability (red) for each actin monomer.*

References:

1. Veigel, C., F. Wang, M. L. Bartoo, J. R. Sellers, and J. E. Molloy. 2002. The gated gait of the processive molecular motor, myosin V. Nature Cell Biology 4:59-65.
2. Batters, C., C. P. Arthur, A. Lin, J. Porter, M. A. Geeves, R. A. Milligan, J. E. Molloy, and L. M. Coluccio. 2004. Myo1c is designed for the adaptation response in the inner ear. Embo Journal 23:1433-1440.
3. Wray, J. 1979. Filament geometry and the activation of insect flight muscles. Nature 280:325-326.
4. Steffen, W., D. Smith, R. Simmons, and J. Sleep. 2001. Mapping the actin filament with myosin. Proc. Natl. Acad. Sci. U. S. A. 98:14949-14954.
5. Abbott, R. H., and P. E. Cage. 1979. Periodicity in insect flight muscle stretch activation. J Physiol, (Lond) 289:32-33p.
6. Cremo, C. R., and M. A. Geeves. 1998. Interactions of actin with ADP with the head domain of smooth muscle myosin: Implications for strain-dependent ADP release in smooth muscle. Biochemistry 37:1969-1978.
7. Kramers, H. A. 1940. Brownian motion in a field of force and the diffusion model of chemical reactions. Physica 7:284-304
8. Huxley, A. F., and R. M. Simmons. 1971. Proposed mechanism of force generation in muscle. Nature 233:533-538.
9. Hill, T. L. 1974. Theoretical formalism for the sliding filament model of contraction of striated muscle: Part I. Progr. Biophys. molec. Biol. 28:267-340.
10. Lymn, R. W., and E. W. Taylor. 1971. The mechanism of adenosine triphosphate hydrolysis by actomyosin. Biochem 10:4617-4624.
11. Finer, J. T., R. M. Simmons, and J. A. Spudich. 1994. Single myosin molecule mechanics: piconewton forces and nanometre steps. Nature 368:113-118.
12. Molloy, J. E., J. E. Burns, J. Kendrick Jones, R. T. Tregear, and D. C. S. White. 1995. Movement and force produced by a single myosin head. Nature 378:209-212.
13. Guilford, W. H., D. E. Dupuis, G. Kennedy, J. R. Wu, J. B. Patlak, and D. M. Warshaw. 1997. Smooth muscle and skeletal muscle myosins produce similar unitary forces and displacements in the laser trap. Biophys. J. 72:1006-1021.
14. Sleep, J., A. Lewalle, and D. Smith. 2006. Reconciling the working strokes of a single head of skeletal muscle myosin estimated from laser-trap experiments and crystal structures. Proc. Natl. Acad. Sci. U. S. A. 103:1278-1282.
15. Veigel, C., L. M. Coluccio, J. D. Jontes, J. C. Sparrow, R. A. Milligan, and J. E. Molloy. 1999. The motor protein myosin-I produces its working stroke in two steps. Nature 398:530-533.
16. Uemura, S., H. Higuchi, A. O. Olivares, E. M. De La Cruz, and S. Ishiwata. 2004. Mechanochemical coupling of two substeps in a single myosin V motor. Nature Structural & Molecular Biology 11:877-883.
17. Lister, I., S. Schmitz, M. Walker, J. Trinick, F. Buss, C. Veigel, and J. Kendrick-Jones. 2004. A monomeric myosin VI with a large working stroke. EMBO Journal 23:1729-1738.
18. Veigel, C., J. E. Molloy, S. Schmitz, and J. Kendrick-Jones. 2003. Load-dependent kinetics of force production by smooth muscle myosin measured with optical tweezers. Nature Cell Biology 5:980-986.
19. Jontes, J. D., E. M. Wilson-Kubalek, and R. A. Milligan. 1995. A 32 degree tail swing in brush border myosin I on ADP release. Nature 378.
20. Whittaker, M., E. M. Wilsonkubalek, J. E. Smith, L. Faust, R. A. Milligan, and H. L. Sweeney. 1995. A 35-Angstrom Movement of Smooth-Muscle Myosin on ADP Release. Nature 378:748-751.
21. Capitanio, M., M. Canepari, P. Cacciafesta, V. Lombardi, R. Cicchi, M. Maffei, F. S. Pavone, and R. Bottinelli. 2006. Two independent mechanical events in the interaction cycle of skeletal muscle myosin with actin. Proc. Natl. Acad. Sci. U. S. A. 103:87-92.
22. Steffen, W., and J. Sleep. 2004. Repriming the actomyosin crossbridge cycle. Proc. Natl. Acad. Sci. U. S. A. 101:12904-12909.
23. Steffen, W., D. Smith, and J. Sleep. 2003. The working stroke upon myosin-nucleotide complexes binding to actin. Proceedings of the National Academy of Sciences U.S.A. 100:6434-6439.
24. Veigel, C., S. Schmitz, F. Wang, and J. R. Sellers. 2005. Load-dependent kinetics of myosin-V can explain its high processivity. Nature Cell Biology 7:861-869.
25. Takagi, Y., E. E. Homsher, Y. E. Goldman, and H. Shuman. 2006. Force generation in single conventional actomyosin complexes under high dynamic load. Biophys. J. 90:1295-1307.
26. Rief, M., R. S. Rock, A. D. Mehta, M. S. Mooseker, R. E. Cheney, and J. A. Spudich. 2000. Myosin-V stepping kinetics: A molecular model for processivity. Proc. Natl. Acad. Sci. U. S. A. 97:9482-9486.
27. Azzu, V., D. Yadin, H. Patel, F. Fraternali, P. D. Chantler, and J. E. Molloy. 2006. Calcium regulates scallop muscle by changing myosin flexibility. European Biophysics Journal with Biophysics Letters 35:302-312.
28. Tyreman, M. J. A., C. Batters, A. E. Knight, L. M. Coiuccio, J. Kendrick-Jones, and J. E. Molloy. 2003. Single molecule mechanical studies on the head and neck of myosin I & II. Biophys. J. 84:328A-328A.
29. Veigel, C., M. L. Bartoo, D. C. S. White, J. C. Sparrow, and J. E. Molloy. 1998. The stiffness of rabbit skeletal actomyosin cross-bridges determined with an optical tweezers transducer. Biophys. J. 75:1424-1438.
30. Dobbie, I., M. Linari, G. Piazzesi, M. Reconditi, N. Koubassova, M. A. Ferenczi, V. Lombardi, and M. Irving. 1998. Elastic bending and active tilting of myosin heads during muscle contraction. Nature 396:383-387.
31. De La Cruz, E. M., A. L. Wells, S. S. Rosenfeld, E. M. Ostap, and H. L. Sweeney. 1999. The kinetic mechanism of myosin V. Proc. Natl. Acad. Sci. U. S. A. 96:13726-13731.
32. Warshaw, D. M., G. G. Kennedy, S. S. Work, E. B. Krementsova, S. Beck, and K. M. Trybus. 2005. Differential Labeling of myosin V heads with quantum dots allows direct visualization of hand-over-hand processivity. Biophys. J. 88:L30-L32.
33. Forkey, J. N., M. E. Quinlan, M. A. Shaw, J. E. T. Corrie, and Y. E. Goldman. 2003. Three-dimensional structural

dynamics of myosin V by single- molecule fluorescence polarization. Nature 422:399-404.
34. Yildiz, A., J. N. Forkey, S. A. McKinney, T. Ha, Y. E. Goldman, and P. R. Selvin. 2003. Myosin V walks hand-over-hand: Single fluorophore imaging with 1.5-nm localization. Science 300:2061-2065.
35. Moore, J. R., E. B. Krementsova, K. M. Trybus, and D. M. Warshaw. 2001. Myosin V exhibits a high duty cycle and large unitary displacement. Journal of Cell Biology 155:625-635.
36. Ruff, C., M. Furch, B. Brenner, D. J. Manstein, and E. Meyhofer. 2001. Single-molecule tracking of myosins with genetically engineered amplifier domains. Nature Structural Biology 8:226-229.
37. Sakamoto, T., F. Wang, S. Schmitz, Y. H. Xu, Q. Xu, J. E. Molloy, C. Veigel, and J. R. Sellers. 2003. Neck length and processivity of myosin V. Journal of Biological Chemistry 278:29201-29207.
38. Watanabe, T. M., H. Tanaka, A. H. Iwane, S. Maki-Yonekura, K. Homma, A. Inoue, R. Ikebe, T. Yanagida, and M. Ikebe. 2004. A one-headed class V myosin molecule develops multiple large (approximate to 32-nm) steps successively. Proc. Natl. Acad. Sci. U. S. A. 101:9630-9635.
39. Tanaka, H., K. Homma, A. H. Iwane, E. Katayama, R. Ikebe, J. Saito, T. Yanagida, and M. Ikebe. 2002. The motor domain determines the large step of myosin-V. Nature 415:192-195.
40. Purcell, T. J., H. L. Sweeney, and J. A. Spudich. 2005. A force-dependent state controls the coordination of processive myosin V. Proc. Natl. Acad. Sci. U. S. A. 102:13873-13878.
41. Sakamoto, T., S. Schmitz, J. E. Molloy, C. Veigel, F. Wang, and J. R. Sellers. 2002. Effect of myosin V neck length on processivity and working stroke. Molecular Biology of the Cell 13:2572.
42. Gebhardt, J. C. M., A. E. M. Clemen, J. Jaud, and M. Rief. 2006. Myosin-V is a mechanical ratchet. Proc. Natl. Acad. Sci. U. S. A. 103:8680-8685.
43. Holt, J. R., S. K. Gillespie, D. W. Provance, K. Shah, K. M. Shokat, D. P. Corey, J. A. Mercer, and P. G. Gillespie. 2002. A chemical-genetic strategy implicates myosin-1c in adaptation by hair cells. Cell 108:371-381.
44. Batters, C., M. I. Wallace, L. M. Coluccio, and J. E. Molloy. 2004. A model of stereocilia adaptation based on single molecule mechanical studies of myosin I. Philos. Trans. R. Soc. Lond. Ser. B-Biol. Sci. 359:1895-1905.

Speaker Paper 7

Mechanochemical coupling in kinesin superfamily motor proteins

F. Jon Kull, Department of Chemistry, Dartmouth College, Hanover, NH 03755

Introduction

Kinesins, as well as the closely related myosins, are molecular motors that utilized the chemical energy stored in ATP to produce directed force along a protein filament (Hirokawa and Takemura, 2004; Vale, 2003). In order to generate this force, molecular motor proteins of the kinesin superfamily must coordinate their catalytic ATP hydrolysis activity with conformational changes in both their microtubule binding and force generating regions. Additionally, different members of the kinesin superfamily are able to move in opposite directions along microtubules; either toward the plus-end or the minus-end, and some subfamilies do not move at all but rather regulate microtubule polymerization and depolymerization (Wordeman, 2005). While not entirely understood, the specific pathways of mechanochemical coupling between the nucleotide binding site, filament binding site, and force generating regions in kinesins have become more clearly described in recent years with the publication of exciting new high resolution crystal structures, medium resolution cryo-EM studies, and spectroscopic experiments. Additionally, structural and functional studies continue to highlight similarities in both the structure and mechanism of kinesins and myosins, allowing a number of comparisons to be made. Taken as a whole, these studies provide a detailed picture of the various pathways of conformational change utilized in kinesin family members in order to generate directional force along microtubules.

Nucleotide binding motifs

The pathway of conformational change in kinesins begins at the nucleotide binding pocket, where three highly conserved structural motifs coordinate both catalytic activity as well as the initial conformational response to nucleotide hydrolysis state. The first motif is the phosphate binding P-loop, whose primary role is to stabilize nucleotide binding through numerous interactions with the phosphates of the ATP and its coordinated Mg^{2+} ion (Figure 1). The P-loop, sometimes referred to as a Walker A motif, is evolutionarily conserved not only in amino acid sequence (GXXXXGKS/T), but also in structure in proteins as diverse as G-proteins, kinesin, myosins, helicases, and kinases. It assumes an essentially rigid structure in almost all known high resolution crystal structures (Kull et al., 1998). The other two motifs, the switch I and switch II loops, are responsible for responding to nucleotide presence, absence, and hydrolysis state, in large part through sensing the presence or absence of gamma-phosphate, thereby instigating an initial conformational change that is passed along to the force generating regions of the motor. It is thought that each of the two loops can be in either an ‘open’ or a ‘closed’ position with respect to the nucleotide, giving four possible configurations for switch I and switch II: open-open, open-closed, closed-open, and closed-closed (Kull and Endow, 2004; Reubold et al., 2003).

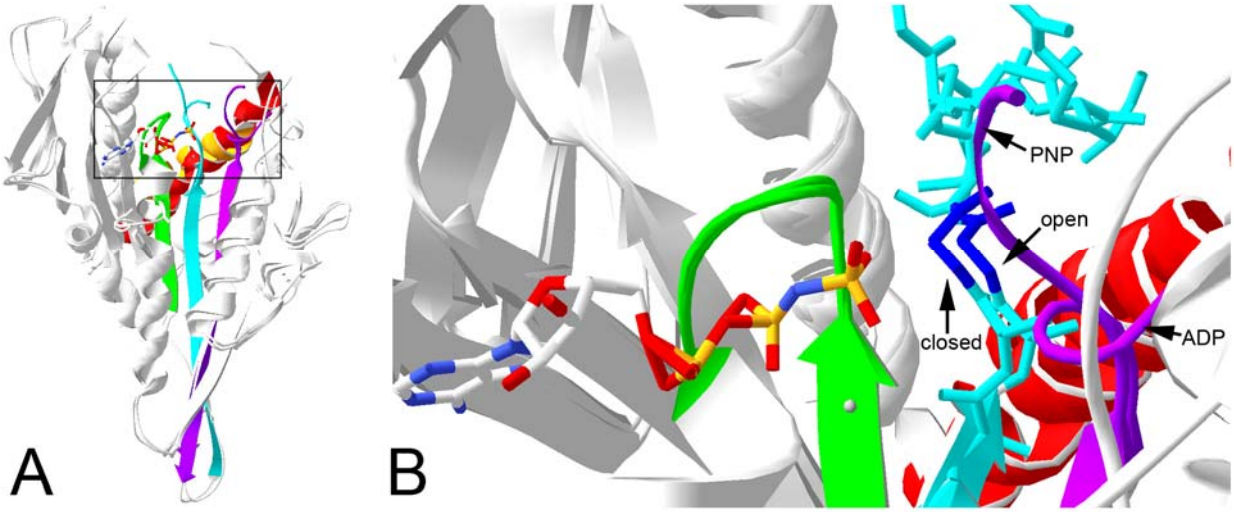

Figure 1: The nucleotide binding switch region of kinesin family molecular motors. A. Global view of superposed Kif1a kinesin motor domains, showing bound nucleotide (AMP-PNP), the P-loop (green), switch I (magenta), switch II (cyan), and the relay helix (orange/red). **B.** Close-up of the region boxed in A showing the change in position of the conserved switch II glycine (dark blue) in the AMP-PNP ('closed') versus ADP ('open') states. The main chain amide of the glycine moves 1.4 Å towards the bound nucleotide in the 'closed' state, forming a hydrogen bond with the gamma-phosphate and triggering a movement of the relay helix (shown in red). Switch I also changes conformation in the two structures (magenta). The Kif1a structures used for figures in this paper are PDB ID number 1I5S (ADP) and 1VFW (AMP-PNP) (Nitta et al., 2004).

The primary gamma phosphate sensor involves a highly conserved glycine residue in switch II, whose amide nitrogen forms a hydrogen bond with the gamma phosphate of ATP, pulling the switch II loop in towards the nucleotide binding site, into what is referred to as the 'closed' position. In the absence of gamma-phosphate, the hydrogen bond can not be formed, and the switch II loop moves out, into the 'open' position. As seen in Figure 1B, the movement of the switch region is only about 1.4 Å between the 'open' and 'closed' conformations; however in myosins the switch II moves 4 Å between the two states. The movement of switch II into and away from the gamma-phosphate region is the initial conformational response of the motor to nucleotide hydrolysis state. From here, the pathway of mechanochemical coupling leads through the relay helix on the opposite side of the motor domain, as discussed in detail below.

The role of switch I in the catalytic region is less clear as in most kinesin family crystal structures the conserved residues (SSR) are contained in a short region of alpha helix, not directly interacting with the Mg^{2+}-ATP, forming the switch I 'open' conformation. However, in several structures the switch I loop takes on alternate structure in which it can form interactions with the nucleotide, assuming the switch I 'closed' conformation. Interestingly, in the related molecular motor myosin, conserved switch I residues are almost always seen interacting with the bound Mg^{2+} ion and nucleotide (switch I 'closed'). As myosins hydrolyze ATP when they are unbound to actin, whereas kinesins hydrolyze ATP when they are bound to microtubules, it is possible that in kinesins the specific interactions of switch I residues with the Mg^{2+} ion that result in a catalytically competent arrangement are stabilized only when kinesin is in a microtubule-bound conformation. This would provide a mechanism by which microtubule binding could activate hydrolysis (Naber et al., 2003).

A final notable feature of the nucleotide binding region is the presence of a salt bridge between a conserved arginine in switch I and a conserved glutamate in switch II. Formation of a salt bridge between these residues, which are conserved in all kinesins as well as all myosins, appears to depend on the relative orientation of the two switch loops. If switch I and switch II are either both 'open' or both 'closed', the salt bridge can form, however if they are in different states, the salt bridge can not form. The exact role the salt bridge plays in the hydrolysis cycle is unclear, but a reasonable role could be in locking the active site into a hydrolysis competent conformation. Another possibility is that in the broken salt bridge conformations charge-charge interactions could be used to assist in the catalytic cycle. For example, the proximity of an unpaired arginine (switch I 'closed', switch II 'open') to the nucleotide binding site could assist in stabilizing ATP binding, while the presence of an unpaired glutamate (switch I 'open', switch II 'closed') could assist in elimination of phosphate following hydrolysis.

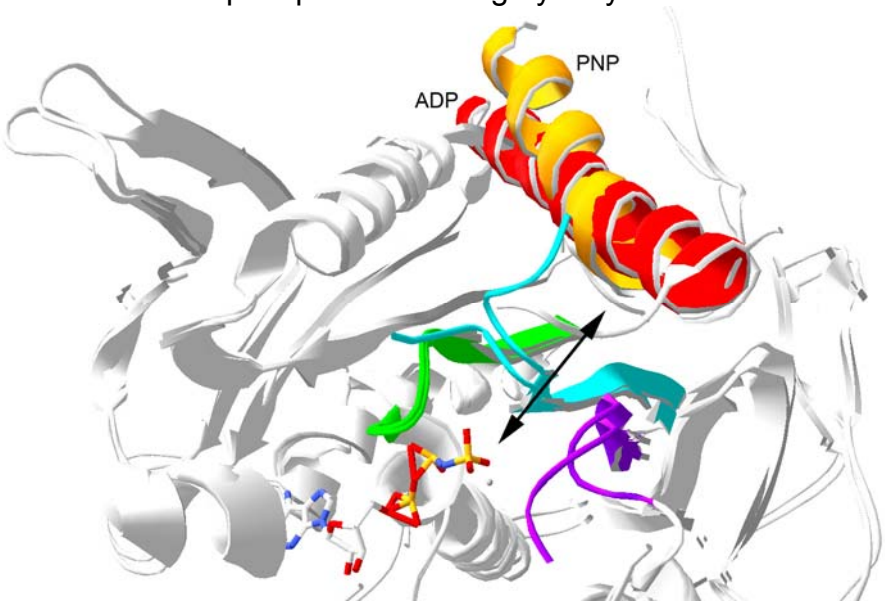

Figure 2: The pathway of mechanochemical transduction between the nucleotide binding site and the relay helix. View of the Kif1a motor domain looking down on the nucleotide binding site, oriented such that the front of the motor domain is at the bottom of the figure and the back is at the top. AMP-PNP and ADP structures are superposed in order to highlight differences in the orientation of the relay helix, shown in red for the ADP state and orange for the AMP-PNP state. The black arrow shows the pathway of conformational change. Note that loop 11 connects switch II (cyan) and the relay helix, but is disordered in these structures.

Relay helix

Following switch II is loop 11, which is disordered in most of the existing kinesin crystal structures. Loop 11 leads into helix α4, also called the relay helix, which is on the opposite side of the motor domain from the nucleotide binding site (Figure 2). The relay helix, which once again has a direct homologue in myosins, is a major component of the microtubule binding interface, which also includes helix α5. The relay helix in various kinesin structures has a different orientation with respect to the rest of the motor domain, and it is thought that movement of the relay helix is triggered by the movements of the switch II region, as is also the case for myosins. Although the loop linking the relay helix and switch II is disordered in many structures, it has been suggested that microtubule binding could serve to stabilize loop 11, creating a

mechanical link between these two elements (Sindelar et al., 2002). In this way, binding to microtubules could affect the position of switch II, and conversely, the nucleotide state could affect the relay helix and microtubule binding interface. Rotation and translation of the microtubule binding region with respect to rest of the motor domain would result in a small movement of the motor domain with respect to the microtubule that would be the same for all types of kinesin motors whether they are plus-end directed, minus-end directed, or non-motile; the specific directionalities of the kinesin subfamilies appears to be dependent on differences in the linker region.

Linker region

The linker region is adjacent to the relay helix and microtubule binding interface and functions to link the motor domain to the coiled-coil dimerization domain. In existing kinesin crystal structures, the linker region takes on either: 1) the form of an extended chain in processive, plus-end directed kinesins, or 2) that of an alpha-helix in non-processive, minus-end directed subfamilies, as typified by Ncd.

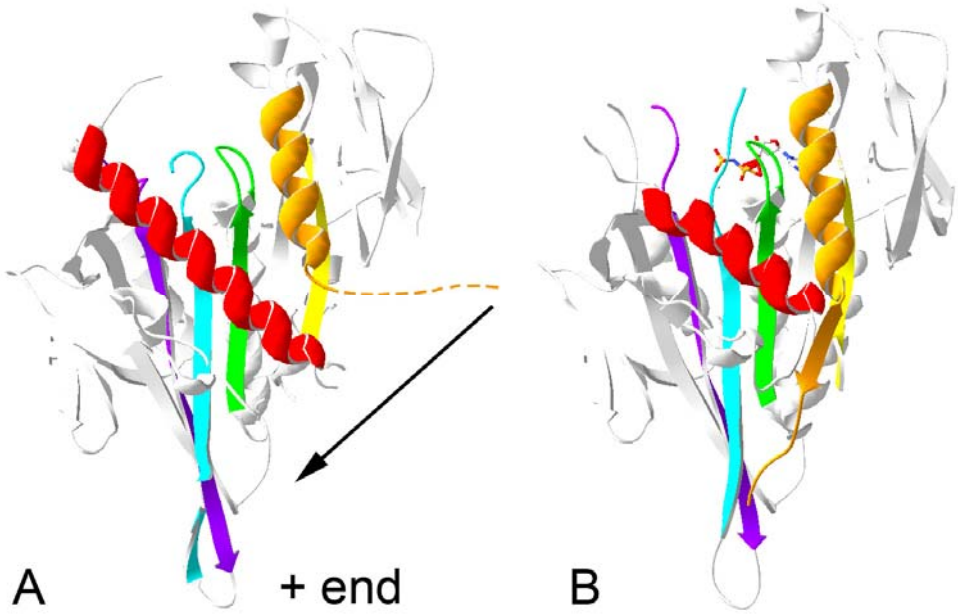

Figure 3: The nucleotide-dependent change in position of the linker region of N-terminal kinesin motor domains resulting in plus-end directed movement. A. In the structure of Kif1a in the ADP-bound state, the C-terminal linker region (orange) is disordered, as indicated by the dashed line. **B.** Upon binding ATP, it is thought that the linker region becomes ordered along the tip of the motor domain, as observed in the structure of Kif1a in the AMP-PNP bound state. The arrow indicates the direction of movement of the end of the linker region, which would be towards the plus end of the microtubule.

A number of high resolution crystal structures have shown that the conventional kinesin linker can be either well-ordered on the motor domain, or detached, and that interconversion is dependent on the state of the bound nucleotide, and to some degree upon whether the motor domain is bound to microtubules (Asenjo et al., 2006; Kikkawa et al., 2001; Rice et al., 1999). Most evidence points to a model in which ATP binding causes the linker to become ordered against the motor domain, while in the ADP-bound form is disordered. It has been suggested that the ordering of the linker in the ATP-bound form would serve to translate the unbound head of the kinesin dimer towards the

plus-end of the microtubule with respect to its position in the presence of ADP or the absence of nucleotide (Figure 3) (Rice et al., 1999).

The linker region in non-processive, minus-end directed kinesins such as Ncd takes on a very different form in which it forms a coiled-coil alpha helix with the second head of the dimer. Although in the original crystal structures of dimeric Ncd the symmetric coiled-coil placed the two heads in an equally symmetric arrangement (Kozielski et al., 1999; Sablin et al., 1998), a recent crystal structure visualized an asymmetric arrangement of heads with respect to the linker (Yun et al., 2003). Furthermore, cryo-EM studies of the Ncd-microtubule complex in the absence of nucleotide or the presence of AMP-PNP or ADP-AlF_4^- indicate that the helical linker region is acting as a lever arm which rotates ~70° towards the minus end of the microtubule as an ATP analogue binds to the motor head (Figure 4) (Endres et al., 2006).

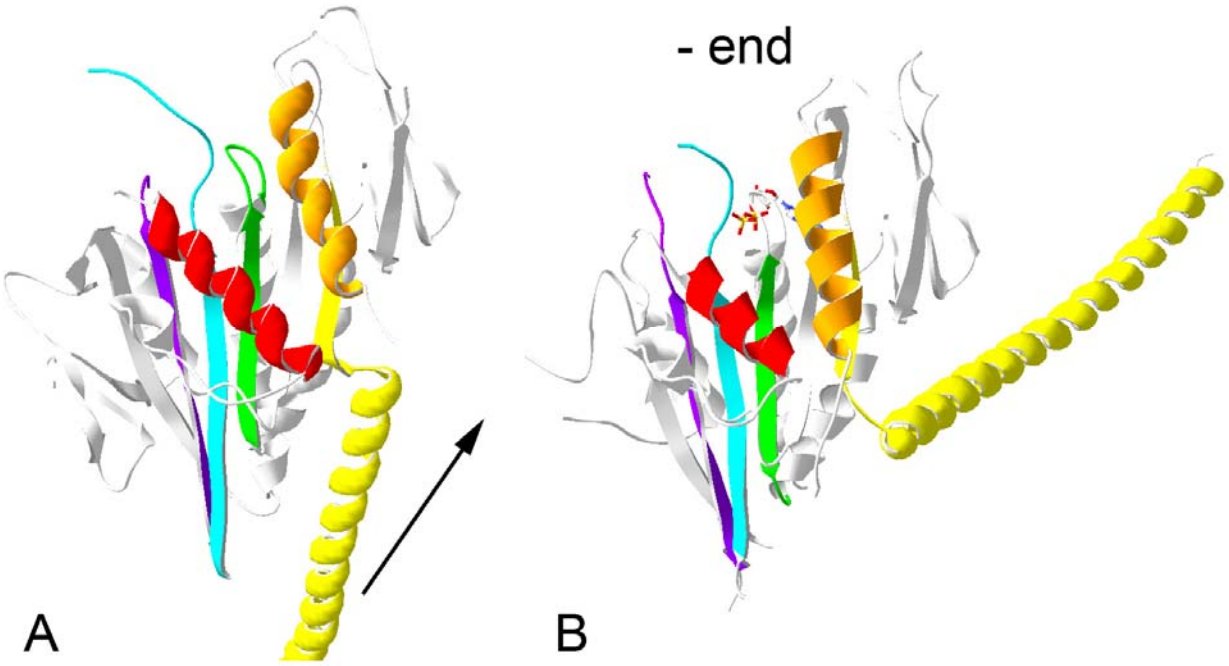

Figure 4: The nucleotide-dependent change in position of the helical linker region of C-terminal kinesin motor domains resulting in minus-end directed movement. A. In the structure of one head of the Ncd dimer, the N-terminal linker region (yellow) is in close contact with the tip of the motor domain. **B.** In the second head of the dimer, the linker helix assumes a very different orientation. The result of the linker movement, as shown by the arrow, is a translation of its end towards the microtubule minus end. The dimeric Ncd structure used in the figures in this paper is unpublished (Kull and Endow, unpublished results) but closely resemble the Ncd structure PDB ID number 1N6M (Endres et al., 2006; Yun et al., 2003).

Despite the fact that the motor domains of kinesin and Ncd are located, respectively, at the N-terminal and C-terminal ends of the molecules and because of this their linkers are at opposite ends of the polypeptide chain, their linker regions emerge from the motor domains separated by only about 4 Å (Figure 5). Due to this proximity, movements of the relay helix and microtubule binding region could easily affect the structure of linker region, allowing the extended linker of conventional kinesin to undergo its transition between an ordered and a disordered state or, similarly,

allowing the helical linker of Ncd to either pack against the motor core or be released from it.

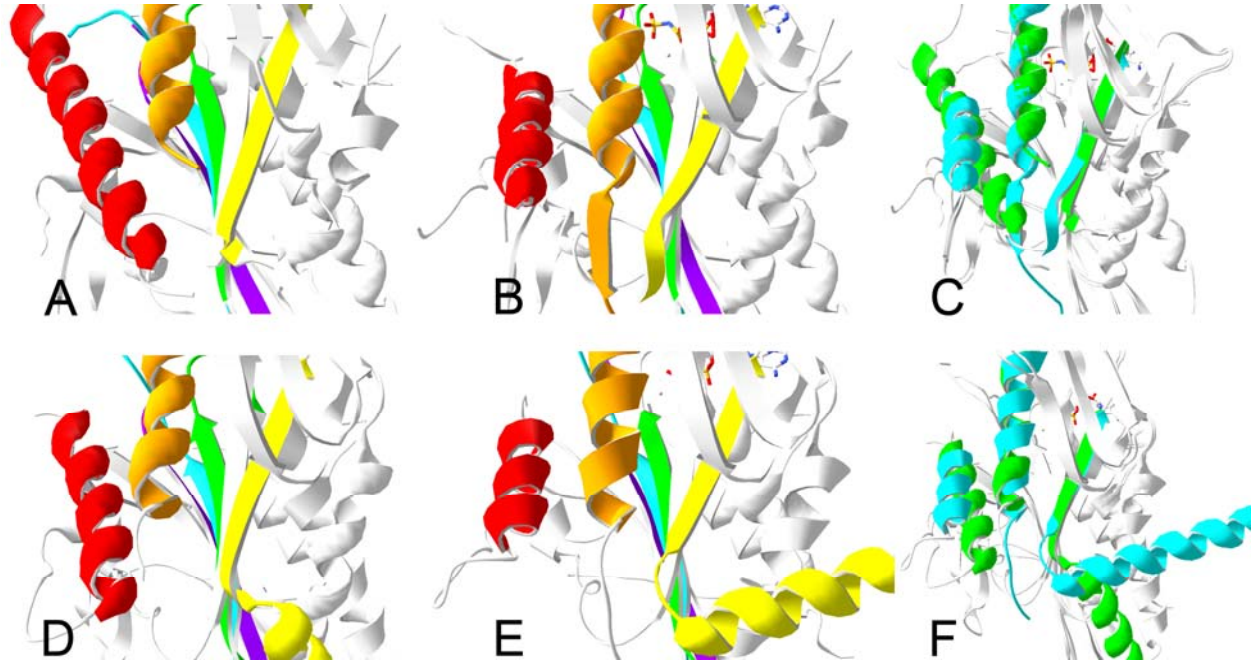

Figure 5: The mechanochemical link between the relay helix and the linker regions in N- and C-terminal kinesin motors. A. Kif1a in the ADP-bound state, as in Figure 3A. The C-terminal linker region is disordered following helix α6 (orange). Note the proximity of the N-terminal β1 strand (yellow) to helix α6. **B.** In Kif1a with AMP-PNP bound, the linker region (orange) is now ordered. **C.** Superposition of the structures shown in A (green) and B (cyan) highlighting the change in conformation of the relay helix, linker region, and N-terminus. **D.** The same structural elements in Ncd as seen in Figure 4A, with the linker helix oriented towards the microtubule plus-end. **E.** Ncd with the linker in the minus-end conformation. **F.** Superposition of D (green) and E (cyan). Note the similarities between the orientations of the relay helices (red) of Kif1a and Ncd in panels A/D and B/E as well as the extended ordering of the C-terminus of Ncd in panel E (extending from the orange α6 helix) in much the same manner as the ordering of the C-terminal linker of Kif1a in panel B.

Frontiers

The structures and studies discussed in this paper reveal a relatively clear picture of the pathway of conformational change leading from the nucleotide binding site of kinesin to its microtubule binding site and linker region. To summarize, the mechanochemical pathway is likely incomplete until the motor binds to microtubules, thereby stabilizing loop 11 and forming a link between switch II and the relay helix. Once this link is established, the presence or absence of gamma phosphate is linked to a movement of the relay helix, an integral part of the microtubule binding region. Translation and rotation of the microtubule binding interface causes a small movement of the motor domain toward the plus-end of microtubules, but, more importantly, affects the conformation of the adjacent linker region. In conventional kinesins, it is thought that ATP binding causes the linker to become ordered on the motor domain, moving the unbound head towards the plus-end of the microtubule. In the minus-end motors, a very similar movement of the microtubule binding interface causes a rearrangement of the helical linker region, resulting in a lever arm swing towards the minus end of the microtubule.

Kinesin family members have used exquisitely clever nanoengineering to utilize a conserved molecular engine to produce movement in different directions or to regulate microtubule polymerization state. Even more intriguing is the observation that myosins use almost exactly the same initial pathway of mechanochemical transduction during force-generation; they have virtually identical switch I and switch II motifs, have a relay helix in the same position, and all three of these structures undergo homologous movements. The mechanism utilized by myosin diverges from that used by kinesin in that its relay helix becomes kinked when switch II is in the 'closed' position. The kink triggers a rotation of the end of the relay helix and the adjacent converter domain, causing myosin's lever arm to swing. As in the case of conventional kinesins and Ncd, myosins have modified the same core motor activity, in this case producing movement along a completely different protein filament.

While crystallographic and other experimental data have illuminated much of the mechanochemical pathway employed by kinesin motors, a major missing piece is the high resolution structure of a kinesin-microtubule complex. Not only would such a structure clarify the exact residues that are involved in the polymer binding interface, but it would likely illuminate the details of how binding to microtubules affects both the linker region and the catalytic pocket. As described above, existing structures of kinesin in the absence of microtubules suggest that polymer binding stabilizes a link to the nucleotide binding site, subsequently allowing switch I and switch II to assume a catalytically competent conformation, however confirmation of this theory, as well as a description of the detailed mechanism awaits the solution a high resolution complex structure.

References

Asenjo, A. B., Weinberg, Y., and Sosa, H. (2006). Nucleotide binding and hydrolysis induces a disorder-order transition in the kinesin neck-linker region. Nat Struct Mol Biol *13*, 648-654.

Endres, N. F., Yoshioka, C., Milligan, R. A., and Vale, R. D. (2006). A lever-arm rotation drives motility of the minus-end-directed kinesin Ncd. Nature *439*, 875-878.

Hirokawa, N., and Takemura, R. (2004). Kinesin superfamily proteins and their various functions and dynamics. Exp Cell Res *301*, 50-59.

Kikkawa, M., Sablin, E. P., Okada, Y., Yajima, H., Fletterick, R. J., and Hirokawa, N. (2001). Switch-based mechanism of kinesin motors. Nature *411*, 439-445.

Kozielski, F., De Bonis, S., Burmeister, W. P., Cohen-Addad, C., and Wade, R. H. (1999). The crystal structure of the minus-end-directed microtubule motor protein ncd reveals variable dimer conformations. Structure *7*, 1407-1416.

Kull, F. J., and Endow, S. A. (2004). A new structural state of myosin. Trends Biochem Sci *29*, 103-106.

Kull, F. J., Vale, R. D., and Fletterick, R. J. (1998). The case for a common ancestor: kinesin and myosin motor proteins and G proteins. J Muscle Res Cell Motil *19*, 877-886.

Naber, N., Minehardt, T. J., Rice, S., Chen, X., Grammer, J., Matuska, M., Vale, R. D., Kollman, P. A., Car, R., Yount, R. G.*, et al.* (2003). Closing of the nucleotide pocket of kinesin-family motors upon binding to microtubules. Science *300*, 798-801.

Nitta, R., Kikkawa, M., Okada, Y., and Hirokawa, N. (2004). KIF1A alternately uses two loops to bind microtubules. Science *305*, 678-683.

Reubold, T. F., Eschenburg, S., Becker, A., Kull, F. J., and Manstein, D. J. (2003). A structural model for actin-induced nucleotide release in myosin. Nat Struct Biol *10*, 826-830.

Rice, S., Lin, A. W., Safer, D., Hart, C. L., Naber, N., Carragher, B. O., Cain, S. M., Pechatnikova, E., Wilson-Kubalek, E. M., Whittaker, M.*, et al.* (1999). A structural change in the kinesin motor protein that drives motility. Nature *402*, 778-784.

Sablin, E. P., Case, R. B., Dai, S. C., Hart, C. L., Ruby, A., Vale, R. D., and Fletterick, R. J. (1998). Direction determination in the minus-end-directed kinesin motor ncd. Nature *395*, 813-816.

Sindelar, C. V., Budny, M. J., Rice, S., Naber, N., Fletterick, R., and Cooke, R. (2002). Two conformations in the human kinesin power stroke defined by X-ray crystallography and EPR spectroscopy. Nat Struct Biol *9*, 844-848.

Vale, R. D. (2003). The molecular motor toolbox for intracellular transport. Cell *112*, 467-480.

Wordeman, L. (2005). Microtubule-depolymerizing kinesins. Curr Opin Cell Biol *17*, 82-88.

Yun, M., Bronner, C. E., Park, C. G., Cha, S. S., Park, H. W., and Endow, S. A. (2003). Rotation of the stalk/neck and one head in a new crystal structure of the kinesin motor protein, Ncd. Embo J *22*, 5382-5389.

How the Voltage Sensor Senses Voltage in Ion Channels: Two Diametrically Opposed Views.

David J. Posson & Paul R. Selvin
Physics Dept., Univ. of Illinois, Urbana-Champaign
1110 W. Green St.
Urbana, IL 61801
Selvin@uiuc.edu

Introduction. Ion channels are membrane proteins responsible for controlling the flow of ions (sodium, potassium, chloride, calcium…) across nerve and other cell membranes. Voltage-controlled sodium and potassium ion channels are a particularly important class of such channels. It is the transient opening and closing of these channels that underlie nerve impulses, or action potentials. The conductivity of these channels are controlled by the voltage across the cell membrane and mutations in these channels cause several diseases, such as a neonatal form of epilepsy (1) and cardiac disorders (3, 4) among others. Despite their importance, and decades of intensive study, the structural changes connecting membrane voltage changes to the open and closed states of the channels are still debated. X-ray crystallography has successfully detailed the permeation pathway (the pore domain) for potassium channels (5-7). However,

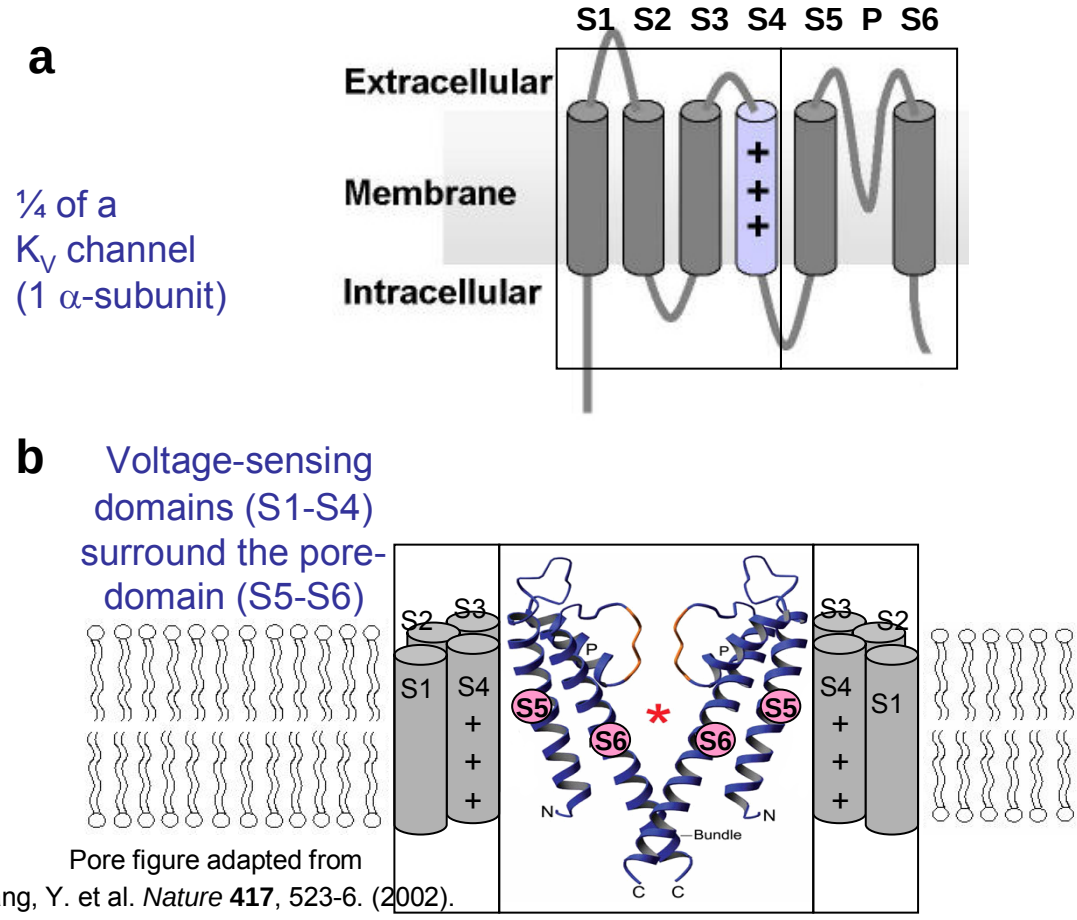

Figure 1. General structure of the voltage-gated K+ channel. **a.** Each subunit consists of 6 transmembrane segments S1-S6. S4 is called the principle voltage-sensor because it carries charged residues that are transported across the membrane by voltage changes. **b.** The voltage-sensing domain is made of segments S1-S4, which surround the pore-domain (S5-S6). Only two subunits are shown for clarity.

the X-ray data for the segments of protein responsible for voltage sensitivity have failed to clarify voltage-sensing. Rather it has incited controversy (8-10), with major questions remaining. Specifically, the highly charged segments, called the **S4 voltage-sensors** (see Fig. 1), move charge across the membrane electric field when the channel opens, but what is the nature of this movement? Is there a significant S4 voltage-sensor translation perpendicular to the membrane (2, 11, 12)? Does this segment rotate, moving charges across a narrow protein-formed gasket (13, 14)? Do the S1 through S3 segments of the voltage-sensing domain move (9, 15, 16)? How are the voltage-sensing subunits structured around the pore domain? Answering these questions is of fundamental importance for a detailed understanding of how voltage-gated channels work.

K_V channels (voltage-gated K^+ channels) are homotetramers, with each subunit containing 6 transmembrane helices, denoted S1-S6 (Fig. 1), and a pore-forming loop (P) that contains the K^+ specific selectivity filter. The channel topology of Fig. 1 is further divided into two major functional parts. S5-S6 is called the 'pore-domain' because these segments make up both the pore and the gate. Every K^+ channel contains a pore domain homologous to S5-S6. S1-S4 is called the 'voltage-sensor domain' because it contains the structural elements responsible for voltage sensitive gating. S4 is called the 'primary voltage-sensor' because it is highly charged and interacts with the membrane electric field in order to couple the gate (open probability) to voltage changes.

Voltage-Sensor Controversy. In 2003, Roderick MacKinnon's lab published a new model of voltage-sensing based on their crystal structure of an archaebacterial voltage-gated channel, KvAP (2). The new model was called the "paddle model" because the principle voltage-sensor S4 was observed to form a helix-turn-helix motif with S3 (actually just part of S3, called S3b), and the structure looked paddle-like (Fig. 2). The paddle model consists of two very striking features which fly in the face of the generally accepted views shared among the conventional models. 1) The S4-voltage-sensor was placed at the

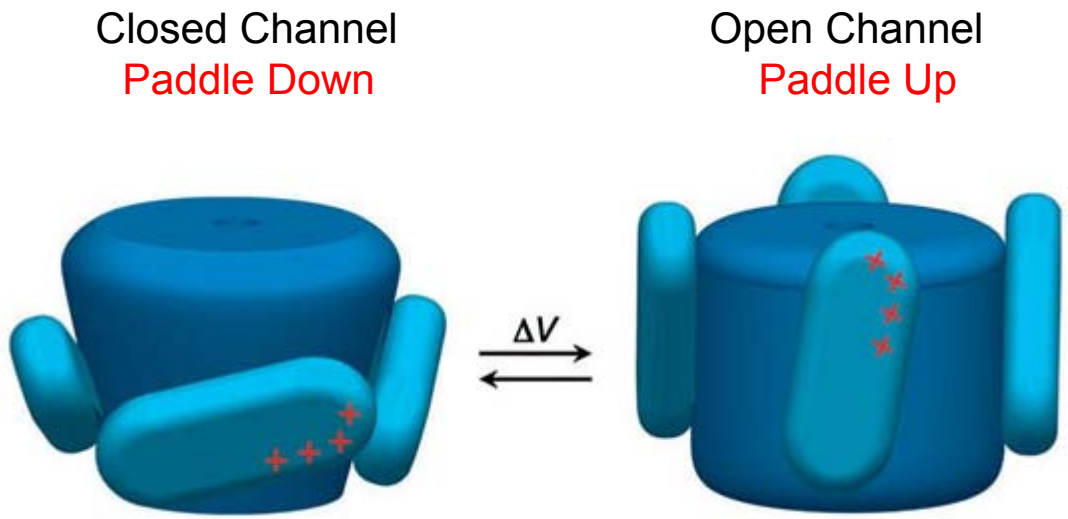

Figure 2. MacKinnon's "paddle model" in cartoon form from Jiang et al. 2003 (2). **Left.** In the closed channel state, the paddles (S3b-S4 segments) are near the intracellular solution at the periphery of the protein. **Right.** Membrane depolarization causes the paddles to move upward towards the outside solution, transporting their charge across the membrane and pulling on the K^+ pathway gate.

periphery of the protein, and in particular, the charges were allowed to make contact with the lipid membrane, despite the energetic cost of such exposure. 2) The S3b-S4 paddle structure was hypothesized to undergo a large transmembrane displacement, generally from the bottom of the membrane to the top (Fig. 2, taken from (2)). Since the paddle was hypothesized to undergo such a large displacement (15-20 Å (2)) through the membrane environment, it was described as a highly mobile *hydrophobic* cation.

MacKinnon and coworkers sought to experimentally test the paddle model. A bacterial toxin-channel called colicin forms a voltage-dependent channel with a charged segment that traverses the membrane bilayer. Finkelstein and coworkers used biotin-linkers attached to the translocating region to show that a biotin-binding protein, called avidin, could attach to the linker from the internal solution or the external solution depending on the state of the channel (17-19). This type of experiment could be described as an accessibility experiment using a fishing line that can determine how deep in the membrane a protein site is located. MacKinnon applied this technique to the KvAP paddle in order to test that the paddle is near the bottom of the membrane when the channel is closed and translocates to the top during opening (Fig. 3) (2).

Sites along S3b and S4 were labeled with the biotin linker fishing line and labeled KvAP was subsequently reconstituted into lipid bilayers so that the channels could be voltage-clamped. A control current trace was recorded before the addition of avidin protein. Next, avidin was added to either the inside or the outside solution and the resulting affect on the current was recorded. For all sites on S3b and sites at the top of S4, current inhibition occurred upon addition of avidin to the external solution. Membrane depolarization significantly speeded up this inhibition. For two sites on S4, inhibition occurred upon addition of avidin to both the internal solution when the channel was closed and the external solution when the paddle was open. This behavior is attributed to the biotin linker being dragged from the inside solution to the external solution upon channel opening. For two sites lower down on S4, inhibition occurred upon addition of avidin from the internal solution and never from the external solution. This pattern of behavior was used to constrain how deep residues on the paddle could be in the membrane as a function of voltage. These results were in agreement with the proposed paddle-model and were reinforced by a more thorough investigation later (20). However, these results are not consistent with the conventional models derived from many different types of biophysical experiments on

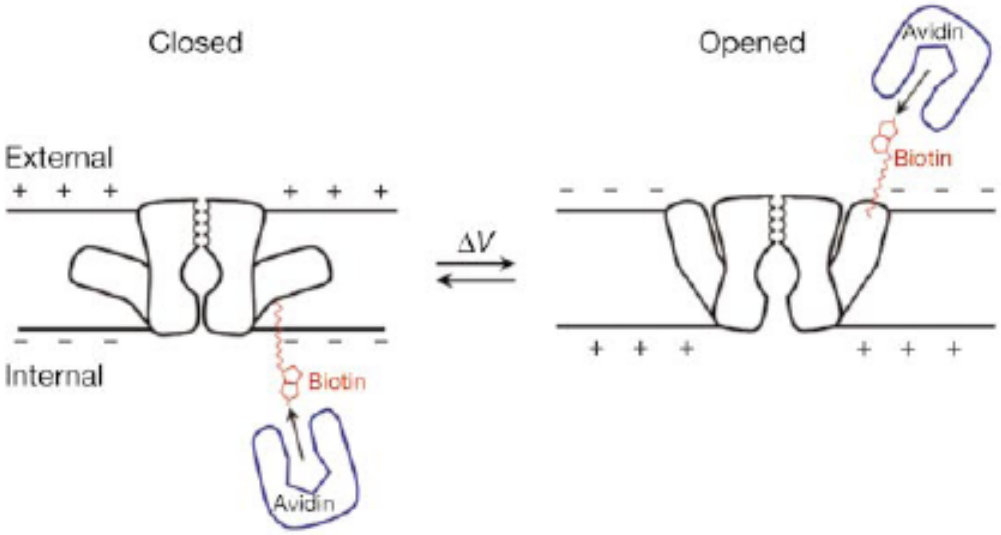

Figure 3. Experimental cartoon for testing KvAP paddle movement using avidin-biotin binding. When the paddle is down, biotin linked sites are expected to bind internal avidin. When the paddle is up, biotin linked sites are expected to bind external avidin. Binding from either side should cause a reduction in K^+ current. Figure taken from Jiang et al., 2003 (2).

eukaryotic potassium channels. Contentious issues have been discussed in numerous reviews (9, 10, 21).

Conventional models. Numerous studies on *Shaker* have established the aqueous accessibility of cysteine substitutions along the S4 to thiol-reactive reagents (MTS reagents) applied from either the inside or the outside solution (11, 22-24). Only a small fraction (~10 amino acids) of S4 is not in contact with water, and moving the channel from closed to open shifts which residues are buried. These changes are shown in a topological cartoon (Fig. 4) taken from Larsson, 1996 (11). Accessibility results demonstrating a watery-environment for S4 motivated a generation of voltage-sensor models that include watery invaginations that penetrate the protein and put much of S4 in contact with the inside and outside solutions. These watery crevices are imagined to form a 'gating canal' or 'gating-pore' through which the S4 moves its gating charges. In general, three types of protein movement have been commonly used to model voltage-gating. 1) S4 translates in the "up" direction perpendicular to the membrane towards the external solution (25); Larsson, 1996 #652; Durell, 1992 #728}. This type of motion is implied in the topological diagram Fig. 4. 2) S4 rotates about its axis, moving charges from one aqueous crevice to another (13, 14). 3) Aqueous crevice reshaping (9, 15, 16). These three types of

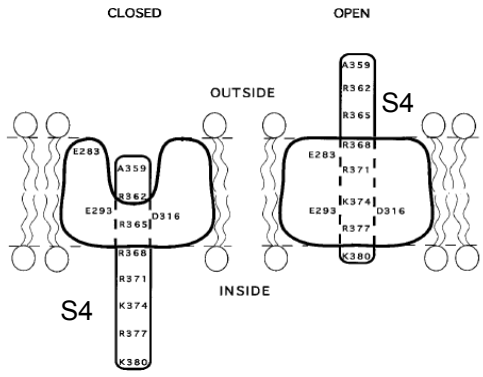

Figure 4 Topological changes in aqueous accessibility along the charged S4 segment moving from closed (left) to open (right) states. Figure taken from Larsson et al., 1996.

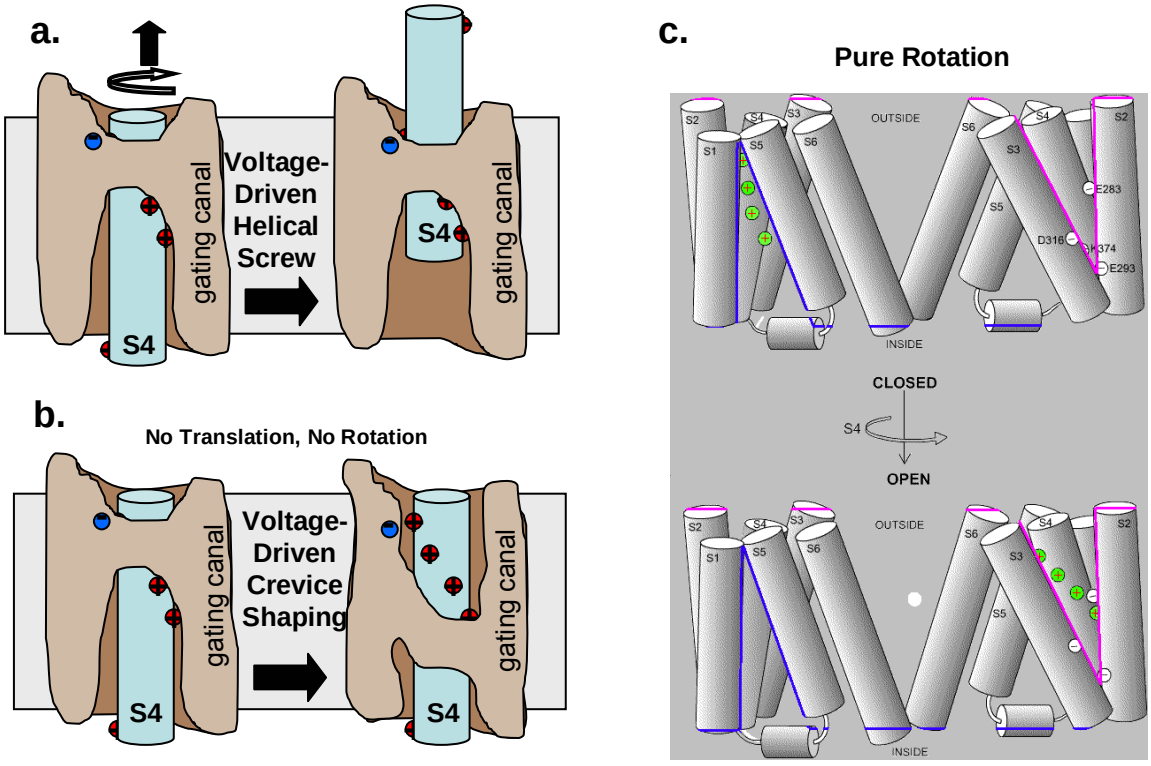

Figure 5 Conventional models of Voltage-sensing. **a.** Helical screw model in which the S4 undergoes vertical translation and rotation. **b.** Crevice reshaping model in which the S4 undergoes very little motion and the surrounding gating canal is reshaped. **c.** Rotation model in which the S4 undergoes a pure rotation, moving charges between aqueous invaginations. Only the gating canal is shown in a. and b.

protein rearrangements can exist in a number of combinations (Fig. 5 a, b, c). For instance, a model that includes both vertical translation and rotation describes the motion of S4 as a 'helical screw' (Fig. 5a). The motivation for adding a twisting movement to a vertical translation of S4 is that the counter-charges located on surrounding protein segments can then be stationary while successive S4 charges pass by. Fig. 5b shows a cartoon version of the crevice reshaping model. Fig. 5c shows the purely rotational model for S4 proposed in Cha et al., 1999 (13).

Energy Transfer Shows Small Vertical S4 Translation. Selvin and Bezanilla's groups (13) and Isacoff's group (14) first tested whether S4 undergoes a substantial vertical motion using fluorescence (FRET) and luminescence resonance energy transfer (LRET). Both are resonance energy transfer technique, with near Angstrom resolution. In both cases the authors came up with clever methods to avoid the problems of non-specific (i.e., non-voltage dependent) labeling. The LRET technique also gets around the "κ^2" orientation problem of FRET: i.e. the inferred distance is essentially independent of the donor's and acceptor's fluorophore's orientation (Formally, the energy-transfer distance is independent of the donor's orientation, leading to a worst case of 12% deviation from $\kappa^2 = 2/3$, the value of complete dis-orientation, and the acceptor's orientation has a millisecond to relax, a million-times longer than the usual ~nanosecond.).

The conclusions of both experiments was that S4-voltage sensor underwent a rotation, with a possible small (< 4Å) translation. Unfortunately, the directions of rotation were in the opposite directions! To this day, it has not been resolved.

More recently, we therefore set out to test, using our LRET technique, whether the voltage-sensor moves a large distance, or a small one. To achieve this, we placed the lanthanide donor probe on the voltage-sensor itself and monitored energy transfer to acceptor dyes that were labeled to the top of the ion channel with the use of a scorpion toxin peptide (Fig. 6). Fig. 7, demonstrating the very small movements of the voltage-sensor domain and supporting the 'standard model', was published in *Nature* as a result (26). The paddle model is not consistent with measurement of distance changes.

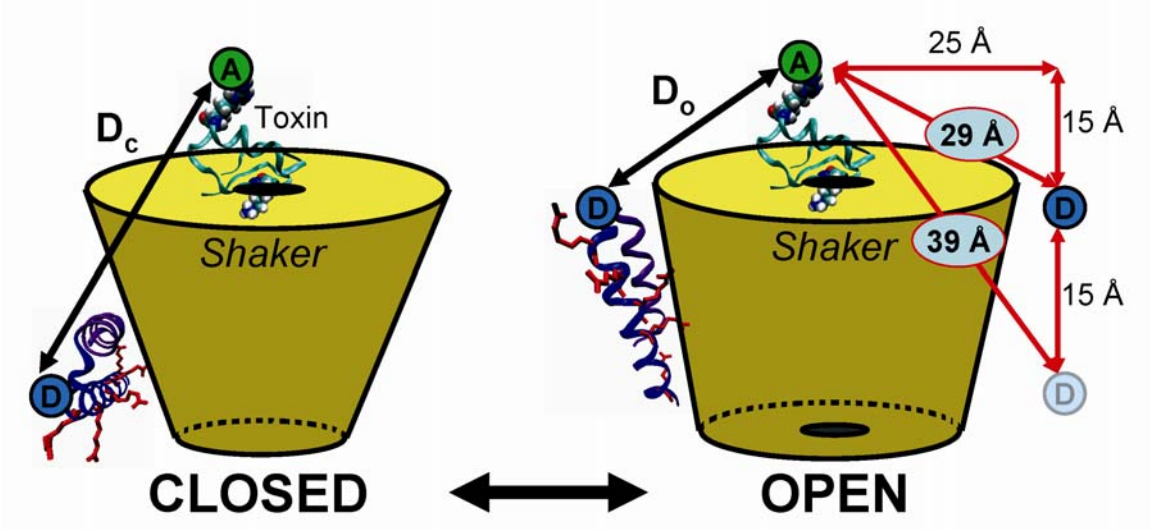

Figure 6 Testing the Paddle model with LRET. Lanthanide donors (D) are labeled to cysteine substitutions on the voltage sensor. Acceptor fluorophores (A) are attached via a scorpion toxin (charybdotoxin). Changes in distance between donor and acceptor are measured, Dc – Do. For the paddle model, distances changes of about 10 Å are expected from a vertical movement of 15-20 Å.

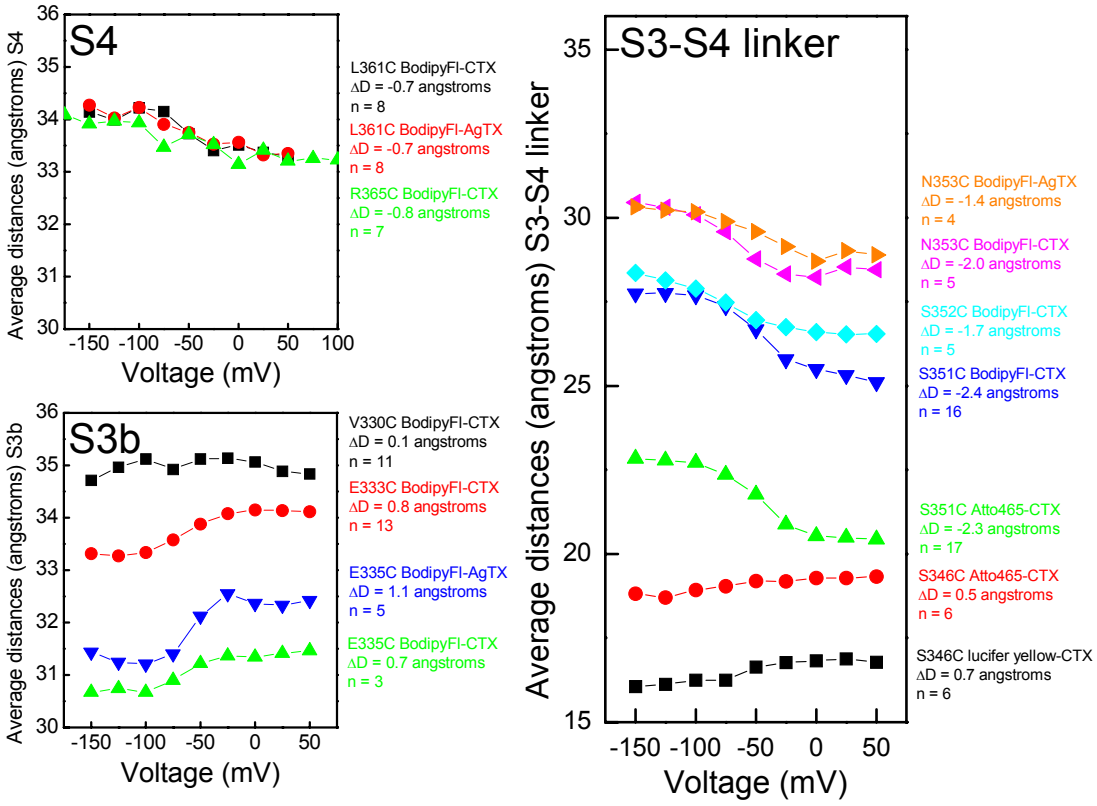

Figure 7 Distance measurements for sites within the voltage-sensor. Small changes on the order of 1-2 Angstroms are observed at multiple sites on S3, S4, or the connecting S3-S4 linker segment. These changes are not consistent with the Paddle model for voltage-sensing.

Reconciliation. It seems likely that the original x-ray crystallography paper in KvAP is a distorted structure. Indeed, it is useful to remember that the paddle model resulted from a crystal structure known to be distorted. Also, a more recent Kv channel structure (27, 28), that of Kv1.2, showed a very different arrangement of S1-S4. At this time, it is unknown how the avidin-binding experiments of MacKinnon can be reconciled with the small movements demonstrated by our LRET experiments. Benoit Roux and Pancho Bezanilla made an unpublished calculation about whether one could get cross-linking between an avidin attached to the voltage sensor, and biotin, based on the ion channel going into a rare conformation. That is, the native conformation of the sensor (N) makes briefs excursions to a distorted state (D) where avidin can trap the biotin (T):

$$N \underset{k_2}{\overset{k_1}{\rightleftharpoons}} D \underset{k_b}{\overset{k_f}{\rightleftharpoons}} T$$

Lifetime of the N state is $1/k_1$, and the probability of being in the distorted state = $k_1/(k_2+k_1) \sim k_1/k_2$ (because $k_1 << k_2$). The well-known biotin-avidin reaction rates: are: $k_{on} = 1.35 \times 10^8 sec^{-1}M^{-1}$; $k_b = 5.4 \times 10^{-6} sec^{-1}$, $K_{eq} = 2.5 \times 10^{13}\ M^{-1}$ and a molecular weight of avidin = 14,000 {Chilkoti, 1995 #2133}. In the Ruta et al. paper (20), the avidin concentration was 40 to 100 μg/ml, so assuming 50 μg/ml, then k_f is about 482 sec^{-1}. This means that if the probability of going into D is only 1/10000, after 2 min of exposure to avidin (their experiments) 100% of the channels get trapped by avidin. Clearly then, it is possible for the ion channel to go into these rare conformations and become trapped by the avidin-biotin. What is

needed is for the Ruta et al. experiments to be repeated where the kinetic rates of the reaction are given, rather than just "one number," and also to repeat them with small concentrations of avidin to eliminate the possibility that trapping is from a distorted state with such a low probability.

On the other hand, realizing that their results were in direct contraction to the LRET results (13, 26) (ignoring the FRET results (14)), Ruta et al. (20), said that the LRET results were not calibrated, i.e. they were not done on a well-defined membrane system of known distances. More relevant is that LRET measurements tend to measure the distance of closest approach between positions. Therefore, some degree of underestimation of distance can occur. This means that the voltage sensor motion may be somewhat larger than the 1-2 Angstrom movements that we measure with LRET, but quite unlikely to be 15-20Å. (In addition, another paper submitted to PNAS has confirmed that the distances in the pore of the KvAP, indicating that the distances measured by LRET are accurate (Anna Correa et al, PNAS, submitted).

Another possibility is that the two ion channels, KvAP, and Shaker, are different, and the KvAP undergoes a trans-membrane movement, and the Shaker does not (29). This rather appealing scenario was presented by Catterall, as a likely (theoretical) possibility. Only more experiments will test the truth of the matter.

References.

1. Biervert, C., Schroeder, B. C., Kubisch, C., Berkovic, S. F., Propping, P., Jentsch, T. J. & Steinlein, O. (1998) *Science* **279,** 403-6.
2. Jiang, Y., Ruta, V., Chen, J., Lee, A. & MacKinnon, R. (2003) *Nature* **423,** 42-8.
3. Bennett, P. B., Yazawa, K., Makita, N. & George, A. L. J. (1995) *Nature* **376,** 683-5.
4. Chen, Q., Kirsch, G., Zhang, D., Brugada, R., Brugada, J., Brugada, P., Potenza, D., Moya, A., Borggrefe, M., Breithardt, G., Ortiz-Lopez, R., Wang, Z., Antzelevitch, C., O'Brien, R., Schulze-Bahr, E., Keating, M., Towbin, J. & Wang, Q. (1998) *Nature* **392:,** 293-6.
5. Zhou, Y., Morais-Cabral, J. H., Kaufman, A. & MacKinnon, R. (2001) *Nature* **414,** 43-48.
6. Jiang, Y., Lee, A., Chen, J., Cadene, M., Chait, B. T. & MacKinnon, R. (2002) *Nature* **417,** 523-6.
7. Zhou, M. & MacKinnon, R. (2004) *J Mol Biol* **338,** 839-46.
8. Miller, G. (2003) *Science* **300,** 2020-2.
9. Ahern, C. A. & Horn, R. (2004) *Trends Neurosci* **27,** 303-7.
10. Cohen, B. E., Grabe, M. & Jan, L. Y. (2003) *Neuron* **39,** 395-400.
11. Larsson, H. P., Baker, O. S., Dhillon, D. S. & Isacoff, E. Y. (1996) *Neuron* **16,** 387-97.
12. Durell, S. R. & Guy, H. R. (1992) *Biophys. J.* **62,** 238-247.
13. Cha, A., Snyder, G. E., Selvin, P. R. & Bezanilla, F. (1999) *Nature* **402,** 809-813.
14. Glauner, K. S., Mannuzzu, L. M., Gandhi, C. S. & Isacoff, E. Y. (1999) *Nature* **402,** 813-817.
15. Vemana, S., Pandey, S. & Larsson, H. P. (2004) *J Gen Physiol* **123,** 21-32.
16. Nguyen, T. P. & Horn, R. (2002) *J Gen Physiol* **120,** 419-36.
17. Slatin, S. L., Qiu, X. Q., Jakes, K. S. & Finkelstein, A. (1994) *Nature* **371,** 158-61.
18. Qiu, X. & Pidgeon, C. (1994) *Biochemistry* **33,** 960-72.
19. Qiu, X. Q., Jakes, K. S., Kienker, P. K., Finkelstein, A. & Slatin, S. L. (1996) *J Gen Physiol* **107,** 313-28.
20. Ruta, V., Chen, J. & MacKinnon, R. (2005) *Cell* **123,** 463-75.
21. Laine, M., Papazian, D. M. & Roux, B. (2004) *FEBS Lett* **564,** 257-63.

22. Yusaf, S. P., Wray, D. & Sivaprasadarao, A. (1996) *Pflugers Arch* **433,** 91-7.
23. Baker, J. E., Brust-Mascher, I., Ramachandran, S., LaConte, L. E. W. & Thomas, D. D. (1998) *Proc. Nat. Acad. Sci. USA* **95,** 2944.
24. Wang, M. H., Yusaf, S. P., Elliott, D. J., Wray, D. & Sivaprasadarao, A. (1999) *J Physiol* **521 Pt 2,** 315-26.
25. Sigworth, F. J. (1994) *Q Rev Biophys* **27,** 1-40.
26. Posson, D. J., Ge, P., Miller, C., Bezanilla, F. & Selvin, P. R. (2005) *Nature* **436,** 848-851.
27. Long, S. B., Campbell, E. B. & Mackinnon, R. (2005) *Science* **309,** 897-903.
28. Long, S. B., Campbell, E. B. & Mackinnon, R. (2005) *Science* **309,** 903-8.
29. Yarov-Yarovoy, V., Baker, D. & Catterall, W. A. (2006) *Proc Natl Acad Sci U S A* **103,** 7292-7.

Torque generation by F1-ATPase

Hiroyuki Noji, Institute of Scientific and Industrial Research, Osaka University, Japan

F_1-ATPase, a water-soluble portion of F_oF_1-ATP synthase, is a rotary molecular motor driven by ATP. The minimum complex of F_1-ATPase as a motor is the $\alpha_3\beta_3\gamma$ complex, in which the γ subunit rotates against the stator cylinder of the $\alpha_3\beta_3$[1]. Recent single molecule studies have revealed fundamental properties of F_1-ATPase as a motor. F_1-ATPase makes a 120 degree step rotation upon one ATP hydrolysis[2]. Each step is resolved into 80 degree and 40 degree substeps, initiated by ATP binding or ATP hydrolysis respectively[3, 4]. The torque F_1-ATPase exerts is estimated to be 40 pNnm irrespective of ATP concentration, viscous load, or rotary angle[2, 5]. Thus, considerable progress has been made in understanding the reaction scheme and molecular mechanism of torque generation of F_1-ATPase, however several critical problems remain to be answered.

One of the most important questions is which chemical step is the major torque-generating step. It is postulated to be ATP binding step on the basis of the observation that 80 degree substep is triggered by ATP binding. However, F_1-ATPase has three catalytic subunits of β which conduct ATP hydrolysis reaction with a strong cooperatively; β subunits are always in different chemical states from each other, and they interconvert the states upon the γ rotation. Therefore, while one β binds an ATP molecule, the others can operate different reactions simultaneously to support torque generation.

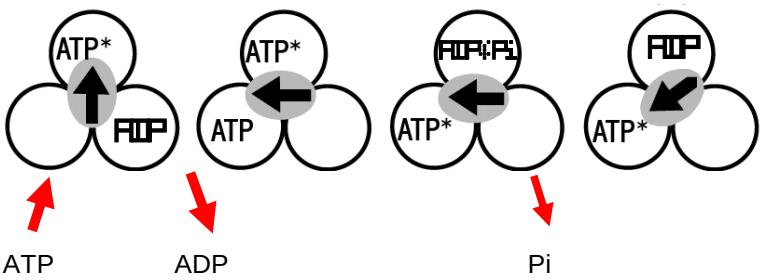

Fig.1 a possible reaction scheme of F_1-ATPase. The scheme dipcts a 120 step rotation consisting of 80 and 40 degree steps and associated reactions. Circles and arrows represent chemical states on the β subunit and rotary angle of the γ subunit.

Another question is how F_1-ATPase modulates the chemical reaction rates and equilibriums upon the rotary angle? This question arises from the reversibility of F_1-ATPase. Previously, we forcibly rotated a single F_1-ATPase molecule with magnetic tweezers to measure ATP production. In this experiment, in order to accumulate synthesized ATP molecules, a F_1-ATPase molecule was encapsulated in an extremely small reaction chamber with a volume of a few femtolitre[6] which allows us highly sensitive detection of ATP. It was revealed that the reverse rotation of the γ subunit in F_1-ATPase leads highly efficient ATP production[7]. This result means that the energetically downhill reaction can be reversed by the mechanical reverse rotation. This reversibility implies that F_1-ATPase modulates, upon the rotary angle, chemical equilibriums of each elementary reaction step such as ATP binding/release, ATP hydrolysis/synthesis, phosphate release/biding, and ADP release/binding. Regarding this point, some hints were given in early biochemical studies[8] that showed that the proton motive force across a membrane in which F_oF_1-ATP synthase molecules are reconstituted modulates chemical reaction equilibriums. However, elucidation on this point remains to be done.

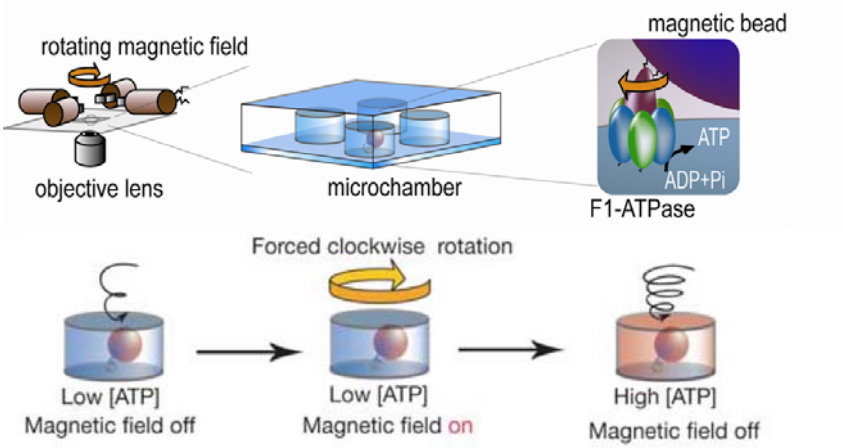

Fig.2: the experimental system for detection of ATP generation by a single F_1 ATPase molecule. F_1 ATPase encapsulated in a femtoliters chamber was reversibly rotated with magnetic tweezers, and then released to let the motor hydrolyzes newly synthesized ATP molecules. The amount of synthesized ATP was determined from the rotary velocity which reports [ATP].

The above two points are associated because the modulation of chemical equilibrium means the free energy change of the reaction; if ATP binding affinity is strongly tightened when the γ subunit rotates ahead, large amount of the free energy of ATP binding should be released upon the binding process, implying that the binding is a major torque-generating step.

Regarding modulation of reaction equilibrium, we found an interesting property of F_1-ATPase. F_1-ATPase is known to lapse into a catalytically inactive state called the ADP-inhibited form in which F_1-ATPase tightly binds ADP on the catalytic site. For re-activation of ADP-inhibited F_1-ATPase, biochemists strip the tightly bound ADP from the enzyme by using gel-filtration. We found that when an inhibited F_1-ATPase molecule was forcibly rotated in the forward direction with magnetic tweezers, F_1-ATPase resumed active rotation[9]. It means that mechanical forward rotation strips the tightly bound ADP from the catalytic site of F_1-ATPase. The probability of the mechanical activation strikingly increased in the forward direction, implying that the affinity of the inhibitory bound ADP decreases upon forward direction. Although the mechanical activation is not relevant to the active catalytic cycle of F_1-ATPase, this experimental results point to an essential property of F_1-ATPase to modulate reaction equilibrium depending on the rotary angle.

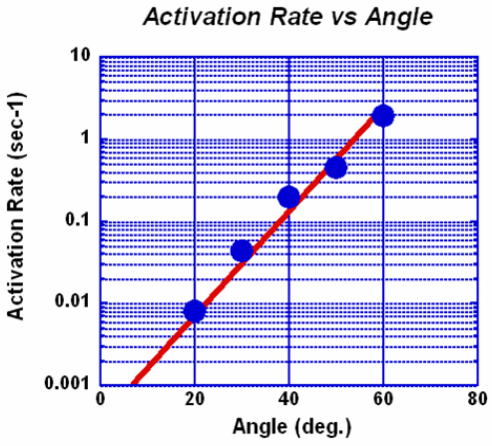

Fig.3. Rate constants of re-activation. F1-ATP molecule in the ADP-inhibited form was manipulated to forcibly rotate with magnetic tweezers. When released from magnetic field, F1-ATPase resumed active rotation with a certain probability. The probability of the resumption depends on the stall time and stall angle. From stall time dependency, the rate constant of re-activation was determined at each angle.

Currently, we are studying how F_1-ATPase modulates the ATP binding/release and ATP hydrolysis/synthesis applying the experimental strategy as same as for mechanical activation of F_1-ATPase in the ADP-inhibited form. Through these experiments, it was found that F_1-ATPase strongly tightens ATP-binding in the forward rotation. The dissociation constant decreases 10^{-4} times for 120-deg. rotation, implying that F_1-ATPase releases up to 40 pNnm of binding energy. This is the first evidence of mechanical modulation by F_1-ATPase, and a strong support for binding-driven torque generation. Interestingly, the reaction equilibrium of hydrolysis/synthesis on F_1-ATPase was found not to depend on the rotary angle as much as found in ATP-binding. It means that chemical reaction on the enzyme can not be a major torque-generating step. In the session, I will present our recent data to discuss about these issues.

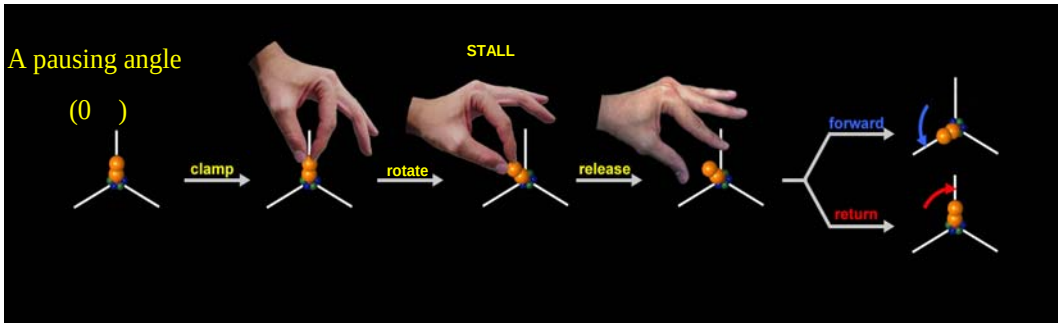

Fig.4. Experimental strategy to determine the mechanical modulation of rate constants and reaction equilibriums of F1-ATPase. 120-deg stepping rotation of F1-ATPase was observed in such a condition that ATP-binding step or ATP hydrolysis step was slowed by decreasing [ATP] or using a mutant F1 with an analog of ATP. During pausing, a motor was clamped to stall at a certain angle for a certain time period, and released. In the case where F1 has undergone an examined reaction when released, F1 jumped to a next pause angle. From the angle- and stall time-dependency, the rate constants of an examined reaction were determined at each rotary angle in the way as same as for mechanical activation.

References

1. Boyer, P. D. The ATP synthase--a splendid molecular machine. Annu Rev Biochem 66, 717-49 (1997).
2. Yasuda, R., Noji, H., Kinosita, K., Jr. & Yoshida, M. F1-ATPase is a highly efficient molecular motor that rotates with discrete 120 degree steps. Cell 93, 1117-24 (1998).
3. Yasuda, R., Noji, H., Yoshida, M., Kinosita, K., Jr. & Itoh, H. Resolution of distinct rotational substeps by submillisecond kinetic analysis of F1-ATPase. Nature 410, 898-904 (2001).
4. Shimabukuro, K. et al. Catalysis and rotation of F1 motor: cleavage of ATP at the catalytic site occurs in 1 ms before 40 degree substep rotation. Proc Natl Acad Sci U S A 100, 14731-6 (2003).
5. Noji, H. et al. Purine but not pyrimidine nucleotides support rotation of F(1)-ATPase. J Biol Chem 276, 25480-6 (2001).
6. Rondelez, Y. et al. Microfabricated arrays of femtoliter chambers allow single molecule enzymology. Nat Biotechnol 23, 361-5 (2005).
7. Rondelez, Y. et al. Highly coupled ATP synthesis by F1-ATPase single molecules. Nature 433, 773-7 (2005).
8. Zhou, J. M. & Boyer, P. D. Evidence that energization of the chloroplast ATP synthase favors ATP formation at the tight binding catalytic site and increases the affinity for ADP at another catalytic site. J Biol Chem 268, 1531-8 (1993).
9. Hirono-Hara, Y., Ishizuka, K., Kinosita, K., Jr., Yoshida, M. & Noji, H. Activation of pausing F1 motor by external force. Proc Natl Acad Sci U S A 102, 4288-93 (2005).

Determinants of Motor Directionality: Points for Discussion

H. Lee Sweeney, Chair

Introduction

Within both the myosin and kinesin superfamilies, reverse direction motors exist (myosin VI and ncd, respectively). We will review the current structural and functional evidence of how directionality reversal was achieved in each case. Do the common themes from these cytoskeletal motors provide any insight into how helicases alter directionality? Bacteria that move via redirecting actin polymerization do so without the use of a motor *per se*. What are the details of this type of movement that uses polymerization to produce force? Here the question of directionality surrounds the mechanism of guidance of the trajectory of the polymerizing filament.

To help guide the discussion, consider the following concepts and questions:

1. For both the myosin and kinesin superfamily, it appears that reversal of directionality involves repositioning of the effective lever arm, but not a redesign of the motor core. First, what are the necessary structural elements necessary for reversal of direction in myosin VI and kinesin? Does the evidence to date suggest that the motor cores of both myosin VI and ncd function as those of myosin and kinesin motors in general? That is to say, is the inherent directionality of the motor core unchanged in myosin VI and ncd? Does this create an opportunity to generate a bidirectional motor under control of a structural switch?

2. Would directionality reversal that requires redesign of the motor imply that the motor would be of a different family (e.g. kinesin vs. dynein)? This is more rhetorical than a point for discussion.

3. Helicases exist that move in either direction on DNA. Is enough known about their motor function to understand how they control directionality? If so, does the strategy for altering directionality have any parallels in the cytoplasmic motors we have been discussing?

4. To create a processive, reverse direction motor, the mechanism of gating must be fundamentally different from that used to gate the normal direction processive motor. While myosin VI has evolved a way to do this, motors in the kinesin superfamily have not. The mechanism of gating in myosin VI is more like that of kinesin than of myosin V. In turn, one could speculate that a processive ncd would have to evolve a gating mechanism that mirrors that of myosin V. Is the fact that this does not seem to have happened due to the fact that cytoplasmic dynein fills the role of a minus-end-directed processive

microtubule motor? Is it possible to alter the ncd kinetics to achieve gating? Certainly without the example of myosin VI, one might have thought that kinesin-like gating was not possible within the myosin superfamily.

5. What are the design features that allow a processive transporter to also function as an anchoring protein? Within the myosin superfamily, does being both an optimal anchor and processive motor require a specific type of gating mechanism (i.e. directionality)? Is myosin VI thus the only myosin well suited to both anchor and processively move cargoes, or have any plus-end directed motors devised a strategy allowing them to fill both niches? By analogy to myosin VI, are kinesins well suited to play an anchoring role in addition to a transport role due to the nature of their gating mechanism? What about reverse-direction kinesins?

6. For bacteria that use actin polymerization for movement rather than motors *per se*, the relevant question for discussion centers on how directed movements are achieved with actin polymerization. What mechanisms have been delineated in bacteria for movement via actin polymerization, and how much do they utilize the normal cellular processes? How is guidance of polymerization achieved (or is it)? Ultimately, what are the advantages to the bacteria of eschewing motors and co-opting actin polymerization? Is part of the advantage being able to control the trajectory of actin polymerization and thus not having to use a motor that runs on a track with a predetermined destination?

The myosin VI structure provides important insights for the mechanism of reverse directionality

J. Ménétrey (a), A. Bahloul (a), P. Llinas (a), H.L. Sweeney (b), A. Houdusse (a).
(a) Structural Motility, Institut Curie CNRS, UMR144, Paris (France)
(b) Department of Physiology, University of Pennsylvania School of Medicine (USA)

Abstract

Myosin VI is perhaps the most unconventional of unconventional myosins. It uses a number of unique mechanisms that are not well understood to accomplish processive movements of similar step sizes to myosin V, but of opposite directionality, for the purposes of anchoring and transporting cargoes within cells. We have solved the structure of this motor at the end of its powerstroke. Comparison of the structure to that of myosin V in the same state demonstrate the role of a 39 residues insert that is unique to the myosin VI class for reversing the direction of the lever arm at the end of the powerstroke.

Nature has evolved a number of molecular motors in order to accomplish motility and/or produce directed forces along cytoskeleton filaments within cells. The myosin superfamily is constituted by motor proteins that use actin filaments as their tracks and as a means to spatially rectify the conversion of chemical energy (provided by ATP hydrolysis) into mechanical energy. The current view of how myosin motors couple ATP hydrolysis and actin binding to movement is known as the "swinging lever arm hypothesis". Briefly, the motor/ATP hydrolysis cycle is coupled to small movements within the motor domain that are amplified and transmitted *via* the "converter" subdomain to an elongated region, called the lever arm. The lever arm (which consists of a target helix and associated light chains) further amplifies the motions of the converter into large directed movements. The release of the ATP hydrolysis products is catalyzed by binding to actin filaments, and coupled to converter/lever arm movements. Following this sequential release of Pi and ADP, rebinding of ATP to the actin-myosin complex at the end of the powerstroke (rigor) causes dissociation from actin, followed by hydrolysis of ATP. The conformation change that allows hydrolysis reprimes the lever arm at the beginning of the powerstroke, and another force/movement generating cycle can then be initiated by again binding to actin.

Myosin VI, like myosin V, has been described as a dimeric processive motor, taking multiple steps along the actin filament before detaching. However, myosin VI, in contrast to all other characterized myosins, moves toward the minus (-) end of the actin filament [1]. Perhaps to serve its vesicle transporting role in cells, myosin VI has another unusual feature: it takes similarly sized steps to those of myosin V [2]. This is despite having a much shorter lever arm, as defined by the number of CaM light chains it binds per head (two for myosin VI and six for myosin V). This property cannot be explained in the context of the "swinging lever arm" theory since its step size is not proportional to its lever arm length when compared to other myosins. Like Myosin V, Myosin VI can undergo 30-36 nm steps, even though its lever arm (defined by CaM-binding sites) appears to be at least three times smaller.

Altogether, this reveals that myosin VI produces directed movements with a different mechanism compared to that of (+)-end myosins, such as myosin V. This is particularly surprising given the high sequence homology in the motor domain of these myosin motors, which suggests that the primary structural features of the motor are unchanged. However, the myosin VI class has however two unique insertions within the motor domain. The first (insert 1) is in the upper 50 KDa domain near switch I. This insert has been shown to slow the rate of

ATP binding [3] and is critical for the coordination between the heads (gating) during processive movement of the two-headed molecule. Myosin VI also contains a specific insert of 39 residues (insert 2) located between the motor domain and the lever arm which, like insert 1, is unique among the myosin superfamily members.

This second unique insert was first proposed to be the basis of the myosin VI reverse directionality due to its critical position following the converter, which could allow repositioning of the lever arm. This was also consistent with cryo-electron microscopy maps of the myosin VI motor bound to actin in rigor [1]. An ADP-mediated conformational change in the distal part of the motor occurred in the opposite direction to that observed for other myosins, and the apparent lever arm was directed toward the (-) end of the actin filament in either the ADP-bound or rigor states [1]. However, molecular engineering studies using myosin V/VI chimera, that either added this insert to myosin V, or removed it from myosin VI, were interpreted to provide evidence that the motor domain itself, and not the unique insert, determined the direction of myosin motility [4].

Quite unexpectedly, we later demonstrated that this unique insert (insert 2) corresponds to a novel target sequence for calmodulin with calcium bound [5]. The calmodulin bound to this insert has a very high affinity for Ca^{2+} ions and plays a critical structural role, not a regulatory role. In contrast, the IQ motif can bind calmodulin with and without Ca^{2+} ions but a stable binding requires $\leq$ 20 additional residues after the IQ motif. Following the insert/Ca^{2+}.CaM, and modified IQ-CaM binding site, there is an additional region of ~60 residues of unknown structure that functions as a lever arm extension (LAE) [6,7]. This is followed by a region that allows dimerization of the native molecule [7], which in turn is followed by a cargo-binding domain.

We have determined the structure of myosin VI in a nucleotide-free state at 2.4 Å resolution (Figure 1). This structure reveals only minor differences in the motor domain as compared to myosin V, which we earlier solved in the same nucleotide-free state [8]. But, a striking difference with myosin V is that the lever arm of myosin VI is directed in the opposite direction towards the (-) end of the actin filament. The good fit obtained by docking this myosin VI structure into electron micrograph maps obtained from actin-myosin VI decoration further confirms that the structural state we have isolated is close to the rigor state (end of powerstroke) of myosin VI. As for (+)-end motors, the position of the myosin VI converter is controlled by two connectors – namely the Relay and the SH1 helix. The converter orientation in this nucleotide-free state is thus in a "down" position like that found for myosin V at the end of its powerstroke. The converter of myosin VI however differs from that of myosin V in the orientation of its last helix as well as in the structure of a highly variable (among myosin classes) loop within the converter. Both of these differences are critical for the proper positioning of the myosin VI unique insert (Figure 2A).

The unique 39-residue insert (insert 2) is a helix that is responsible for the reversal of the lever arm. After the last helix of the converter, the proximal part of the insert turns at Pro774, wraps around the converter and interacts strongly with the variable loop of the converter. This is in sharp contrast to (+)-end motors whose lever arm helix emerges as a straight helix, continuing the last helix of the converter (Figure 2B). The distal part of the insert 2 forms a previously unseen calmodulin-binding motif. Both the insert and its associated calmodulin make specific interactions with the converter. The net result of these interactions is that the lever arm emerges ~120° from the position of the lever arm found in (+)-end motors. This structure at the end of the powerstroke, thus largely accounts for myosin

VI reverse directionality. At the end of the stroke, the lever arm is directed towards the (-) end of the actin filament. Moreover, in redirecting the lever arm, the insert creates a bias for binding of the second head of a dimer towards the (-) end of the actin filament.

In light of the myosin VI structure, it is clear why adding insert 2 from myosin VI into the myosin V converter did not lead to a reversal of direction [4]. First a clash between W702 of the myosin V converter and F763 of the last helix of the converter would have prevented the last helix to be oriented as found in myosin VI (Figure 2). Moreover, to be positioned properly, the insert requires the specific interactions with the variable loop of the converter, which only the myosin VI converter provides. Unable to wrap around the converter, the insert in the context of a myosin V/myosin VI chimera likely would simply have lengthened the lever arm of a (+)-end motor. The directionality of the three other chimeras reported between myosin V and myosin VI are less easily explained, but it is important to note that they all moved very poorly [4]. Why removal of the insert from myosin VI did not lead to a plus-end motor is at odds with our structural results, which show that without the insert, the lever arm would point towards the plus-end at the end of the stroke. It is also difficult to understand why the myosin V motor could not direct the myosin VI converter/insert in order to produce force towards the (-) end of the actin filament. These studies need to be re-investigated with constructs containing longer lever arms, so as to increase the motility speed of the chimeras in order to determine their directionality unambiguously.

In agreement with our structural study that shows that change in the lever arm orientation is sufficient to reverse directionality, an elegant engineering study has revealed that redirecting the lever arm 180° in a (+)-end myosin motor (myosin I) leads to the reversal of its directionality [9]. It is clear from modeling of the powerstroke using a normal (+) end converter rotation, that it is essential for the lever arm to be long enough to compensate for the (+) end directed movement of the converter [3]. This is indeed the case for this engineered myosin.

However, modeling of the myosin VI conformation at the beginning of the stroke using the motor domain of myosin II in the pre-powerstroke state reveals that the stroke produced would be much smaller (2.5 nm) than that experimentally measured (11 nm) (Figure 3). In contrast, similar modeling for myosin V accounts for the 7 nm stroke produced by a construct containing a single IQ-motif (Figure 3). Myosin VI thus must have a different pre-powerstroke conformation, as compared to the (+)-end motors. It is possible that the Relay and the SH1 helix re-orient the converter such that it directs the insert-2 helix and the lever arm in the opposite direction (towards the (+) end of the actin filament) in the pre-powerstroke state. Another possibility is that rather than keeping the converter rotation of plus-end motors, myosin VI has essentially abolished it. In this hypothesis, a specific region (SH1 helix) unfolds to uncouple the lever arm from the motor domain prior to force generation. Its refolding upon actin binding would impose a stroke that could be as large as 11 nm (Figure 2). This mechanism is reminiscent of the kinesin-like uncoupling/docking mechanism and could fully explain the movements due to the myosin VI motor. Thus to progress further in our understanding of how myosin VI works, the structure of the motor in other conformations is required.

References

[1] Wells AL, Lin AW, Chen LQ, Safer D, Cain SM, Hasson T, Carragher BO, Milligan RA, Sweeney HL. Myosin VI is an actin-based motor that moves backwards. *Nature* **401**:505-8 (1999).

[2] Rock RS, Rice SE, Wells AL, Purcell TJ, Spudich JA, Sweeney HL. Myosin VI is a processive, backwards motor with a large step size. *Proc. Natl. Acad. Sci. USA* **98**: 13655-13659 (2001).

[3] Menetrey J, Bahloul A, Wells AL, Yengo CM, Morris CA, Sweeney HL, Houdusse A. The structure of the myosin VI motor reveals the mechanism of directionality reversal. *Nature* **435**: 779-85 (2005).

[4] Homma K, Yoshimura M, Saito J, Ikebe R, Ikebe M. The core of the motor domain determines the direction of myosin movement. *Nature* **412**:831-4 (2001).

[5] Bahloul A, Chevreux G, Wells AL, Martin D, Nolt J, Yang Z, Chen LQ, Potier N, Van Dorsselaer A, Rosenfeld S, Houdusse A, Sweeney HL. The unique insert in myosin VI is a structural calcium-calmodulin binding site. *Proc Natl Acad Sci U S A*. **101**:4787-92 (2004).

[6] Rock RS, Ramamurthy B, Dunn AR, Beccafico S, Morris C, Spink B, Rami B, Franzini-Armstrong C, Spudich JA, Sweeney HL. A flexible domain is essential for the large step size and processivity of myosin VI. *Mol. Cell*. **17**: 603-9 (2005).

[7] Park H, Ramamurthy B, Travaglia M, Safer D, Chen L.-Q, Franzini-Armstrong C, Selvin PR, Sweeney HL. Full-length myosin VI dimerizes and moves processively along actin filaments upon monomer clustering. *Mol. Cell*. **21**: 331-336 (2006).

[8] Coureux PD, Wells AL, Menetrey J, Yengo CM, Morris CA, Sweeney HL, Houdusse A. A structural state of the myosin V motor without bound nucleotide. *Nature* **425**:419-23 (2003).

[9] Tsiavaliaris G, Fujita-Becker S, Manstein DJ. Molecular engineering of a backwards-moving myosin motor. *Nature*. **427**:558-61 (2004).

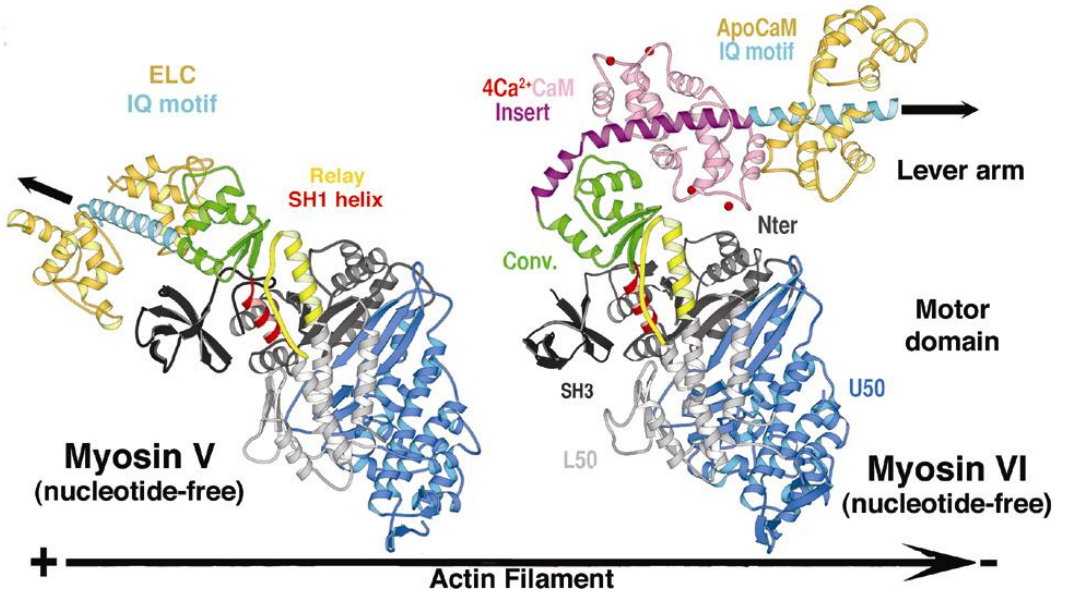

Fig. 1: The structure of nucleotide-free myosin VI (right) is compared to that of myosin V (left). Note the difference in the position of the lever arm (IQ motif, cyan) due to the unique insert (purple) and its associated-calmodulin (pink).

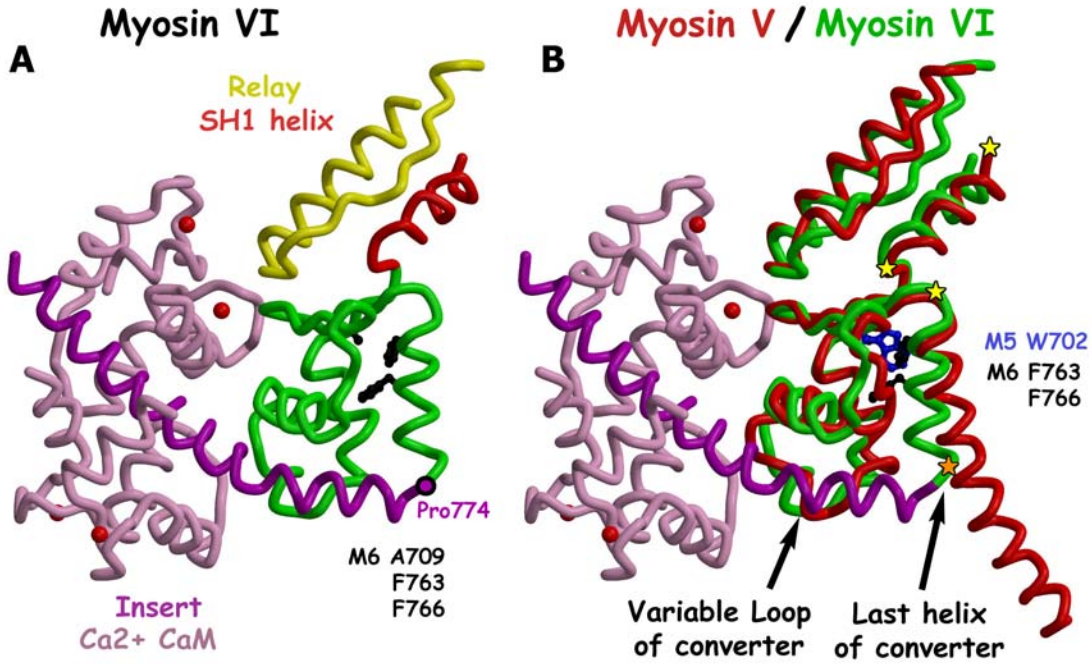

Fig. 2: The converter/insert of myosin VI (left) is compared to that of myosin V (red on the right). Note that the two connectors Relay and SH1 helix interact with the converter in myosin VI as found for myosin V and other plus-end motors. The major difference in the myosin VI converter (green) is found in the orientation of the last helix and the structure of a variable loop of the converter. The insert (purple) starts at Pro774 and wraps around the converter. Its distal sequence recruits CaM with four Ca^{2+} ions bound.

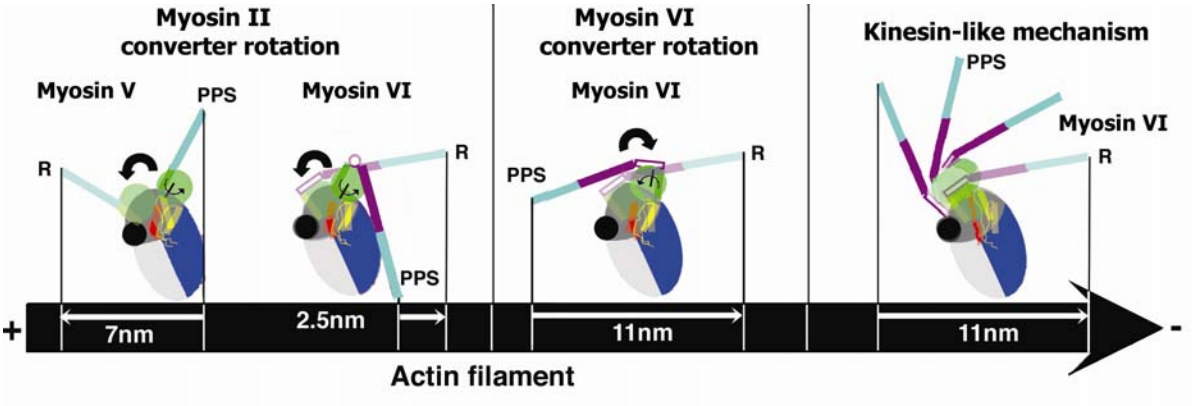

Fig. 3: Reversal directionality mechanisms. Light chains are omitted for clarity. (R) Rigor state: the nucleotide-free high affinity state for actin filament that follows force production. (PPS) Pre-powerstroke state: the ADP.Pi state of weak affinity for actin filament that preceeds force production.

Motor Directionality in the Kinesins.

Ronald A. Milligan and Craig Yoshioka.

Department of Cell Biology, The Scripps Research Institute, 10550 North Torrey Pines Road, La Jolla, CA 92037.

Members of the kinesin superfamily exhibit three types of behavior: plus end directed motion, minus end directed motion and microtubule depolymerization activity. Plus end directed motors are processive – one dimeric molecule takes many consecutive steps along the microtubule without dissociating. Minus end directed motors are also generally dimeric, but the individual dimers are non-processive although ensembles of dimers may mediate continuous association between microtubule and cargo to bring about long range transport. The third type of kinesin targets to microtubule ends where it actively bends and destabilizes the protofilaments to bring about depolymerization. The detailed mechanism of these depolymerization machines is not well understood and they do not seem to move along microtubules in a directional, ATP-dependent fashion. For these two reasons, they will not be discussed further here. It should be noted that these three behaviors are not mutually exclusive. Some plus-end and minus-end directed kinesins also exhibit depolymerization at microtubule ends, although this activity is “weak” and not as robust as that of the seemingly non-motile depolymerizers. In this presentation, we will focus on discussing some thoughts on the mechanisms underlying plus and minus-end directed motion.

Cycles of hydrolysis, motor-track interaction and conformational change.

It is perhaps useful to think of the problem of movement and directionality in cytoskeletal motors by setting aside the wealth of detailed information that is available and considering the basic features of the system. In this simple view, three cycles are operating as a motor molecule moves along its track: the ATP hydrolysis cycle, the motor track interaction cycle and what may be conveniently called the mechanical cycle – the work-related, conformational cycle. The way in which the cycles are coordinated or coupled is the key to understanding the mechanisms of directional motion. Clearly it would not be productive for the cycles to operate independently of one another; it is the job of the motor core to coordinate the cycles so that they function together to produce useful, directional movement. We will briefly discuss the cycles themselves before exploring the ways in which they may be coupled, and comparing these possibilities with what nature has done (see also Vale and Milligan, 2000).

The ATP hydrolysis cycle requires ATP binding to the motor, hydrolysis (ATP –> ADP + Pi), and finally sequential release of the products of hydrolysis (Pi, then ADP). Thus there are four main states, nucleotide-free, ATP-bound, ADP.Pi-

bound and ADP-bound, and it is generally believed that significant work is associated with ATP binding and with Pi release. Amino acid sequences directly involved in the ATPase cycle are among the most highly conserved regions of the motor core.

The motor track interaction cycle simply describes the repeated attached (bound) and detached (free) states of the motor relative to the track. The bound state may be further divided into an initial, weakly bound state, a transition to a strongly bound state, and then reversion to a (different) weakly bound state which precedes detachment. It is likely that productive force can only be generated while the motor is strongly bound to the underlying track.

The third cycle describes the conformational changes that produce motility. It involves a mechanical element changing its orientation with respect to the underlying track. In the simplest sense, a structural element swings back and forth between a forward (+) pointing and a backward (-) pointing position.

Coordinating the three cycles.

A moment's thought about this simple scheme for the cycle of conformational change underscores the need for coordination with the motor-track interaction cycle. If all possible conformational transitions occur while the motor is attached (or detached), no net motility occurs. It is only when a specific conformational transition is coupled exclusively with an attached or detached state that directional movement can occur. Therefore forward motion results when the backward-pointing to forward-pointing transition takes place while the motor is bound to its track (and the recovery stroke occurs when it is detached). The ATPase cycle is coordinated with these already-linked activities by virtue of its modulation of motor track interactions and its powering of the cycle of conformational change.

If we consider a hypothetical motor, the design of which is loosely based on the coupling relationships of plus-end directed kinesins, we have a mechanical element in the motor that may have backward (-) pointing or forward pointing (+) conformations. A forward stroke (backward to forward transition) occurs while the motor is strongly bound to the underlying track and is associated with the ATP binding step of the ATPase cycle. Recovery of the backward pointing conformation occurs while the motor is detached from the track and about to begin its next cycle of interaction (Figure 1a).

In principle, there are two simple ways in which we could alter the coupling relationships of the three cycles to reverse the directionality of this motor. The first is to maintain the coordination between the ATPase cycle and the cycle of conformational change, but change the phase of the motor-track interaction cycle. In this case, the "forward stroke" would occur on the detached motor, and

the ”recovery stroke” would happen while the motor was bound to the track, leading to direction reversal (Figure 1b). Practically speaking, one might expect this method of direction reversal to require re-engineering the parts of the motor that are involved in communication between the ATP hydrolysis site and the track. Note that the coupling relationships in this model (Figure 1b) bear certain similarities to those of conventional myosin, which may have evolved from a kinesin-like proto-motor.

The second simple way of reversing the directionality is to maintain the coupling relationship between the ATPase cycle and the motor track interaction cycle, but to change the coordination with the cycle of conformational change of the mechanical element. Thus ATP binding (and strong track binding) would be associated with reorientation of the mechanical element from a forward-pointing to a backward-pointing orientation (Figure 1c). In this case, re-engineering of the communication between the ATP site and the mechanical element is necessary.

Nature’s solution.

In the kinesin superfamily, nature appears to have used this latter method to bring about direction reversal. Minus and plus-end directed and kinesins have highly conserved ATP hydrolysis and microtubule binding sites and very similar microtubule binding cycles. However, their mechanical elements are quite different structurally and behaviorally. Conventional kinesin’s neck linker executes a plus-end directed stroke upon ATP binding to the microtubule-attached motor domain, while the coiled coil neck of the minus-end directed kinesin, Ncd, swings towards the minus end of the microtubule at the same stage of the ATPase and attachment cycles. ATP binding to conventional kinesin creates a binding surface allowing the neck linker to dock onto the motor domain, and this action constitutes the forward stroke. Disruption of the neck linker binding site – probably at the Pi release step when the motor domain detaches from the microtubule – initiates the recovery stroke (Rice et al., 1999; Vale and Milligan, 2000). In Ncd, there are two distinct positions in which the coiled coil neck can interact with the motor domain. ATP binding must disrupt the interactions between the motor and its plus-end pointing neck, at the same time creating a binding site for the neck in a minus-end pointing orientation. The opposite sequence of events takes place later in the cycle to reset the neck when the motor is detached (Wendt et al., 2002; Yun et al., 2003; Endres et al, 2006).

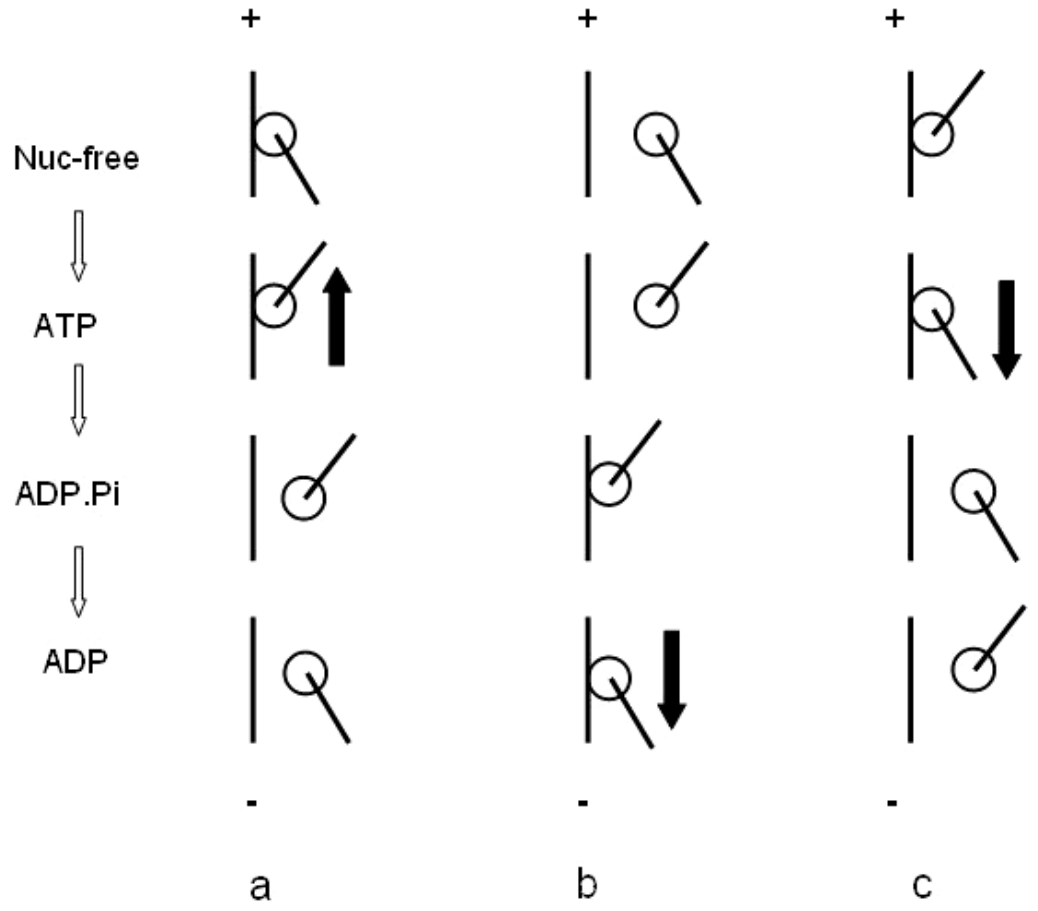

Figure 1. Schemes for direction reversal in a hypothetical motor. The nucleotide states during one round of the ATPase cycle are shown at left and are sequenced from top to bottom. The coordination between ATPase, attachment and conformation cycles in (a) is similar to that of a conventional plus-end directed kinesin motor domain. Direction reversal can be accomplished by maintaining the relationship between the ATPase and conformation cycles and changing the phase of the attachment cycle (b). This scheme is similar to the situation in conventional myosin. A second way to reverse motility, (c) is to maintain the relationship between the ATPase and attachment cycles and to change the coordination with the conformational cycle. Minus-end directed kinesins such as Ncd appear to use this scheme.

References.

Endres, N.F., et al. 2006. A lever arm rotation drives motility of the minus-end-directed kinesin, Ncd. Nature 439: 875-878.

Rice, S., et al. 1999. A structural change in the kinesin motor protein that drives motility. Nature 402:778-784.

Vale, R.D. and R.A. Milligan. 2000. The way things move: Looking under the hood of molecular motor proteins. Science 288:88-95.

Wendt T.G. et al., 2002. Microscopic evidence for a minus-end-directed power stroke in the kinesin motor Ncd. EMBO J. 21:5969-5978.

Yun, M. et al., 2003. Rotation of the stalk / neck and one head in a new crystal structure of the kinesin motor protein, Ncd. EMBO J. 22:5382-5389.

hsicHelicases: Origin of directionality

Taekjip Ha

Department of Physics, University of Illinois, Urbana-Champaign
Howard Hughes Medical Institute
tjha@uiuc.edu

Helicases are cellular enzymes that unwind double stranded DNA or RNA using ATP hydrolysis. They are found in all kingdoms of life and extremely numerous: our genome contains more than 200 putative helicases. It turns out many of the putative helicases identified through sequence comparison are not actually helicases as they do not show the ability to unwind the double stranded nucleic acid molecules. Rather, non-canonical functions of these enzymes have been discovered including translocation on single and double stranded DNA, branch migration of a Holliday junction, chromatin remodeling, protein displacement and remodeling of ribonucleic-protein complexes. These diverse functions are powered by the common translocation engine formed by the walker A and walker B motifs (Figure 1).

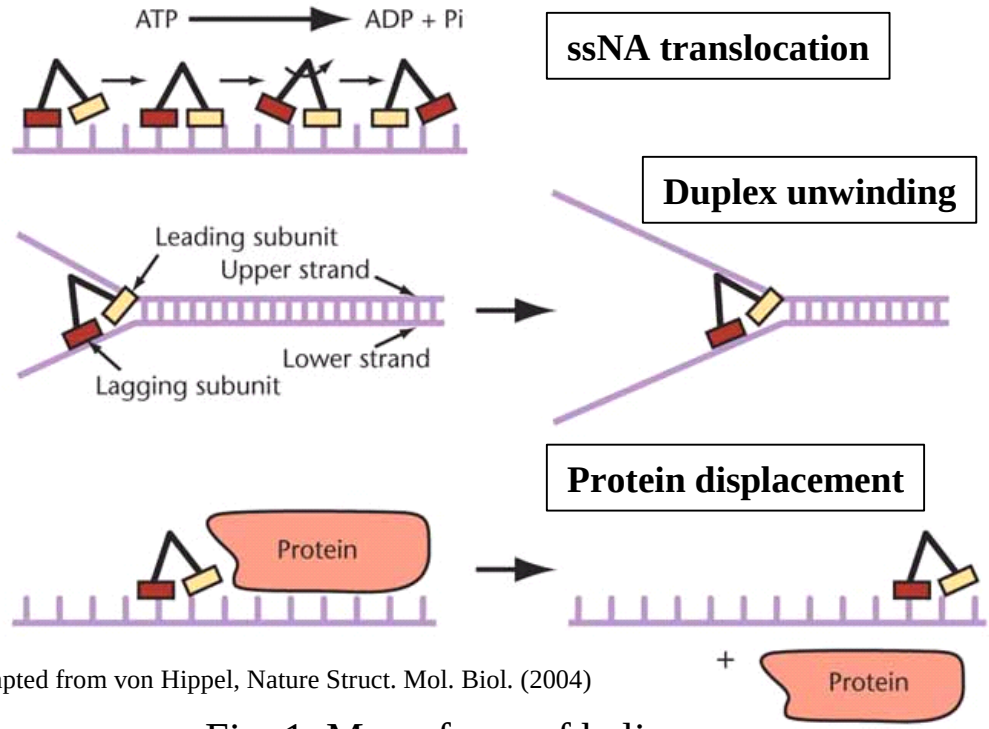

Adapted from von Hippel, Nature Struct. Mol. Biol. (2004)

Fig. 1. Many faces of helicase.

Helicases are classified into two groups, 3'-5' and 5'-3' helicases. Since the duplex DNA does not have any polarity, what is meant here is that a 3' single stranded tail is required for observing unwinding activity in vitro for 3'-5' helicases and vice versa. Presumably, the 3' tail is required for loading the 3'-5' helicase and then the protein moves on the

loading strand in the 3’-5’ direction and in the process displaces the other strand. In fact, many 3’-5’ helicases have been shown to move on a ssDNA in the 3’-5’ direction using a variety of biophysical techniques.

A helicase moving on a ssDNA in a directional matter powered by ATP hydrolysis may be considered a motor protein, just like cytoskeleton motors moving directionally on tracks such as actin filaments and microtubules. In fact, PcrA and Rep helicases show the translocation activity as a monomer of about 600 amino acids, among the smallest of any motor protein, and several high resolution crystal structures are available. Therefore, one might even argue that these helicases are the ideal model systems for understanding the motor protein functions in general.

It is currently unknown what determines the directionality of helicase translocation. My lab is working toward the engineering of a helicase mutant that reverses its natural direction. If successful, such an attempt would reveal important insight on the translocation mechanism. Below, I will first argue why such an attempt is not entirely absurd and then sketch the multi-pronged approaches we are taking towards this pie in the sky.

Studies by Tim Lohman and Dale Wigley have shown that Rep, UvrD and PcrA helicases move on ssDNA in the 3’-5’ direction as a monomer. The speed is on the order of 100 bases per second. It appears that about 1 ATP is used per base although this has not been firmly established. All three helicases belong to the same helicase superfamily (SF1). Kevin Raney demonstrated that another SF1 helicase, Dda, moves on ssDNA in the 5’-3’ direction. This is the first hint that it may not take a very drastic modification to change the directionality because they all belong to the same superfamily yet showed the opposite directionality.

We can conceive two different ways of achieving directionality reversal. The first is that the protein binds to the ssDNA in the reverse orientation but still moves in the same direction as before. The second is that the protein binds to the ssDNA in the same orientation but moves backward. Since the latter would be expected to require smaller modification to the protein, such a scenario would give us a better hope of engineering a reversal mutant. Steve Kowalczykowski has shown that RecBCD is a bipolar helicase where RecB and RecD are both helicases but with opposite directionality. Both RecB and RecD are SF1 helicases. The crystal structure of RecBCD obtained by Wigley and Kowalczykowski showed very compelling evidence that RecB and RecD bind to the ssDNA in the same orientation, so their opposite directionality must come from rather subtle differences on the energetic barriers between the forward and backward movements. This is the second hint that a reversal mutant may be engineered with relatively small amount of modifications.

The third hint comes from the Khan lab who examined the unwinding polarity of several different PcrA proteins from different organisms and found that some preferentially unwound DNA with a 5’ tail. If the observation is also confirmed by the direct

measurements of ssDNA translocation directionality, this would be the most compelling basis for our hope of directionality reversal.

What are the approaches we are taking? The first is the computational approach utilizing the available crystal structures, notably PcrA which has been crystallized in two forms, with ATP and without ATP. Wigley made an insightful proposal how ATP may modulate the differential affinity to the ssDNA of two RecA-like domains, giving rise to the directionality. However, his proposal was ad hoc in the sense that which domain binds to ssDNA more tightly in which ATP bound form was assigned in order to match the known directionality of PcrA. We sought to provide a quantitative rationalization of such a proposal. In collaboration with Klaus Schulten, we have run molecular dynamic simulations and calculated the DNA interaction energies of the two RecA-like domains in the two different crystal forms. We found that indeed the binding affinities were alternating for the two domains as ATP binds and dissociates in a manner consistent only with the 3'-5' direction (Yu, Ha and Schulten, Biophysical Journal, *in press*). The study also identified key residues that contribute to the differential binding energy. This type of computational study will help us design mutants and rationalize future experimental observations.

The second approach is the brute force characterization of many different highly related helicases, for example, PcrA. Imagine a database of many 3-5' and 5'-3' helicases that are extremely similar in primary sequence. Then, extensive sequence and structural gauzing may offer mutations to try experimentally.

The third approach would be to select, from a random pool of helicase mutants, a mutant that goes backward. The current challenge is the adequate selection method.

So far, I have only discussed the helicases that move on ssDNA as a monomer. However, there are hexameric ring helicases that move on ssDNA in a directional manner. A really exciting crystal structure of one such helicase, E1 helicase, was reported just now by Leemor Joshua-Tor. This structure was the first with DNA bound to a ring helicase and showed that each monomer was interacting with each nucleotide (six in all) in a sequential manner, suggesting a very straightforward circular staircase mechanism. In particular, the structure showed ATP, ADP and apo forms of monomers in succession, clearly suggesting the direction of translocation consistent with the known direction of 3'-5'. This is analogues to the case of F1-ATPase where the crystal structure of the trimer with one ATP bound, the second ADP bound, and the third empty suggested the rotation direction with was later confirmed by single molecule measurements. Many ring helicases also move on dsDNA but how would the mechanism found from E1 translocation in ssDNA apply to dsDNA translocation? Does it require that the two strands to be separated inside the ring and the protein is simply undergoing ssDNA translocation? The jury is still out there.

Biophysical Society Discussion Meeting 2006

Bacteria and polymerization motors

Daniel A. Fletcher

Bioengineering & Biophysics, UC Berkeley
Berkeley, CA 94720
fletch@berkeley.edu

Summary

Several species of pathogenic bacteria have been found to move intracellularly and intercellularly by means of actin-based motility. After invasion of a host cell, bacteria such as *Listeria monocytogenes* harness host cell factors to form branched and cross-linked actin filament networks that propel them at speeds of microns per minute through the cytoplasm. These networks of polymerizing actin filaments, sometimes described as polymerization motors, generate protrusions into neighboring cells that facilitate entry and spread of the bacteria. Despite extensive biochemical knowledge of the components necessary for actin-based motility of bacterial pathogens, many biophysical questions remain about the mechanism and control of actin network growth and about how network architecture influences behavior. This abstract summarizes several aspects of actin-based motility of bacterial pathogens and highlights current topics of interest in the field.

Intracellular bacterial motility

Many bacteria use the rotary motion of external appendages such as flagella to swim through liquids. For pathogenic bacteria that spend at least part of their life cycle infecting host cells, swimming with flagella is not an effective means of movement through cytoplasm. Some bacteria, such as *Spiroplasma melliferum*, have adopted alternate techniques for swimming in high viscosity environments [1], but others have developed strategies that makes use of cytoskeletal proteins in the host cell cytoplasm for movement. Intracellular bacterial pathogens including *Listeria monocytogenes*, *Shigella flexneri*, *Rickettsia rickettsii*, *Mycobacterium marinum*, and *Burkhoderia pseudomallei* harness actin-based motility to move through and between host cells in a process that resembles the formation of actin-rich protrusions in eukaryotic cells [2, 3].

Reproducing and spreading within host cells, as opposed to outside, has several advantages for the invading bacteria. One is that remaining inside of a host cell hinders detection by the host cell immune system. A second is the ready availability of nutrients for growth and division. A third advantage is the abundance of cytoskeletal proteins that can be harnessed for motility. Each of the bacteria listed above expresses a different surface protein that either directly or indirectly activates the Arp2/3 complex, a protein in the host cell cytoplasm that binds to the side of actin filaments and nucleates the growth

of daughter filaments. Activation of the Arp2/3 at the bacterial cell surface leads to the formation of branched actin networks like those that drive lamellipodial protrusions of eukaryotic cells (Fig. 1).

Growth of branched actin networks

The cytoskeletal protein actin polymerizes into non-covalent polymer filaments that are organized by actin-binding proteins into branched and cross-linked actin filament networks. Actin polymerization indirectly links ATP hydrolysis with steady-state assembly and disassembly of the polymer in a cycle that can do work, a process known as “treadmilling” [4] (Fig. 2). Growing actin networks generate mechanical forces necessary for a wide range of cell movements such as motility, cytokinesis, and phagocytosis [5, 6].

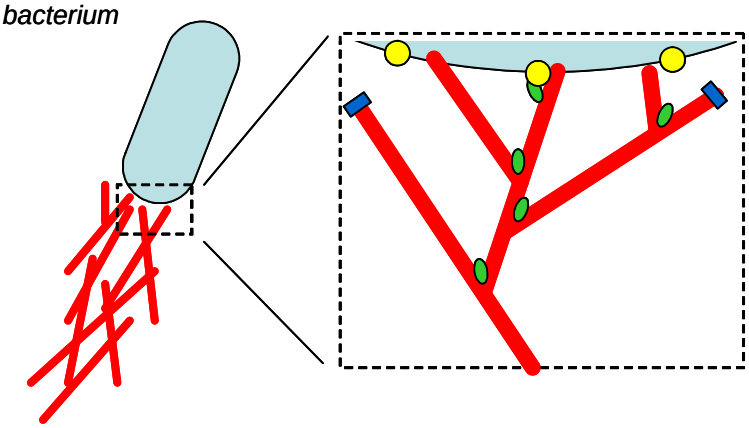

Figure 1: Actin-based motility of a bacterial pathogen. (a) Branched actin networks form at the poles of pathogenic bacteria after invasion and propel them through the host cell cytoplasm. (b) The *Listeria monocytogenes* surface protein ActA (yellow circle) activates the Arp2/3 complex (green oval) and promotes branching of new actin filaments (red lines), which can later be capped (blue rectangle).

More than 60 actin-binding proteins are at work in eukaryotic cells, many of which control the architecture of actin filament networks as they grow [7]. Cellular control of branching, crosslinking, capping, sequestering, severing, and nucleating proteins affects when, where, and how actin networks are formed. Some actin binding proteins, such as ADF/cofilin, can affect several aspects of network architecture, such as stiffness and growth rate, making the net effect on a network’s ability to displace a load difficult to predict. In some cases, nucleation promoting factors can be spatially organized on the bacterial cell surface to influence the location of network formation [8].

The networks formed by filament growth must elastically transmit forces as well as generate forces. In the lamellipodium of crawling cells, branched and crosslinked actin networks formed between points of substratum adhesion and the membrane leading edge must be stiff compared to the resistance to forward motion. Otherwise, growing filaments at the leading edge will compress the internal actin network rather than extend the cell membrane forward. Hence, both the mechanical properties and the growth rate are subject to forces that may influence actin network dynamics.

Measurements of actin-based motility

Actin-based motility of bacterial pathogens has been studied with video microscopy and laser tracking using both whole bacteria and *in vitro* reconstitutions

based on key proteins. A diverse set of behaviors has been observed, including micron-scale "hopping" [9] and nanometer-scale stepping [10]. Motility assays based on beads and vesicles, microneedle force measurements, and atomic force microscopy studies have made important contributions to understanding actin-based motility and force generation.

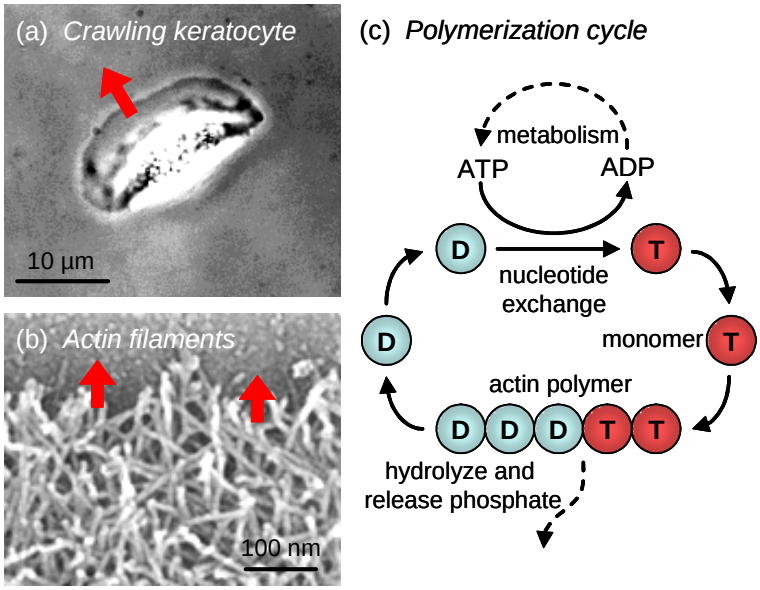

Figure 2: Actin polymerization in eukaryotic cells. (a) Crawling fish keratocyte powered by actin polymerization. (b) Electron microscopy of actin filaments at the leading edge of a crawling cell (from Svitkina *et al.*, 1997). (c) Work is done in the actin polymerization cycle by addition of a monomer to the polymer.

<u>Bead motility assays have guided understanding of actin-based motility</u>: Actin-based movements of micron-sized particles that mimic intracellular bacterial pathogens have been extensively used to investigate growing actin networks [11]. The surface protein ActA derived from *Listeria monocytogenes* can be purified and coated onto polystyrene beads or other inert particles, causing them to exhibit actin-based motility when immersed in cytoplasmic extract from *Xenopus laevis* eggs [12]. Electron micrographs demonstrate a striking similarity between the architecture of these reconstituted networks and the lamellipodia of motile cells [13]. Bead movement can tracked over time with video microscopy, and bead velocity can be studied as a function of factors including bead diameter, surface density of ActA, and extract concentration [14-16]. However, this method only provides a lower bound for the force produced by actin polymerization (balanced by viscous drag), which is typically on the order of femtonewtons – three orders of magnitude smaller than the nanonewtons of force expected from thermodynamic arguments for the actin network formed against a moveable surface [17]. Actin network forces under small loads have been estimated from the curvature of deformable vesicles [18, 19] and oil droplets [20].

<u>A minimum set of proteins are required for directed movement</u>: Though bead motility assays cannot probe the load-dependence of actin network dynamics, they have served as the basis for identifying a purified or "minimum" motility system. The minimum motility system is a solution of purified soluble proteins that can replace cytoplasmic extract as the medium in which ActA-coated beads will exhibit actin-based motility. Loisel *et al.* published a purified motility system containing four components – Arp 2/3 complex, actin, cofilin, and capping protein – in addition to ActA [15]. Other actin-binding proteins, such as profilin and α-actinin, influence actin network assembly and disassembly but were not necessary for movement in a low-force environment dominated by viscous drag. Interestingly, significant differences in velocity have been

reported between beads moving in the minimum motility system and those moving in cytoplasmic extract [14, 15, 21], and this discrepancy has raised questions about whether the properties of actin network growth in each system are the same.

Force microscopy measurements enable application of larger forces: Marcy *et al.* made a more direct measurement of actin polymerization forces using a flexible fiber as a force probe [22]. They measured the force-velocity relationship for actin networks growing from a 2-μm-diameter bead attached to the fiber, pulling on the growing actin network with an aspirated micropipette. However, like the bead motility assays, this measurement was also not able to stall the actin network growth. Recent atomic force microscopy (AFM) measurements have succeeded in stalling actin network growth and revealed a different force-velocity relationship than previously seen. Parekh *et al*. found that growing actin networks in extract were insensitive to force over a significant portion of the force range prior to stall [23].

Modeling of actin-based motility

Over the last decade, several models have been developed to couple actin network growth with forward movement of a load such as an intracellular pathogen [24]. The architectural complexity of actin networks has made modeling network properties a significant challenge. Currently, neither force-velocity models nor mechanical property models are able to capture some behaviors that have been observed in growing actin networks, such as stress-softening and loading-history dependence of growth velocity. However, each model highlights important properties and current thinking about growing actin networks.

Polymerization can generate a force: Unlike single-molecule motors, like myosin and kinesin, polymerization motors generate force by monomer addition. The ability of actin networks to displace a load depends on the fact that monomer addition is thermodynamically favorable even in the presence of a force. In 1982, Hill & Kirshner used thermodynamics to argue that protein polymerization accompanied by free energy release ($\Delta G<0$) is theoretically capable of generating a force [17]. The simplest case of this is one-dimensional polymerization against a moveable load (Fig. 3). Addition of monomers to the end of a growing filament leads to a force-dependent rate of filament growth, v, given by

$$v = \delta\left(k_{on}[A]e^{-\frac{F\delta}{kT}} - k_{off} \right)$$

for reaction-limited polymerization, where $[A]$ is the monomeric actin concentration, F is the load, δ is the step size, k is the Boltzmann constant, T is the temperature, k_{on} is the monomer addition rate, and k_{off} is the monomer release rate (unloaded). While this theoretical expression gives a simple relationship between force and velocity based only on actin concentration and reaction rates, the behavior of multi-filament networks involving numerous actin-binding proteins is significantly more complex.

Brownian ratchet models explain monomer addition by thermal fluctuations: The first Brownian ratchet model was based on the idea that polymerization of actin filaments could rectify the thermal motions of loads and create directed motion [25]. In this model by Oster and colleagues, gaps created by random motion of a load near an

actin network allow addition of a monomer to the filaments in the network, biasing movement of the load in the direction of monomer addition. This model was modified in 1996 to focus on fluctuations of the elastic filaments rather than fluctuations of the load, and it became known as the Elastic Brownian ratchet model [26]. The Tethered Elastic Brownian ratchet is the most recent revision of the model, which considers growth of a network of filaments and includes the observation that filaments are transiently bound to the moveable load with significant forces [27]. The tethered model depends on detachment rates of actin filaments and predicts a biphasic force-velocity curve with the velocity decaying convexly – rapidly at first and then more slowly with increasing force.

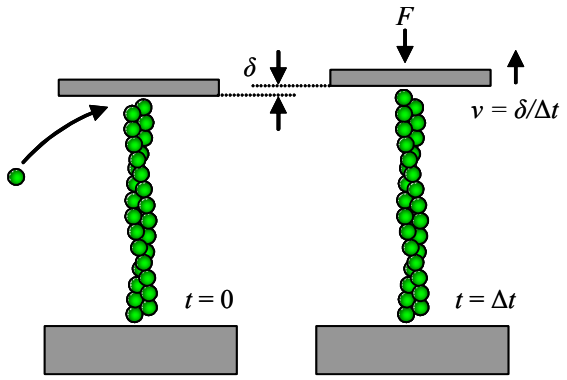

Figure 3: Thermodynamic model of force generation by actin polymerization under a moveable load from Hill & Kirshner (1982). Brownian ratchet models explain monomer addition by thermal fluctuation of the filaments and/or the load.

Building on the idea that single filaments act like Brownian ratchets, Carlsson has proposed an autocatalytic dendritic branching model for actin-based motility [28, 29]. While it is microscopically similar to the Brownian ratchet models, it predicts a flat force-velocity relationship, assuming a rigid network, based on the branching, capping, and growth of actin filaments near the nucleating surface. An increase in the load force stimulates branching locally, increasing the number of filaments pushing on the load, which allows the network to displace the load at its original velocity. A separate class of models is based on the existence of an end-tracking motor that couples ATP hydrolysis to protrusion [30].

Elastic energy storage models account for surface curvature: In the elastic energy storage model, velocity is predicted based on a balance of elastic energy storage and release by the gel. Gerbal *et al.*'s elastic theory of propulsion [31] proposes that *Listeria*, shaped like an oblate spheroid, moves due to asymmetric buildup of elastic stresses in the actin network. The addition of actin monomers at the bacterium surface pushes the existing network of actin outwards, stretching it elastically. This buildup of stress is continuously relaxed by movement of the bacterium forward, similar in principle to the slipping of a wet bar of soap when squeezed tightly at one end. In the limiting case of infinite curvature (i.e. a flat surface), the elastic gel model modifies Hill and Kirschner's relation by additionally considering the actin tail to be compressing elastically. While Prost and his collaborators have shown that several experimental results agree with their elastic theory [22, 32, 33], the mechanical properties of actin networks – and the microscopic origin of elasticity – are far from clear.

Questions for discussion

Several questions about intracellular bacterial motility and polymerization motors are the focus of active research:

1. How do specific actin binding proteins contribute to the dynamic behavior and microstructural architecture of growing actin networks?
2. How is the trajectory of actin-propelled bacteria determined, and what role doe surface attachments play?
3. What dynamic models correctly describe the force-velocity relationships of growing actin networks?
4. What mechanical models correctly describe the rheological properties of static actin networks?

Advancements in biophysical instrumentation and biochemical characterization of actin binding proteins will help to reveal the complex behavior and biological importance of organized actin network growth.

References

[1] J. W. Shaevitz, J. Y. Lee, and D. A. Fletcher, "Spiroplasma swim by a processive change in body helicity," *Cell*, vol. 122, pp. 941-5, 2005.

[2] E. Gouin, M. D. Welch, and P. Cossart, "Actin-based motility of intracellular pathogens," *Curr Opin Microbiol*, vol. 8, pp. 35-45, 2005.

[3] J. M. Stevens, E. E. Galyov, and M. P. Stevens, "Actin-dependent movement of bacterial pathogens," *Nat Rev Microbiol*, vol. 4, pp. 91-101, 2006.

[4] J. A. Theriot, "The polymerization motor," *Traffic*, vol. 1, pp. 19-28., 2000.

[5] A. Mogilner and G. Oster, "Polymer motors: pushing out the front and pulling up the back," *Curr Biol*, vol. 13, pp. R721-33, 2003.

[6] T. D. Pollard and G. G. Borisy, "Cellular motility driven by assembly and disassembly of actin filaments," *Cell*, vol. 112, pp. 453-65, 2003.

[7] D. Bray, *Cell Movements*, 2 ed. New York: Garland Publishing, 2001.

[8] S. M. Rafelski and J. A. Theriot, "Bacterial shape and ActA distribution affect initiation of Listeria monocytogenes actin-based motility," *Biophys J*, vol. 89, pp. 2146-58, 2005.

[9] A. Bernheim-Groswasser, S. Wiesner, R. M. Golsteyn, M. F. Carlier, and C. Sykes, "The dynamics of actin-based motility depend on surface parameters," *Nature*, vol. 417, pp. 308-11, 2002.

[10] S. C. Kuo and J. L. McGrath, "Steps and fluctuations of Listeria monocytogenes during actin-based motility," *Nature*, vol. 407, pp. 1026-9, 2000.

[11] A. Upadhyaya and A. van Oudenaarden, "Biomimetic systems for studying actin-based motility," *Curr Biol*, vol. 13, pp. R734-44, 2003.

[12] L. A. Cameron, P. A. Giardini, F. S. Soo, and J. A. Theriot, "Secrets of actin-based motility revealed by a bacterial pathogen," *Nat Rev Mol Cell Biol*, vol. 1, pp. 110-9., 2000.

[13] L. A. Cameron, T. M. Svitkina, D. Vignjevic, J. A. Theriot, and G. G. Borisy, "Dendritic organization of actin comet tails," *Current Biology*, vol. 11, pp. 130-135, 2001.

[14] L. A. Cameron, M. J. Footer, A. van Oudenaarden, and J. A. Theriot, "Motility of ActA protein-coated microspheres driven by actin polymerization," *Proc Natl Acad Sci U S A*, vol. 96, pp. 4908-13, 1999.

[15] T. P. Loisel, R. Boujemaa, D. Pantaloni, and M. F. Carlier, "Reconstitution of actin-based motility of Listeria and Shigella using pure proteins," *Nature*, vol. 401, pp. 613-616, 1999.

[16] L. A. Cameron, J. R. Robbins, M. J. Footer, and J. A. Theriot, "Biophysical parameters influence actin-based movement, trajectory, and initiation in a cell-free system," *Molecular Biology of the Cell*, vol. 15, pp. 2312-2323, 2004.

[17] T. L. Hill and M. W. Kirschner, "Bioenergetics and kinetics of microtubule and actin filament assembly- disassembly," *Int Rev Cytol*, vol. 78, pp. 1-125, 1982.

[18] A. Upadhyaya, J. R. Chabot, A. Andreeva, A. Samadani, and A. van Oudenaarden, "Probing polymerization forces by using actin-propelled lipid vesicles," *Proc Natl Acad Sci U S A*, vol. 100, pp. 4521-6, 2003.
[19] P. A. Giardini, D. A. Fletcher, and J. A. Theriot, "Compression forces generated by actin comet tails on lipid vesicles," *Proc Natl Acad Sci U S A*, vol. 100, pp. 6493-8, 2003.
[20] H. Boukellal, O. Campas, J. F. Joanny, J. Prost, and C. Sykes, "Soft Listeria: actin-based propulsion of liquid drops," *Phys Rev E Stat Nonlin Soft Matter Phys*, vol. 69, pp. 061906, 2004.
[21] A. Bernheim-Groswasser, S. Wiesner, R. M. Golsteyn, M. F. Carlier, and C. Sykes, "The dynamics of actin-based motility depend on surface parameters," *Nature*, vol. 417, pp. 308-311, 2002.
[22] Y. Marcy, J. Prost, M. F. Carlier, and C. Sykes, "Forces generated during actin-based propulsion: a direct measurement by micromanipulation," *Proc Natl Acad Sci U S A*, vol. 101, pp. 5992-7, 2004.
[23] S. H. Parekh, O. Chaudhuri, J. A. Theriot, and D. A. Fletcher, "Loading history determines the velocity of actin-network growth," *Nature Cell Biology*, vol. 7, pp. 1119-1123, 2005.
[24] A. Mogilner, "On the edge: modeling protrusion," *Curr Opin Cell Biol*, vol. 18, pp. 32-9, 2006.
[25] C. S. Peskin, G. M. Odell, and G. F. Oster, "Cellular motions and thermal fluctuations: the Brownian ratchet," *Biophys J*, vol. 65, pp. 316-24, 1993.
[26] A. Mogilner and G. Oster, "Cell motility driven by actin polymerization," *Biophys J*, vol. 71, pp. 3030-45, 1996.
[27] A. Mogilner and G. Oster, "Force Generation by Actin Polymerization II: The Elastic Ratchet and Tethered Filaments," *Biophys J*, vol. 84, pp. 1591-605, 2003.
[28] A. E. Carlsson, "Growth of branched actin networks against obstacles," *Biophys J*, vol. 81, pp. 1907-23, 2001.
[29] A. E. Carlsson, "Growth velocities of branched actin networks," *Biophys J*, vol. 84, pp. 2907-18, 2003.
[30] R. B. Dickinson, L. Caro, and D. L. Purich, "Force generation by cytoskeletal filament end-tracking proteins," *Biophys J*, vol. 87, pp. 2838-54, 2004.
[31] F. Gerbal, P. Chaikin, Y. Rabin, and J. Prost, "An elastic analysis of Listeria monocytogenes propulsion," *Biophys J*, vol. 79, pp. 2259-75, 2000.
[32] F. Gerbal, V. Laurent, A. Ott, M. F. Carlier, P. Chaikin, and J. Prost, "Measurement of the elasticity of the actin tail of Listeria monocytogenes," *Eur Biophys J*, vol. 29, pp. 134-40, 2000.
[33] V. Noireaux, R. M. Golsteyn, E. Friederich, J. Prost, C. Antony, D. Louvard, and C. Sykes, "Growing an actin gel on spherical surfaces," *Biophys J*, vol. 78, pp. 1643-54, 2000.

Regulating Myosin Function – Progress and Questions

Margaret A. Titus, Department of Genetics, Cell Biology & Development
University of Minnesota, Minneapolis, MN 55455

Motor protein function must be controlled both temporally and spatially in vivo. This is accomplished by regulating several different aspects of motor behavior: enzymatic activity, processivity, structural organization and localization. The best-studied and most widely known means of controlling myosin enzymatic activity is via the neck-associated light chains. This occurs either through phosphorylation of the RLC (in the case of smooth and non-muscle Myo2) or by Ca^{2+} binding to variable numbers of neck-associated calmodulin light chains (as seems to be the case for many of the unconventional myosins). While Ca^{2+}-calmodulin based regulation appears to be a dominant and common mode of regulation, additional mechanisms have been described that may be unique to a given myosin – these include monomer-dimer transitions and regulated localization. The first challenge is to identify the varied levels of regulation that affect myosin function and then understand how these are integrated within the cell to drive various motilities.

Regulating Processivity. Dimerized Myo6 moves processively, consistent with its role as an organelle motor, but cellular Myo6 appears to be monomeric (Lister et al, 2004). The apparent contradiction between these two observations can be resolved if dimer formation, and by extension processivity, itself is regulated. Several different potential mechanisms for doing so have emerged. First, Myo6 monomers may be recruited to dimeric binding proteins and this interaction the converts the myosin to a dimer that moves processively. Optineurin has been proposed to have such a role (Sahlender et al, 2005) and indirect support for this model comes from the observation that binding of anti-Myo6 antibodies to the tail region promotes dimerizaton and processive movement (Park et al., 2006). Another means of converting monomeric Myo6 to a dimer is via actin binding (Park et al, 2006). Motors that are in regions of high actin concentrations within the cells might then be converted to dimers by actin binding bringing the tail regions into close proximity. Once dimerized, the Myo6 would then be ready to bind and transport organelles. A third proposed mechanism is that cargo binding itself is sufficient to promote processive motility. Monomeric Myo6 bound to a relatively large cargo such as a bead is observed to move processively (Iwaki et al, 2006). This may result from the organelle acting as a "diffusional anchor", slowing the diffusion of the motor-cargo complex away from the actin filament, and thus promoting processivity. It is not clear that this is an effective mechanism as the length of the runs observed with the monomeric Myo6 are much shorter than found for dimeric Myo6. However, the limited increase in processivity may be useful for generating needed short-range translocation in certain contexts.

The in vitro data establish that conversion of Myo6 to a dimer changes the nature of its movement. It now remains to be established that Myo6 dimers do exist in vivo. This

will require the development of tools, most likely fluorescence-based, that can report on the monomer-dimer state of the Myo6 in vivo. It will also be necessary to have sufficient resolution to detect these in the cell against a background of monomers, and the ability to determine whether or not they are typically associated with Myo6 cargo.

The length of a processive motor's runs can also be modulated. In the case of Myo5, binding of Ca^{2+} to neck-associated light chains can cause dissociation of the calmodulin and terminate a run (Lu et al, 2006). It has been recently shown that Ca^{2+} promotes actin binding and increased nucleotide exchange and this may explain how Ca^{2+} may end a processive run (Olivares et al, 2006). How the neck region communicates with the active site to promote changes in nucleotide binding remains an open question.

Intramolecular Interactions. The best example of this type of regulation is the reversible assembly of Myo2 filaments that occurs during cytokinesis in non-muscle cells, most likely controlled via heavy chain phosphorylation. The Myo2 filaments drive the contraction and constriction ceases once cell division is complete and the filament are disassembled. Intramolecular interactions between the head and tail of myosins may also play an important role in regulating activity. The inhibited state of smooth muscle Myo2 is characterized by a folding over of the tail domain that causes one of the two heads binds to the actin binding region of the other head (Wendt et al, 1999). Interestingly, Myo5a may also use this inhibitory mechanism (Liu et al; Thirumurugan et al., 2006). The Myo5a tail region is folded over such that the C-terminal globular tail region lies close to the ATPase site. Consistent with the structural observations, the isolated tail domain has been shown to inhibit the activity of the Myo5a motor region (Li et al, 2006). Thus, intramolecular interactions between the motor domain and tail may play a critical role in modulating enzymatic activity. It should be noted that Ca^{2+} binding to the calmodulin LCs relieves this inhibition by promoting an extended, active state (Krementsov et al; Li et al, 2004). In addition, cargo binding is also likely to be capable of directly disrupting the head-tail interaction and switching the myosin to the active state.

Several questions are raised by these recent findings. Once again, how does Ca^{2+} binding to calmodulin at the neck region contribute to the regulation of motor activity (i.e. actin binding and ATP hydrolysis)? Are there changes in the flexibility of the neck that impinge on motor function? The answers will probably have general implications for any myosin that employs calmodulin as a LC (that's likely to be quite a few of them). Another question is whether or not the folded state observed for Myo5 exists in vivo. Detection may prove to be challenging, however it should be possible to develop spectroscopic probes for real-time detection of conformational transitions as Myo5 goes from the active to an inactive state. Ideally, the ability to correlate these with cargo binding, movement and local changes in calcium concentration would allow for a detailed understanding of how myosin function is controlled at the cellular level.

Localization. Activation of a given motor is meaningful only if this event occurs when and where motor function is needed. A few myosins are present in seemingly fixed structures (i.e myosin thick filaments in muscle, the actin-rich microvilli of epithelial cells), but many myosins must be recruited to their intracellular targets before functioning. For example, Myo5a is responsible for actin-dependent distribution of melanosomes and it is recruited to the melanosome membrane via small G-protein dependent interaction with its binding partner melanophilin (Provance et al.; Strom et al; Wu et al, 2002). The interaction of a myosin with its binding partner could regulate activity at two levels – first, by the mere act of localizing the motor to its site of action and second, the binding to its targeting molecule may turn the motor on (e.g. as has been reported for Myo5a binding to melanophilin; Li et al, 2005).

The localization of several different myosins is highly dynamic. The *Dictyostelium* Myo7, for example, is present on the plasma membrane of migrating and phagocytosing cells (Tuxworth et al, 2001) and this localization is transient. Myo7 is associated with the growing phagosome shortly after the cell engages a particle but once the phagosome is fully formed it disappears (Fig. 1). Similar dynamics are observed for Myo7 at the leading edge of a migrating cell. Myo7 is present while the membrane is being extended but is rapidly released as protrusion ceases. Preliminary FRAP data reveal that Myo7 turnover on the membrane is quite rapid in migrating cells (~t1/2 = 1 sec; Galdeen et al). What regulates this rapid association and disassociation? It is of interest to note that Myo7 is present in regions of the cell where dynamic actin polymerization occurs. This may promote the assembly of a receptor-cytoskeleton complex that has high affinity for Myo7. Termination of polymerization signals may then result reorganization of this complex and release of Myo7 from the membrane. Functional analysis of the Myo7 tail domain reveals that the both of the FERM domains found in the tail are essential for membrane binding (Titus & Stephens). These domains could promote interaction with the cytoplasmic tails of receptor proteins or phospholipids. Ongoing efforts to identify the mechanism of membrane binding should aid in identifying how Myo7 localization and function are tightly controlled in *Dictyostelium*.

Summary. The regulation of myosin function entails controlling fundamental aspects of motor function, structure and intracellular localization. Many myosins may share common modes of regulation but as progress is made in characterizing additional family members new paradigms are sure to emerge. The overall goal will continue to be the dissection of the molecular basis of regulatory mechanisms and how these are engaged by the cell.

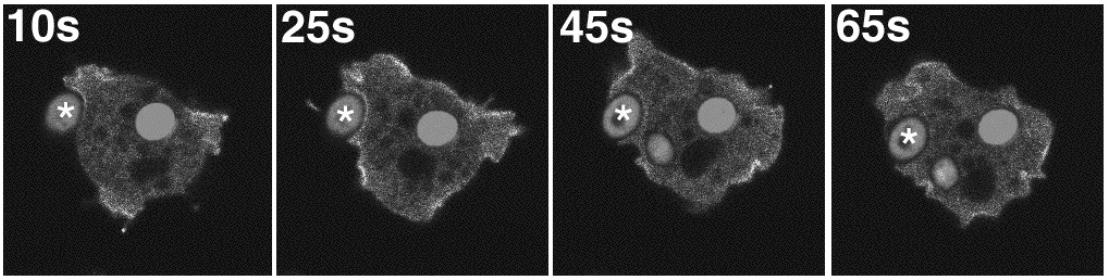

Fig. 1. Localization of GFP-M7 during phagocytosis of yeast (*). Note the rim of fluorescence around the particle that disappears after cup formation is complete (modified from Tuxworth et al, 2001).

MOLECULAR MOTORS KIFs AND CARGO BINDING AND REGULATION

Nobutaka Hirokawa

Department of Cell Biology and Anatomy, Graduate School of Medicine, University of Tokyo, Hongo 7-3-1, Bunkyo-ku, Tokyo 113-0033, JAPAN
Tel: +81-3-5841-3326
Fax: +81-3-5689-4856
E-mail address: hirokawa@m.u-tokyo.ac.jp

Intracellular transport is fundamental for cellular morphogenesis, function and survival. Many proteins are selectively transported to their destinations as membranous organelles and protein complexes. In addition, some specific mRNAs are transported for local translation. Kinesin superfamily proteins (KIFs) participate in selective transport by using adaptor/scaffolding proteins to recognize and bind cargoes(Figs.1-3)(1-7). Here I discuss the molecular mechanisms of directional transport with specific emphasis on the role of motor proteins and their mechanisms of cargo recognition based on maily works from our laboratory.

Kinesin superfamily proteins

The kinesin superfamily is a large gene family of microtubule-dependent motors with 45 members in mice and humans(Figs. 1,2)(4,5,7).

All KIFs have a globular motor domain that shows high degrees of homology and contains a microtubule-binding sequence and an ATP-binding sequence, but the sequence outside the motor domain is unique to each KIF(3,-8). These regions form the cargo-binding domains, and their diversity explains why KIFs transport many different cargoes. Many KIFs are expressed in the nervous system, but KIFs are also expressed in other tissues and participate in various types of intracellular transport(3,5,7).

Motors and Cargoes(Fig. 3)

KIF1A and KIF1Bβ transport synaptic vesicle precursors along nerve axons. Although mature synaptic vesicles are relatively uniform spheres of about 50 nm in diameter, these structures are usually not observed in axons. Instead, the components of synaptic vesicles are transported in tubulovesicular organelles as precursors, and assembled into synaptic vesicles at synaptic terminals(15). The synaptic vesicle precursor that is transported by KIF1A contains synaptic vesicle proteins such as synaptotagmin, synaptophysin and Rab3A, but not presynaptic membrane proteins such as syntaxin 1A or SNAP-25(4,9,14).

When the cargoes of KIF1A and KIF1Bβ are isolated by immunoprecipitation, they are found to contain synaptic vesicle proteins. Furthermore, mice that lack either KIF1A or KIF1Bβ show a reduced density of synaptic vesicles at synaptic terminals, and impaired sensory and motor nerve functions(13,14). KIF1Bα (formerly KIF1B), an isoform that is derived from the same gene as KIF1Bβ by alternative splicing, transports mitochondria anterogradely(10). The N-terminal motor domain of KIF1Bα and KIF1Bβ are identical, but their C-terminal tails share no significant homology, whereas the C-terminal tails of KIF1A and KIF1Bβ have 61% amino-acid identity.

The cargo vesicles of KIF5(5A,5B,5C) also contain proteins such as GAP-43 and VAMP2(17). KIF5, like KIF1Bα, also transports mitochondria(16,18). The fact that mitochondria are transported by both KIF5 and KIF1Bα might not be surprising, given that mitochondria could have many potential binding sites for motor proteins. KIF5 also transports oligomeric tubulin in large transporting complex distinct from those of stable polymers or other cytosolic proteins. Movement of fluorescently-labeled tubulin microinjected to axons at a compatible speed of slow axonal transport is perturbed by the functional blocking anti-kinesin antibody, thus indicating that KIF5 also participates in slow axonal transport(19).

The KIF3A/KIF3B-KAP3 complex transports vesicles, 90 to 160 nm in diameter, distinct from synaptic vesicles precursors and from vesicles carried by other motors such

as KIF5 that are associated with fodrin, through an interaction between KAP3 and fodrin and important for neurite extension(11,12,20).

Molecules that are transported in nerve dendrites include those associated with postsynaptic densities, neurotransmitter receptors, ion channels, and specific mRNAs. These include the mRNA for microtubule-associated protein-2 (MAP2), which is specifically expressed in dendrites, and for the α-subunit of calcium/calmodulin-dependent protein kinase II (CaMKIIα) and activity-regulated cytoskeleton-associated protein (Arc), both of which are involved in long-term potentiation. First, N-methyl-D-aspartate (NMDA) glutamate receptors are transported in dendrites by KIF17. KIF17 is an N-kinesin and a plus-end-directed motor that is localized mainly in dendrites, colocalizes with the NR2B subunit of NMDA receptors, and moves away from the cell body towards the postsynaptic region at an average speed of 0.76 μm/s(24,26). The physiological importance of the transport of NMDA receptors by KIF17 has been shown in transgenic mice. The overexpression of KIF17 enhances working or episodic-like memory and spatial learning and memory in transgenic mice. Moreover, the genes for KIF17 and NR2B are coregulated so that overexpression of KIF17 leads to the upregulation of NR2B. This process might involve the increased phosphoryation of a transcription factor, the cAMP response element-binding protein (CREB)(25).

Second, α-amino-3-hydroxy-5-methylisoxazole-4-propionate (AMPA) glutamate receptors are transported by KIF5s (KIF5A, KIF5B, and KIF5C)(27). In this case, the binding of AMPA receptors apparently steers KIF5 to dendrites, as discussed below.

Third, it has been shown that KIF5s also transport a large multisubunit complex composed of 42 proteins that includes the mRNAs for CaMKIIα and Arc(28). The S value of this complex is estimated to be 1000 or more, because it sediments more than 12 times as fast as synaptic vesicle marker (115S) or free ribosome marker (80S) in a sucrose density gradient centrifugation. This complex is transported exclusively in dendrites at a forward speed of about 0.1 μm/s, although the tug-of-war between forward and backward movements decreases the "net" speed to 0.01-0.05 μm/s. The proteins in this complex are those associated with RNA transport, such as Fragile X mental retardation proteins (FMR1, FXR1, and FXR2), Purα, Purβ, and staufen; those associated with protein synthesis, such as elongation factors (for example, EF-1α and eIF2α); RNA helicases (such as DDX1 and DDX3); heterogeneous nuclear ribonucleoproteins (such as hnRNP-U and hnRNP-A/B); and other RNA-associated proteins such as polypyrimidine tract-binding protein-associated splicing factor (PSF)(28).

Cargo Recognition by Motors(Fig.4)

It was initially assumed that transmembrane cargo proteins would bind directly to specific motors. However, it is become clear that KIFs tend to use an adaptor/scaffolding protein complex for cargo recognition and binding(24,27,30).

Binding of KIF13A to AP-1 adaptor. KIF13A was one of the first examples of the involvement of adaptor/scaffolding proteins in the binding of KIFs to cargoes(30). KIF13A transports vesicles containing the mannose-6-phosphate receptor (M6PR). KIF13A is ubiquitously expressed in various tissues and transports vesicles containing M6PR from the *trans*-Golgi network to the plasma membrane. Mannose-6-phosphate (M6P) serves as a recognition signal for intracellular sorting; newly synthesized lysosomal hydrolases carrying M6P bind to M6PR in the *trans*-Golgi network. The cytoplasmic side of M6PR binds to the AP-1 adaptor complex and is transported by clathrin-coated vesicles primarily to endosomes but also to the cell surface. In transporting M6PR-containing vesicles, KIF13A binds to M6PR via the AP-1 adaptor complex; therefore, the AP-1 adaptor complex serves as an adaptor for both the motor and clathrin coats. The AP-1 adaptor complex comprises β1-, γ-, μ1-, and δ1-adaptin subunits, and the C-terminal tail of KIF13A binds to β1-adaptin, which is also the binding partner of clathrin. However, KIF13A and clathrin bind to different domains of β1-adaptin.

Binding of KIF17 to scaffolding proteins. One of the first clear examples of the use of scaffolding proteins by molecular motors was KIF17. The interaction between KIF17 and its cargo vesicles, which contain NMDA receptors, is mediated by a tripartite protein

complex that contains mLin-10 (Mint1), mLin-2 (CASK), and mLin-7 (Velis/MALS). This complex is involved in the localization of proteins in polarized cells such as neurons and epithelial cells, including synaptic vesicle exocytosis and the organization of the postsynaptic density. All three proteins contain PDZ domains, but these domains do not bind to each other , leaving them free to recruit other proteins to the complex. The C-terminal tail domain of KIF17 interacts directly with the first PDZ domain of mLin-10, which then sequentially interacts with mLin-2, and then mLin-7. The PDZ domain of mLin-7/Velis/MALS binds to the C-terminus of the NMDA receptor subunit NR2B. Therefore, NMDA receptors are transported by KIF17 through its binding to the scaffolding protein complex for NMDA receptors(24).

Binding via KIF5. The binding of the C-terminal tail of KIF5 to AMPA receptors, which is bridged by a scaffolding protein, glutamate receptor-interacting protein (GRIP1), transports vesicles to dendrites. GRIP1 is a cytoskeletal postsynaptic density protein with seven PDZ domains that can interact with various proteins and is involved in the clustering of AMPA receptors. The minimal GRIP1-binding site of KIF5 at its C-terminal tail (amino acid residues 807-934) overlaps with the cargo-binding domain of the fungus kinesin and is contained in all KIF5 family genes (KIF5A, KIF5B, and KIF5C). When the KIF5-binding domain of GRIP1 (amino acid residues 753-987), which is between the sixth and seventh PDZ domains, is overexpressed, endogenous KIF5 predominantly accumulates in the somatodendritic area; by contrast, when JIP-3 (JSAP1), which binds to KLC, is overexpressed, KIF5 accumulates in the somatoaxonal area, indicating that cargo binding to KIF5 steers cargoes to dendrites(27).

RNA-containing granules, which are transported to dendrites, also bind to the C-terminal tail of KIF5 . The minimal binding site for RNA-containing granules is a 59-amino-acid region of KIF5 (amino acid residues 865-923), which is also conserved among KIF5A, KIF5B, and KIF5C. Among the 42 or more proteins that constitute the large RNA-containing granule, Purα and Purβ are two of the most strongly bound components. However, the direct binding partner of KIF5 is unknown. When cultured neurons are transfected with both green fluorescent protein (GFP)-Purα and cyan fluorescent protein (CFP)-KIF5, Purα-containing granules are transported exclusively to dendrites, although CFP-KIF5 distributes to both axons and dendrites. However, when a dominant negative mutant of KIF5 (CFP-ΔN1), which contains the C-terminal tail RNA granule-binding site but lacks the N-terminal motor domain, is expressed, the movement of RNA-containing granules towards distal dendrites is inhibited. CaMKIIα and Arc mRNAs colocalize with Purα-containing granules, but tubulin mRNA does not. When RNA interference (RNAi) is used to suppress expression of component proteins of the RNA-containing granules such as hnRNP-U, staufen, Purα, and PSF, mRNA transport is suppressed. These results show that RNA-containing granules are transported to dendrites as a result of their direct binding to the C-terminal tail of KIF5(28).

Directional transport and sorting

As discussed above, cargo recognition seems to have important roles in directional transport. However, neurons use many mechanisms to selectively sort and transport proteins to axons and dendrites.

Microtubules have intrinsic polarity, which differs between axons and dendrites. This difference could be used to achieve polarized transport into the axon and dendrites. It has been proposed that the post-Golgi transport of dendritic proteins might be mediated mainly by minus-end-directed motors. However, as discussed above, there is increasing evidence that this is not the case.

Rather, membrane proteins are transported to dendrites as well as to axons by plus-end-directed motors. For example, NMDA receptors are transported by KIF17, and AMPA receptor and mRNA complexes by KIF5. However, the use of plus-end-directed motors for both axonal and dendritic transport poses an inherent problem. How do motors differentiate axons from dendrites? Some motors, such as KIF17 might be able to differentiate them. In the case of KIF5, the direction of transport might be determined by whether cargoes bind via KLC or directly to KIF5.

Microtubules in initial segment as cue. Although axonal and dendritic transport are often dealt with as two similar, alternative pathways, in reality the requirements for the two are

very different. A typical neuron has several dendrites with large diameters in their proximal segments. By contrast, each neuron has only one axon, and the diameter of a typical axon from the initial segment onwards is very small. If the diameter of an axon is one-tenth of that of the cell body, axonally transported materials need to be propelled from the cell body in only about 0.25% of all possible directions to enter the axon. Some structural components, rather than a diffusible signal, must provide a directional cue for efficient sorting and transport to the axon.

It has recently been shown that microtubules at the initial segment serve as the cue for the KIF5 motor domain to enter the axon. When the GFP-KIF5 motor domain is expressed in hippocampal neurons, it accumulates at the tips of axons, indicating that preferential axonal transport of KIF5 is attributed to its motor domain. Moreover, a mutated form of KIF5 that can be recruited to microtubules but cannot translocate along nor dissociate from microtubules (rigor-KIF5) accumulates in the initial segment of axons, indicating that the KIF5 motor domain, as a default, prefers microtubules in the initial segment(17).

What makes microtubules at the initial segment unique? Electron microscopy has shown that microtubules in the initial segment have a high density; however, how this organization is maintained is unclear. Yellow fluorescent protein (YFP)-EB1, which binds to the tips of growing microtubules, shows a particularly high affinity for microtubules in the initial segment, indicating there is a specific property of initial segment microtubules that might be recognized by both KIF5 and EB1. To maintain the difference between microtubules in the initial segment and those in dendrites, a continuous turnover of microtubules might be needed. If the dynamics of microtubule turnover are changed by treatment with a low concentration of taxol, KIF5 loses its ability to preferentially bind to microtubules in the initial segment and to mediate directional transport to the axon(17).

Conclusions and future perspectives

Neurons use many complex mechanisms to maintain the polarity of axons and dendrites, and motor proteins are vital for these mechanisms. Proteins are sorted and transported in various organelles and protein complexes, and they are specifically recognized by different motors and selectively transported to specific destinations. mRNAs are also transported as large protein-RNA complexes. Motors seem to recognize these cargoes through adaptor complexes or scaffolding proteins. Some proteins directly associate with adaptor complexes or scaffolding proteins, but others can be transported by associating with these proteins. Targeting sequences can, therefore, bind to adaptor or scaffolding complexes, motors, or other proteins that are necessary for proteins to associate in organelles.

Other proteins are transported nonselectively throughout the neuron, before being selectively eliminated from inappropriate destinations by endocytosis. They are presumably retained in the desired location by associating with cytoskeletal complexes. In this case, signals that are recognized by the endocytotic apparatus might in effect serve as targeting signals.

Although many issues need to be clarified further, motors are important in all selective transport processes. Motors can intrinsically distinguish between axons and dendrites, perhaps being cued by microtubules. The mode of binding of cargoes to motors can also affect the direction of transport, presumably by changing the conformation of the motors. Previous structural studies have helped to clarify the characteristics of individual motors. For example, KIF1A is a unique monomeric motor, and single molecule biophysics, optical trapping, cryoelectron microscopy, and X-ray crystallography have revealed how it moves(31-34). The X-ray crystallography of KIF2 has revealed the structural attributes that underlie its unique microtubule-depolymerizing activity(22,23). Structural studies that compare motors in terms of axonal versus dendritic transport and their interaction with microtubules might provide important information.

Because of the variety of molecules that are transported selectively to axons and dendrites, it is not surprising that many different mechanisms are used. Some of these mechanisms might be redundant, because any sorting machinery is not likely to have 100% efficiency. A basic understanding of the transport process from the viewpoint of motors and their association with cargoes will help to clarify the common principles by which cargoes are selectively sorted and transported.

There are still motors whose functions are unknown, and we do not yet know largely how transport is regulated — for example, how are the association and dissociation of cargoes with motors controlled?

Our recent research on KIF4 shed a light on this question(Fig.5)(41). In brain development, apoptosis is a physiological process that controls the final numbers of neurons. Our recent study revealed that the activity-dependent prevention of apoptosis in juvenile neurons is regulated by KIF4. The C-terminal domain of KIF4 is a module that suppresses the activity of poly(ADP-ribose)polymerase-1(PARP-1), a nuclear enzyme known to maintain cell homeostasis by repairing DNA and serving as a transcriptional regulator. When neurons are stimulated by membrane depolarization, calcium signaling mediated by CaMKII induces dissociation of KIF4 from PARP-1, resulting in upregulation of PARP-1 activity, which supports neuron survival. After dissociation from PARP-1, KIF4 enters into the cytoplasm from the nucleus and moves to the distal part of neuritis in a microtubule-dependent manner. We suggested that KIF4 controls the activity-dependent survival of postmitotic neurons by regulating PARP-1 activity in brain development. This study showed that a motor dissociates from binding partner by phosphorylation(Fig.5)(41). However, these problems are important subject of ongoing and future studies for most of KIFs and cargo interactions.

1. Hirokawa, N. Cross-linker system between neurofilaments, microtubules, and membranous organelles in frog axons revealed by the quick-freeze, deep-etching method. ***J Cell Biol*** 94, 129-142 (1982).
2. Hirokawa, N. Molecular architecture and dynamics of the neuronal cytoskeleton. in *Neuronal Cytoskeleton* (ed. Burgoyne, R. D.) 5-74 (Wiley-Liss, Inc., New York, 1991).
3. Hirokawa, N. Kinesin and dynein superfamily proteins and the mechanism of organelle transport. ***Science*** 279, 519-526 (1998).
4. Aizawa, H., Sekine, Y., Takemura, R., Zhang, Z., Nangaku, M. & Hirokawa, N. Kinesin family in murine central nervous system. ***J Cell Biol*** 119, 1287-1296 (1992).
5. Miki, H., Setou, M., Kaneshiro, K. & Hirokawa, N. All kinesin superfamily protein, KIF, genes in mouse and human. ***Proc Natl Acad Sci U S A*** 98, 7004-7011 (2001).
6. Hirokawa, N. & Takemura, R. Kinesin superfamily proteins. in *Molecular Motors* (ed. Schliwa, M.) 79-109 (Wiley-VCH, Weinheim, 2003).
7. Hirokawa, N. & Takemura, R. Molecular motors and mechanisms of directional transport in neurons. ***Nat Rev Neurosci*** 6,201-214 (2005)
8. Hirokawa, N., Pfister, K. K., Yorifuji, H., Wagner, M. C., Brady, S. T. & Bloom, G. S. Submolecular domains of bovine brain kinesin identified by electron microscopy and monoclonal antibody decoration. ***Cell*** 56, 867-878 (1989).
9. Okada, Y., Yamazaki, H., Sekine-Aizawa, Y. & Hirokawa, N. The neuron-specific kinesin superfamily protein KIF1A is a unique monomeric motor for anterograde axonal transport of synaptic vesicle precursors. ***Cell*** 81, 769-780. (1995).
10. Nangaku, M., Sato-Yoshitake, R., Okada, Y., Noda, Y., Takemura, R., Yamazaki, H. & Hirokawa, N. KIF1B, a novel microtubule plus end-directed monomeric motor protein for transport of mitochondria. ***Cell*** 79, 1209-1220. (1994).
11. Yamazaki, H., Nakata, T., Okada, Y. & Hirokawa, N. KIF3A/B: A heterodimeric kinesin superfamily protein that works as a microtubule plus end-directed motor for membrane organelle transport. ***J. Cell Biol.*** 130, 1387-1399 (1995).
12. Yamazaki, H., Nakata, T., Okada, Y. & Hirokawa, N. Cloning and characterization of KAP3: A novel kinesin superfamily-associated protein of KIF3A/3B. ***Proc Natl Acad Sci USA*** 93, 8443-8448 (1996).
13. Yonekawa, Y., Harada, A., Okada, Y., Funakoshi, T., Kanai, Y., Takei, Y., Terada, S., Noda, T. & Hirokawa, N. Defect in synaptic vesicle precursor transport and neuronal cell death in KIF1A motor protein-deficient mice. ***J Cell Biol*** 141, 431-441 (1998).
14. Zhao, C., Takita, J., Tanaka, Y., Setou, M., Nakagawa, T., Takeda, S., Yang, H. W., Terada, S., Nakata, T., Takei, Y., Saito, M., Tsuji, S., Hayashi, Y. & Hirokawa, N. Charcot-Marie-Tooth disease type 2A caused by mutation in a microtubule motor KIF1Bbeta. ***Cell*** 105, 587-597 (2001).
15. Nakata, T., Terada, S. & Hirokawa, N. Visualization of the dynamics of synaptic vesicle and plasma membrane proteins in living axons. ***J Cell Biol*** 140, 659-674 (1998).
16. Tanaka, Y., Kanai, Y., Okada, Y., Nonaka, S., Takeda, S., Harada, A. & Hirokawa, N. Targeted disruption of mouse conventional kinesin heavy chain, *kif5B*, results in abnormal perinuclear clustering of mitochondria. ***Cell*** 93, 1147-1158 (1998).
17. Nakata, T. & Hirokawa, N. Microtubules provide directional cues for polarized axonal transport through interaction with kinesin motor head. ***J. Cell Biol.*** 162, 1045-1055 (2003).
18. Kanai, Y., Okada, Y., Tanaka, Y., Harada, A., Terada, S. & Hirokawa, N. KIF5C, a novel neuronal kinesin enriched in motor neurons. ***J Neurosci*** 20, 6374-6384 (2000).
19. Terada, S., Kinjo, M. & Hirokawa, N. Oligomeric tubulin in large transporting complex is transported via kinesin in squid giant axons. ***Cell*** 103, 141-155. (2000).
20. Takeda, S., Yamazaki, H., Seog, D. H., Kanai, Y., Terada, S. & Hirokawa, N. Kinesin superfamily protein 3 (KIF3) motor transports fodrin- associating vesicles important for neurite building. ***J Cell Biol*** 148, 1255-1265 (2000).
21. Noda, Y., Sato-Yoshitake, R., Kondo, S., Nangaku, M. & Hirokawa, N. KIF2 is a new microtubule-based anterograde motor that transports membranous organelles distinct from those carried by kinesin heavy chain or KIF3A/B. ***J Cell Biol*** 129, 157-167 (1995).
22. Ogawa, T., Nitta, R., Okada, Y. & Hirokawa, N. A common mechanism for microtubule destabilizers-M type kinesins stabilize curling of the protofilament using the

class-specific neck and loops. ***Cell*** 116, 591-602 (2004).

23. Homma, N., Takei, Y., Tanaka, Y., Nakata, T., Terada, S., Kikkawa, M., Noda, Y. & Hirokawa, N. Kinesin superfamily protein 2A (KIF2A) functions in suppression of collateral branch extension. ***Cell*** 114, 229-239 (2003).
24. Setou, M., Nakagawa, T., Seog, D. H. & Hirokawa, N. Kinesin superfamily motor protein KIF17 and mLin-10 in NMDA receptor-containing vesicle transport. ***Science*** 288, 1796-1802 (2000).
25. Wong, R. W., Setou, M., Teng, J., Takei, Y. & Hirokawa, N. Overexpression of motor protein KIF17 enhances spatial and working memory in transgenic mice. ***Proc Natl Acad Sci U S A*** 99, 14500-14505 (2002).
26. Guillaud, L., Setou, M. & Hirokawa, N. KIF17 dynamics and regulation of NR2B trafficking in hippocampal neurons. ***J. Neurosci.*** 23, 131-140 (2003).
27. Setou, M., Seog, D. H., Tanaka, Y., Kanai, Y., Takei, Y., Kawagishi, M. & Hirokawa, N. Glutamate-receptor-interacting protein GRIP1 directly steers kinesin to dendrites. ***Nature*** 417, 83-87 (2002).
28. Kanai, Y., Dohmae, N. & Hirokawa, N. Kinesin transports RNA; isolation and characterization of an RNA-transporting granule. ***Neuron*** 43, 513-525 (2004).
29. Saito, N., Okada, Y., Noda, Y., Kinoshita, Y., Kondo, S. & Hirokawa, N. KIFC2 is a novel neuron-specific C-terminal type kinesin superfamily motor for dendritic transport of multivesicular body-like organelles. ***Neuron*** 18, 425-438 (1997).
30. Nakagawa, T., Setou, M., Seog, D., Ogasawara, K., Dohmae, N., Takio, K. & Hirokawa, N. A novel motor, KIF13A, transports mannose-6-phosphate receptor to plasma membrane through direct interaction with AP-1 complex. ***Cell*** 103, 569-581 (2000).
31. Okada, Y. & Hirokawa, N. A processive single-headed motor: kinesin superfamily protein KIF1A. ***Science*** 283, 1152-1157 (1999)
32. Kikkawa, M., Sablin,E.P., Okada,Y., Yajima, H., Fletterick, R.J., and Hirokawa, N. Switch-based mechanism of kinesin motors. ***Nature*** 411, 439-445 (2001).
33. Okada, Y., Higuchi, H. & Hirokawa, N. Processivity ofthesingle-headekinesinKIF1A through biased binding to tubulin. ***Nature*** 424, 574-577 (2003).
34. Nitta, R., Kikkawa, M., Okada, Y. & Hirokawa, N. KIF1A alternately uses two loops to bind microtubules. ***Science*** 305, 678-683 (2004).
35. Nakata, T. & Hirokawa, N. Point mutation of adenosine triphosphate-binding motif generated rigor kinesin that selectively blocks anterograde lysosome membrane transport. ***J Cell Biol*** 131, 1039-1053 (1995).
36. Nonaka, S., Tanaka, Y., Okada, Y., Takeda, S., Harada, A., Kanai, Y., Kido, M. & Hirokawa, N. Randomization of left-right asymmetry due to loss of nodal cilia generating leftward flow of extraembryonic fluid in mice lacking KIF3B motor protein. ***Cell*** 95, 829-837 (1998).
37. Takeda, S., Yonekawa, Y., Tanaka, Y., Okada, Y., Nonaka, S. & Hirokawa, N. Left-right asymmetry and kinesin superfamily protein KIF3A: new insights in determination of laterality and mesoderm induction by *kif3A*$^{-/-}$ mice analysis. ***J Cell Biol*** 145, 825-836 (1999).
38. Sekine, Y., Okada, Y., Noda, Y., Kondo, S., Aizawa, H., Takemura, R. & Hirokawa, N. A novel microtubule-based motor protein (KIF4) for organelle transports, whose expression is regulated developmentally. ***J. Cell Biol.*** 127, 187-201 (1994).
39. Noda, Y., Okada, Y., Saito, N., Setou, M., Xu, Y., Zhang, Z. & Hirokawa, N. KIFC3, a microtubule minus end-directed motor for the apical transport of annexin XIIIb-associated Triton-insoluble membranes. ***J Cell Biol*** 155, 77-88 (2001).
40. Xu, Y., Takeda, S., Nakata, T., Noda, Y., Tanaka, Y. & Hirokawa, N. Role of KIFC3 motor protein in Golgi positioning and integration. ***J Cell Biol*** 158, 293-303 (2002).
41. Midorikawa, R., Takei, Y., & Hirokawa, N. KIF4 motor regulates activity-dependent neuronal survivial by suppressing PARP-1 enzymatic activity. ***Cell*** 125, 371-383 (2006)

Figure legend

Figure 1: Quick-frozen, deep-etched axons in which various types of crossbridges(arrows) are identified between membranous organelles and microtubules as candidates for molecular motors.

Figure 2: Upper left; The domain structures of the principal KIFs. KIF1Bα and KIF1Bβ are alternative transcripts of KIF1B. The motor domains are indicated in purple, the ATP-binding consensus sequence by a thin red line, the microtubule-binding consensus sequence by a thick red line, and the dimerization domains by yellow hatched boxes. The number of amino acids in each molecule is shown on the right. KIF1A, KIF1Bα and KIF1Bβ, KIF1C, KIF3A, KIF3B, KIF4A, KIF5A, KIF5B, KIF5C, KIF13A, and KIF17 have the motor domains in the N-terminus and are therefore N-kinesins[5,14,15]. KIF2A has the motor domain in the middle of the molecule and is therefore an M-kinesin. KIFC2 and KIFC3 have the motor domains in the C-terminal and are therefore C-kinesins.
Lower left; Diagrams constructed on the basis of electron microscopy(left) or predicted from the analysis of their primary structures are shown on the right (Red ovals in each diagram indicate motor domains). KIF5 forms a homodimer and kinesin light chains (KLC; blue) associate at the C-terminus to form fanlike ends. KIF1A and KIF1Bα are monomeric and globular. KIF2A forms a homodimer and its motor domains (red ovals) are in the middle (N-terminal non-motor domain, blue). KIF3A and KIF3B form a heterodimer (α-helical coiled-coil domains and C-terminal tail of KIF3A and KIF3B are expressed in red and blue) and kinesin superfamily-associated protein 3 (KAP3; shown in green) associates at the C-terminal end. KIF4 forms a homodimer. KIFC2 also forms a homodimer, but its motor domain is on the opposite side (N-terminal tail and α-helical coiled-coil domains, blue and C-terminal motor domains, red)(3,7). Scale bar, 100 nm.
Upper right; Phylogenetic comparison of mouse and human KIFs(5)

Figure 3: (a) A typical neuron extending several dendrites on the left and a single thin axon on the right from the cell body is shown with its microtubule polarity and the rough endoplasmic reticulum. In the axon, microtubules are unipolar, the plus ends pointing towards the synaptic terminal. Microtubules form special bundles at the initial segment, which may serve as the cue for axonal transport. Tubulovesicular organelles are transported anterogradely along microtubules by KIFs. In the growth cone of an axon collateral, KIF2A controls microtubule dynamics and extension of collaterals. Rough endoplasmic reticula are abundant in most parts of the cell body, except for the axon hillock. Dendrites contain some rough endoplasmic reticula. Microtubules have mixed polarity in proximal dendrites, but are unipolar in distal dendrites. Membranous organelles and RNA-containing granules are transported along microtubules by KIFs. (b)In the axon mitochondria are transported by KIF5 and KIF1Bα. KIF3 transports vesicles associated with fodrin. KIF1A/KIF1Bβ transports synaptic vesicle precursors. (c) In dendrites, KIF5 transports vesicles containing AMPA receptor by interaction between KIF5 and GRIP1. RNA-containing granules are also transported by interacting directly with KIF5. KIF17 transports vesicles containing NMDA receptor by interacting via the LIN complex(7)

Figure 4: A schema showing how KIFs recognize and binds their cargoes.
In many cases KIFs tail domain binds scaffolding protein or adaptor protein complexes and recognizes and binds cargo proteins(24,27,30).

Figure 5: Schematic model of the involvement of KIF4 in the regulation of the survival of developing neurons. (1) KIF4 binds to PARP-1 and inhibits PARP-1 activity. (2) After membrane depolarization, elevated Ca++ activates CaMKII, which phosphorylates PARP-1. (3) PARP-1 is automodified(Homburg et al., 2000). (4) KIF4 is dissociated from poly ADP-ribosylated PARP-1 and moves into neurites. Upregulated PARP-1 activity promotes expression of genes and modifies nuclear proteins to support cell survival(41)

Some thoughts on the regulation of bi-directional transport

Steven Gross
U.C. Irvine
sgross@uci.edu

(*This manuscript is NOT intended for distribution outside the attendees of the Point-Counterpoint meeting***)**

Many cargos, including numerous classes of vesicles, mitochondria, mRNA particles, intermediate filament fragments and virus particles move bi-directionally along microtubules, employing both dynein and a kinesin-family motors. Here, as a motivation for the upcoming discussion, I briefly review what we know so far of the mechanics and regulation of such motion. As background, interested readers may want to consult two relatively recent reviews on the subject[1, 2]; my treatment of topics discussed in those reviews will be somewhat abbreviated. As this paper is meant simply to be used to stimulate discussion, it is not intended as a complete review of this extensive topic; important contributions by numerous labs have certainly been missed.

Cargos that move bi-directionally typically reverse course every seconds or two. Because transport velocities are usually between 300 nm/s and 1-2 microns per second, this means that the typical run length (i.e. the distance traveled in a given direction before either a reversal or pause) in different systems can be anywhere between 300 nm and 4-6 microns. To control net (average) travel, the cell must control the relative length of plus-end versus minus-end runs. There appear to be two ways that this happens. In many systems, the run length in one direction is left approximately constant, and the run length in the other is increased or decreased. Examples of such systems include Xenopus pigment granules (minus-end run lengths are altered) [3], mitochondria (plus-end run lengths are altered)[4] and lipid droplets (plus-end run lengths are altered) [5]. There are also systems where runs in both directions are altered, such as pigment granules in Fish cells[6].

These frequent changes in direction indicate that the cargo is alternatively transported by plus-end kinesin-family motors and minus-end dynein motors. There are three basic scenarios for how opposite polarity motors could work together. In the first, they engage in a tug-of-war, and the instantaneous direction of cargo transport is determined by whichever set of motors exerts more force. In this scenario, regulation would influence the frequency with which a given set of motors 'wins' the tug-of-war, e.g. by altering the average number of engaged motors of one class. A second scenario posits that coordination is achieved between motors, so that they do not engage in a tug-of-war, by only having one set of motors on the cargo at any given time. In this model, the cargo switches direction when one group of motors is released, and the alternative motors are bound. The third scenario suggests that both classes of motors remain bound to the cargo the entire time, but that there is coordination between opposite motors, so that only one set is engaged at any given time.

There have been a number of studies from different groups, and most favor some variant of the third scenario. That is, in general it appears that both classes of motors remain on the cargo, but do not engage in a constant tug-of-war (see for example, [3, 7-9]

and also further discussion in the reviews mentioned above). There is clearly functional coupling between opposite polarity motors on the same cargos, because alteration (impairment) of function of one set of motors (via mutations or antibodies) routinely alters (impairs) the function of the other set. Representative publications describing these effects include (but are not limited to) [10, 11]and [7].

Given a model where both sets of motors are on the cargo simultaneously, but usually only one set is active at any instant, we then must ask how is one set turned off, and the other set turned on, and also how interference between the opposite motors is avoided. We do not really know, but there are a number of known elements that have bearing on a final answer; I'll summarize them in the next few pages.

First, quite a few studies, in different systems, and using a variety of techniques, suggest that cargos may be moved by multiple motors, likely between 1 and 5 [5, 9, 12]. This is important because recent experimental work in our lab on dynein [13] and past experimental work from the Schnapp lab on kinesin [14], and finally recent theoretical work on multiple motors (either kinesin or dynein) [15] all suggest that cargos moved by more than one motor should go very long distances. What this means is that a cargo moved by multiple motors is expected to go very far unless something actively cuts short the run (i.e. the period of uninterrupted travel in the same direction). I will call the process that cuts short the run the 'switch'.

Mechanistically, what does the switching process involve? Motors could be turned off in a number of ways. First, single-molecule studies in vitro[16, 17] show that a motor's mean velocity and also processivity (i.e. how far it moves along the Microtubule before detaching) are decreased by an opposing force, or load. The more load, the larger the decrease. Thus, in principle, motors could be induced to detach from their tracks by applying a load; the more load the shorter the cargo would travel before the motors would detach. Where could such a load come from? There have been a number of studies [9, 18] suggesting that the cytosol itself provides significant drag, which in principle could reduce effective cargo processivity. Whether such drag is really sufficient to cause enough load to significantly cut short runs still remains an open question; a number of the studies observe changes in velocity of the cargos as they move, and conclude that these velocity changes are due to changes in the number of active motors moving the cargo.

Because we know that for processive motors functioning under no load, velocity is essentially independent of the number of motors, and kinesin and dynein are processive, this suggestion that velocity changes are due to changes in the number of motors requires the assumption that the cargos are moving under significant load. While this in principle may be true, it requires further study because in vivo there are potentially many factors affecting velocity. For instance, cytosolic properties may vary at different locations, so that applied load per motor might not be constant due to changes in the environment, rather than changes in the number of motors. Similarly, factors such as phosphorylation of the motor, or the presence or absence of accessory factors, could change the motors kinetics, independent of load. Obviously, these kinds of factors are not present in *in vitro* studies. Intriguingly, a recent *in vivo* study[19] of quantum dots *known* to be moved by only a single kinsin motor found mean sustained velocities of the same dot (at different times) that ranged between 0.26 and 0.67 microns/sec, suggesting velocities can vary quite significantly even when the cargo is always moved by a single motor and is presumably not under much load (the dots are 30 nm in diameter). So, cytosolic drag

could in principle load down motors inducing reversals, but any interpretation of changes in velocity *in vivo* needs to carefully evaluate the magnitude of such effects, as well as the possibility of other causes resulting in changes in cargo velocity.

If viscosity were playing an important role, one might expect that the mean travel distance in a given direction would be controlled by alteration of the mean number of motors engaged in a given direction. Two recent studies suggested that this might be the case[9, 20], though the conclusions on the number of motors were based solely on the distributions of observed velocities, which could have other causes as discussed above.

In principle, opposing load could also be applied via a cargo-MT linkage other than the currently motors moving the cargo. Such a load could come from the opposite polarity motors that would somehow be turned on by an external motor-control machinery. Alternatively, it could come from the dynactin complex which has been implicated in playing a role in coordination between opposite polarity motors and switching[7]. This is somewhat supported by a recent study[8] that found that for mitochondria loss of dynactin in axons (due to RNAi) resulted in increased velocity and run lengths in each direction, consistent with an applied load that had been lost. However, in this case motion was still bi-directional, and switching was still observed, so the exact role of dynactin in the switching process still remains to be investigated.

In addition to a load-based mechanism, one can imagine an essentially chemical mechanism, where a process essentially turns off one set of motors by blocking their enzymatic activity in some form. Innumerable mechanisms along these lines could be imagined. For instance, kinesin's tail is known to bind to its head, preventing futile hydrolysis when the tail is not attached to a cargo; this tail-to-head binding turns kinesin off. There could be proteins that mimic kinesin's tail and similarly bind to its head, thus turning it off; locally increasing or decreasing such functional tail mimics could then be used to turn kinsin off or on. Similarly, direct phosphrylation of the motor itself could alter its activity; this has been reported for both kinesin and dynein. We do not currently know the relative importance of load-based mechanisms versus essentially chemical mechanisms, and this will certainly be an important focus in the future.

What do we know about regulation in specific systems? Directly related to understanding bi-directional transport, there has been the most work done on pigment granules, mitochondria, and lipid droplets. There is also increasing work on virus transport and mRNA transport[21, 22] which I will not review here.

Part of the skin of Fish and frogs includes Melanophore cells, packed with pigment granules. By changing the distribution of these granules inside the cells, the animal can camouflage itself and change its color: dispersed pigment makes the cell the color of the pigment, while pigment granules aggregated to the cell center pile on top of each other, and thus the cell turns clear (or grey) with a small dot of pigment color at its center. Dispersion reflects net plus-end transport, whereas aggregation reflects net minus-end transport. Although Dispersion is due to the combined activities of both a kinesin-family member and Myosin-V (moving along actin), here I neglect the contribution of the actin/M-V system. The net direction of transport has been shown to be predominantly controlled by cAMP levels, which control the activity of PKA[23], and indeed in one system tuning cAMP levels or PKA activity artificially can be uses to tune run lengths[6]. In some cases PKC plays a minor role as well. We do not know all of the downstream targets of PKA, but a recent paper[24] showed that the MAK/ERK pathway is

downstream of PKA; the involvement of the ERK pathway had already been established in regulating melanophore motion. Ultimately, how these kinases together result in changes in the minus-end run length to control net aggregation or dispersion is not clear, however it is likely not due to overall recruitment of additional motors to the cargo, because western blot analysis indicates that the neither the amount of kinisin or dynein bound to the cargo changes between aggregation and dispersion[3]. If the average number of *engaged* motors does change, it is not immediately clear how that determines the mean length of runs--in the drosophila lipid droplet system (see below), force measurements *in vivo* suggest that the number of active minus-end motors changes between different developmental phases, but the mean minus-end run length remains approximately constant. In conclusion, then, the two kinases PKA and ERK are both localized to the cargo, and involved in regulating run lengths, but exactly what proteins are targeted by their kinase activity remain unknown.

Like pigment granule motion, lipid droplets have also been used as a model system to understand bi-directional transport. Control of the net direction of droplet transport starts with small, basic protein called Halo, whose levels are developmentally controlled[25]. In order to up-regulate plus-end motion, the embryo increases halo levels. It is not yet clear whether halo directly binds to the droplets, however changes in halo levels are correlated with changes in phosophorylation of the droplet-bound protein LSD2[26]. LSD2 is a key protein involved in regulating droplet motion, because in LSD2-null flies droplets move but their motion no longer is altered in response to developmental cues. LSD2 interacts with klar[26], another droplet-bound protein that is essential for normal droplet transport. Loss of klar tremendously impairs both plus-end and minus-end motion[5], and there is some evidence suggesting klar might interact directly with dynein. Thus, there is a suggested regulatory pathway, where halo levels somehow facilitate the activity of a kinase that phosphorylates LSD2, and potentially this phosphorylation then alters LSD2's interaction with klar, and klar then directly communicates with the kinesin-family and dynein motors to somehow regulate their activity. This pathway is speculative in a number of ways (for instance, other proteins like dynactin clearly play a role in droplet motion), but it none the less provides a starting point for future studies.

Mitochondria also move bi-directionally, to locations where the cell need energy (ATP) production. There has been a recent explosion of studies investigating various aspects of mitochondrial motion and its regulation. An excellent recent review [27] summarizes much of what is known, and here I only briefly discuss some of what is presented there. Just as overall motion of pigment granules can be altered by controlling ERK kinase activity[24], the total amount of anterograde organelle transport in axoplasm can be reduced by activation of GSK3[27], which phosphorylated KLC causing the release of kinesin-1 from the organelle surface. However, TNF activity also apparently causes phosphorylation and a decrease in kinesin function, while leaving kinesin attached to mitochondria[27], so the exact details of the pathway and its control remain to be elucidated. Nonetheless, direct regulation of kinesin function via phosphorylation appears to be one important aspect of regulation of mitochondrial motion. There are a number of other recently identified proteins such as the GTPase Miro[28] that also play a role in mitochondrial transport.

In conclusion, then, we are starting to identify some of the proteins that enable correct bi-directional transport, but we don't know how they work together to allow robust function and control. There are quite a number of open issues. These include clarifying the importance of physical mechanisms (such as load) on determining transport vs direct (chemical) activation/inactivation of motors. The implications of the number of motors that are instantaneously active, and how that is controlled, remains to be determined. Details of track usage are also not firmly established--under what conditions can a cargo simultaneously move along more than one MT, and is this useful/physiologically important? How much is alteration of tracks (via polymerization dynamics, MAPs, etc) used to control transport? In addition, the overall use of physical properties of motion (such as velocity), and what they tell us either about the sub-cellular environment or instantaneous state of motor activity, remain to be clarified. Finally, the mechanism that coordinates opposite polarity motors (or whether they functionally coordinate simply due to stochastic variations), and how motor coordination is linked to turning one set of motors on or off, remains to be clarified.

1. Gross, S.P. (2004). Hither and yon: a review of bi-directional microtubule-based transport. Phys Biol *1*, R1-11.
2. Welte, M.A. (2004). Bidirectional transport along microtubules. Curr Biol *14*, R525-537.
3. Gross, S.P., Tuma, M.C., Deacon, S.W., Serpinskaya, A.S., Reilein, A.R., and Gelfand, V.I. (2002). Interactions and regulation of molecular motors in Xenopus melanophores. J Cell Biol *156*, 855-865.
4. Morris, R.L., and Hollenbeck, P.J. (1993). The regulation of bidirectional mitochondrial transport is coordinated with axonal outgrowth. J Cell Sci *104 (Pt 3)*, 917-927.
5. Welte, M.A., Gross, S.P., Postner, M., Block, S.M., and Wieschaus, E.F. (1998). Developmental regulation of vesicle transport in Drosophila embryos: forces and kinetics. Cell *92*, 547-557.
6. Rodionov, V., Yi, J., Kashina, A., Oladipo, A., and Gross, S.P. (2003). Switching between microtubule- and actin-based transport systems in melanophores is controlled by cAMP levels. Curr Biol *13*, 1837-1847.
7. Gross, S.P., Welte, M.A., Block, S.M., and Wieschaus, E.F. (2002). Coordination of opposite-polarity microtubule motors. J Cell Biol *156*, 715-724.
8. Pilling, A.D., Horiuchi, D., Lively, C.M., and Saxton, W.M. (2006). Kinesin-1 and Dynein are the primary motors for fast transport of mitochondria in Drosophila motor axons. Mol Biol Cell *17*, 2057-2068.
9. Levi, V., Serpinskaya, A.S., Gratton, E., and Gelfand, V. (2006). Organelle transport along microtubules in Xenopus melanophores: evidence for cooperation between multiple motors. Biophys J *90*, 318-327.
10. Martin, M., Iyadurai, S.J., Gassman, A., Gindhart, J.G., Jr., Hays, T.S., and Saxton, W.M. (1999). Cytoplasmic dynein, the dynactin complex, and kinesin are interdependent and essential for fast axonal transport. Mol Biol Cell *10*, 3717-3728.

11. Brady, S.T., Pfister, K.K., and Bloom, G.S. (1990). A monoclonal antibody against kinesin inhibits both anterograde and retrograde fast axonal transport in squid axoplasm. Proc Natl Acad Sci U S A *87*, 1061-1065.
12. Ashkin, A., Schutze, K., Dziedzic, J.M., Euteneuer, U., and Schliwa, M. (1990). Force generation of organelle transport measured in vivo by an infrared laser trap. Nature *348*, 346-348.
13. Mallik, R., Petrov, D., Lex, S.A., King, S.J., and Gross, S.P. (2005). Building complexity: an in vitro study of cytoplasmic dynein with in vivo implications. Curr Biol *15*, 2075-2085.
14. Block, S.M., Goldstein, L.S., and Schnapp, B.J. (1990). Bead movement by single kinesin molecules studied with optical tweezers. Nature *348*, 348-352.
15. Klumpp, S., and Lipowsky, R. (2005). Cooperative cargo transport by several molecular motors. Proc Natl Acad Sci U S A *102*, 17284-17289.
16. Visscher, K., Schnitzer, M.J., and Block, S.M. (1999). Single kinesin molecules studied with a molecular force clamp. Nature *400*, 184-189.
17. Coppin, C.M., Pierce, D.W., Hsu, L., and Vale, R.D. (1997). The load dependence of kinesin's mechanical cycle. Proc Natl Acad Sci U S A *94*, 8539-8544.
18. Hill, D.B., Plaza, M.J., Bonin, K., and Holzwarth, G. (2004). Fast vesicle transport in PC12 neurites: velocities and forces. Eur Biophys J *33*, 623-632.
19. Courty, S., Luccardini, C., Bellaiche, Y., Cappello, G., and Dahan, M. (2006). Tracking individual kinesin motors in living cells using single quantum-dot imaging. Nano Lett *6*, 1491-1495.
20. Kural, C., Kim, H., Syed, S., Goshima, G., Gelfand, V.I., and Selvin, P.R. (2005). Kinesin and dynein move a peroxisome in vivo: a tug-of-war or coordinated movement? Science *308*, 1469-1472.
21. Bullock, S.L., Nicol, A., Gross, S.P., and Zicha, D. (2006). Guidance of bidirectional motor complexes by mRNA cargoes through control of dynein number and activity. Curr Biol *16*, 1447-1452.
22. Ling, S.C., Fahrner, P.S., Greenough, W.T., and Gelfand, V.I. (2004). Transport of Drosophila fragile X mental retardation protein-containing ribonucleoprotein granules by kinesin-1 and cytoplasmic dynein. Proc Natl Acad Sci U S A *101*, 17428-17433.
23. Reilein, A.R., Tint, I.S., Peunova, N.I., Enikolopov, G.N., and Gelfand, V.I. (1998). Regulation of organelle movement in melanophores by protein kinase A (PKA), protein kinase C (PKC), and protein phosphatase 2A (PP2A). J Cell Biol *142*, 803-813.
24. Deacon, S.W., Nascimento, A., Serpinskaya, A.S., and Gelfand, V.I. (2005). Regulation of bidirectional melanosome transport by organelle bound MAP kinase. Curr Biol *15*, 459-463.
25. Gross, S.P., Guo, Y., Martinez, J.E., and Welte, M.A. (2003). A determinant for directionality of organelle transport in Drosophila embryos. Curr Biol *13*, 1660-1668.
26. Welte, M.A., Cermelli, S., Griner, J., Viera, A., Guo, Y., Kim, D.H., Gindhart, J.G., and Gross, S.P. (2005). Regulation of lipid-droplet transport by the perilipin homolog LSD2. Curr Biol *15*, 1266-1275.

27. Hollenbeck, P.J., and Saxton, W.M. (2005). The axonal transport of mitochondria. J Cell Sci *118*, 5411-5419.
28. Fransson, S., Ruusala, A., and Aspenstrom, P. (2006). The atypical Rho GTPases Miro-1 and Miro-2 have essential roles in mitochondrial trafficking. Biochem Biophys Res Commun *344*, 500-510.

Filament regulation of motors: Kinesin-5 Motor Dynamics in the Budding Yeast Mitotic Spindle

M.K. Gardner[1], L.V. Paliulis[2], E.D. Salmon[2], K. Bloom[2], and D.J. Odde[1]

[1]Department of Biomedical Engineering, University of Minnesota, Minneapolis, MN;
[2]Department of Biology, University of North Carolina at Chapel Hill, Chapel Hill, NC

ABSTRACT

During mitosis in budding yeast, plus-end directed homotetrameric Kinesin-5 motor proteins cross-link dynamic microtubules to exert extensional sliding forces in the mitotic spindle. A key question regarding this system, and motor systems in general, is: to what extent are motor dynamics controlled by the local density, orientation, and assembly dynamics of microtubules?

Our previously developed stochastic model for metaphase kinetochore microtubule (kMT) dynamics in budding yeast was able to quantitatively reproduce the dynamics of kMTs across multiple fluorescence imaging and FRAP experiments. Here we extend our model to include Kinesin-5 motor proteins, such that interactions between the spindle motor proteins (Cin8p and Kip1p) and the dynamics of microtubule polymerization/depolymerization are quantitatively described in live cell simulations. Through FRAP experiments characterizing fluorescent motor protein dynamics in live cells, we find that, although kinesin motor proteins turn over rapidly as compared to microtubules, a gradient in motor turnover exists along the length of the mitotic spindle that mirrors a similar gradient in kMT turnover. Modeling of these results combined with quantitative analysis of fluorescent motor protein position in the mitotic spindle indicates that: (1) motor motility is frustrated by kinetochore attachment at the plus-ends of microtubules, (2) motors turn over more slowly in regions of the spindle with a high density of stable anti-parallel microtubules, and (3) depolymerization of kinetochore-attached microtubules may mediate motor detachment from plus-ends. Thus, through quantitative live-cell fluorescence imaging combined with computational modeling of the imaging (an approach we call model-convolution), it appears that microtubule orientation, density, and dynamics all contribute significantly to regulating kinesin-5 dynamics and distribution in the budding yeast mitotic spindle.

INTRODUCTION

During mitosis, dynamic arrays of kinetochore-associated microtubules (kMTs) are organized via molecular motors into a mitotic spindle that subsequently serves to accurately segregate chromosomes into daughter cells. In yeast, a kinetochore-associated microtubule (kMT) minus end is stably anchored at the spindle pole body (SPB), while the plus end is associated with a kinetochore (Fig. 1). Cytoplasmic microtubules in yeast have been observed to exhibit dynamic instability, stochastically switching between extended periods of polymerization and depolymerization [3], and oscillations of fluorescent probes on chromosome arms suggest that kMT plus-ends are dynamic as well [4,5]. In addition, longer interpolar microtubules are attached at the SPBs and run nearly the length of the spindle, although they are significantly less numerous than kMTs (Fig. 1). Thus, the function of molecular motors in the mitotic spindle is likely to be dictated at least in part by the interaction of these motors with dynamic spindle microtubules.

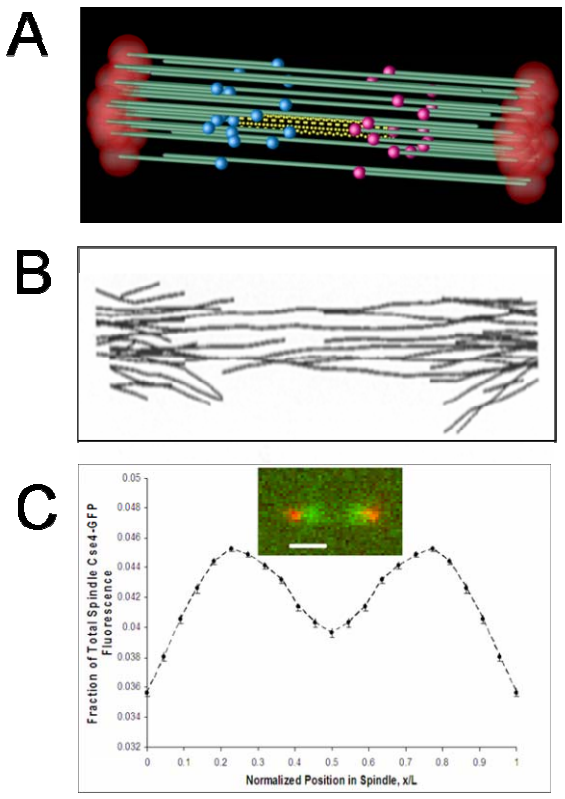

Figure 1: The budding yeast mitotic spindle. (A) Spindle structure cartoon: SPBs (red), anchor kMTs (green) at their minus-ends. Kinetochores (blue, left SPB attach, magenta, right SPB attach) are attached at kMT plus-ends. Chromatin (yellow spring, typical for one pair), is stretched between sister kinetochores. Interpolar microtubules (green) have minus-ends anchored in the SPBs, but generally run the length of the spindle and do not have kinetochores attached at plus-ends. (B) Electron microscope reconstruction of spindle microtubules, reprinted from [1]. Note shorter kMTs on right and left of spindle, with longer interpolar microtubules running through the center of the spindle. (C) Top: typical experimental fluorescence image. Spindle pole body (SPB) markers are red, and kinetochore-associated fluorescence clusters are green. (Scale bar 1000 nm) Bottom: Kinetochore-associated fluorescence is quantified by spindle position. There is a peak in kinetochore-associated fluorescence midway between the spindle equator and each SPB, indicating that kinetochores tend to cluster in these positions.

Computer simulation of microtubule dynamics can provide a bridge between mitotic spindle phenotypes and the individual kMT dynamics that produce these phenotypes. We found that by simulating kMT dynamics, we can predict kMT lengths and kinetochore distributions in mitotic spindles [6,7]. By

convolving these computer-generated predictions with the experimentally measured microscope point spread function and background noise, we can generate simulated images suitable for quantitative comparison to experimental images. Our previously developed stochastic model for metaphase kinetochore microtubule (kMT) dynamics in yeast was able to quantitatively reproduce the dynamics of kMTs across multiple fluorescence imaging and FRAP experiments [6,7]. Here we expand our model to include Kinesin-5 motor proteins, such that interactions between the spindle motor proteins and the dynamics of microtubule polymerization/depolymerization are quantitatively described in live cell simulations.

Cin8p and Kip1p are plus-end directed homotetrameric proteins of the Kinesin-5 family that have been implicated in the mitotic spindle function of budding yeast. They are function as active mechanical elements that separate SPBs during pro-metaphase and then act to prevent spindle collapse during metaphase, and they appear to have somewhat redundant function in the yeast mitotic spindle [8-11]. Cells remain viable despite deletion of either one of these proteins, although the spindles have high rates of chromosome loss and undergo frequent spindle collapse [11]. In addition, over-expression of Cin8p leads to aberrant spindle elongation [12,13]. Together, Cin8p and Kip1p are essential since the deletion of both proteins is lethal [14]. Similar to other motors in the Kinesin-5 family, it is thought that Cin8p and Kip1p complexes are dumbbell shaped, with two globular motor heads on each end separated by a ~60 nm stalk composed of a pair of coiled-coils [8,15,16]. It may be that Cin8p and Kip1p work to separate SPBs by attachment of their motor heads to oppositely oriented (anti-parallel) spindle microtubules. As motor heads then walk in opposite directions, motor protein stalk stretching exerts a sliding force, pushing anti-parallel microtubules apart. One might view the kinesin-5 function as analogous to muscle myosin in the sarcomere, except in reverse: kinesin-5 generates outward extensional force, whereas muscle myosin generates inward contractile force. In this way, a stable metaphase spindle length could be established by the balance of outwardly directed forces generated by Kip1p and Cin8p opposed by inwardly directly forces resulting from the elastic stretch of chromatin between sister kinetochores.

Previous *in vivo* work in *Xenopus* extract spindles found that populations of kinesin Eg5 dynamics were static while fluorescent tubulin molecules in spindle microtubules moved steadily toward the spindle poles [17]. This observation led to the conclusion that mitotic kinesin motors may be associated with a static “spindle matrix” rather than with dynamic spindle microtubules. In addition, recent *in vivo* work with kinesin motors Cin8p and Kip1p resulted in a similar characterization, although motors were thought to be stably associated with kinetochores rather than a spindle matrix [18]. In either case, it is not clear how motor attachment to dynamic MTs could provide a steady outwardly directed force to mediate stable spindle lengths during mitosis (reviewed in [8]).

Observation of microtubule turnover is possible by performing fluorescence recovery after photobleaching (FRAP) experiments with a green fluorescent protein labeled tubulin (GFP-Tubulin) marker [19]. This experiment

quantifies microtubule turnover by measuring FRAP due to tubulin subunit exchange in a ~300 nm box placed over a bleached spindle-half.

We recently developed a method for rapid temporal and high spatial resolution imaging and analysis of GFP-Tubulin photobleaching experiments in yeast [2]. In this way, we were able to quantify FRAP rate in ~65 nm intervals along the length of the mitotic spindle. By computing half-maximal recovery times as a function of spindle position, a spatial gradient of recovery rates is observed in metaphase spindles, such that GFP-Tubulin fluorescence recovery is most rapid at the approximate location of peak kinetochore density in metaphase spindles (Fig. 2). This result suggests that kMT plus-ends are constrained to the location of most rapid GFP-Tubulin turnover in the spindle. Thus, quantification of FRAP rate by position within the spindle allows for sensitive discrimination of fluorescent protein dynamics in sampling intervals that are significantly less than the diffraction limit of the microscope (~220 nm), in this case ~65 nm.

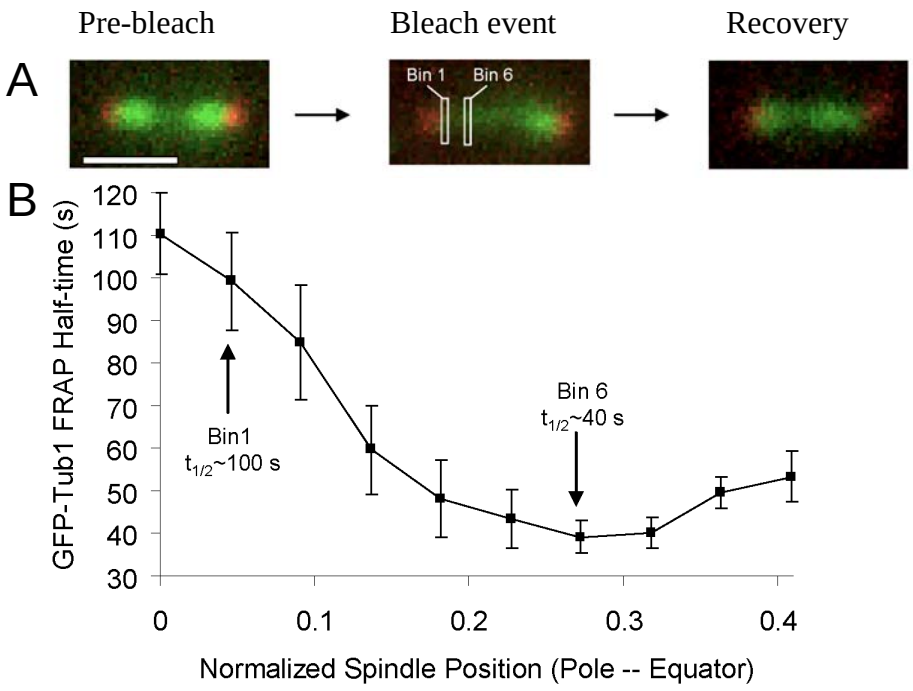

Figure 2: Experimental data from the GFP-Tubulin FRAP by spindle position [2]. (A) Typical experimental images (red, SPB marker, green, tubulin marker). (B) Recovery half times are fastest mid-way between the spindle pole and the spindle equator (Bin 6), where kMT plus-ends tend to cluster during metaphase. Recovery takes place more slowly towards the spindle poles (Bin 1) (n=22 cells). (scale bar, 1000 nm)

Here, we performed spatially resolved FRAP experiments using fluorescently tagged kinesin motor proteins in yeast (Cin8p and Kip1p). These results were then directly compared to similar experiments with Tubulin-GFP that quantify kMT dynamics in yeast [2] to explore kinesin motor dynamics relative to kMT dynamics in the yeast mitotic spindle. We find that although kinesin motor proteins turn over rapidly as compared to microtubules, a gradient in motor turnover exists along the length of the mitotic spindle that mirrors a similar gradient in kMT turnover. In addition, modeling of Cin8p and Kip1p localization in the mitotic spindle constrains the rules for behavior of motors interacting with

kMT plus-ends at kinetochores. Together, these results indicate that (1) Cin8p and Kip1p may tip-track spindle microtubules via motor motility towards kMT plus-ends *in vivo*, and (2) Cin8p and Kip1p turnover may be regulated by dynamics at the plus-ends of kinetochore-attached microtubules.

RESULTS AND DISCUSSION

Cin8p binds more efficiently to spindle microtubules than Kip1p

The localization of fluorescently tagged Cin8p and Kip1p molecular motors was quantitatively analyzed relative to SPBs (Fig. 3). As shown in Fig. 3D, both Kinesin-5 motors in the yeast mitotic spindle are unevenly distributed along the length of the mitotic spindle. In comparing absolute fluorescence signal between Cin8p-GFP and Kip1p-GFP, the mean spindle-bound Cin8p signal is ~1.4X higher than that of Kip1p, while background signal of Kip1p is ~3X higher than that of Cin8p. These results suggest that while the behavior and function of these motors may be similar, Cin8p has a higher affinity for microtubules, and thus is expected to be more important than Kip1p in establishing stable spindle lengths during metaphase. This could explain why *cin8Δ* mutants require checkpoint and have a more severe chromosome loss phenotype as compared to *kip1Δ* mutants [9,20,21].

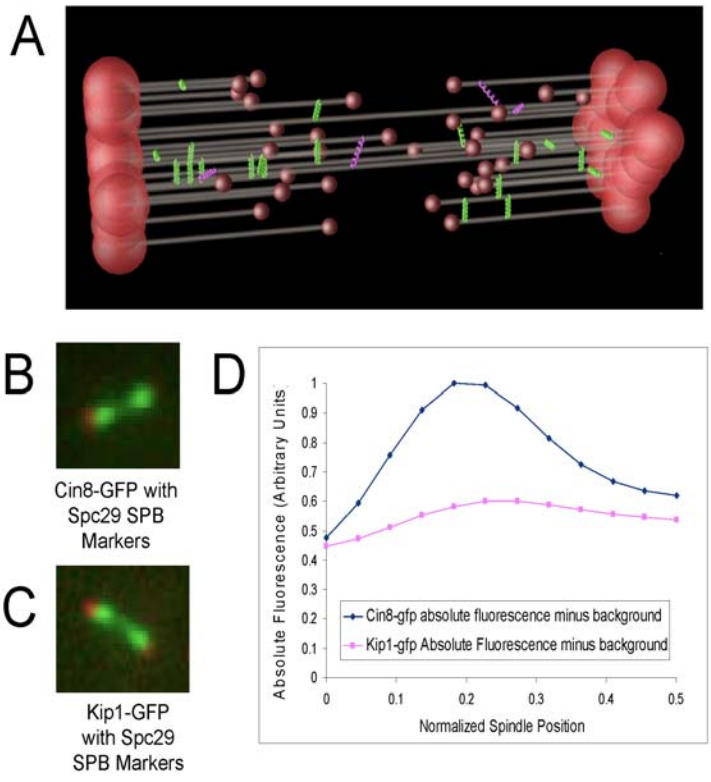

Figure 3: Molecular motors in the yeast mitotic spindle. (A) A model for the yeast metaphase spindle: microtubules (grey) are attached to spindle pole bodies (red). kMTs have plus-end attached kinetochores (brown spheres), that link to a sister kinetochore through a sister chromatid pair (not shown). Kinesin-5 molecular motors are shown as springs in green (parallel-attached) and magenta (anti-parallel attached). (B) Typical experimental fluorescence image of Cin8p-GFP (green) with SPB markers (red) (C) Experimental image of Kip1p-GFP (green) with SPB markers (red) (scale bar, 1000 nm) (D) Quantification of Cip8p-GFP and Kip1p-GFP fluorescence distribution. Absolute fluorescence is plotted as a function of spindle position. Only half of the spindle is shown, with the spindle equator at position 0.5, and SPB at position 0. Cin8p had more intense fluorescence than Kip1p.

Spindle kinesin-5 motor signal is offset from kinetochore clusters

In comparing motor-associated fluorescence localization in the mitotic spindle to Nuf2-GFP, a kinetochore associated protein, motor fluorescence is characteristically located "behind" the kinetochore towards the SPBs, in the location where kMT density is high (Fig. 3A). For example, the peak in Cin8p-GFP fluorescence is ~180 nm from the peak in Nuf2-GFP fluorescence, and the peak in Kip1p-GFP is ~110 nm away (Fig. 4A). This localization argues that a significant fraction of kinesin-5 motors may be cross-linking parallel-oriented kMTs, and that motor localization and dynamics are regulated by kMT plus-end dynamics. The difference in localization between Cin8p-GFP and Kip1p-GFP could be a result of differences in their affinities for microtubules, as discussed below.

Computational modeling predicts that motor-based motility results in kMT tip tracking, and that kMT depolymerization mediates kinesin-5 motor detachment

Random motor attachment and crosslinking of microtubules, motor head movement, and detachment from microtubules were then simulated in conjunction with plus-end kMT dynamics in the yeast mitotic spindle. Simulated Cin8p and Kip1p fluorescence images were then generated using different rules for motor dynamics relative to microtubule plus-end dynamics, and the results quantitatively compared to experimental motor localization. Selected model assumptions are listed in Table 1, and a typical animated simulation output is shown in Figure 3A.

As shown in Fig. 4A, a reasonable model fit to experimental kinesin motor spindle localization could be achieved by allowing random attachment and crosslinking of motors, combined with subsequent motor movement and detachment. Importantly, model-predicted motor localization is highly dependent on the rules for motor behavior and dynamics at kMT plus-ends, i.e., at kinetochores. For this reason, three possible models for motor behavior at kinetochores were tested, as listed in Table 1. The best fit between experiment and theory is achieved when parallel-attached kinesin-5 motors are initially allowed to walk toward and, upon arrival, track polymerizing kMT plus-ends. Then, by allowing kinesin-5 motors to detach upon kMT catastrophe and depolymerization, the average motor position moves away from kinetochore clusters and toward the SPBs, as is experimentally observed (Fig. 4A). If simulated kinesin-5 motors do not track kMT plus-ends, but instead immediately walk off the plus-ends of polymerizing or depolymerizing kMTs, the simulated distribution of motor-associated fluorescence is diffuse, without the characteristic fluorescence peak that is experimentally observed (Fig. 4C). In contrast, if motors are allowed to track both polymerizing and depolymerizing kMT plus-ends, the peak in motor localization is exactly co-localized with the peak in kinetochore-associated fluorescence, which is not experimentally observed (Fig. 4B). Thus, an acceptable model for interaction between kMT plus-ends and kinesin-5 motors was one in which motors are able to track polymerizing but not depolymerizing kMT plus-ends (Fig. 4D). Differences in simulated run lengths

between Cin8p and Kip1p can account for quantitative differences in their mean positions relative to kinetochores.

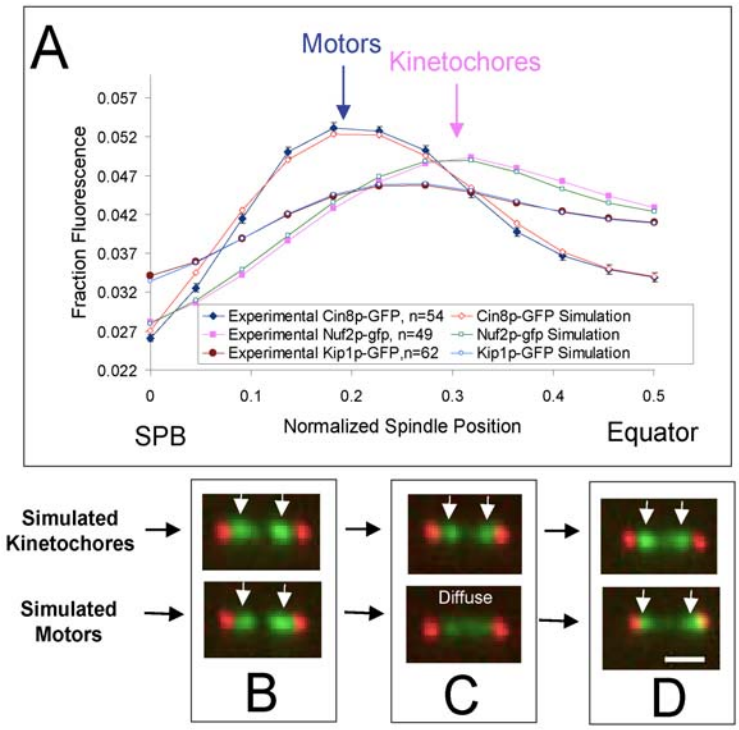

Figure 4: Modeling predicts motor behavior at kinetochores. (A) Experimental and simulation comparison of Kip1p and Cin8p localization relative to kinetochores. Cin8p clustering is ~180 nm behind kinetochores, and Kip1p clustering is ~110 nm behind kinetochores. In (B-D) are simulation predictions for motor localization relative to kinetochores. In (B) motors track both polymerizing and depolymerizing kMTs, so motor clustering mirrors kinetochore clustering. In (C) motors do not track kMT plus-ends, so motor clustering is diffuse relative to kinetochores. In (D), motors track polymerizing but not depolymerizing kMT plus ends, such that motors cluster "behind" kinetochores. Quantitative motor simulation results for the model in (D) are shown in (A). (scale bar 1000 nm)

Spatially resolved FRAP experiments reveal a gradient in kinesin-5 spindle motor turnover as predicted by mediation of motor turnover via kMT depolymerization

The computational model for interaction of kinesin-5 motors with kMT plus-ends indicates that kMT depolymerization could mediate turnover of motors, such that motor turnover may be most rapid in the location of plus-end clustering, similar to the spatial gradient in kMT dynamics as described above (Fig. 2). In addition, the reduced spindle-bound Kip1p fluorescence signal as compared to Cin8p (Fig 3D) suggests that Kip1p has a lower affinity for microtubules than Cin8p, and thus Kip1p would be predicted to turn over more rapidly on the spindle. In order to test these predictions, we performed the spatially-resolved FRAP experiment with fluorescently tagged Kip1p and Cin8p motor proteins.

FRAP experiments on Cin8-GFP and Kip1-GFP strains were performed and fluorescence recovery analyzed in ~65 nm bins along the length of the mitotic spindle (Fig. 5). In general, kinesin-5 motors turn over rapidly, with FRAP half-times 2-3 times faster than that of tubulin polymer. These results indicate that motor protein interactions with the mitotic spindle are dynamic relative to microtubules. Also, as predicted by its weak fluorescence intensity on the spindle relative to Cin8p-GFP, the Kip1p-GFP had more rapid dynamics, consistent with a higher off-rate constant, which implies a lower affinity and

shorter run length relative to Cin8p. Importantly, FRAP half-times for motor proteins vary by spindle position, almost perfectly coordinated with the observed gradient in tubulin turnover in the mitotic spindle (Fig. 5). Recent *in vitro* data on the kinesin-5 motor Eg5 indicate that these motors tend to dissociate from microtubules before slowing substantially, and that they can sustain loads as high as 7 pN without detachment [22]. Thus it may be that *in vivo* kMT catastrophe and subsequent depolymerization of kMT plus-ends could mediate turnover of kinesin-5 motors in yeast by physically dissociating motor heads from kMT tubulin subunits, although modeling of the spatially-resolved FRAP experiment will help to account for many factors that could influence this result, in particular motor off and on rate constants, the effect of force on motor velocities and off-rates, and the motility of motors on both parallel and anti-parallel attached microtubules. This hypothesis would be in contrast to another recent *in vitro* study indicating that Eg5 motors tend to remain attached to dynamic microtubule plus-ends for considerably longer than typical motor turnover times [23].

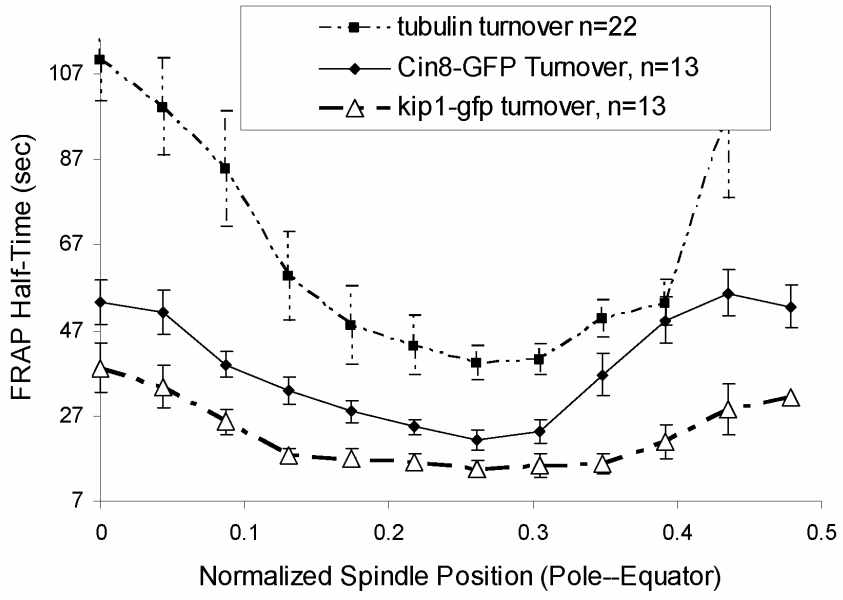

Figure 5: Experimental results for fluorescence recovery after photobleaching (FRAP) by spindle position. GFP-Tubulin FRAP recovery is most rapid in the position of plus-end clustering, as was previously reported [2]. The kinesin motors Cin8-GFP and Kip1-GFP have shorter FRAP half-times, indicative of a rapid protein turnover. The observed gradient in motor FRAP half-times suggests that motor turnover may be mediated in part by kMT plus-end dynamics.

CONCLUSIONS

By using quantitative fluorescence microscopy in concert with computational simulations of fluorescent motor protein dynamics, we found that the microtubule dynamics are likely regulating the turnover and dynamics of kinesin-5 motors. From the analysis, the observed behavior is consistent with a model where: (1) motor motility is frustrated by kinetochore attachment at the plus-ends of microtubules, (2) motors turn over more slowly in regions of the spindle with a high density of stable anti-parallel microtubules, and (3) depolymerization of kinetochore-attached microtubules may mediate motor detachment from plus-ends. These results indicate that the kMT dynamics are important in controlling the dynamics kinesin-5 motors in budding yeast mitosis, and suggest that, in general, MT dynamics may regulate motor activities.

Table 1: Selected Model Assumptions

CATEGORY	MODEL ASSUMPTION AND/OR TEST
Motor attachment & movement	• All motor heads restricted from attaching to same MT • All motor heads have no preference of attachment to interpolar MTs or kinetochore MTs, parallel or anti-parallel attachment • Individual motor heads move per force velocity relationship such that at stall force velocity is zero, singly attached heads move at unloaded velocity • Random attachment with on-rate constant based on weighted MT array • Both motor heads attach during one time step
Motor Properties	• In determining force, motors act as hookean springs
Motor Detachment	• Off-rate constant is force dependent based on stretching of motors • Both motor heads detach during one time step • *Motor behavior at kinetochore:* *Option 1*: Motor heads immediately walk off ends of microtubules upon arriving at kinetochores. *Option 2*: Motor heads track polymerizing and depolymerizing kMT plus-ends at kinetochores. *Option 3*: Motors track polymerizing plus-ends at kinetochores but detach immediately upon kMT depolymerization. • Motor heads immediately “walk off” of interpolar microtubule plus-ends

REFERENCES

1. Winey M, Mamay CL, O'Toole ET, Mastronarde DN, Giddings TH, Jr., McDonald KL, McIntosh JR: **Three-dimensional ultrastructural analysis of the Saccharomyces cerevisiae mitotic spindle**. *Journal of Cell Biology* 1995, **129**:1601-1615.
2. Pearson CG, Gardner MK, Paliulis LV, Salmon ED, Odde DJ, Bloom K: **Measuring Nanometer Scale Gradients in Spindle Microtubule Dynamics Using Model Convolution Microscopy**. *Mol Biol Cell* 2006.
3. Carminati JL, Stearns T: **Microtubules orient the mitotic spindle in yeast through dynein-dependent interactions with the cell cortex**. *J Cell Biol* 1997, **138**:629-641.
4. Pearson CG, Maddox PS, Salmon ED, Bloom K: **Budding Yeast Chromosome Structure and Dynamics during Mitosis**. *J. Cell Biol.* 2001, **152**:1255-1266.
5. He X, Asthana S, Sorger PK: **Transient Sister Chromatid Separation and Elastic Deformation of Chromosomes during Mitosis in Budding Yeast**. *Cell* 2000, **101**:763-775.
6. Gardner MK, Pearson CG, Sprague BL, Zarzar TR, Bloom K, Salmon ED, Odde DJ: **Tension-dependent Regulation of Microtubule Dynamics at Kinetochores Can Explain Metaphase Congression in Yeast**. *Mol Biol Cell* 2005, **16**:3764-3775.
7. Sprague BL, Pearson CG, Maddox PS, Bloom KS, Salmon ED, Odde DJ: **Mechanisms of Microtubule-Based Kinetochore Positioning in the Yeast Metaphase Spindle**. *Biophys J* 2003, **84**:1-18.
8. Hildebrandt ER, Hoyt MA: **Mitotic motors in Saccharomyces cerevisiae**. *Biochim Biophys Acta* 2000, **1496**:99-116.
9. Geiser JR, Schott EJ, Kingsbury TJ, Cole NB, Totis LJ, Bhattacharyya G, He L, Hoyt MA: **Saccharomyces cerevisiae genes required in the absence of the CIN8-encoded spindle motor act in functionally diverse mitotic pathways**. *Mol Biol Cell* 1997, **8**:1035-1050.
10. Hildebrandt ER, Hoyt MA: **Cell cycle-dependent degradation of the Saccharomyces cerevisiae spindle motor Cin8p requires APC(Cdh1) and a bipartite destruction sequence**. *Mol Biol Cell* 2001, **12**:3402-3416.
11. Hoyt MA, He L, Loo KK, Saunders WS: **Two Saccharomyces cerevisiae kinesin-related gene products required for mitotic spindle assembly**. *J Cell Biol* 1992, **118**:109-120.
12. Saunders W, Hornack D, Lengyel V, Deng C: **The Saccharomyces cerevisiae kinesin-related motor Kar3p acts at preanaphase spindle poles to limit the number and length of cytoplasmic microtubules**. *J Cell Biol* 1997, **137**:417-431.
13. Saunders W, Lengyel V, Hoyt MA: **Mitotic Spindle Function in Saccharomyces cerevisiae Requires a Balance between Different Types of Kinesin-related Motors**. *Molecular biology of the cell* 1997, **8**:1025-1033.
14. Saunders WS, Hoyt MA: **Kinesin-related proteins required for structural integrity of the mitotic spindle**. *Cell* 1992, **70**:451-458.
15. Gheber L, Kuo SC, Hoyt MA: **Motile properties of the kinesin-related Cin8p spindle motor extracted from Saccharomyces cerevisiae cells**. *J Biol Chem* 1999, **274**:9564-9572.
16. Kashina AS, Baskin RJ, Cole DG, Wedaman KP, Saxton WM, Scholey JM: **A bipolar kinesin**. *Nature* 1996, **379**:270-272.
17. Kapoor TM, Mitchison TJ: **Eg5 is static in bipolar spindles relative to tubulin: evidence for a static spindle matrix**. *J Cell Biol* 2001, **154**:1125-1133.
18. Tytell JD, Sorger PK: **Analysis of kinesin motor function at budding yeast kinetochores**. *J Cell Biol* 2006, **172**:861-874.
19. Maddox P, Bloom K, Salmon ED: **Polarity and Dynamics of Microtubule Assembly in the Budding Yeast *Saccharomyces cerevisiae***. *Nature Cell Biology* 2000, **2**:36-41.
20. Hoyt MA, He L, Loo KK, Saunders WS: **Two Saccharomyces cerevisiae kinesin-related gene products required for mitotic spindle assembly**. *Journal of Cell Biology* 1992, **118**:109-120.
21. Roof DM, Meluh PB, Rose MD: **Kinesin-related proteins required for assembly of the mitotic spindle**. *Journal of Cell Biology* 1992, **118**:95-108.
22. Valentine MT, Fordyce PM, Krzysiak TC, Gilbert SP, Block SM: **Individual dimers of the mitotic kinesin motor Eg5 step processively and support substantial loads in vitro**. *Nat Cell Biol* 2006, **8**:470-476.
23. Kapitein LC, Peterman EJ, Kwok BH, Kim JH, Kapoor TM, Schmidt CF: **The bipolar mitotic kinesin Eg5 moves on both microtubules that it crosslinks**. *Nature* 2005, **435**:114-118.

Kiehart, Edwards & Venakides: Biophysical Discussions

Introduction: We investigate the forces that connect the genetic program of development to morphogenesis in *Drosophila*. We focus on dorsal closure, a model system for cell sheet morphogenesis, in order to provide insight into the mechanisms of morphogenesis in general. It is an excellent model system that is amenable to genetic, transgenic, cell biological and biophysical analyses (e.g., Kiehart et al., 2000; Harden, 2002; Jacinto et al., 2002; Hutson et al., 2003). Understanding the morphogenetic movements that underlie metazoan development requires detailed knowledge of cellular kinematics (the analysis of cell movements) and cellular dynamics (the analysis of the forces that underlie those movements) and the biological processes that regulate such movements. Bard (1990) observes that epithelial movements "are remarkable phenomena in biology" and in vertebrate embryos, are responsible for much of morphogenesis, at least through neurulation. There is a history of applying quantitative modeling to development and such studies unavoidably require analysis of the forces responsible for movements, either at the subcelluar or tissue levels (Odell et al., 1981; Brodland and Clausi, 1995; Meinhardt and Roth, 2002; Eldar et al., 2003; Grill et al., 2003; Orr et al., 2006)., Tissue explants that at least in part recapitulate morphogenetic movements, provide essential access for the analysis of force measurements on tissues *in vitro* (reviewed in Keller et al., 2000; Keller et al., 2003; reviewed in Shook and Keller, 2003). We reasoned that analyzing forces *in vivo* would provide new biophysical insight into the mechanisms of morphogenesis. This is especially true in *Drosophila*, an organism that allows for facile experimental manipulation of gene expression and for which the genetic program of development is arguably the best understood. As described below we have successfully identified the forces for dorsal closure; established their relative magnitude; have begun to identify their molecular basis; and generated an underdetermined but plausible model for closure that promises to inform future experimental work (see Hutson et al., 2003; Yang et al., In Preparation).

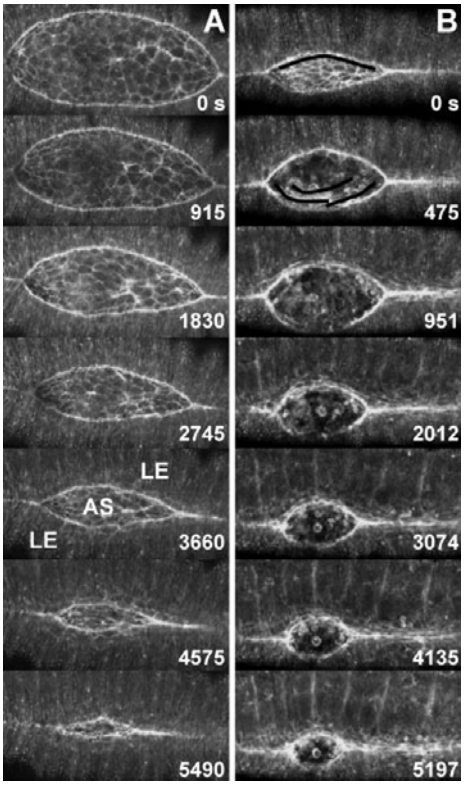

Figure 1. Dorsal Closure

Summary of morphogenesis in dorsal closure: In the early stages of closure, the dorsal surface of the embryo is covered by the large, flat polygonal cells of the amnioserosa. The rest of the embryo is covered by smaller, cuboidal-to-columnar cells of the lateral and ventral epidermis. The visible area of the amnioserosa is shaped roughly like a human eye, with a wide central section that tapers to canthi, the corners of the eye (see Fig. 1, taken from Hutson et al., 2003; Yang et al., In Preparation). With time, this eye-like structure "closes" (Fig. 1A, 0s-5490s, time in seconds). A single row of amnioserosa cells is tucked under the lateral epidermis throughout closure (Kiehart et al., 2000; this is a feature missed in many reviews). Where these cell sheets overlap, the dorsal-most row of lateral epidermis cells comprise a third, distinct tissue known as the leading edge of the lateral epidermis (see below, Foe, 1989; see below, Kiehart et al., 2000; Stronach and Perrimon, 2001). The cells of the leading edge on each flank of the embryo contain an actomyosin-rich "purse-string" or "actin-cable" (Young et al., 1993; Kiehart, 1999; Kiehart et al., 2000). In addition, these cells extend dynamic finger-like filopodia, ~10 μm in length (Jacinto et al., 2000). At the canthi, pairs of these filopodia can span the gap between opposing leading edges. As dorsal closure progresses, the actin

cytoskeleton is re-modeled and each structure changes (Young et al., 1993; Jacinto et al., 2000; Kiehart et al., 2000; Wood et al., 2002). Cells of the lateral epidermis are stretched (or elongate) towards the dorsal midline; the purse-strings contract along their length; and cells of the amnioserosa actively change shape as their apical surfaces contract to help draw the lateral epidermal sheets together. The two flanks of the lateral epidermis adhere to one another or are zipped together – filopodia and lamellipodia from opposing leading edges interdigitate and a seam is formed (Jacinto et al., 2000; Bloor and Kiehart, 2002). At the end stages, the arcs flatten out and closure occurs "edge-to-edge" as numerous contacts are made simultaneously between the opposing sheets. Once the tissues from opposing flanks are sutured together, the actin rich purse-string dissolves. Ultimately the dorsal surface is covered by a continuous epithelium that appears seamless. The bulk of closure requires ~2-3 hours. Within each epithelium, neither cell division, nor rearrangements of cells that cause them to change neighbors contribute significantly to the movements of dorsal closure (*e.g.*, there are no movements comparable to convergent extension).

Genetic Approaches – the Dorsal Closure (DC) Genes: In all, there are over 60 genes whose products participate in dorsal closure (reviewed in Harden, 2002; Jacinto et al., 2002). Genetic analysis of loss of function alleles of DC genes and/or analyses with a variety of different kinds of transgenes (*e.g.*, ones that encode wild type, "constitutively active" or "dominant negative" proteins) indicate that malfunction or mis-function of the various DC genes results in a range of dorsal closure phenotypes. In some cases, analysis is restricted to a dorsal open phenotype – for example, dorsal closure mutants were recognized by their cuticle phenotypes as a discrete class of embryonic lethal mutations in the screens performed by Nüsslein-Volhard, Wieschaus and colleagues (Jurgens et al., 1984; Nusslein-Volhard et al., 1984; Wieschaus et al., 1984). In other mutations, discrete aspects of cell sheet movement during dorsal closure were shown to be compromised. Thus, a number of mutations affect the distribution of filopodia at the leading edge of the lateral epidermis (Jacinto et al., 2000; Harden, 2002; Jacinto et al., 2002; Wood et al., 2002); other mutations appear to affect the elongation or stretching (17 identified thus far) of the leading edge of the lateral epidermis or the elongation or stretching (3 identified so far) of the lateral epidermis ventral to the leading edge (Harden, 2002; Jacinto et al., 2002). In our reverse genetic analysis of *zip*/myoII, we provided a limited analysis of the cell sheet movements (through analysis of fixed and antibody-stained specimens) that characterize dorsal closure and demonstrated the existence of an actomyosin-rich, purse-string (Young et al., 1993) and recently used a novel transgenic mosaic approach to further elucidate the role of *zip*/MyoII in this process (Franke et al., 2005 and see below).

Overall, the DC genes fall into three general, molecular classes. One group is involved in signaling, a second in transcriptional regulation and a third are so called "structural proteins". Clearly many genes can be described as falling into more than one camp, especially with respect to their contribution to dorsal closure (*e.g.*, *myospheroid*, which encodes the β_{PS} subunit of integrin, see below). Together the DC mutants provide a rich collection of biological specimens to examine.

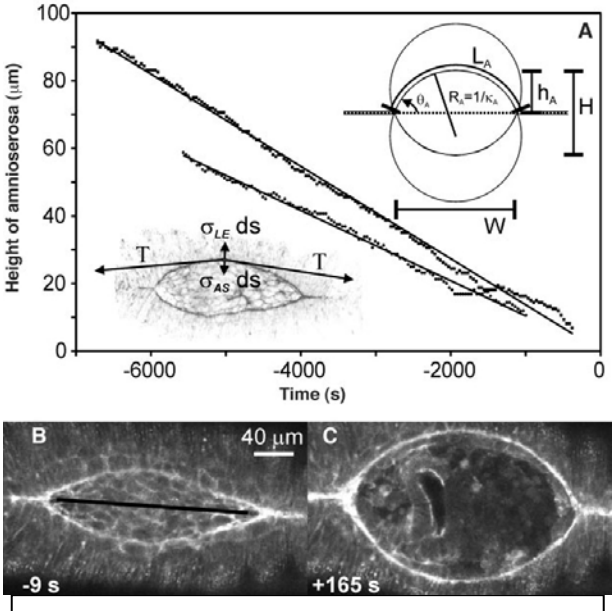

Fig. 2. Quantitative Analysis of Dorsal Closure – Laser Interrogated Closure

Biophysical Analysis of Dorsal Closure: To

understand better the cell biology of the dorsal closure process we use a biophysical approach to complement genetic ones (Kiehart et al., 2000; Hutson et al., 2003; Kiehart et al., 2006; Peralta et al., Submitted to Biophysical Journal). Initially we used a laser macro-beam (5-10 μm diameter at the specimen plane) to establish that both the amnioserosa and the leading edge of the lateral epidermis are contractile. We next refined our macro-beam into a near-diffraction limited micro-beam. Moreover, we used beam steering for laser-microsurgery and automated analysis of data from large stacks of high-resolution confocal images to describe quantitatively the various movements that characterize closure. In addition, we used the quantitative and predictive capabilities of physical modeling to address the important question of the cellular origin and the relative magnitude of the forces required for dorsal closure. We focused on the middle to late stages of dorsal closure when the entire leading edge can be imaged in a single focal plane (Fig. 2B shows a laser cut diagrammed on intact tissue, Fig. 2C shows dorsal opening after the rapid recoil of the leading edge and the lateral epidermis away from the dorsal midline as a consequence of surgically removing the amnioserosa). A summary of our modeling approach follows. It allows us to describe in detail the cellular bases of force production for this cell sheet movement.

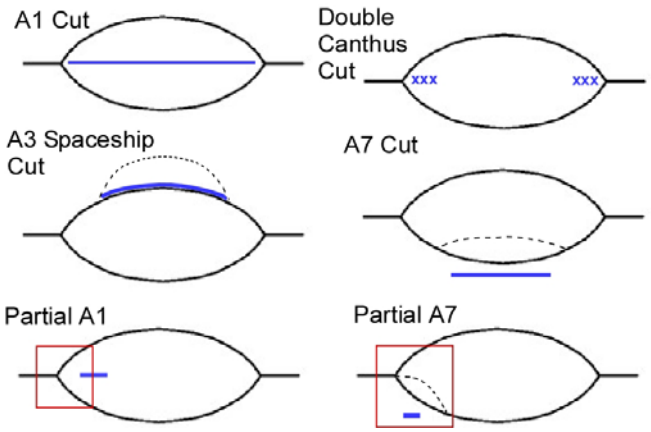

Fig. 3. Diagram of Diagnostic Cuts

Mechanical jump experiments: We are able to evaluate dynamically the forces on the tissues that contribute to dorsal closure through judicious laser surgical interrogation (*i.e.*, tissue ablation with a near diffraction limited beam). Of particular utility are "mechanical jump" experiments that use the laser microbeam to rapidly remove the forces contributed by one or more of the tissues that provide force for movement (Fig. 3 diagrams the diagnostic cuts). Included are cuts that remove the mechanical integrity of the AS (A1); double canthus cuts that remove zipping; cuts that remove the contractility of the contractile purse-string (A3 Spaceship, see below); and cuts that relieve tension generated by the lateral epidermis (which recall, opposes closure, A7 cut). By analyzing movements before and the recoil after the removal of the tissue, we can describe that tissue's contribution to the net forces driving the movement.

Forces for Closure are Redundant: Surgical removal of any one tissue or process fails to block closure – removal of the mechanical integrity of the supracellular purse-string, the amnioserosal or zipping at the canthi all fail to block closure (Kiehart et al., 2000; Hutson et al., 2003). Thus individual forces that participate in closure must be regulated in order to compensate for the loss of force contribution by the ablated tissue (see Newtonian Force Balance Equation, below).

A corollary of this observation is that removal of more than one of the force producing tissues blocks closure, as do mutations in a number of distinct genes – presumably mutations in those genes that encode proteins that contribute to forces generated in more than one tissue or process (Young et al., 1993; Kiehart et al., 2000; Franke et al., 2005). Indeed, *zip*/MyoII is expressed in all cells of the embryo and severe mutations in *zip*/MyoII block closure by affecting *zip*/MyoII function in the leading edge of the lateral epidermis and in the amnioserosa. Nevertheless, by targeting *zip*/MyoII transgene expression to either the amnioserosa; the leading edge of the lateral epidermis; or all of the

lateral epidermis in animals homozygous for *zip*/MyoII null mutations, we showed that expression in any one tissue can rescue the defects in closure (Franke et al., 2005).

Zipping is Not Required for Bulk Cell Sheet Movements During Closure: We used laser surgical ablation experiments to eliminate zipping at the canthi and showed that dorsal closure proceeds at native rates (compare short dashed lines in Fig. 4 to the solid lines that show the behavior of two "native" embryos that were not laser manipulated or the dot dash line that shows the results of the removal of the amnioserosa, Hutson et al., 2003). This observation indicates that the progress of the leading edge towards the dorsal midline does not require zipping. Nevertheless, additional analysis demonstrates that zipping plays a key role in maintaining the curvature of the leading edge and participates at the end stages of dorsal closure to complete edge-to-edge tissue suturing.

Newtonian force balance equation: In the absence of force produced by zipping, we can write a Newtonian force balance equation (see diagram in lower left of Fig. 2) that describes the forces that impinge on a small segment (*ds*) of the leading edge of the lateral epidermis:

$$(dT/ds + \sigma_{LE} + \sigma_{AS})ds - b\,ds v = \rho ds\, a \qquad (1)$$

The term in parentheses describes the balance between the tensions T due to an actomyosin rich purse-string (that in native closure, favors closure – see below), the sheet forces ($\sigma_{AS}ds$) in the amnioserosa (that favor closure) and the sheet forces ($\sigma_{LE}ds$) in the remainder of the lateral epidermis (that oppose closure). The next term is a viscous drag term (*b ds v*) that opposes closure (*b* is the drag coefficient and *v* is the velocity of closure; where $v = dh/dt$ and h is the distance from the dorsal midline to the leading edge, see Fig. 2, diagram in upper right). The term on the right side of the equation is equivalent to the inertial term (*i.e.*, the force due to acceleration, $ma = mdv/dt$ where $\rho ds = m$). Under the conditions of low Reynolds number present in the embryo (viscous forces are ~10^5 times greater than inertial forces), this inertial term is inconsequential and can be treated essentially as 0. Equation (1) can therefore be re-written:

$$T\kappa + \sigma_{AS} - \sigma_{LE} = b\, dh/dt \qquad (2)$$

Where κ is the curvature and Tκ represents the components of T along the direction of motion. The velocity (dh/dt=v) is constant and very small during native closure – the leading edge moves towards the dorsal midline at only 6 nm/s (it moves toward the other leading edge at $V=dH/dt = 2dh/dt$=12 nm/sec) . In contrast, the leading edge retracts following laser-surgical removal of the amnioserosa at >940 nm/s (see Fig. 1 and 2, time at which each frame was taken is shown in seconds). While our treatment strictly applies only to the symmetry point (where H, see Fig. 2A, is maximum), the vector sum of forces applies in a more general sense to a large segment of the leading edge. Moreover, we are developing approaches to better understand dynamics near the canthus, where equation (1) lacks a term for zipping.

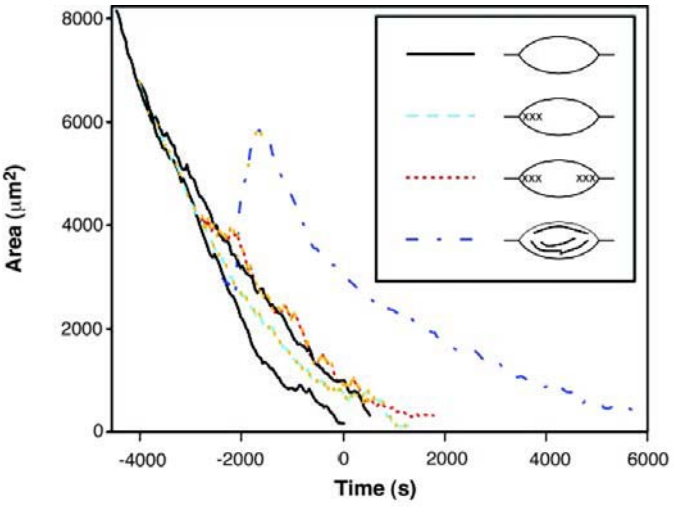

Fig. 4. Quantitative Analysis of Laser Cuts

Empirical rate equation: In addition to this force balance equation on the leading edge, we treat zipping with a rate equation that is approximated by the change in the width of the tissue W with time (*i.e.*, the rate at which the leading edge disappears into the seam). This equation was originally based on empirical fits to experimental data but now has been derived based on a model for the dynamic geometry of the dorsal opening, thereby providing a geometric basis for its formulation (Peralta et al., Submitted to Biophysical Journal).

$$dW/dt = -\frac{k_z}{\tan(\theta_A/2)+\tan(\theta_B/2)} = \frac{-k_z}{2H} \qquad (3)$$

Thus dW/dt is a function of a rate constant, k_z, and can be expressed as either an inverse function of the angle between the two sheets of leading edge tissues at the canthus (the tanθ terms) or the height of the exposed amnioserosa (H). This equation, along with the observation of constant V (for the vast majority of closure, see Fig. 2 and discussion above) fits the data very well (Fig. 5) and has the biologically pleasing property that zipping proceeds more quickly if the angle between the cell sheets becomes more acute. The pairs of eye shaped structures in Fig. 5 B,C and D are actual data traces (upper) and model generated shapes (bottom). Factors other than the geometry effect their influence on zipping through the rate constant k_z. Another measure of closure is f_z, which describes the fractional contribution of zipping to the velocity of the leading edge (described more fully in Hutson et al., 2003).

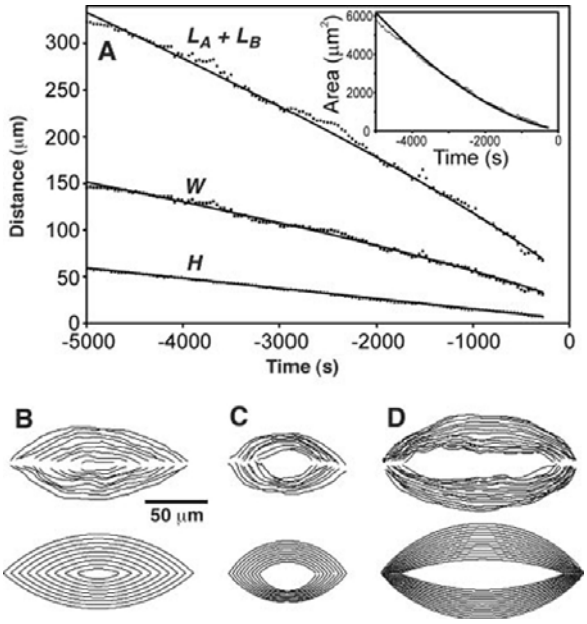

Fig. 5. Biophysical Analysis and Modeling of Closure

Biophysical parameters that characterize dorsal closure: Analysis of native closure yields three kinetic parameters that are useful descriptors of the closure process: for wild type embryos, $V = dH/dt$ = 12 nm/s; k_z = 16 nm/s; and f_z = 33.4%. Analysis of laser cut embryos yields the relative magnitude of the forces in a "force ladder" relationship (σ_{AS}:σ_{LE}:Tκ:bv). In wild type embryos, the relative magnitudes of the force contributions in this ladder are bracketed between the ratios ~120:80:40:1 and ~160:80:80:1. Note that while Tκ is modest, T is the most significant force – T:$\sigma_{AS}\Delta s_{AS}$:$\sigma_{LE}\Delta s_{LE}$ is ~36:2:1 (where Δs_{AS} and Δs_{LE} the cellular dimensions, 10 μm and 3 μm, respectively, upon which the relevant sheet forces, σ, act). This is because only a small component of T is resolved in the direction of movement. Thus, a useful and encompassing biophysical description of dorsal closure is provided by the three kinetic values and the force ladder. Quantitative analysis points to a key and measurable role for cellular adhesion or zipping during closure.

Previously, zipping had been identified by Jacinto et al. (2000) as a potential driving force for dorsal closure. As described above, double canthus cut experiments indicates that adhesion-mediated zipping coordinates the forces produced by the purse-strings through its role in maintaining the curvature of the purse-strings and thus the projection of its tension T along the direction of motion. At the end-stages, zipping is of course essential for forming a seamless epithelium.

Quantitative approaches to a DC mutant reveal an unsuspected function for β_{PS}-integrin in dorsal closure: Applying this model to the ß$_{PS}$-integrin mutant, *myospheroid* (*mys*), we quantified the mutant phenotype and specified the force-generating process(es) to which the protein contributes. *mys* mutants fail in zipping. Compare Fig. 5B, which shows a data set from native closure in a wild type embryo, upper panel, and the fit of the model, lower panel; to Fig. 5D, which shows data and the model fit for a native *mys* embryo. Our model indicates that compromised zipping is a key feature of the *mys* phenotype. This failure in zipping is followed by disintegration of the junction between the lateral epidermis and the amnioserosa (occasionally, failure is within one of the tissues, rather than between them).

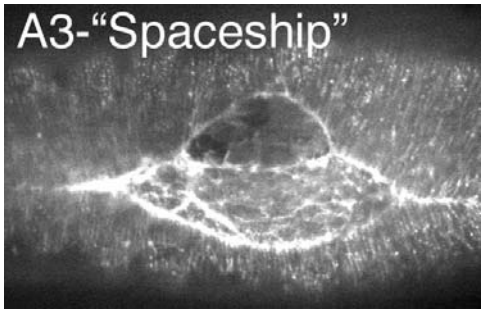

Fig. 6. A3-Spaceship cut

The molecular basis of contractility – quantitative analysis of zip/myoII mutants: Since Hutson et al. (2003) was published, we have extended our observations in several key ways. First, to investigate the contractile purse-strings, we surgically removed one of the purse-strings through laser microbeam ablation of approximately one half of the cells of the leading edge on one side of the embryo. This A3 cut causes the reproducible formation of what we refer to as the "space ship" morphology (Fig. 6, Rodriguez et al., In preparation). Uncut regions of the leading edge proceed to close on schedule. In contrast, the cut region forms a new "wound" purse-string (see Kiehart et al., 2000), more distant from the dorsal midline than the native purse-string it replaces. After a brief delay, closure proceeds at nearly wild type rates. We hypothesize that the purse-string is a key part of closure, and its loss induces the embryo to generate a new one that subsequently contributes to closure.

Next, we have addressed the molecular basis of contractility. We (Young et al., 1993 and unpublished data), and others (Wood et al., 2002) have shown that the abundance of both actin and myosin are severely reduced in *zip*/myoII mutant animals and that dorsal closure fails in such mutants. Wood and co-workers focused on homozygotes that complete closure – we have concentrated on homozygotes with a more severe dorsal closure defect. Video time-lapsed analysis shows that the mechanical integrity of two of the three tissues involved in closure – amnioserosa and leading edge – fail. Our hypothesis is that failure occurs when the level of maternally loaded myosin heavy chain drops below some critical level (robust zyogotic expression of zip/myoII begins at 4-8 hrs of development, Kiehart et al., 1989). Immunofluorescent analysis of *zip*/myoII in mutant embryos incapable of zygotic expression of *zip*/myoII show that the level of myosin begins to drop by the time of dorsal closure (onset at 10.3 to 11 hrs). We showed that the bulk of progress toward closure is driven by contractility that requires nonmuscle myosin II (Franke et al., 2005). The macro-molecular assemblies of actin and myosin in the supra-cellular "purse-strings" of the leading edge of the lateral epidermis are distinct from the sub-plasma membrane, cortical arrays in the amnioserosa. Cortical arrays of acto-myosin II in the bulk of the lateral epidermis are likely analogous to the cortical arrays in the amnioserosa, but the cells are a different shape and contractility in the lateral epidermis impedes closure. Adhesion-mediated zipping, which also requires nonmuscle myosin II function coordinates the forces produced by the purse-strings and is essential for the end stages of seam formation – ensuring that a seam is formed between cells that have the same sub-segmental, cellular identity.

We have begun to analyze quantitatively native *zip*/myoII embryos. Preliminary analysis indicates that rates of closure prior to failure are about 84 % of wild type (dh/dt =5.1 nm/s vs. 6.0 nm/s), with

the rate constant for zipping slightly higher than wild type (k_z = 17.4 nm/s vs. 16.0 nm/s) but the total contribution from zipping is nearly 130% of wild type (f_z = 43.0% vs. 33.4%). We hypothesize that the small change in *V* is due to effects on forces that both contribute to and oppose dorsal closure. We note that the most significant change is the contribution of zipping to closure, which we interpret as due to a decrease in contractility (shortening) of the purse-string. Further analysis of the mutant phenotype through surgical cuts will allow us to further evaluate the force ladder that distinguishes *zip*/myoII mutants from wild type embryos.

Up-regulation of forces for dorsal closure in surgically manipulated embryos: We have also begun to analyze forces in the embryo following removal of zipping at the canthi. Dorsal closure proceeds in the absence of zipping and an "internal" seam is formed. In contrast to native closure, this leads to a convexed versus a concaved shape for the leading edge, such that the force generated by contractility of the actomyosin rich purse-string at the leading edge of the lateral epidermis opposes closure. Nevertheless, the rate of closure is nearly identical to native closure (the slight decrease in rate is very likely the result of damage to the amnioserosa that underlies the canthus). This indicates that tension generated by the amnioserosa has to increase or tension in the lateral epidermis has to decrease. Analysis of experiments that surgically inhibit zipping, then remove the amnioserosa (double canthus cuts followed by A1 cuts, Fig. 3) demonstrates that the tension in the amnioserosa increases by 25-50% (Peralta et al., Submitted to Biophysical Journal). Moreover, theoretical modeling of the laser inhibited zipping experiments indicate that σ_{AS} increases by 50 to 350% (Y. Tokutake, Ph.D. thesis). We are beginning to investigate the mechanism by which this interesting regulation occurs.

We are theoretically modeling these movements in additional ways. We (Yang et al., In Preparation) have been exploring non-Hookean models for closure comparable to the force velocity relationships in muscle developed by Hill (1938) and Huxley and Simmons (1971).

Ramifications for morphogenesis: A significant feature of our findings is that they demonstrate that the net force that drives dorsal closure is the vector sum of forces, each of which is up to one to two *orders of magnitude greater* than the net force during native closure and each of which depends on one or more biological processes. These forces include contraction of the amnioserosa, contraction of the purse-string or actin cable; cell sheet adhesion or zipping; and contraction of lateral and ventral epidermis (this last force opposes closure). We find that these individual forces are redundant – laser microsurgery can be used to eliminate contribution from one of these forces and dorsal closure proceeds at essentially native rates (sometimes after a brief recovery period). If we remove more than one force, dorsal closure fails. To maintain closure at native rates after the removal of one tissue, biological processes in the remaining tissues must be up-regulated to compensate for the loss. This remarkable resiliency may well be related to the regulatory factors that insure nearly balanced forces in native closure – feed back mechanisms must be in place to insure that no one force overwhelms the others, and that dorsal closure proceeds to completion (see e.g., Orr et al., 2006). Of equal significance is that we have been able to apply our quantitative approach to the analysis of mutant phenotypes. We demonstrate that closure in the DC gene *myospheroid*, which encodes β_{PS}-integrin, has an early, important role in zipping. Later, the junction between the amnioserosa and the leading edge of the lateral epidermis fails, and the embryo rips itself apart.

Pharmacological analysis of dorsal closure: We have also developed methods to pharmacologically investigate dorsal closure. We use a micro-pipette to disrupt the vitelline envelope on the ventral side of embryos during germ band elongation stages whilst they are immersed in growth medium (Robb's medium, Echalier, 1997). These embryos continue to develop normally and we can follow dorsal

closure using standard methods. We have analyzed of the effects of a number of different compounds. For example, we have shown that once dorsal closure begins, the embryo can complete dorsal closure even in sufficient concentrations of cyclohexamide to completely inhibit metabolic incorporation of labeled ^{35}S-leucine. When applied early, cyclohexamide blocks closure – we are currently determining when in closure new transcription and protein synthesis are no longer necessary. We have also tested drugs that perturb the function of the actin cytoskeleton. Not surprisingly, cytochalasin disrupts the purse-string and blocks closure, while jasplakinolide (which functions as a cell-permeant phalloidin) increases the number and length of filopodia and the amount of actin in the actomyosin purse-string. It causes the purse-string to kink and actin to remain assembled even after a mature seam forms and actin is usually dispersed. We also find that low doses of colchicine inhibits dorsal closure in a 366 nm light-reversible fashion. The leading edge cells of wild type embryos contain a robust microtubule cytoskeleton (see also Kaltschmidt et al., 2002). Our observations indicate microtubules are required for dorsal closure. Collectively, these preliminary studies show that we can use pharmacological studies to analyze dorsal closure.

Dorsal closure provides an excellent model system for the study morphogenesis. The advantage of using a genetic system like fly that is also amenable to biophysical analysis cannot be over estimated. *Drosophila* offers a powerful window on the cellular and molecular basis of cell sheet movements that are a fundamental part of morphogenesis throughout phylogeny. Many cell movements observed in fly closely parallel those seen in vertebrates and a number of the contractile proteins are highly conserved. The powerful set of genetic and molecular tools available are reviewed elsewhere (Wolfner and Goldberg, 1994; Adams and Sekelsky, 2002; St Johnston, 2002; Hawley and Walker, 2003).

Important questions regarding dorsal closure remain unresolved: Quantitative analysis and biophysical modeling reveals that we have only begun to understand the phenotypes due to mutations in DC genes – further analysis of cellular kinematics and dynamics in DC mutant embryos will be required to describe the process fully and understand it in terms of molecular and cellular processes. Moreover, kinematic analysis remains incomplete. For example, elegant genetic manipulation of dorsal ventral patterning mutants establishes that the leading edge is defined by the juxtaposition of the amnioserosa and the lateral epidermis (Stronach and Perrimon, 2001). Nevertheless, a kinematic description of the events that lead up to the overlap of leading edge cells and amnioserosa that characterizes the morphology of the embryo at the start of dorsal closure is not available. Moreover, few studies have analyzed the changes in embryo structure that accompany dorsal closure at the electron microscope level and no one has done so in a systematic fashion.

Emerging Biophysical Questions:

1) So far we approximate the relative magnitude of forces that drive closure – ultimately, a complete model will require measurements of absolute force. The embryo is surrounded by a tough vitelline envelope whose mechanical properties would predominate if attempts are made to introduce flexible micro-pipettes. The ability to apply forces to magnetic beads introduced into the embryo may be the best strategy for measuring directly the individual forces that contribute.

The individual forces that the embryo applies to dorsal closure are far in excess of their vector sum. Moreover, the embryo can compensate for the laser removal of forces that contribute to closure. Indeed, we showed that inhibition of zipping causes the force applied by the amnioserosa to increase by 25-50%.

2) How does the embryo, or how do particular tissues in the embryo sense the forces applied to them?

3) Are comparable sensing mechanisms responsible for maintaining the balance between large forces such that the next force applied for closure remains of a proper sign (*i.e.*, favoring closure) and causes closure at a rate that is astonishingly constant even in the presence of mutations that are known to influence closure (6.0 ± 0.8 nm/sec).

4) How is the sensing mechanism for closure transduced into increases in applied force?

5) Is there a governor that maintains constant speed?

6) What is the "parts list" for the contractile and elastic components required for closure – though we can separate elastic from contractile theoretically, can we do so in practice?

References:

Adams, M.D., and J.J. Sekelsky. 2002. From sequence to phenotype: reverse genetics in *Drosophila melanogaster*. *Nat Rev Genet.* 3:189-198.

Bard, J. 1990. Morphogenesis: the cellular and molecular processes of developmental anatomy. Cambridge University Press, Cambridge; New York. xi, 303 pp.

Bloor, J.W., and D.P. Kiehart. 2002. *Drosophila* RhoA regulates the cytoskeleton and cell-cell adhesion in the developing epidermis. *Development.* 129:3173-3183.

Brodland, G.W., and D.A. Clausi. 1995. Cytoskeletal mechanics of neurulation: insights obtained from computer simulations. *Biochem Cell Biol.* 73:545-553.

Echalier, G. 1997. *Drosophila* Cells in Culture. Academic Press, San Diego.

Eldar, A., D. Rosin, B.Z. Shilo, and N. Barkai. 2003. Self-enhanced ligand degradation underlies robustness of morphogen gradients. *Dev Cell.* 5:635-646.

Foe, V.E. 1989. Mitotic domains reveal early commitment of cells in *Drosophila* embryos. *Development.* 107:1-22.

Franke, J.D., R.A. Montague, and D.P. Kiehart. 2005. Nonmuscle myosin II generates forces that transmit tension and drive contraction in multiple tissues during dorsal closure. *Curr Biol.* 15:2208-2221.

Grill, S.W., J. Howard, E. Schaffer, E.H. Stelzer, and A.A. Hyman. 2003. The distribution of active force generators controls mitotic spindle position. *Science.* 301:518-521.

Harden, N. 2002. Signaling pathways directing the movement and fusion of epithelial sheets: lessons from dorsal closure in *Drosophila*. *Differentiation.* 70:181-203.

Hawley, R.S., and M.Y. Walker. 2003. Advanced genetic analysis: finding meaning in a genome. Blackwell Pub., Malden, MA. xv, 239 pp.

Hill, A.V. 1938. The heat of shortening and the dynamic constants of muscle. *Proc. Roy. Soc. Lond.* B126:136-195.

Hutson, M.S., Y. Tokutake, M.S. Chang, J.W. Bloor, S. Venakides, D.P. Kiehart, and G.S. Edwards. 2003. Forces for morphogenesis investigated with laser microsurgery and quantitative modeling. *Science.* 300:145-149.

Huxley, A.F., and R.M. Simmons. 1971. Proposed mechanism of force generation in striated muscle. *Nature.* 233:533-538.

Jacinto, A., W. Wood, T. Balayo, M. Turmaine, A. Martinez-Arias, and P. Martin. 2000. Dynamic actin-based epithelial adhesion and cell matching during *Drosophila* dorsal closure. *Curr Biol.* 10:1420-1426.

Jacinto, A., S. Woolner, and P. Martin. 2002. Dynamic analysis of dorsal closure in *Drosophila*: from genetics to cell biology. *Dev Cell.* 3:9-19.

Jurgens, G., E. Wieschaus, C. Nüsslein-Volhard, and H. Kluding. 1984. Mutations affecting the pattern of the larval cuticle in *Drosophila melanogaster*: II. Zygotic loci on the third chromosome. *Roux's Archives of Developmental Biology.* 193:283-294.

Kaltschmidt, J.A., N. Lawrence, V. Morel, T. Balayo, B.G. Fernandez, A. Pelissier, A. Jacinto, and A. Martinez Arias. 2002. Planar polarity and actin dynamics in the epidermis of *Drosophila*. *Nat Cell Biol*. 4:937-944.

Keller, R., L. Davidson, A. Edlund, T. Elul, M. Ezin, D. Shook, and P. Skoglund. 2000. Mechanisms of convergence and extension by cell intercalation. *Philos Trans R Soc Lond B Biol Sci*. 355:897-922.

Keller, R., L.A. Davidson, and D.R. Shook. 2003. How we are shaped: the biomechanics of gastrulation. *Differentiation*. 71:171-205.

Kiehart, D.P., M.S. Lutz, D. Chan, A.S. Ketchum, R.A. Laymon, B. Nguyen, and L.S.B. Goldstein. 1989. Identification of the gene for fly non-muscle myosin heavy chain: *Drosophila* myosin heavy chains are encoded by a gene family. *EMBO J*. 8:913-922.

Kiehart, D.P. 1999. Wound healing: the power of the purse string. *Curr. Biol*. 9:R602-R605.

Kiehart, D.P., C.G. Galbraith, K.A. Edwards, W.L. Rickoll, and R.A. Montague. 2000. Multiple forces contribute to cell sheet morphogenesis for dorsal closure in *Drosophila*. *J. Cell Biol.* 149:471-490.

Kiehart, D.P., Y. Tokutake, M.-S. Chang, M.S. Hutson, J. Wiemann, X.G. Peralta, Y. Toyama, A.R. Wells, A. Rodriguez, and G.S. Edwards. 2006. Ultraviolet laser microbeam for dissection of *Drosophila* embryos. *In* Cell Biology: A Laboratory Handbook, 3rd Ed. Vol. 3. J.E. Celis, editor. Elsevier Academic Press, San Diego, CA. 87-103.

Meinhardt, H., and S. Roth. 2002. Developmental biology: sharp peaks from shallow sources. *Nature*. 419:261-262.

Nusslein-Volhard, C., E. Wieschaus, and H. Kluding. 1984. Mutations affecting the pattern of the larval cuticle in *Drosophila melanogaster*: I. Zygotic loci on the second chromosome. *Roux's Arch Dev.Biol.* 193:267-282.

Odell, G.M., G. Oster, P. Alberch, and B. Burnside. 1981. The mechanical basis of morphogenesis. I. Epithelial folding and invagination. *Dev*. 85:446-462.

Orr, A.W., B.P. Helmke, B.R. Blackman, and M.A. Schwartz. 2006. Mechanisms of mechanotransduction. *Dev Cell*. 10:11-20.

Peralta, X.G., Y. Toyama, M.S. Hutson, R.A. Montague, S. Venakides, D.P. Kiehart, and G.S. Edwards. Submitted to Biophysical Journal. Upregulation of forces and morphogenic asymmetries in dorsal closure during *Drosophila* development.

Rodriguez, A., D.L. Abravanel, G.S. Edwards, and D.P. Kiehart. In preparation. Force production during morphogenesis: the contribution of the actomyosin cable to dorsal closure in *Drosophila* investigated by UV laser microsurgery.

Shook, D., and R. Keller. 2003. Mechanisms, mechanics and function of epithelial-mesenchymal transitions in early development. *Mech Dev*. 120:1351-1383.

St Johnston, D. 2002. The art and design of genetic screens: *Drosophila melanogaster*. *Nat Rev Genet*. 3:176-188.

Stronach, B.E., and N. Perrimon. 2001. Investigation of leading edge formation at the interface of amnioserosa and dorsal ectoderm in the *Drosophila* embryo. *Development*. 128:2905-2913.

Wieschaus, E., C. Nusslein-Volhard, and G. Jurgens. 1984. Mutations affecting the pattern of the larval cuticle in *Drosophila melanogaster*: III. Zygotic loci on the X-chromosome and fourth chromosome. *Roux's Archives of Developmental Biology*. 193:296-307.

Wolfner, M.F., and M.L. Goldberg. 1994. Harnessing the power of *Drosophila* genetics. *Methods Cell Biol*. c:33-80.

Wood, W., A. Jacinto, R. Grose, S. Woolner, J. Gale, C. Wilson, and P. Martin. 2002. Wound healing recapitulates morphogenesis in *Drosophila* embryos. *Nat Cell Biol*. 4:907-912.

Yang, G.-Q., A.T. Layton, G.S. Edwards, D.P. Kiehart, and S. Venakides. In Preparation. Modeling the mechanics of *Drosophila* dorsal closure. *for Math Biol.*

Young, P.E., A.M. Richman, A.S. Ketchum, and D.P. Kiehart. 1993. Morphogenesis in *Drosophila* requires nonmuscle myosin heavy chain function. *Genes & Development*. 7:29-41.

Mitotic Spindle Assembly

The assembly of a microtubule-based bipolar spindle is essential for the equal segregation of replicated DNA during cell division. I will focus on our current understanding of vertebrate cell division and discuss some of the questions that remain unanswered.

Recent advances in high-resolution microscopy, including the development of fluorescent speckle microscopy, have led to a quantitative description of spindle microtubule dynamics. Well-documented features of these dynamics include: (1) turnover occurs with half-lives of less than 100s, (2) the microtubule lattice fluxes towards each spindle pole at ~2 micron/min (or slower), and (3) microtubule plus-ends grow at ~10 micron/min. Sophisticated analysis tools have revealed heterogeneity in the dynamics of different microtubule populations (e.g. kinetochore and non-kinetochore), and at different sites within spindles (near poles or chromatin). Molecular perturbations, combined with high-resolution imaging, have allowed a number of spindle components to be linked to different aspects of these fast microtubule dynamics. While essentially all of the proteins, including microtubule-based motor proteins, required for proper cell division are now known, without a deeper understanding of the properties of key spindle proteins our descriptions of the most basic aspects of mitotic spindle self-organization, such as how spindle size and shape are determined, remain largely incomplete.

In current models, bipolar spindle formation requires the proper regulation of two processes: (1) microtubule transport, involving plus-end directed (e.g. kinesin-5s) and minus-end directed (e.g. kinesin-14s and dynein) motor proteins; and (2) microtubule polymerization, involving a number of non-motor microtubule associated proteins (e.g. Eb1, Op18) and depolymerizing kinesins (kinesin-13s). The characterization of post-translational modifications and binding partners for these proteins has led to an emphasis on biochemical regulation, through kinases and GTPases. Gradients of such signals have been measured and found to be on scales comparable to spindle size. Models for how these gradients may regulate microtubule nucleation and stabilization as well as motor protein dynamics have also been proposed. However, as we better understand micromechanical properties of the proteins involved in bipolar spindle formation, the importance of mechanical-sensing and force-based regulation will likely become as important as biochemical regulation.

Xenopus egg extracts have been developed as a model system to study vertebrate spindle assembly. Compatibility with biochemical manipulation and straightforward control over cell cycle progression are some of the advantages of this system. In addition, the following powerful simplifications are possible: (1) the absence of cell walls excludes physical constraints and the supply of proteins needed for assembly, (2) spindle assembly without centrosomes, relevant for many meiotic and plant divisions, can be examined, (3) chromatin linked to

beads, lacking kinetochores or pairs of sister chromatids, can support bipolar spindle assembly. While many of these simplifications raise questions about the physiological relevance of this system, a number of discoveries regarding spindle assembly mechanisms made using this system have been broadly relevant. We find that this model system provides a level of experimental control that is better suited than others for examining the basic principles underlying spindle self-organization.

We will focus on the following questions, discussing some of our recent findings:

1) **How does the spatial organization of regulatory signals influence spindle size?**

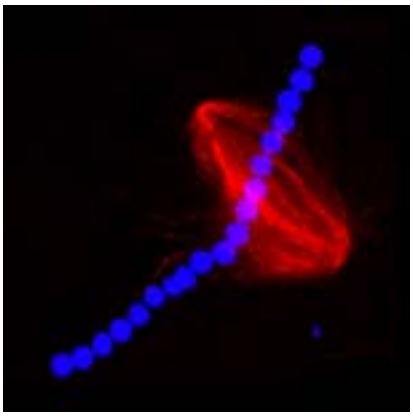

Figure 1. Spindle assembly on linear chromatin arrays.

Chromatin generates signals that play important roles in regulating spindle assembly. In many systems, chromatin alone is sufficient for providing cues for microtubule assembly and spindle organization. RanGTP and Aurora kinases are believed to be mediators of chromatin signaling and the gradients of these diffusible signals from chromatin have been imaged using FRET-based sensors. Based on these observations, Turing-like models, incorporating enzymatic reaction and diffusion properties of these signaling molecules, have been developed to account for the size and shape of the metaphase spindle. While molecule-specific perturbations support the basic model, the question of whether changes in the shape of chromatin signals affect spindle morphology remains unanswered. We have developed an in vitro assay system to manipulate chromatin structures in cytoplasm to examine how the spatial organization of the chromatin signals influences spindle assembly. We used paramagnetic chromatin-beads, and magnetic fields for their alignment, in Xenopus egg extracts and examined spindle assembly. We found that for linear chromatin-structures varying 8-fold in length, metaphase spindle size and shape were constant (Fig. 1). The restriction of microtubule distribution to a ~20 μm region, depends on proper function of the microtubule-based motor proteins, cytoplasmic dynein and kinesin-5. Our findings indicate that while chromatin provides cues for microtubule formation, metaphase spindle organization is controlled by microtubule-based motors.

2) **How is spindle width determined?**

To account for our observations of chromatin-directed spindle assembly, we have proposed a simple model that serves as a basis for additional experiments. Microtubule assembly occurs proximal to chromatin, and this region of assembly and/or stabilization can be set up by gradients of RanGTP, Op18 and other

signaling molecules. Dynein/dynactin crosslinks these microtubules and transports them to bring their minus-ends together (Fig. 2). Dynamic microtubules explore distances greater than 50 μm from each spindle pole, as revealed by observations of Eb1 dynamics. These microtubules provide tracks for the continuous recruitment of newly formed microtubules to spindle poles.

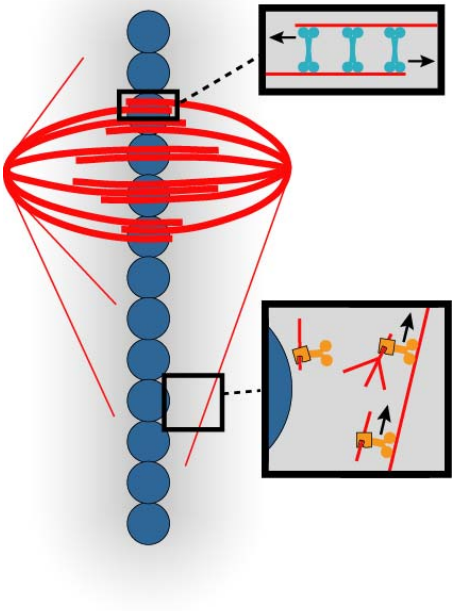

Figure 2. A model for the roles of kinesin-5 and dynein/dynactin during spindle assembly.

We hypothesize that spindle width is determined by the length of stable microtubules in the spindle and geometric constraints on the cross-linking of antiparallel microtubule arrays. Kinesin-5 can crosslink microtubules and can push these microtubules apart to maintain spindle bipolarity. With no kinesin-5 function, but active dynein-dependent microtubule recruitment to spindle poles, we observed that only one monopolar spindle forms on chromatin-bead strings. It is reasonable to assume the force kinesin-5 generates depends on the extent of antiparallel overlap in the spindle and the angle of incidence between two microtubules anchored at spindle poles. With increased spindle width, the angle of incidence and extent of overlap between microtubules emanating from each spindle pole would change. At larger distances from the spindle poles, the number of kinesin-5 cross-links between two microtubules would be reduced due to microtubule rigidity and the finite flexibility and size of the kinesin-5 protein. In contrast, two precisely parallel or anti-parallel microtubules would have a large linear distance over which cross-linking could occur and a very large number of available sites for kinesin-5-mediated cross-linking. For chromatin signals that extend over a wider region along the axis of the metaphase plate, the geometric constraints on maintaining stable antiparallel microtubule overlap by kinesin-5, and spindle pole focusing by dynein-dynactin, would limit spindle width.

3) How is steady-state spindle microtubule length set?

Plus-ends in spindles undergo bounded dynamic instability such that they do not grow indefinitely, but undergo catastrophe at a frequency that sets their average length. Non-specific agents like 2-methylpentane-2,4-diol, that promote protein association and can induce tubulin polymerization, and more specific agents, such as antibodies to MCAK, a kinesin-13 that promotes microtubule catastrophe, have been used to examine microtubule length regulation in the spindle. At high doses, these agents induce spontaneous microtubule polymerization in the entire

cytoplasm. At lower doses, while microtubule density increases, only a modest change in spindle size is observed or time-dependent changes in spindle organization are achieved. Perturbations that change steady-state microtubule length have not been characterized.

4) Where are microtubule minus-ends located? How dynamic are minus-ends in spindles?

It is generally accepted that microtubules in the spindle depolymerize at their minus-ends. In current models, polewards microtubule transport, plus-end assembly rates and minus-end disassembly are precisely coupled to allow steady-state metaphase spindle size to be maintained. Kinesin-13s, which can depolymerize microtubules from both ends in vitro, localize to spindle poles where minus-ends are believed to concentrate. Based on inhibition of kinesin-13 family members it has been suggested that these proteins actively depolymerize microtubule minus-ends in spindles. However, a probe for visualizing microtubule minus-ends in the spindle is not available and therefore, it has not been possible to directly show that minus-ends in the spindle actively disassemble. In fact, the precise distribution of microtubule minus-ends in the spindle remains unknown. The possibility remains that the minus-ends of microtubules are capped and all disassembly occurs via plus-end dynamic instability.

5) How does the spindle respond to mechanical perturbations?

Studies examining the loss-of-function (or knock-down) phenotypes of essentially all molecules needed for spindle assembly are now complete. Systematic mechanical perturbations of metaphase spindles may be combined with these molecular perturbations to test current models for force balance and distribution in the metaphase spindle.

Biophysical Discussions on Molecular Motors
Asilomar, 22 October 2006

Summary: What have we learnt and where are we going?

Jonathon Howard

MPI-CBG
Pfotenhauerstr. 108
01307 Dresden
Germany
howard@mpi-cbg.de

Introduction

This meeting has shown that we have learnt a lot about Molecular Motors since the last Biophysical Discussions meeting on the subject that was organized by Roger Cooke in 1994. There has been lots of healthy discussion, argument and disagreement over the last few days. This has tended to obscure the fact that our understanding of how molecular motors work has increased dramatically over the last dozen years. Here I will summarize our current level of understanding and give some hints of what the outstanding open questions are and how they might be approached. Many of these issues were raised by Yale Goldman in his opening talk.

Directionality

Motor proteins move in a directional manner. This is what distinguishes “active transport” from diffusion, which is randomly directed. Directed motion requires an energy source, and for motor proteins this energy is provided by the free energy associated with the hydrolysis of ATP.

The directed motion of motor proteins relies on three properties. First, the filaments are polar. Microtubules and actin filaments are made of asymmetric building blocks that associate in a head-to-tail manner that confers asymmetry to the whole polymer. Second, motor proteins bind stereospecifically to the filament such that the asymmetric motor domain binds in a specific orientation to the asymmetric surface of the filament. And third, the motor protein undergoes a “stroke”, a conformational change that has a specific direction with respect to the axis of the filament. This stroke is coupled to the hydrolysis of ATP, and this is how energy dissipation is coupled to directed motion. If the motor is fixed, the stroke will move the filament in a particular direction. If the filament is fixed, and the motor has two motor domains, then a stroke by one motor domain will move the second motor domain nearer to the next binding site in the direction of travel.

Thus the stroke is the key to directionality and this is why so much effort – especially x-ray crystallography and high-resolution single-molecule tracking – has gone into defining the it.

For myosin, several structures suggest that the stroke corresponds to rotation of a lever-like light-chain-binding domain. For kinesin, there is no lever arm and one

popular model is the neck-linker docking hypothesis, though I believe that there are a number of problems with the hypothesis (Schief and Howard, 2001). For dynein, the stroke is thought to involve rotation of the microtubule-binding stalk with respect to the ring-like AAA domain. I would like to draw attention to one very surprising result bearing on the structural basis for directionality: Andrew Carter rotated the microtubule-binding domain at the end of dynein's stalk by 180 degrees by modifying the sequence of the coiled coil in the stalk, but found that the motor still went in the same direction. This puzzling result seems to contradict the essential role of stereospecific binding. Because the structure and dynamics of the motor changes upon binding the filament, a key future goal is to solve the structure of a motor-filament complex at atomic resolution.

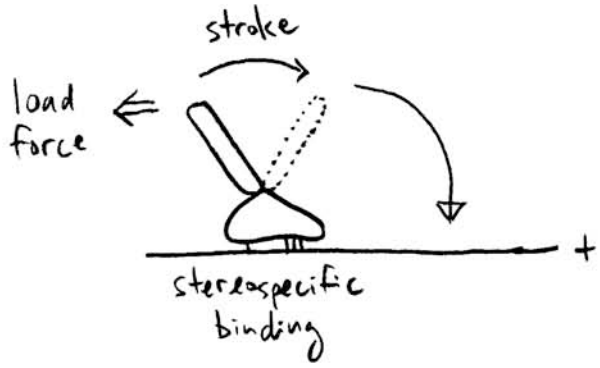

Figure 1: Directionality relies on a polar filament (one end marked with a plus), stereospecific binding, and a directed stroke.

The stroke also offers a way to understand the action of force. That a motor can generate force means that it still moves in a directed manner in the presence of a load force. If the protein is flexible, then we can think of a load force as countering the stroke, decreasing its amplitude and thereby decreasing the directionality of the motor. There is a beautiful paper from Nick Carter and Rob Cross that illustrates this point for kinein-1 by showing that increasing the force leads to an exponential increase in the ratio of backward to forward steps (Carter and Cross, 2005).

Strokes and Steps

The stroke is a conformational change of the motor. Its purpose is to get the motor closer to the next binding site on the filament (in the right direction). The distance to the next binding site is called the step size. But these two distances, the stroke and step sizes, are not necessarily the same. For example, single molecule studies on myosin V show that the stroke is about 25 nm, some 10 nm short of the next binding site on the actin filament. The shortfall is thought to be made up by thermal/diffusional fluctuations, and the key idea is that the light-chain binding domain is flexible so that its thermally-driven distortion allows the motor domain to reach the next biding site.

The shortfall problem is especially acute for myosin VI which has a much shorter light-chain binding domain than myosin V. Perhaps this domain unfolds in order to make up the shortfall. The problem is even more dire for kinesin-1 which has no obvious lever. A key future goal of single-molecule work is to directly resolve this

putative diffusive part of the cycle. In which phase of the hydrolysis cycle does the diffusive search take place?

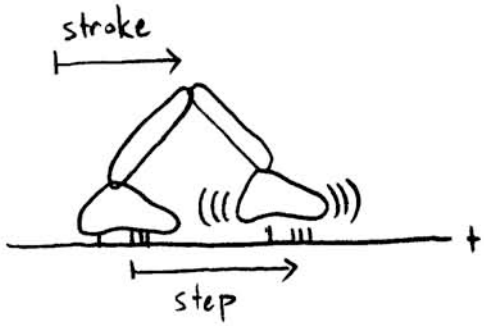

Figure 2: Steps and strokes. A conformational change in one motor domain brings the second motor domain closer to the next binding site. Any shortfall must be made up by thermally driven distortions.

Gating: strain dependence

Processive motors proteins take tens or hundreds of steps along a filament before dissociating. Processivity requires that the motor always maintains attachment to the filament because if the motor detached for even a microsecond it would diffuse away. Two-headed motors like kinesin-1 and myosin-V maintain attachment by coordinating the attachment and detachment of their two motor domains. This is particularly well illustrated for the case of kinesin where the detachment rate of an isolated motor domain is ~1 s^{-1} in ADP or ADP-Pi but ~100 s^{-1} , about 100 times faster, when it is in the two-headed molecule (Hancock and Howard, 1999).

It has been hypothesized that coordination between the motor domains is mediated by intramolecular strain. The idea is that if attachment of both motor domains to the filament requires distortion, and if the filament is rigid, then the region in the motor molecules between the motor domains will be tensed (or compressed). This tensile force might then influence the attachment of the motor domains or in some way alter the kinetics of the ATP hydrolysis cycle. In this way, intramolecular strain is said to "gate" the transition from one structural or nucleotide state to the next. This is an area of great current interest, and was addressed in several presentations. Questions include: is the leading or trailing head regulated, or are they both? In the case of kinesin, does strain prevent ATP binding, or does it prevent ADP release? Or does it accelerate rear motor domain detachment? For myosin V and VI: Does strain accelerate ADP release?

Figure 3: Gating. If the attachment of both motor domains creates intramolecular strain, then this strain might be used to coordinate the two motor domains. For example, it might accelerate the detachment of the rear head or to alter the kinetics of the ATP hydrolysis cycle.

Regulation

In the context of the cell, the regulation of motor activity is extraordinarily complex: many signaling pathways converge on motor output during mitosis or cell locomotion. The fundamental question is: how does one switch a motor protein on and off? There are two known mechanisms. The first is folding: both myosin II and kinesin-1 can exist in compact, folded inactive states and in open, unfolded active states. The switch between these states can be thrown by phosphorylation or cargo-binding. The second mechanism is dimerization: processive motors must be dimeric in order to attain optimal motor activity, though single-headed constructs are capable of limited motility. There is evidence that both myosin VI and kinesin-3 are regulated by dimerization. An important goal of future work is to use structural information to design probes (such as FRET) that can be used to test whether these switching transitions also occur in cells. Then it might be possible to determine how the switch is regulated, in turn, by the cell's signaling machinery.

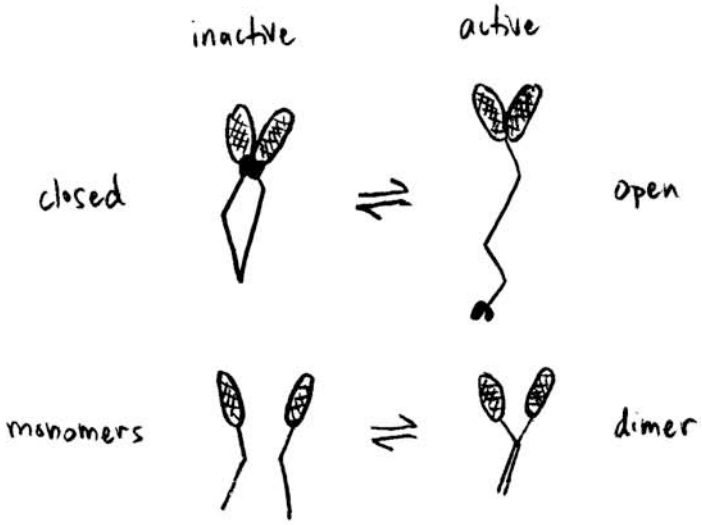

Figure 4: Regulation. There are two known mechanisms for switching motor proteins on and off: unfolding/ folding and dimerization.

"One head many tails"

Humans have 41 different kinesins, defined as proteins containing domains with high sequence similarity to the motor domain of kinesin-1. Why so many? There is a similar number of human myosins and about half as many dyneins. After the discovery of the large kinesin superfamily, it was initially hypothesized that the diversity served to link a generic motor to different cellular cargos: one motor, many tails. However, cell biological and genetic studies soon proved this hypothesis to be unsatisfactory. For example, mitosis comprises several stages, each requiring a different kinesin-family protein. But the type of motion differs considerably from one phase to another. For example, during prophase the microtubule arrays slide apart, while during anaphase the microtubules shorten. The fact that the respective proteins, kinesin-5 and kinesin-13, have a common motor domain doesn't explain anything.

In the face of this diversity of motor activities, it is was very satisfying that different kinesins were found to have very different activities. For example, some go in one direction (kinesin-1), while others go in the other direction (kinesin-14). Similarly it is found that different myosin superfamily members move in different directions along actin filaments. Some kinesins are sliding motors, meaning that they cause sliding of antiparallel microtubules, similar to myosin II which causes sliding between antiparallel actin filaments. Other kinesins are not even motors. Kinesin-13 triggers microtubule depolymerization: it is a depolymerases. Other kinesins may even be polymerases. There is even a kinesin that is both a processive motor and a depolymerase (kinesin-8). This dual activity gives kinesin-8 the intriguing property that the depolymerization rate is depends on the length of the microtubule! In other words, microtubule length feeds back on the polymerization dynamics, offers a potential mechanism for precise regulation of microtubule length in cells. The diversity of kinesin activity is summarized in Table 1.

Kinesin Subfamily	Translocase	Depolymerase
Kinesin-1	Yes (+ end)	No
Kinesin-5 (Eg5)	Yes (+ end)	No
Kinesin-13 (MCAK)	No (diffusive)	Yes (+ end & - end)
Kinesin-8 (Kip3p)	Yes (+ end)	Yes(+ end)
Kinesin-4 (chromo)	Yes (+ end)	?
Kinesin-14 (ncd, kar3)	Yes (- end)	?

Table 1. Microtubule Translocases and Depolymerases.

Future Goals

1. The atomic structure of a motor bound to its filament is needed. Only with this structure in hand might we understand the three-way communication that takes place between the nucleotide, the filament and the stroke. A kinesin-13/tubulin dimer co-crystal is the best hope at that moment because the depolymerase activity of kinesin-13 inhibits tubulin polymerization.
2. A complete hydrolysis cycle of a motor protein that can account for e.g. force-velocity curves is still lacking. This requires measurement of all the rate constants and estimating their load dependence. Kinesin-1 and myosin-V are the most promising candidates at the moment.
3. There are still lots of motors in all three motor families to assay. I expect that there are many surprises left.
4. Cells have a great number other macromolecular machines in cells; motor proteins can provide a technical and conceptual framework for understanding them.
5. We need new tools to measure single-molecule fluorescence and single-molecule forces in cells and tissues.
6. We need to put it all together to explain how mechanical signaling can coordinate cellular motility and locomotion

References

Carter, N.J., and R.A. Cross. 2005. Mechanics of the kinesin step. *Nature* 435(7040):308-312.

Hancock, W.O., and J. Howard. 1999. Kinesin's processivity results from mechanical and chemical coordination between the ATP hydrolysis cycles of the two motor domains [In Process Citation]. *Proc Natl Acad Sci U S A* 96(23):13147-13152.

Schief, W.R., and J. Howard. 2001. Conformational changes during kinesin motility. *Curr Opin Cell Biol* 13(1):19-28.